

Gerhard von der Emde
Eric Warrant *Editors*

The Ecology of Animal Senses

Matched Filters for Economical Sensing

 Springer

The Ecology of Animal Senses

Gerhard von der Emde • Eric Warrant
Editors

The Ecology of Animal Senses

Matched Filters for Economical Sensing

 Springer

Editors

Gerhard von der Emde
Institut für Zoologie
Universität Bonn
Bonn, Germany

Eric Warrant
Lund Vision Group
Department of Biology
University of Lund
Lund, Sweden

ISBN 978-3-319-25490-6

ISBN 978-3-319-25492-0 (eBook)

DOI 10.1007/978-3-319-25492-0

Library of Congress Control Number: 2015958346

Springer Cham Heidelberg New York Dordrecht London

© Springer International Publishing Switzerland 2016

This work is subject to copyright. All rights are reserved by the Publisher, whether the whole or part of the material is concerned, specifically the rights of translation, reprinting, reuse of illustrations, recitation, broadcasting, reproduction on microfilms or in any other physical way, and transmission or information storage and retrieval, electronic adaptation, computer software, or by similar or dissimilar methodology now known or hereafter developed.

The use of general descriptive names, registered names, trademarks, service marks, etc. in this publication does not imply, even in the absence of a specific statement, that such names are exempt from the relevant protective laws and regulations and therefore free for general use.

The publisher, the authors and the editors are safe to assume that the advice and information in this book are believed to be true and accurate at the date of publication. Neither the publisher nor the authors or the editors give a warranty, express or implied, with respect to the material contained herein or for any errors or omissions that may have been made.

Printed on acid-free paper

Springer International Publishing AG Switzerland is part of Springer Science+Business Media (www.springer.com)

Preface

Almost 30 years ago, the celebrated German biologist Rüdiger Wehner published a landmark paper in the *Journal of Comparative Physiology* entitled “Matched filters – neural models of the external world” (Wehner 1987), and with it ushered in an entirely new way of understanding how peripheral sensory structures and sensory neural circuits have evolved to deal with complex, constant and seemingly infinite sensory information. The essence of his message was that any given species *does not* deal with all of this information – in fact *cannot* deal with it – at least not with the overwhelming majority of it. Instead, Wehner recognised that sensory systems rely on “matched filters” to extract the most pressing sensory stimuli that are crucial to the animal’s chances of survival and reproduction, and to suppress or even reject other stimuli. By matching the properties of neurons, circuits and sensory structures to the characteristics of the most crucial sensory stimuli that need to be detected, these stimuli can be directly and reliably extracted for further processing. Moreover, this extraction can be done with a minimum of neural tissue. To sense “the world through such a matched filter”, to quote Wehner himself, “severely limits the amount of information the brain can pick up from the outside world, but it frees the brain from the need to perform more intricate computations to extract the information finally needed for fulfilling a particular task”. An example of a classic matched filter can be found in the ears of certain species of moths, which are tuned to the high frequency sonar pulses of the bats that hunt them, and perceive little else. For these moths no other sound embodies the same danger or requires a behavioural response of the same urgency, and their entire auditory investment – from the morphology of the ear to the physiology of the auditory neural circuits – is devoted to the detection and analysis of that one narrow range of sonic frequencies (see also Chap. 4 by Römer in this volume).

In the years that have followed Wehner’s landmark contribution, it has become increasingly apparent that brains and nervous systems are energetically extremely expensive and that the cost of maintaining a nervous system represents a substantial fraction of an animal’s total energy budget. The main reason for this expense is the cost of maintaining the resting potential of neurons in readiness for electrical signalling. The resting potential, which is usually many tens of millivolts negative relative to the external cellular medium, is maintained (and restored following signalling) by active ion pumps that use energy from ATP molecules to pump sodium and potassium ions across the neuronal membrane against their passive

electrical and concentration gradients. This energetic cost is substantial and is incurred even in the absence of signalling. The extra cost of signalling is simply added to this (Niven et al. 2007). Thus, during evolution, nervous systems have been under pressure to become as lean and as efficient as possible (Sterling and Laughlin 2015), and not surprisingly this fact is inextricably linked to the evolution of matched sensory filters. To quote Wehner above, because matched filters “severely limit information picked up by the brain”, the energetic costs that would have been associated with coding superfluous information are effectively eliminated. And “freeing the brain” not only frees it from the need to perform intricate computations, it also frees it from the significant energetic costs that would have arisen by possessing the neural circuits necessary to make these computations. Simply put, matched filtering saves energy by stripping away unnecessary energetic investments and efficiently redirecting the remaining energy to where it is needed most.

Matched sensory filtering thus has two main evolutionary advantages: firstly it substantially enhances an animal’s ability to detect and analyse ecologically crucial sensory stimuli, and secondly it does so with the most efficient use of the animal’s limited energy supply. In this book we hope to showcase these advantages across the senses, in both vertebrates and invertebrates, and to show how matched sensory filtering is intimately linked to the ecologies of animals. This “ecology of sensing” – with its inherent use of matched filters – provides some of the most beautiful and remarkable products of natural selection that can be found in the natural world, and many of these are described in the pages that follow.

The nine chapters of this book are arranged according to the evolutionary origin of the different senses of animals. Chemoreception – the sensing of chemicals related to smell or taste – is the most ancient sense in the animal kingdom and even occurs in single-celled organisms. Many animals, such as insects, can detect important olfactory stimuli with remarkable sensitivity and at a millisecond time scale. In their review on insect olfactory systems, Riffell and Hildebrand explain how the insect peripheral and central olfactory systems filter meaningful chemical information from a noisy environment full of “unimportant” chemical components. Important olfactory information is perceived by a combination of active and passive processes, during which neural plasticity plays an essential role.

Various animal senses such as hearing, touch, whisking and several others (e.g. infrared perception in some insects) can be attributed to mechanoreception, involving sensory cells that respond to mechanical pressure or distortion. Mechanoreception is also a very old sense and, like chemoreception, even occurs in single-celled organisms. In this book, four chapters deal with matched filtering in the various senses based on mechanoreception. Friedrich Barth uses spiders’ sense of touch to explain the functioning of the large numbers of mechanoreceptive hairs on their exoskeleton. Even though natural stimulus patterns are frighteningly complex, spiders rely on a highly specialised sensory periphery to solve complex behavioural tasks.

Tactile facial hairs, called whiskers or vibrissae, are also used by many mammals. Grant and Arkley explain how, during active whisking, whisker

specialists can extract information about size, texture, shape and position by moving their whiskers over an object. Here again a great deal of processing is conducted by matched filters at the sensory periphery, with the spatial layout and properties of the sensors being matched to the problem at hand. In addition, a mapping of the peripheral arrangement of tactile hairs in the cortex allows for eloquent and economical processing of sensory information.

Two additional chapters on mechanoreception deal with audition, explaining how insects and certain vertebrates acquire sensory information using sound. Heiner Römer presents several examples of sensory matching in the acoustic domain of insects. By concentrating on only some aspects of a sound stimulus and ignoring the rest, insects can match the tuning of their receptors to the carrier frequency of the relevant sound or to the temporal parameters of songs. Economic filtering additionally occurs in the intensity domain and begins already in the peripheral receptors. Acoustic matched filters are also found in other animal groups, and Narins and Clark present examples in the auditory systems of several selected vertebrates. They point out how matched filters can be effective detection tools when examples of the desired signal are available a priori.

Visual matched filters have evolved for all aspects of life in both insects (described in Chap. 6 by Warrant) and vertebrates (described in Chap. 7 by Douglas and Cronin). In insects, the pressing ecological challenges and the overriding energy constraints of small brains and sense organs have led to an enormous variety and sophistication of visual matched filters in insect eyes. Vertebrates also show an enormous diversity of specialisations, including pigment filters, optical adjustments and retinal sampling variations. This plasticity, which is based on a single fundamental eye design, enhances the utility of visual perception in a particular habitat and simultaneously reduces the energetic costs of vision.

The last two chapters deal with the so-called sixth senses, those that fall outside Aristotle's original canon of five senses (sight, hearing, touch, smell, and taste). Infrared perception, absent in most animals, can be found in a few pyrophilous insect species and in some snakes, as outlined in Chap. 8 by Schmitz and colleagues. Despite their different functional principles, insect IR receptors all show the same built-in filter properties, which are based on a match of the absorption properties of the atmosphere and the chemical composition of the insect cuticle. Even electroreception in some aquatic vertebrates can be considered a sixth sense, with this sense probably already present in the earliest vertebrates. As von der Emde and Ruhl point out in their chapter (Chap. 9), weakly electric fish have developed a complex set of matched filters that match the properties of the incoming electrical signal to the properties of the peripheral sense organs. This matching allows electric fish to economically perceive objects in the near field. Interestingly, objects located at greater distances are perceived visually, again with eyes functioning as matched filters for specific visual stimuli.

This book provides a new and updated synthesis of sensory ecology in animals and builds upon the classic 2001 Springer volume *Ecology of Sensing*, edited by Friedrich Barth – one of our current authors – and Axel Schmid. By exploring sensory ecology in the context of matched filtering and energetic constraints, we

hope not only to honour Rüdiger Wehner's immense contribution to the field but also to highlight how the finite energy budgets of animals have been critically important in the evolution of sensory processing. We wish to thank our authors for their excellent contributions to this book and our editors and production staff at Springer for their patience and guidance as this book was being completed.

Bonn, Germany
Lund, Sweden

Gerhard von der Emde
Eric Warrant

References

- Barth FG, Schmid A (2001) Ecology of sensing. Springer, Berlin/Heidelberg/New York
Niven JE, Anderson JC, Laughlin SB (2007) Fly photoreceptors demonstrate energy-information trade-offs in neural coding. PLoS Biol 5(4):e91
Sterling P, Laughlin S (2015) Principles of neural design. MIT Press, Cambridge, MA
Wehner R (1987) "Matched filters" – neural models of the external world. J Comp Physiol A 161:511–531

Contents

Part I Chemoreception

- 1 Adaptive Processing in the Insect Olfactory System** 3
Jeffrey A. Riffell and John G. Hildebrand

Part II Mechanoreception and Audition

- 2 A Spider's Sense of Touch: What to Do with Myriads of Tactile Hairs?** 27
Friedrich G. Barth
- 3 Matched Filtering in Active Whisker Touch** 59
Robyn A. Grant and Kendra P. Arkley
- 4 Matched Filters in Insect Audition: Tuning Curves and Beyond . . .** 83
Heiner Römer
- 5 Principles of Matched Filtering with Auditory Examples from Selected Vertebrates** 111
Peter M. Narins and Grace A. Clark

Part III Vision

- 6 Matched Filtering and the Ecology of Vision in Insects** 143
Eric J. Warrant
- 7 Visual Matched Filtering in Vertebrates** 169
R.H. Douglas and T.W. Cronin

Part IV Infrared-Perception

- 8 Matched Filter Properties of Infrared Receptors Used for Fire and Heat Detection in Insects** 207
Helmut Schmitz, Anke Schmitz, and Erik S. Schneider

Part V Electoreception

**9 Matched Filtering in African Weakly Electric Fish:
Two Senses with Complementary Filters** 237
Gerhard von der Emde and Tim Ruhl

Index 265

Part I

Chemoreception

Adaptive Processing in the Insect Olfactory System

1

Jeffrey A. Riffell and John G. Hildebrand

Contents

1.1	Introduction	4
1.2	The Olfactory Environment	7
1.2.1	Combined Analytical and Neurophysiological Methods for Identification of VOC Stimuli	10
1.3	Peripheral Processing	10
1.4	Central Processing	12
1.4.1	Mechanisms for Selective Filtering in the Antennal Lobe	12
1.4.2	Higher Brain Centers: The Lateral Protocerebrum	13
1.4.3	Higher Brain Centers: The Mushroom Body	15
1.4.4	Aminergic and Peptidergic Plasticity	16
1.5	Summary and Future Directions	17
	References	18

Abstract

Insects live in a complex olfactory environment containing thousands of volatile organic compounds (olfactory stimuli) at various intensities and mixture proportions, yet insects can detect and respond to specific olfactory stimuli at millisecond timescales. In this chapter, we describe the mechanisms by which the insect olfactory system can efficiently process an olfactory stimulus and how it filters the signal from background noise. Highlighting recent results from a variety of insect species, we consider: (1) the nature of the olfactory environment, (2) how olfactory information is filtered in the periphery, and (3) how the

J.A. Riffell (✉)

Department of Biology, University of Washington, Seattle, WA 98195, USA

e-mail: jriffell@uw.edu

J.G. Hildebrand

Department of Neuroscience, University of Arizona, Tucson, AZ 85721-0077, USA

central nervous system efficiently and adaptively processes olfactory information. We propose that plasticity encoded in state- and learning-related processes allows the insect olfactory system to process and distinguish olfactory signals efficiently from background and to allow both the large-scale (e.g., meaning or value) and fine-scale (e.g., identity and composition) features of a stimulus to be encoded.

Abbreviations

AL	Antennal lobe
GABA	γ -Aminobutyric acid
GC	Gas chromatography
GC-EAD	Gas chromatography coupled with electroantennographic detection
iLPN	Interneuron in the lateral protocerebrum
LN	Local interneuron
LP	Lateral protocerebrum
MB	Mushroom body
OBP	Odorant binding protein
OR	Olfactory receptor
ORC	Olfactory receptor cell
PN	Projection neuron
VOC	Volatile organic compound

1.1 Introduction

The insect olfactory system is an exquisite example of a finely tuned chemical detection system. This system enables insects to detect volatile organic chemical stimuli (hereinafter, VOC stimuli) at extremely low chemical concentrations with an intensity threshold on the order of zeptomolar (equivalent to a teaspoon of sugar dissolved in a volume of water greater than Lake Michigan) and with sampling frequencies on sub-second timescales. Furthermore, insects have the ability to discriminate among closely related stimulus sources and to do so even when the behaviorally important stimulus is embedded in an olfactory environment that shares some of the same constituents as the “meaningful” stimulus itself. Examples of these processes are abundant among diverse insect species. Moths can locate patches of flowers and mates that are tens or hundreds of meters distant (Stockhouse 1976), honeybees can discriminate between VOC stimuli that differ only in one compound (Reinhard et al. 2004; Wright and Smith 2004; Fernandez et al. 2009), and cockroaches can sample a fluctuating VOC stimulus at millisecond timescale (Lemon and Getz 1997, 2000). An insect’s ability to extract, or filter, meaningful

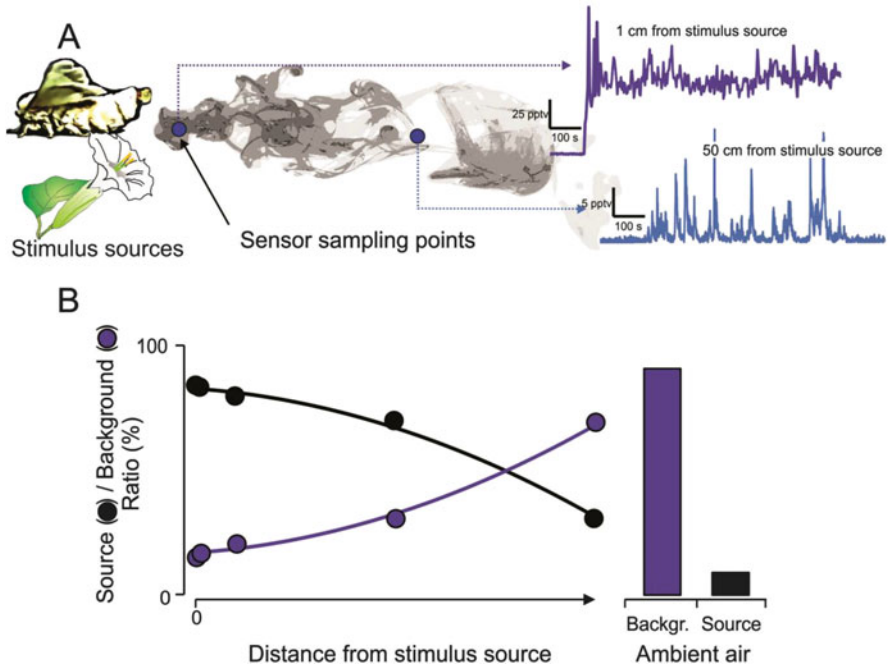


Fig. 1.1 Olfactory stimuli—whether emitted from a female moth or a flower—are dynamic in both space and time (a, left) and are rapidly mixed by turbulent movement of the ambient air. (a, right) Near the source (<5 cm), stimulus intensities are high and rarely reach the ambient baseline. However, intensities still fluctuate even above baseline. Farther away from the source, wind breaks up the plume, causing it to become patchy in both space and time. (b) Mixing also begins to embed the “background” VOCs of the ambient environment into the plume. As the plume is dispersed in space, mixing with the background VOCs increases, thereby causing the ratio of source-to-background volatiles to change. Background VOCs can make it difficult for insects to filter the “meaningful” olfactory stimulus from background (Modified from Riffell et al. 2014)

olfactory information raises the question: how does the insect’s olfactory system accomplish these tasks?

Studies of a range of insect species have enriched our understanding of peripheral and central processing of olfactory information in the last two decades. Work in the fruit fly *Drosophila melanogaster* has shown that olfactory receptor proteins (ORs) are rapidly divergent, either through evolutionary drive or genetic drift, and the number and location in the animal of neurons bearing these ORs can in some cases reflect ecological adaptation among closely related species (Dekker et al. 2006). In the insect brain, the number and wiring of neurons in the central nervous system that are devoted to specific VOC stimuli can reflect specialization and possible ecological adaptation (Hansson and Stensmyr 2011; Strausfeld 2012; Clifford and Riffell 2013). Together, these filtering mechanisms—one occurring in the periphery and the other, at the central level—provide the insect with the ability to extract chemical information from the environment, discriminate signal from noise, and resolve distance and orientation to the source (Figs. 1.1, 1.2, and 1.3).

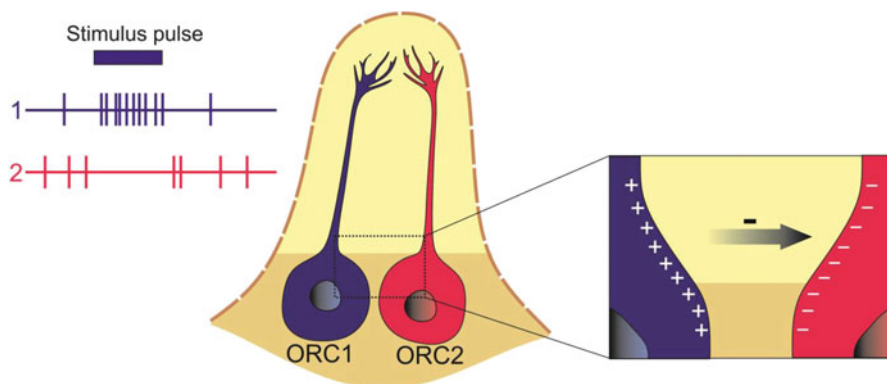


Fig. 1.2 Olfactory receptor cells (ORCs)—each expressing one or two distinct receptor proteins—are housed within the same sensillum (*left*). Although the ORCs are not synaptically coupled, they do interact, where the excitatory activity of one ORC (ORC1) inhibits its neighbor (ORC2). The inhibition may be mediated through the electrical field generated by the apposing ORC, termed ephaptic coupling (*right*) (Modified from Su et al. 2012; Shimizu and Stopfer 2012)

Concurrently with new work on the olfactory processing centers of insects, there has been significant progress in analytical chemical methods required for analysis of the insect olfactory system, identification of bioactive VOC stimuli, and determination of filtering mechanisms in the insect brain (Harris et al. 2008; Riffell et al. 2008; Goldsmith et al. 2011). Insect olfactory systems sample the environment and process VOC stimuli faster than once per second; however, most analytical chemical methods for VOCs require extended time periods for sample collection, preparation, and separation (Tholl and Röse 2006). Thus, temporal resolution of olfactory information has traditionally been lost to scientists. New analytical technologies involving rapid (<1 s or <1 min) sampling times and quantitative resolution are becoming available for chemical ecologists, thereby providing a means for chemical sampling of the volatile environment at timescales approaching those achieved by insect olfactory systems. Furthermore, the ability to combine these new analytical technologies directly with the insect nervous system and behavioral responses has permitted rapid progress in identifying important signal compounds and their physiological effects.

In this review, we focus on how the insect nervous system filters meaningful chemical information from a noisy environment. In particular, we consider pioneering neurophysiological studies that have determined how olfactory information is processed, how the chemical and physical environment itself affects the level of VOC stimulus available to the animal, and the behavioral strategy of the recipient insect. We further consider the roles of peripheral and central olfactory systems in assessing the chemical landscape and processing acquired sensory information. We argue that the combination of active and passive behaviors with adaptive modulation provides insects with an enhanced ability to extract and filter important olfactory information.

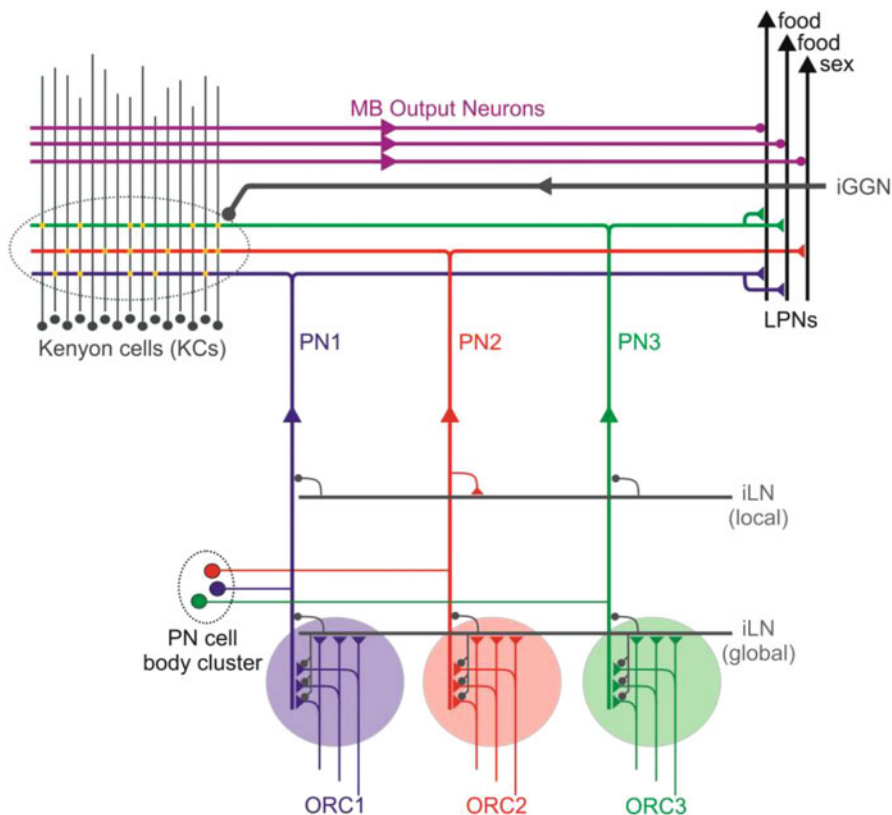


Fig. 1.3 Schematic diagram of the insect olfactory system. ORCs in the antenna and maxillary and/or labial palps project to and converge on a few PNs in each glomerulus (*large shaded circles*). Inhibitory LNs (*gray lines*; local and global) form a network between glomeruli and can project back on the ORC-PN synapse for gain control or synapse on the PN for local contrast enhancement. PNs project to both the MB (learning and memory) and LP (stimulus evaluation and meaning). PNs synapse on a large population of KCs, thereby creating a distinct stimulus “library.” MB output neurons are activated by the KCs and project to the LP. LP neurons can “sum” the input from multiple PNs for one type of stimulus (e.g., food) or receive distinct input from a PN that represents a different type of stimulus (e.g., sex). A giant GABAergic neuron (iGGN) projects back to the MB and possibly mediates the sparse activity of the KCs (Modified from Galizia 2014)

1.2 The Olfactory Environment

VOCs are defined as relatively nonpolar organic compounds of low molecular weight (<300 Da). Because of these chemical and physical constraints, there are a few thousand natural VOCs in the natural environment (El-Sayed 2014). Insects typically respond behaviorally to a mixture of VOCs, not to one compound in a mixture. The proportional composition of the stimulus mixture is important for its

identification and behavioral responses to it (reviewed by Hansson and Stensmyr 2011). Mixtures of VOCs can vary in their complexity and concentration. For example, certain VOC stimuli may contain a few compounds of a particular chemical class, but these VOCs may be particularly important in attracting a given insect (Peakall 1990; Schiestl et al. 1999, 2003; Ayasse et al. 2000). Examples include the night-blooming cereus flower, *Peniocereus greggii*, which emits a fragrance dominated by benzenoid compounds that are attractive to crepuscular hawk moths (Raguso et al. 2003; Riffell et al. 2013). Other VOC stimuli can be complex in the number chemical classes of VOCs and/or, in many cases, the insect olfactory system filters this complexity by processing only a few VOCs in the scent in recognizing the stimulus (Wright and Smith 2004; Riffell et al. 2009a, b; Reinhard et al. 2010).

Once VOC molecules are emitted from a source into a moving fluid—air or water—they are instantly advected into the turbulent fluid flow to form a plume. Although diffusive forces occur, ambient motion has a much stronger role in distributing the compounds. Several excellent reviews of the instantaneous structure of plumes have been published (e.g., Murlis 1992; Murlis et al. 1992; Weissburg 2000; Koehl 2006). Here, we briefly describe plumes as well as the rapidly evolving analytical technology that may be used to characterize and identify behaviorally effective VOCs in airborne plumes.

At spatial scales >1 cm, the olfactory environment is spatiotemporally dynamic. This is crucial for a navigating insect, as behavioral studies in diverse insect species have shown that the near-instantaneous (<1 s) information in a plume, and not the time-averaged properties (Elkinton et al. 1987), is a key requirement for VOC-guided navigation (Mafrá-Neto and Cardé 1994; Vickers and Baker 1994). This is because turbulent VOC plumes are spatially and temporally patchy and composed of spikes or filaments of high VOC concentration interspersed with regions of low concentration (Cardé and Willis 2008). The temporal dynamics of the plume can be due to advective and turbulent forces of the fluid transporting and mixing the plume (Yee et al. 1993a, b; Zimmer and Zimmer 2008) and the position of the source of the compounds in the plume in the boundary layer (Finelli et al. 1999, 2000; Moore and Crimaldi 2004).

In addition to its temporal dynamics, the structure of the plume changes as a function of the distance from the source (Mylne and Mason 1991; Yee et al. 1993a, b; Mole and Jones 1994). These effects were examined first by atmospheric scientists studying pollutant transport and subsequently by chemical ecologists interested in the dispersal and transport insect pheromones. The effects of boundary-layer turbulence and the physical environment are becoming more clearly understood. For example, Dinar and coworkers (1988) and Riffell and coworkers (2014) have found that high concentrations of VOCs in a plume were present at a position <1 m downwind from the source approximately 75 % of the time, but concentrations decreased to 20 % and occurred only 20 % of the time at greater distances. The turbulent eddies that mix and transport the plume occur at multiple spatial scales, both larger and smaller than the width of the plume. Sampling the stimulus plume at a given distance downwind from the source can

reflect the large- and small-scale motions of the eddies, where high-intensity, rapidly fluctuating bursts of the signal (reflecting the small-scale eddies) can be followed by longer periods of no signal (reflecting the larger eddies causing the plume to meander). In the plume centerline, the concentration of VOC fluctuations may drop with distance from the source as a result of turbulent mixing and diffusion, although some VOC filaments with high concentration may occur, albeit much less frequently than close to the source.

Large- and small-scale fluctuations in the plume have important effects on plume mixing with the background VOCs in the environment. Although strong turbulent mixing and diffusion cause background VOCs to become completely mixed, the time required for this process to occur is long (on the order of seconds) compared with an insect's olfactory response time (<1 s). Nevertheless, behavioral studies have shown that background VOCs can have strong effects—both positive and negative—on an insect's ability to locate stimulus sources. For example, if the insect can detect background VOCs that also are found in the behaviorally important VOC stimulus, then exposure to background VOCs can cause adaptation and/or sensitization, thereby reducing the insect's ability to locate the source (Schröder and Hilker 2008; Riffell et al. 2014). In some cases, the background VOCs may be dissimilar to those in the behaviorally relevant VOC stimulus (e.g., vegetative VOCs and sex pheromones) but interfere with location of the stimulus source, presumably through peripheral or central olfactory mechanisms (Pregitzer et al. 2012). Alternatively, background VOCs can increase the contrast between the stimulus VOCs and background and thus improve the stimulus-tracking ability of the insect (Kárpáti et al. 2013).

Beyond the passive effects of airflow on chemical signal transmission, chemical information may be modified further before detection by the insect in three different ways: movement of the VOC stimulus source, dynamic changes in VOC release, and active sensing by the insect. Examples of active movement of the VOC source include the active pumping of sex pheromone into the air by certain female moths (Conner et al. 1980) and the manner in which flower positions oscillate owing to biomechanical properties (Sprayberry and Daniel 2007). Intermittent release of VOC stimulus and movement of a stimulus source influence the temporal structure of the resulting plume, thereby creating a biologically mediated intermittency coupled to physically turbulent airflow. In addition, active and passive movement of the insect modifies the boundary layer around olfactory appendages, thereby changing stimulus input. For example, wing-fanning by moths causes passive oscillation of the antennae, thus thinning the boundary layer and potentially increasing the flux of stimulus molecules contacting the olfactory sensilla (Loudon et al. 1994; Loudon and Koehl 2000; Bau et al. 2005; Sane 2006; Sane and Jacobson 2006). Similar effects could occur as a result of active behavior of the insect, including behavioral maneuvers during flight or walking. Changes in the velocity of locomotion also change the boundary layer around the antennae and other sensory appendages. Thus, both the chemical environment and the active movement of the insect can serve to prefilter the type(s) of olfactory information received by the navigating insect.

1.2.1 Combined Analytical and Neurophysiological Methods for Identification of VOC Stimuli

There are two requirements for studying how an insect's olfactory system processes information about VOC stimuli. First, natural, behaviorally effective stimuli at natural concentrations and compositions should be used. Second, robust methods for identifying the VOCs emitted from the source, and specifically those that mediate behaviors of interest, are required. In the last 50 years, research on insect sex pheromones (Roelofs et al. 1971) and food-related scents (Riffell et al. 2009a, b; Schubert et al. 2014) has revealed that the behavioral effectiveness of a VOC mixture often resides in a few key component compounds. Identifying those key components is important for understanding how the olfactory system filters behaviorally relevant chemosensory information from background in a concentration-independent manner.

Insect olfactory research has benefitted from the combination of analytical chemical techniques for isolation and identification of VOCs with neurophysiological methods for testing the ability of individual VOCs to elicit physiological responses at the peripheral and central levels. The primary technique for identification of VOCs that are sensed by an insect's antenna is gas chromatography coupled with electroantennographic detection (GC-EAD) (Moorhouse et al. 1969; Arn et al. 1975). Electroantennographic recording of antennal responses to olfactory stimuli was developed originally by Dietrich Schneider (1957) and later was integrated with GC to constitute GC-EAD for precise identification of VOCs emitted by insects or plants. This method permits simultaneous registration of the VOCs eluting from a GC column and small electrophysiological depolarizations they may evoke in an antennal stimulation by stimulating olfactory receptor cells (ORCs) throughout much of the antenna. Other physiological methods that interface with a GC include the recording of electrophysiological responses of individual ORCs in single olfactory sensilla (GC-single sensillum recording) and responses in the antennal lobe (AL) by means of imaging technology (GC imaging) or multichannel electrodes (GC multichannel recording) (Riffell et al. 2009, 2013; Schubert et al. 2014).

We cite these methods because of their importance in the field of olfactory neurobiology and chemical ecology. By first identifying physiologically active VOCs and then determining their role in behavior, the field of olfactory neurobiology can link the chemical signal, its transmission dynamics, the molecular basis of receptor binding and transduction, and the neural mechanisms in the CNS that mediate behavior (Hansson and Stensmyr 2011).

1.3 Peripheral Processing

Olfactory receptor cells (ORCs), located in sensilla (e.g., sensory hairs or pegs) on appendages (mainly the antennae but also maxillary and/or labial palps), are exquisitely sensitive to the type, intensity, and temporal dynamics of olfactory

stimuli. There have been several excellent reviews on the evolution and function of insect ORCs (e.g., Hansson and Stensmyr 2011; Leal 2013). In this section, we focus on examples of insect ORCs and olfactory receptor proteins (ORs) that exhibit selective filtering of olfactory information.

To transduce the information in the fluctuating stimulus plume, ORCs must quickly respond to the presence of stimulus VOCs. The temporal response profiles of ORCs are typically measured by recording from the sensilla housing the ORCs while delivering pulses of the stimulus at various frequencies. ORCs can detect short (20 ms) pulses of stimulus at relatively high frequencies (5 s^{-1} ; Kaissling and Thorson 1980; Kaissling 1986; Rumbo and Kaissling 1989; Marion-Poll and Tobin 1992). Mixtures of stimulus VOCs can modify the ORC responses. For example, single-sensillum recordings from ORCs of the male moth *Agrotis segetum* specific to the female's sex-pheromone mixture revealed that an ORC specifically tuned to one pheromone component rapidly adapted to the fluctuating plume (Baker et al. 1988). By contrast, the neighboring ORC, located in the same sensillum but specific to the other pheromone component, did not adapt. Thus, individual ORCs can detect and transmit information about the temporal dynamics of specific compounds and together encode the intensity and composition of the mixture.

ORCs each express a single OR, and individual olfactory sensilla contain various numbers of ORCs, each with distinct chemosensory tuning that depends on the OR it expresses (de Bruyne et al. 2001). Alterations in the olfactory periphery may take the form of changes in the tuning of ORs or the abundance of a given type of ORC. A well-studied example of an ecological change is the relationship between a species of *Drosophila* and its host plant *Morinda citrifolia*. *Drosophila sechellia* is closely related to the model organism *D. melanogaster*, which is an ecological generalist. By contrast, *D. sechellia* is highly specialized, ovipositing exclusively on the fruit of *Morinda citrifolia* (Farine et al. 1996; Dekker et al. 2006). To detect *Morinda*-specific VOCs, *D. sechellia* has increased expression of a specific type of antennal sensillum (the ab3 sensillum). This sensillum houses the ab3A and ab3B ORCs that are sensitive to VOCs emitted by *Morinda* fruit, in particular hexanoate esters (ab3a) and 2-heptanone (ab3B) (Ibba et al. 2010). Both of these VOCs are important for attracting *D. sechellia* to *Morinda* fruit (Dekker et al. 2006; Ibba et al. 2010). *D. sechellia* has 150–200 % more ab3 sensilla than *D. melanogaster*, and the ab3A neurons of *D. sechellia* are ten times more sensitive to methyl hexanoate than those of *D. melanogaster* (Dekker et al. 2006). This *D. sechellia* specialization comes at a cost, however; *D. sechellia* has 60–95 % fewer ab1 and ab2 sensilla than *D. melanogaster*.

On a mechanistic level, interactions between different VOC molecules occupying a given OR, or between ORCs in the same sensillum, also may influence the coding of olfactory information. Thus, vegetative VOCs have been shown to modulate pheromone reception in moths when presented in isolation or simultaneously (Van der Pers et al. 1980), and host-plant VOCs can potentiate pheromone-evoked responses (Ochieng et al. 2002). Further work in *D. melanogaster* revealed similar nonadditive effects that can operate on a single OR, presumably through competitive binding (Su et al. 2011) and through interactions between ORCs

housed in the same sensilla (Su et al. 2012). For example, when the ab3A cell expressing OR22 was stimulated with a mixture of methyl hexanoate (which evokes excitation) and 2-heptanone (which evokes suppression), the temporal response characteristics were modified (Su et al. 2011, 2012). In the ab3 sensillum, the response of the ab3A cell was non-synaptically inhibited by transient activation of the ab3B cell. Thus, non-synaptic information flow between ORCs in the same sensillum via an extracellular electrical field may mediate responses to combinations of stimulus VOCs in the same headspace and may contribute to the filtering of olfactory information.

1.4 Central Processing

1.4.1 Mechanisms for Selective Filtering in the Antennal Lobe

Olfactory systems enable insects to distinguish behaviorally relevant VOC stimuli from irrelevant ones and to separate important stimuli from a background of shared VOCs (Baker 2008; Ibba et al. 2010; Riffell et al. 2013). After airborne VOCs are transduced into electrophysiological signals in the ORCs, they are processed in the AL, which is the first-order center in the insect brain for processing of afferent olfactory information (Hildebrand and Shepherd 1997). As in most other animals, these primary olfactory centers are characterized by an array of condensed neuropil structures called glomeruli. A common feature for many insects is that the axons of ORCs expressing a given OR project to the same glomerulus in the AL (Bargmann 2006), thereby forming a chemotropic map. The temporal and spatial activity of this map encodes properties of olfactory stimuli such as identity and concentration. The spatial patterns of glomerular activity that encode a given stimulus compound or mixture are often consistent within a species (Galizia et al. 1999), indicating that conspecifics detect VOCs and process information about them similarly in the AL. ORCs, projection neurons (PNs), and local interneurons (LNs) interact in glomeruli (Homberg et al. 1989; Silbering and Galizia 2007). Thus olfactory information transmitted to the AL by the ORCs is processed through intra- and interglomerular synaptic circuitry, and PNs that innervate the glomeruli convey the results of that processing to higher brain centers such as the lateral protocerebrum and mushroom body. The temporal features of PN activity, such as spike synchrony and latency (reviewed by Laurent 2002; Martin et al. 2011), are important for coding chemical and temporal features of a stimulus plume (Lei et al. 2002, 2004; Riffell et al. 2009b).

Modulation by LNs plays an important role in filtering “significant” stimuli from background and enables processing of the temporal dynamics of the stimulus plume. Neurites of LNs are limited to the AL, and LNs connect glomeruli so that activity in one glomerulus can modify activity in another when both are stimulated. LN activity can modify the representation of stimuli provided by the ORCs (Matsumoto and Hildebrand 1981; Christensen et al. 1993; Hildebrand 1995; Olsen and Wilson 2008). Depending on the insect species in question, AL LNs

are mostly or entirely inhibitory and GABAergic (Hildebrand et al. 1992; Olsen et al. 2007; Olsen and Wilson 2008), but some may be excitatory and cholinergic (Olsen et al. 2007; Yaksi and Wilson 2010). The overall effect of interglomerular inhibition dominates that of excitation (Olsen and Wilson 2008). LN activity can influence a variety of AL coding mechanisms, including gain, which alters the relative strength of output to input, and synchronized activity of PNs, which helps to bind neural representations of mixture components into unitary percepts. LN-mediated inhibition also enhances the accuracy of the onset and offset time of a stimulus (Christensen et al. 1993; Sachse and Galizia 2002; Mwilaria et al. 2008) and the temporal response when the fluctuating stimulus is presented in the presence of background VOCs (Riffell et al. 2014). Importantly, pharmacological or genetic manipulation of LN activity modifies the perception of the stimulus and the behavior it evokes (Acebes et al. 2011) and plays a crucial role in navigation in a VOC plume (Lei et al. 2009; Riffell et al. 2014).

In *Drosophila*, there are two broad types of LNs (local and global) that may mediate AL responses to different kinds and intensities of stimulus VOCs. Global LNs play an important role in gain control, because global lateral inhibition scales with input to the ALs (Root et al. 2007). It has been suggested that glomerular innervation is correlated with ORC input, with higher LN innervation associated with those glomeruli that receive greater ORC responses (Chou et al. 2010; Olsen et al. 2010). In a related manner, interglomerular inhibition increases as the number of constituents in a VOC mixture increases, thus providing a gain-control mechanism for stimuli with high intensities and/or complexity and background. By contrast, LNs that are limited in their innervation patterns may be involved in selective sharpening and increasing the contrast of glomerular responses, although they too are involved in suppression of mixture-evoked responses (Silbering and Galizia 2007). Sharpening of the representation of an olfactory stimulus occurs when inhibitory LNs prevent weak afferent input from contributing to the representation, thus allowing responses of glomeruli that receive the strongest input (Wilson et al. 2004; Linster et al. 2005; Galizia and Sachse 2010). The effects of global and local LNs on gain control and input sharpening may be effective filters as an insect navigates to a stimulus plume in a complex background. As the animal gets closer to the source, which is associated with an increase in stimulus intensity, the representation of the stimulus will become clearer and the effects of gain and signal-to-noise ratio may become important features that are integrated with other sensory mechanisms to resolve the spatial location of a stimulus source (van Breugel and Dickinson 2014).

1.4.2 Higher Brain Centers: The Lateral Protocerebrum

After synaptic processing in the AL, PNs convey information about the olfactory stimulus to higher-order olfactory centers in the protocerebrum including the mushroom bodies (MBs) and lateral protocerebrum (LP). Anatomical and physiological studies show that there is substantial convergence in the AL from the ORCs

to the PNs; however, from the AL there is substantial divergence as PNs synapse on multiple postsynaptic neurons in both the MBs and LP (e.g., the lateral horn, the inferior lateral protocerebrum, and the lateral accessory lobe) (Kanzaki et al. 1989, 1991, 1994; Stocker et al. 1990; Hansson et al. 1996; Wong et al. 2002; Seki et al. 2005; Kirschner et al. 2006; Jefferis et al. 2007). In diverse insects, the LP receives input from both uniglomerular PNs (uPNs) and multiglomerular PNs (mPNs) that arborize in multiple glomeruli (Galizia and Rössler 2010). The PN types differ, as uPNs are excitatory and cholinergic, and send axons first to the MB and then terminate in the LP. By contrast, mPNs are primarily inhibitory and GABAergic and send axons first to the LP and then terminate in the MB (Kanzaki et al. 2003; Rø et al. 2007; Galizia and Rössler 2010). Thus, there are substantial divergence and connectivity between the MB and the LP and a combination of feed-forward excitation and inhibition to the LP.

The LP was traditionally thought to be a premotor or behavioral processing center for innately important stimuli such as sex pheromones. More recent work, however, in fruit flies, bees, and moths suggests that the LP is important for encoding the valence of a stimulus, which determines whether it is a food scent or a sex pheromone (Jefferis et al. 2007; Lei et al. 2013; Liang et al. 2013; Martin et al. 2013; Roussel et al. 2014). In fruit flies (*D. melanogaster*) and honeybees (*Apis mellifera*), the pattern of activated glomeruli correlates with the behavioral bias between pairs of olfactory stimuli, and those with different valences also have greater separation in their respective pattern of glomerular responses. These valences are reflected by the spatial activity in the LP that receives the stimulus from excitatory PNs; innately attractive food VOCs are represented spatially distinctly from those of innately attractive pheromones (Jefferis et al. 2007; Parnas et al. 2013; Roussel et al. 2014). In *Drosophila*, specific LP neurons sum the input from multiple glomeruli (the DM1, DM2, and DM4 glomeruli) that together encode innately attractive food VOCs related to yeast (Fişek and Wilson 2013). In addition to feed-forward excitatory input, activity by inhibitory PNs plays an important role in increasing separation of stimuli, and differences in this input may reflect the functions of the LP circuitry (Parnas et al. 2013; Fişek and Wilson 2013). In the giant sphinx moth *Manduca sexta*, sex pheromone and plant-related VOCs elicit specific and selective responses in LP neurons, and computations in the LP may infrequently reflect the composition of a behaviorally effective stimulus (Lei et al. 2013). These moths exhibit strong ratio-specific behaviors to synthetic sex pheromone mixtures, and synchronized activity by AL PNs maximally occurs upon stimulation with the most behaviorally effective ratio of pheromone components (Martin et al. 2013). The coincident arrival of stimulatory spikes from the PNs may be sufficient to drive a small proportion (20 %) of pheromone-sensitive LP neurons, thus enabling ratio-specific coding to occur (Lei et al. 2013; Martin et al. 2013). A majority of recorded LP neurons, however, do not discriminate the ratio of components in the sex pheromone mixture. This result suggests that these neurons may be similar to those of *Drosophila* and instead encode the general type and/or value of the stimulus rather than its fine features.

LP neurons may play important roles in sensory fusion and multimodal behavior. For example, in the locust (*Schistocerca americana*) and in moths, LP neurons respond to light (Gupta and Stopfer 2012) and mechanosensory stimuli (Lei et al. 2013). In *M. sexta* moths, these multimodal LP neurons, with arborizations in ventral protocerebral (VPC) neuropil, are thought to be involved in mediating stimulus-tracking behavior (Kanzaki et al. 1994), when the merging of olfactory and mechanosensory information is needed for moths to navigate effectively in the stimulus plume. Other LP-VPC neurons have processes that extend into the contralateral optic lobes and may respond to visual input (Lei et al. 2013). Thus, these neurons may be crucial for the integration of sensory information involved in flight control and may function as pattern generators for controlling the source-searching (casting) behaviors.

1.4.3 Higher Brain Centers: The Mushroom Body

For various insects, processes and excitatory input from the AL form synaptic connections with a large population of Kenyon cells (KCs) in the calyces of the MBs. This is reflected in the numbers of KCs (approximately 2,500 in *D. melanogaster* and 180,000 in *A. mellifera*) that receive input from a much smaller number of AL PNs (approximately 150 for *Drosophila* and 800 for honeybees). Each KC is driven by the population of PNs providing synaptic input to it. Thus, this across-fiber pattern of input to KCs supports a higher-dimensional library of stimulus-evoked patterns. For this reason, the MB is thought to be involved in identification of VOC stimuli. A large body of experimental evidence shows that the MB is an important site of olfactory learning, further supporting this hypothesis (Heisenberg et al. 1985; de Belle and Heisenberg 1994; Durst et al. 1994; Strausfeld et al. 1995; Dubnau et al. 2001; Perez-Orive et al. 2002; Heisenberg 2003).

In contrast to the overlapping glomerular representations of olfactory stimuli in the AL, KC responses are sparse and more distinct (Perez-Orive et al. 2002; Turner et al. 2008; Szyszka et al. 2008). Each KC receives input from multiple PNs and must receive convergent input from multiple glomeruli to respond (Turner et al. 2008). The convergent input enables KCs to represent diverse stimuli. When combined with modulation through learning (detailed below), the coding space increases further and provides an enhanced ability to filter olfactory information. However, given the multiglomerular input from the AL, how do KC responses remain sparse? Originally thought to be mediated through a population of GABAergic interneurons in the LP (iLPNs) that extend processes to the MB, the dynamic excitation from the AL was thought to be rapidly followed by inhibition from the iLPNs, thus creating a sparse KC response (Perez-Orive et al. 2002). More recent work has shown that these iLPNs were misidentified and are not GABAergic (Gupta and Stopfer 2012). Although the MB receives inhibitory input from giant GABAergic neurons (also classified as C5 neurons), it is unclear what might be

driving them, although they extend arborizations into the MB calyx and provide the greatest source of inhibitory input to the KCs (Gupta and Stopfer 2012).

Output (extrinsic) neurons in the MB α -lobe receive input from a varied population of KCs and project to other regions of the brain including the LP (Rybak and Menzel 1993; Okada et al. 2003). In untrained insects, these output neurons show broad tuning to olfactory input from the KCs; similar to LP neurons, they do not represent the fine features of an olfactory stimulus (Strube-Bloss et al. 2011). α -Lobe output neurons, however, change their responses after olfactory conditioning (Strube-Bloss et al. 2011). Recording ensemble responses of α -lobe output neurons during olfactory conditioning of honeybees revealed that 50 % of the neurons underwent changes in their response profiles. Output neurons also showed greater responses to the rewarded stimulus (CS+) than the unrewarded stimulus (CS-). The change in responses to rewarded, unrewarded, or control stimuli might reflect increased PN drive to KCs via aminergic modulation and change in synaptic density of KC responses during learning. The α -lobe ensemble responses showed quicker discrimination times than the AL PN responses, suggesting that a subpopulation of AL PNs may play an important role in fast decision times and α -lobe computations and feedback (Strube-Bloss et al. 2012).

1.4.4 Aminergic and Peptidergic Plasticity

It is unclear why the peripheral olfactory system appears to filter olfactory information at a fine level (e.g., VOC identities, concentrations, and mixture proportions), whereas higher brain regions (e.g., the LP and MB α -lobe output neurons) appear to filter olfactory information more grossly (significance and/or type of stimulus). This filtering may be due to the plasticity in these areas of the olfactory system. Plasticity, particularly in the AL, has been demonstrated in many insect species, including moths, bees, and flies (Faber et al. 1999; Daly et al. 2004; Denker et al. 2010; Clifford and Riffell 2013; Riffell et al. 2013). The AL receives input from a variety of aminergic neurons (including cells containing serotonin, dopamine, octopamine, and histamine) and peptidergic neurons that project from higher-order brain regions (Anton and Homberg 1999), which may alter the K^+ conductances of AL neurons and modulate neuronal activity (reviewed by Ellen and Mercer 2012). The neurons that release these neuromodulators may signal the context of the olfactory stimulus. It is thought that serotonin modulates olfactory responses based on circadian rhythm (Kloppenborg and Mercer 2008), dopamine modulates responses based on association of the stimulus with an aversive one (Dacks et al. 2012), and octopamine modulates responses based on association of the stimulus with an appetitive one (Schwaerzel et al. 2003). Although these neuromodulators may signal different behavioral contexts, their gross effects on AL responses can be quite similar (Dacks et al. 2012; Riffell et al. 2013).

AL responses are modified after olfactory conditioning to a particular stimulus; glomerular activity patterns change, PN responses are enhanced, and PN temporal responses (synchronized activity between PNs and response latencies) change

(Daly et al. 2004; Riffell et al. 2013). Modulation increases the discrimination of glomerular patterns and PN ensemble responses to closely related stimuli (Yu et al. 2004; Barrozo et al. 2010; Dacks et al. 2012; Riffell et al. 2013). Thus, increased synaptic drive, via increases in firing rate responses and synchronized activity between PNs, strengthens connections with downstream KCs and enhances stimulus identification and filtering. The MB calyx and the AL are sites for convergence of modulatory neurons known to encode appetitive and aversive olfactory stimuli (Hammer 1993; Dacks et al. 2012). KC responses change for both rewarded and unrewarded stimulus recognition (Szyszka et al. 2005).

What role might this modulation play in efficient olfactory coding and behavior? As mentioned above, the olfactory environment is complex, with background VOCs overlapping with “meaningful” VOCs that are emitted from behaviorally significant sources. Adaptive modulation of PN and KC responses may allow the insect olfactory system to learn positive associations rapidly between a novel stimulus and a reward and enable extraction of olfactory information from a mélange of related and non-related sources (Riffell et al. 2014).

The behavioral or physiological state of the insect can play an important role in its response to olfactory stimuli; the time of day, feeding status, and mating status may modify the importance or salience of a stimulus (Barrozo et al. 2010; Root et al. 2011). In *D. melanogaster*, appetitive state is signaled by insulin, which upregulates a peptide receptor on the ORCs that innervate the DM1 glomerulus. Activation of the DM1 glomerulus is sufficient to drive the fly to search for food (Root et al. 2011). State-dependent effects can influence olfactory responses in the periphery. For example, the feeding status of mosquitoes can affect the regulation of olfactory binding proteins, which in turn can influence the sensitivity of ORCs in the periphery. Aminergic modulation can influence the gain of neurons at peripheral and central levels (Tomchik and Davis 2009). Modulation of different levels of the olfactory system through different mechanisms can adaptively and efficiently influence olfactory processing.

1.5 Summary and Future Directions

Recent advances in a range of insect taxa provide opportunities for determining how the olfactory system extracts behaviorally significant olfactory stimuli from background noise and how insects efficiently process meaningful VOC stimuli to elicit adaptive behaviors. In particular, our understanding of how olfactory stimuli are filtered and extracted at different levels of the olfactory system—processed first in the periphery, then in the glomeruli of the AL, and ultimately in the neural networks of higher-order regions such as the MBs and LP—remains open for future work. The contribution of processes such as competition between VOCs for access to receptor sites in ORs, ephaptic coupling among ORC axons, and modulatory feedback during state-dependent and learning-related behaviors could be studied in greater depth. The interaction between MB α -lobe output neurons and LP neurons

remains a fruitful avenue of research, in part because of the interaction between learned and innate behaviors. The LP may encode the valence (positive or negative) of the stimulus, whereas the α -lobe neurons may encode its identity. Understanding how glomerular representations in the AL change during learning and how complex olfactory stimuli composed of many VOCs are efficiently encoded seems now to be within reach and beckons to new investigators.

Acknowledgments We thank E. Warrant and G. von der Emde for their invitation to be included in this book. We also thank H. Lei, C. Reisenman, E. Shlizerman, and M. Dickinson for discussions on olfactory filtering and processing. Funding was provided by National Science Foundation (IOS-1354159 and DMS-1361145), the National Institutes of Health (R01DC013693, R01DC02751), and the Human Frontier Science Program (A87616).

References

- Acebes A, Martín-Peña A, Chevalier V, Ferrús A (2011) Synapse loss in olfactory local interneurons modifies perception. *J Neurosci* 31:2734–2745
- Anton S, Homberg U (1999) Antennal lobe structure. In: Hansson BS (ed) *Insect olfaction*. Springer, Berlin, pp 97–124
- Arn H, Städler E, Rauscher S (1975) The electroantennographic detector—a selective and sensitive tool in the gas chromatographic analysis of insect pheromones. *Z Naturforsch Sect C Biosci* 30:722–725
- Ayasse M, Schiestl FP, Paulus HF, Löfstedt C, Hansson B, Ibarra F, Francke W (2000) Evolution of reproductive strategies in the sexually deceptive orchid *Ophrys sphegodes*: how does flower-specific variation of odor signals influence reproductive success? *Evolution* 54:1995–2006
- Baker TC (2008) Balanced olfactory antagonism as a concept for understanding evolutionary shifts in moth sex pheromone blends. *J Chem Ecol* 34:971–981
- Baker TC, Hansson BS, Löfstedt C, Löfqvist J (1988) Adaptation of antennal neurons in moths is associated with cessation of pheromone-mediated upwind flight. *Proc Natl Acad Sci U S A* 85:9826–9830
- Bargmann CI (2006) Comparative chemosensation from receptors to ecology. *Nature* 444:295–301
- Barrozo RB, Gadenne C, Anton S (2010) Switching attraction to inhibition: mating-induced reversed role of sex pheromone in an insect. *J Exp Biol* 213:2933–2939
- Bau J, Justus KA, Loudon C, Cardé RT (2005) Electroantennographic resolution of pulsed pheromone plumes in two species of moths with bipectinate antennae. *Chem Senses* 30:771–780
- Cardé RT, Willis M (2008) Navigational strategies used by insects to find distant, wind-borne sources of odor. *J Chem Ecol* 34:854–866
- Chou Y, Spletter ML, Yaksi E, Leong JCS, Wilson RI, Luo L (2010) Diversity and wiring variability of olfactory local interneurons in the *Drosophila* antennal lobe. *Nat Neurosci* 13:439–449
- Christensen TA, Waldrop BR, Harrow ID, Hildebrand JG (1993) Local interneurons and information processing in the olfactory glomeruli of the moth *Manduca sexta*. *J Comp Physiol A* 173:385–399
- Clifford MR, Riffell JA (2013) Mixture and odorant processing in the olfactory systems of insects: a comparative perspective. *J Comp Physiol A* 199:911–928
- Conner WE, Eisner T, Vander Meer RK, Guerrero A, Ghiringelli D, Meinwald J (1980) Sex attractant of an arctiid moth (*Utetheisa ornatrix*): a pulsed chemical signal. *Behav Ecol Sociobiol* 7:55–63

- Dacks AM, Riffell JA, Martin JP, Gage SL, Nighorn AJ (2012) Olfactory modulation by dopamine in the context of aversive learning. *J Neurophysiol* 108:539–550
- Daly KC, Christensen TA, Lei H, Smith BH, Hildebrand JG (2004) Learning modulates the ensemble representations for odors in primary olfactory networks. *Proc Natl Acad Sci U S A* 101:10476–10481
- De Belle J, Heisenberg M (1994) Associative odor learning in *Drosophila* abolished by chemical ablation of mushroom bodies. *Science* 263:692–695
- De Bruyne M, Foster K, Carlson JR (2001) Odor coding in the *Drosophila* antenna. *Neuron* 30:537–552
- Dekker T, Ibbá I, Siju KP, Stensmyr MC, Hansson BS (2006) Olfactory shifts parallel superspecialism for toxic fruit in *Drosophila melanogaster* sibling, *D. sechellia*. *Curr Biol* 16:101–109
- Denker M, Finke R, Schaupp F, Grün S, Menzel R (2010) Neural correlates of odor learning in the honeybee antennal lobe. *Eur J Neurosci* 31:119–133
- Dinar N, Kaplan H, Kleiman M (1988) Characterization of concentration fluctuations of a surface plume in a neutral boundary layer. *Bound-Layer Meteorol* 45:157–175
- Dubnau J, Grady L, Kitamoto T, Tully T (2001) Disruption of neurotransmission in *Drosophila* mushroom body blocks retrieval but not acquisition of memory. *Nature* 411:476–480
- Durst C, Eichmüller S, Menzel R (1994) Development and experience lead to increased volume of subcompartments of the honeybee mushroom body. *Behav Neural Biol* 62:259–263
- Elkinton JS, Schal C, Onot T, Cardé RT (1987) Pheromone puff trajectory and upwind flight of male gypsy moths in a forest. *Physiol Entomol* 12:399–406
- Ellen CW, Mercer AR (2012) Modulatory actions of dopamine and serotonin on insect antennal lobe neurons: insights from studies in vitro. *J Mol Histol* 43:401–404
- El-Sayed AM (2014) The pherobase: database of pheromones and semiochemicals. <http://www.pherobase.com/>
- Faber T, Joerges J, Menzel R (1999) Associative learning modifies neural representations of odors in the insect brain. *Nat Neurosci* 2:74–78
- Farine J-P, Legal L, Moreteau B, Le Quere J-L (1996) Volatile components of ripe fruits of *Morinda citrifolia* and their effects on *Drosophila*. *Phytochemistry* 41:433–438
- Fernandez PC, Locatelli FF, Person-Rennell N, Deleo G, Smith BH (2009) Associative conditioning tunes transient dynamics of early olfactory processing. *J Neurosci* 29:10191–10202
- Finelli CM, Pentcheff ND, Zimmer-Faust RK, Wetthey DS (1999) Odor transport in turbulent flows: constraints on animal navigation. *Limnol Oceanogr* 44:1056–1071
- Finelli CM, Pentcheff ND, Zimmer RK, Wetthey DS (2000) Physical constraints on ecological processes: a field test of odor-mediated foraging. *Ecology* 81:784–797
- Fişek M, Wilson RI (2013) Stereotyped connectivity and computations in higher-order olfactory neurons. *Nat Neurosci* 17:280–288
- Galizia CG (2014) Olfactory coding in the insect brain: data and conjectures. *Eur J Neurosci* 39:1784–1795
- Galizia CG, Rössler W (2010) Parallel olfactory systems in insects: anatomy and function. *Annu Rev Entomol* 55:399–420
- Galizia CG, Sachse S (2010) Odor coding in insects. In: Menini A (ed) *The neurobiology of olfaction*. CRC Press, Boca Raton, pp 35–70
- Galizia CG, Sachse S, Rappert A, Menzel R (1999) The glomerular code for odor representation is species specific in the honeybee *Apis mellifera*. *Nat Neurosci* 2:473–478
- Goldsmith BR, Mitala JJ Jr, Josue J, Castro A, Lerner MB, Bayburt TH, Khamis SM, Jones RA, Brand JG, Sligar SG (2011) Biomimetic chemical sensors using nanoelectronic readout of olfactory receptor proteins. *ACS Nanotechnol* 5:5408–5416
- Gupta N, Stopfer M (2012) Functional analysis of a higher olfactory center, the lateral horn. *J Neurosci* 32:8138–8148
- Hammer M (1993) An identified neuron mediates the unconditioned stimulus in associative olfactory learning in honeybees. *Nature* 366:59–63

- Hansson BS, Stensmyr MC (2011) Evolution of insect olfaction. *Neuron* 72:698–711
- Hansson BS, Ochieng SA, Grosmaître X, Anton S, Njagi PGN (1996) Physiological responses and central nervous projections of antennal olfactory receptor neurons in the adult desert locust, *Schistocerca gregaria* (Orthoptera: Acrididae). *J Comp Physiol A* 179:157–167
- Harris GA, Nyadong L, Fernandez FM (2008) Recent developments in ambient ionization techniques for analytical mass spectrometry. *Analyst* 133:1297–1301
- Heisenberg M (2003) Mushroom body memoir: from maps to models. *Nat Rev Neurosci* 4:266–275
- Heisenberg M, Borst A, Wagner S, Byers D (1985) *Drosophila* mushroom body mutants are deficient in olfactory learning. *J Neurogenet* 2:1–30
- Hildebrand J (1995) Analysis of chemical signals by nervous systems. *Proc Natl Acad Sci U S A* 92:67–74
- Hildebrand JG, Shepherd GM (1997) Mechanisms of olfactory discrimination: converging evidence for common principles across phyla. *Annu Rev Neurosci* 20:595–631
- Hildebrand JG, Christensen TA, Arbas EA, Hayashi JH, Homberg U, Kanzaki R, Stengl M (1992) Olfaction in *Manduca sexta*: cellular mechanisms of responses to sex pheromone. In: Duce IR (ed) *Neurotox'91 – molecular basis of drug and pesticide action*. Elsevier Applied Science, London, pp 323–338
- Homberg U, Christensen TA, Hildebrand JG (1989) Structure and function of the deutocerebrum in insects. *Annu Rev Entomol* 34:477–501
- Ibba I, Angioy A, Hansson B, Dekker T (2010) Macrogglomeruli for fruit odors change blend preference in *Drosophila*. *Naturwissenschaften* 97:1059–1066
- Jefferis GS, Potter CJ, Chan AM, Marin EC, Rohlfsing T, Maurer CR Jr, Luo L (2007) Comprehensive maps of *Drosophila* higher olfactory centers: spatially segregated fruit and pheromone representation. *Cell* 128:1187–1203
- Kaissling K (1986) Temporal characteristics of pheromone receptor cell responses in relation to orientation behaviour of moths. In: Payne TL, Birch MC, Kennedy CEJ (eds) *Mechanisms in insect olfaction*. Clarendon Press, Oxford, pp 193–199
- Kaissling KE, Thorson J (1980) Insect olfactory sensilla: structural, chemical and electrical aspects of the functional organization. In: Sattelle DB, Hall LM, Hildebrand JG (eds) *Receptors for neurotransmitters, hormones and pheromones in insects*. Elsevier/North Holland Biomedical Press, Amsterdam, pp 261–282
- Kanzaki R, Arbas EA, Strausfeld NJ, Hildebrand JG (1989) Physiology and morphology of projection neurons in the antennal lobe of the male moth *Manduca sexta*. *J Comp Physiol A* 165:427–453
- Kanzaki R, Arbas E, Hildebrand J (1991) Physiology and morphology of descending neurons in pheromone-processing olfactory pathways in the male moth *Manduca sexta*. *J Comp Physiol A* 169:1–14
- Kanzaki R, Ikeda A, Shibuya T (1994) Morphological and physiological-properties of pheromone-triggered flipflopping descending interneurons of the male silkworm moth, *Bombyx mori*. *J Comp Physiol A* 175:1–14
- Kanzaki R, Soo K, Seki Y, Wada S (2003) Projections to higher olfactory centers from subdivisions of the antennal lobe macrogglomerular complex of the male silkworm. *Chem Senses* 28:113–130
- Kárpáti Z, Knaden M, Reinecke A, Hansson BS (2013) Intraspecific combinations of flower and leaf volatiles act together in attracting hawkmoth pollinators. *PLoS One* 8:e72805
- Kirschner S, Kleineidam CJ, Zube C, Rybak J, Grünwald B, Rössler W (2006) Dual olfactory pathway in the honeybee, *Apis mellifera*. *J Comp Neurol* 499:933–952
- Kloppenborg P, Mercer AR (2008) Serotonin modulation of moth central olfactory neurons. *Annu Rev Entomol* 53:179–190
- Koehl MAR (2006) The fluid mechanics of arthropod sniffing in turbulent odor plumes. *Chem Senses* 31:93–105

- Laurent G (2002) Olfactory network dynamics and the coding of multidimensional signals. *Nat Rev Neurosci* 3:884–895
- Leal WS (2013) Odorant reception in insects: roles of receptors, binding proteins, and degrading enzymes. *Annu Rev Entomol* 58:373–391
- Lei H, Christensen TA, Hildebrand JG (2002) Local inhibition modulates odor-evoked synchronization of glomerulus-specific output neurons. *Nat Neurosci* 5:557–565
- Lei H, Christensen TA, Hildebrand JG (2004) Spatial and temporal organization of ensemble representations for different odor classes in the moth antennal lobe. *J Neurosci* 24:11108–11119
- Lei H, Riffell J, Gage S, Hildebrand J (2009) Contrast enhancement of stimulus intermittency in a primary olfactory network and its behavioral significance. *J Biol* 8:21
- Lei H, Chiu H-Y, Hildebrand JG (2013) Responses of protocerebral neurons in *Manduca sexta* to sex-pheromone mixtures. *J Comp Physiol A* 199:997–1014
- Lemon W, Getz W (1997) Temporal resolution of general odor pulses by olfactory sensory neurons in American cockroaches. *J Exp Biol* 200:1809–1819
- Lemon WC, Getz WM (2000) Rate code input produces temporal code output from cockroach antennal lobes. *Biosystems* 58:151–158
- Liang L, Li Y, Potter CJ, Yizhar O, Deisseroth K, Tsien RW, Luo L (2013) GABAergic projection neurons route selective olfactory inputs to specific higher-order neurons. *Neuron* 79:917–931
- Linster C, Sachse S, Galizia CG (2005) Computational modeling suggests that response properties rather than spatial position determine connectivity between olfactory glomeruli. *J Neurophysiol* 93:3410–3417
- Loudon C, Koehl MAR (2000) Sniffing by a silkworm moth: wing fanning enhances air penetration through and pheromone interception by antennae. *J Exp Biol* 203:2977–2990
- Loudon C, Best BA, Koehl MAR (1994) When does motion relative to neighboring surfaces alter the flow-through arrays of hairs. *J Exp Biol* 193:233–254
- Mafra-Neto A, Carde RT (1994) Fine-scale structure of pheromone plumes modulates upwind orientation of flying moths. *Nature* 369:142–144
- Marion-Poll F, Tobin T (1992) Temporal coding of pheromone pulses and trains in *Manduca sexta*. *J Comp Physiol A* 171:505–512
- Martin JP, Beyerlein A, Dacks AM, Reisenman CE, Riffell JA, Lei H, Hildebrand JG (2011) The neurobiology of insect olfaction: sensory processing in a comparative context. *Prog Neurobiol* 95:427–447
- Martin JP, Lei H, Riffell JA, Hildebrand JG (2013) Synchronous firing of antennal-lobe projection neurons encodes the behaviorally effective ratio of sex-pheromone components in male *Manduca sexta*. *J Comp Physiol A* 199:963–979
- Matsumoto SG, Hildebrand JG (1981) Olfactory mechanisms in the moth *Manduca sexta*: response characteristics and morphology of central neurons in the antennal lobes. *Proc R Soc Lond B* 213:249–277
- Mole N, Jones C (1994) Concentration fluctuation data from dispersion experiments carried out in stable and unstable conditions. *Bound-Layer Meteorol* 67:41–74
- Moore P, Crimaldi J (2004) Odor landscapes and animal behavior: tracking odor plumes in different physical worlds. *J Mar Syst* 49:55–64
- Moorhouse JE, Yeadon R, Beever PS, Nesbitt BF (1969) Method for use in studies of insect chemical communication. *Nature* 223:1174–1175
- Murlis J, Elkinton JS, Carde RT (1992) Odor plumes and how insects use them. *Annu Rev Entomol* 37:505–532
- Mwilaria EK, Ghatak C, Daly KC (2008) Disruption of GABA A in the insect antennal lobe generally increases odor detection and discrimination thresholds. *Chem Senses* 33:267–281
- Myrne KR, Mason P (1991) Concentration fluctuation measurements in a dispersing plume at a range of up to 1000 m. *Q J R Meteorol Soc* 117:177–206
- Ochieng S, Park K, Baker T (2002) Host plant volatiles synergize responses of sex pheromone-specific olfactory receptor neurons in male *Helicoverpa zea*. *J Comp Physiol A* 188:325–333

- Okada R, Sakura M, Mizunami M (2003) Distribution of dendrites of descending neurons and its implications for the basic organization of the cockroach brain. *J Comp Neurol* 458:158–174
- Olsen SR, Wilson RI (2008) Lateral presynaptic inhibition mediates gain control in an olfactory circuit. *Nature* 452:956–960
- Olsen SR, Bhandawat V, Wilson RI (2007) Excitatory Interactions between olfactory processing channels in the *Drosophila* antennal lobe. *Neuron* 54:89–103
- Olsen SR, Bhandawat V, Wilson RI (2010) Divisive normalization in olfactory population codes. *Neuron* 66:287
- Parnas M, Lin AC, Huetteroth W, Miesenböck G (2013) Odor discrimination in *Drosophila*: from neural population codes to behavior. *Neuron* 79:932–944
- Peakall R (1990) Responses of male *Zaspilothynnus trilobatus* turner wasps to females and the sexually deceptive orchid it pollinates. *Funct Ecol* 159–167
- Perez-Orive J, Mazor O, Turner GC, Cassenaer S, Wilson RI, Laurent G (2002) Oscillations and sparsening of odor representations in the mushroom body. *Science* 297:359–365
- Pregitzer P, Schubert M, Breer H, Hansson BS, Sachse S, Krieger J (2012) Plant odorants interfere with detection of sex pheromone signals by male *Heliothis virescens*. *Front Cell Neurosci* 6:42
- Raguso RA, Henzel C, Buchman SL, Nabhan GP (2003) Trumpet flowers of the Sonoran Desert: floral biology of *Peniocereus cacti* and Sacred Datura. *Int J Plant Sci* 164:877–892
- Reinhard J, Srinivasan MV, Guez D, Zhang SW (2004) Floral scents induce recall of navigational and visual memories in honeybees. *J Exp Biol* 207:4371–4381
- Reinhard J, Sinclair M, Srinivasan MV, Claudianos C (2010) Honeybees learn odour mixtures via a selection of key odorants. *PLoS ONE* 5:e9110
- Riffell JA, Abrell L, Hildebrand JG (2008) Physical processes and real-time chemical measurement of the insect olfactory environment. *J Chem Ecol* 34:837–853
- Riffell JA, Lei H, Christensen TA, Hildebrand JG (2009a) Characterization and coding of behaviorally significant odor mixtures. *Curr Biol* 19:335–340
- Riffell JA, Lei H, Hildebrand JG (2009b) Neural correlates of behavior in the moth *Manduca sexta* in response to complex odors. *Proc Natl Acad Sci U S A* 106:19219–19226
- Riffell JA, Lei H, Abrell L, Hildebrand JG (2013) Neural basis of a pollinator's buffet: olfactory specialization and learning in *Manduca sexta*. *Science* 339:200–204
- Riffell JA, Shlizerman E, Sanders E, Abrell L, Medina B, Hinterwirth AJ, Kutz JN (2014) Flower discrimination by pollinators in a dynamic chemical environment. *Science* 344:1515–1518
- Rø H, Müller D, Mustaparta H (2007) Anatomical organization of antennal lobe projection neurons in the moth *Heliothis virescens*. *J Comp Neurol* 500:658–675
- Roelofs WL, Comeau A, Hill A, Milicevic G (1971) Sex attractant of the codling moth: characterization with electroantennogram technique. *Science* 174:297–299
- Root CM, Semmelhack JL, Wong AM, Flores J, Wang JW (2007) Propagation of olfactory information in *Drosophila*. *Proc Natl Acad Sci U S A* 104:11826–11831
- Root CM, Ko KI, Jafari A, Wang JW (2011) Presynaptic facilitation by neuropeptide signaling mediates odor-driven food search. *Cell* 145:133–144
- Roussel E, Carcaud J, Combe M, Giurfa M, Sandoz J-C (2014) Olfactory coding in the honeybee lateral horn. *Curr Biol* 24:561–567
- Rumbo E, Kaissling K-E (1989) Temporal resolution of odour pulses by three types of pheromone receptor cells in *Antheraea polyphemus*. *J Comp Physiol A* 165:281–291
- Rybak J, Menzel R (1993) Anatomy of the mushroom bodies in the honey bee brain: the neuronal connections of the alpha-lobe. *J Comp Neurol* 334:444–465
- Sachse S, Galizia CG (2002) Role of inhibition for temporal and spatial odor representation in olfactory output neurons: a calcium imaging study. *J Neurophysiol* 87:1106–1117
- Sane SP (2006) Induced airflow in flying insects I. A theoretical model of the induced flow. *J Exp Biol* 209:32–42
- Sane SP, Jacobson NP (2006) Induced airflow in flying insects II. Measurement of induced flow. *J Exp Biol* 209:43–56

- Schiestl FP, Ayasse M, Paulus HF, Löfstedt C, Hansson BS, Ibarra F, Francke W (1999) Orchid pollination by sexual swindle. *Nature* 399:421–421
- Schiestl FP, Peakall R, Mant JG, Ibarra F, Schulz C, Franke S, Francke W (2003) The chemistry of sexual deception in an orchid-wasp pollination system. *Science* 302:437–438
- Schneider D (1957) Elektrophysiologische Untersuchungen von Chemo- und Mechanorezeptoren der Antenne des Seidenspinners *Bombyx mori* L. *J Comp Physiol A* 40:8–41
- Schröder R, Hilker M (2008) The relevance of background odor in resource location by insects: a behavioral approach. *Bioscience* 58:308–316
- Schubert M, Hansson BS, Sachse S (2014) The banana code—natural blend processing in the olfactory circuitry of *Drosophila melanogaster*. *Front Physiol* 5:59
- Schwaerzel M, Monastirioti M, Scholz H, Friggi-Grelin F, Birman S, Heisenberg M (2003) Dopamine and octopamine differentiate between aversive and appetitive olfactory memories in *Drosophila*. *J Neurosci* 23:10495–10502
- Seki Y, Aonuma H, Kanzaki R (2005) Pheromone processing center in the protocerebrum of *Bombyx mori* revealed by nitric oxide-induced anti-cGMP immunocytochemistry. *J Comp Neurol* 481:340–351
- Shimizu K, Stopfer M (2012) Olfaction: intimate neuronal whispers. *Nature* 492:44–45
- Silbering AF, Galizia CG (2007) Processing of odor mixtures in the *Drosophila* antennal lobe reveals both global inhibition and glomerulus-specific interactions. *J Neurosci* 27:11966–11977
- Sprayberry JD, Daniel TL (2007) Flower tracking in hawkmoths: behavior and energetics. *J Exp Biol* 210:37–45
- Stocker RF, Lienhard MC, Borst A, Fischbach K-F (1990) Neuronal architecture of the antennal lobe in *Drosophila melanogaster*. *Cell Tissue Res* 262:9–34
- Stockhouse REI (1976) A new method for studying pollen dispersal using micronized fluorescent dusts. *Am Midl Nat* 96:241–245
- Strausfeld NJ (2012) Arthropod brains: evolution, functional elegance, and historical significance. Belknap Press of Harvard University Press, Cambridge, MA
- Strausfeld NJ, Bushbeck EK, Gomez RS (1995) The arthropod mushroom body: its functional roles, evolutionary enigmas and mistaken identities. In: Breidback O, Kutsch W (eds) *The nervous system of invertebrates, a evolutionary and comparative approach*. Birkhäuser, Basel, pp 349–381
- Strube-Bloss MF, Nawrot MP, Menzel R (2011) Mushroom body output neurons encode odor–reward associations. *J Neurosci* 31:3129–3140
- Strube-Bloss MF, Herrera-Valdez MA, Smith BH (2012) Ensemble response in mushroom body output neurons of the honey bee outpaces spatiotemporal odor processing two synapses earlier in the antennal lobe. *PLoS One* 7:e50322
- Su C-Y, Martelli C, Emonet T, Carlson JR (2011) Temporal coding of odor mixtures in an olfactory receptor neuron. *Proc Natl Acad Sci U S A* 108:5075–5080
- Su C-Y, Menuz K, Reisert J, Carlson JR (2012) Non-synaptic inhibition between grouped neurons in an olfactory circuit. *Nature* 492:66–71
- Szyszka P, Ditzen M, Galkin A, Galizia CG, Menzel R (2005) Sparsening and temporal sharpening of olfactory representations in the honeybee mushroom bodies. *J Neurophysiol* 94:3303–3313
- Szyszka P, Galkin A, Menzel R (2008) Associative and non-associative plasticity in Kenyon cells of the honeybee mushroom body. *Front Syst Neurosci* 2:3
- Tholl D, Röse USR (2006) Detection and identification of floral scent compounds. In: Dudareva N, Pichersky E (eds) *Biology of floral scent*. CRC Taylor Francis, Boca Raton, pp 3–25
- Tomchik SM, Davis RL (2009) Dynamics of learning-related cAMP signaling and stimulus integration in the *Drosophila* olfactory pathway. *Neuron* 64:510–521
- Turner GC, Bazhenov M, Laurent G (2008) Olfactory representations by *Drosophila* mushroom body neurons. *J Neurophysiol* 99:734–746
- Van Breugel F, Dickinson MH (2014) Plume-tracking behavior of flying *Drosophila* emerges from a set of distinct sensory-motor reflexes. *Curr Biol* 24:274–286

- Van Der Pers J, Thomas G, Den Otter C (1980) Interactions between plant odours and pheromone reception in small ermine moths (Lepidoptera: Yponomeutidae). *Chem Senses* 5:367–371
- Vickers N, Baker T (1994) Reiterative responses to single strands of odor promote sustained upwind flight and odor source location by moths. *Proc Natl Acad Sci U S A* 91:5756–5760
- Weissburg M (2000) The fluid dynamical context of chemosensory behavior. *Biol Bull* 198:188–202
- Wilson RI, Turner GC, Laurent G (2004) Transformation of olfactory representations in the *Drosophila* antennal lobe. *Science* 303:366–370
- Wong AM, Wang JW, Axel R (2002) Spatial representation of the glomerular map in the *Drosophila* protocerebrum. *Cell* 109:229–241
- Wright GA, Smith BH (2004) Variation in complex olfactory stimuli and its influence on odour recognition. *Proc R Soc Lond Ser B* 271:147–152
- Yaksi E, Wilson RI (2010) Electrical coupling between olfactory glomeruli. *Neuron* 67:1034–1047
- Yee E, Kosteniuk P, Chandler G, Biloft C, Bowers J (1993a) Statistical characteristics of concentration fluctuations in dispersing plumes in the atmospheric surface layer. *Bound-Layer Meteorol* 65:69–109
- Yee E, Wilson D, Zelt B (1993b) Probability distributions of concentration fluctuations of a weakly diffusive passive plume in a turbulent boundary layer. *Bound-Layer Meteorol* 64:321–354
- Yu D, Ponomarev A, Davis RL (2004) Altered representation of the spatial code for odors after olfactory classical conditioning: memory trace formation by synaptic recruitment. *Neuron* 42:437–449
- Zimmer RK, Zimmer C (2008) Dynamic scaling in chemical ecology. *J Chem Ecol* 34:822–836

Part II

Mechanoreception and Audition

A Spider's Sense of Touch: What to Do with Myriads of Tactile Hairs?

2

Friedrich G. Barth

Contents

2.1	Introduction	28
2.2	Numbers and Morphological Types	29
2.3	Distribution	34
2.4	Coping with the Stimulus by Well-Matched Micromechanics	34
2.4.1	The "Clever" Hair Shaft	34
2.4.2	The Coupling of the Sensory Dendrites	37
2.4.3	Forces, Torques, and Directionality	38
2.5	Types of Physiological Responses and Information Encoding	41
2.6	Matched to Specific Behaviors?	41
2.6.1	Actively Gained Contact Information for the Adaptive Control of Locomotion	42
2.6.2	Simple Stereotyped Behavior	45
2.7	Concluding Remarks	52
	References	54

Abstract

Some spiders are densely covered by an intriguingly large number of mechanoreceptive hairs on their exoskeleton, the wandering spider *Cupiennius salei* being the main example examined here. All of these hairs represent first-order lever arms, whose deflection triggers nervous impulses in the sensory cells ending at their base. Their sensitivities differ greatly. By far the most sensitive hairs are the trichobothria. They respond to the frictional forces contained in the slightest movement of air. The large majority of the hairs, however, are much less sensitive. They represent touch receptors, including proprioceptive hairs, which monitor the movements of joints. The mechanical properties of the hairs such as their resistance to deflection and their directional properties vary as do

F.G. Barth (✉)

Department for Neurobiology, Faculty of Life Sciences, University of Vienna, Althanstr. 14,
1090 Vienna, Austria

e-mail: friedrich.g.barth@univie.ac.at

details of their morphology (like structure of socket and outer hair shaft, length, angle of hair insertion). Although such differences are graduated, the distributions of some main morphological types form stereotyped patterns on the spider exoskeleton. The functional significance of these patterns in regard to particular behaviors is largely unknown. The enormous versatility of the tactile sense nevertheless clearly emerges from the analysis of prominent examples of hairs and their relation to behavior. Like in other senses, stimulus transformation turns out to be a most important evolutionary playground for biologically applied physics and to a large extent to be responsible for the fine-tuned match between the sensor and the adequate stimulus patterns which it is meant to receive for different behavioral tasks.

2.1 Introduction

The diversity and ingenuity of animal sensors have evolved to enable organisms to behave in favor of their fitness. Animal sensors absorb energy of different form in tiny quantities and generate electrical signals which carry the relevant information about their inside and outside world to the central nervous system. To a large extent the picture the central nervous system creates of an animal's environment and *in*vironment is based on this information. However, this information is by no means comprehensive in a physical sense but instead a highly filtered, limited, distorted, and species-specific image of what can be measured objectively. Like art (according to a saying by Pablo Picasso, Wilson 1984), sensory images are lies that help the animal to recognize the biologically relevant truth. Once we know these images, they also help us to recognize the role a specific sense organ plays as a mediator between the environment and behavior. We therefore expect to find important aspects of an animal's habitat to be reflected in the properties of sense organs and in the way the information provided by them is handled. This is what sensory ecology and this book mainly is about (see also Dusenbery 1992; Barth and Schmid 2001; Barth 2002a).

Sensory ecology has old roots, dating back at least to the early twentieth century, when Jacob von Uexküll (1909, 1920) stressed the subjectivity and predetermination of an organism's relations to its environment and their species-specific uniqueness. Thus, a sensor's technical refinement is only one side of this coin. The other side, brilliantly demonstrated by the work of Karl von Frisch (1965) and his many followers, is its match to specific features of the biologically relevant stimulus patterns and the performance of the entire organism in its habitat (Barth 2002a). As pointed out by Wehner (1987) in his seminal paper on "matched filters" in spatial orientation, animals often use surprisingly simple information to solve a complex behavioral task. They then largely rely on a highly specialized sensory periphery while dealing with natural stimulus patterns of sometimes frightening complexity.

For many if not most spiders, the mechanical senses are particularly important for the guidance of their behavior. Their mechanical senses are very well developed (Barth 1997, 2002a, b, 2004, 2012b, 2014; Fratzl and Barth 2009). Computational biomechanics and mathematical modeling not only revealed many of the physical constraints underlying their operation but also helped to understand tendencies of adaptation and to predict optimizing tendencies of natural selection (Dechant et al. 2001; Bathellier et al. 2005, 2012; Höbl et al. 2006, 2007, 2009, 2014; Humphrey and Barth 2008). Spider mechanosensors respond to a wide range of stimuli. These include the energy contained in minute substrate vibrations down to displacement values of 10^{-7} m (Barth and Geethabali 1982), the slightest whiff of air down to velocities as small as 0.15 mm/s (Barth and Höller 1999; Barth 2014), micro-strains in their exoskeleton, and deformations resulting from them on the order of nanometers (Hössl et al. 2009; Schaber et al. 2012).

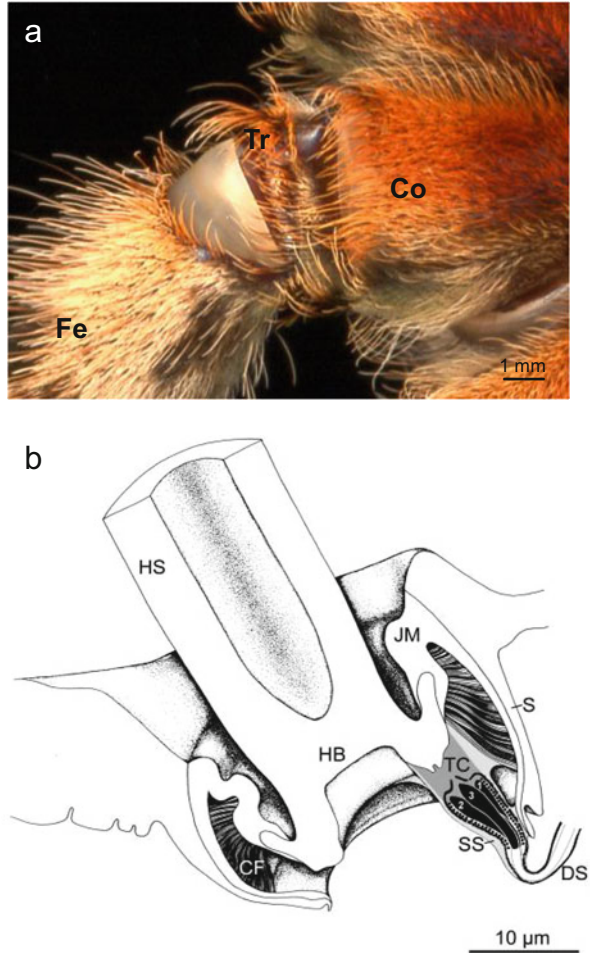
Even when considering all senses including vision, a spider's sensory space is small. There are no long distance senses like our hearing and vision. However, despite its limitation to a few meters at most (vibration sense), the sensory world of spiders is rich, not the least due to a remarkable technical refinement of its mechanoreceptors. Combining research into the behavior, ecology and physical properties of natural stimuli have given us some idea about the evolutionary selection pressures that must have led to the adaptedness of slit sensilla, trichobothria, and tactile hairs (Lit. see above) (for chemoreceptive hairs, see Tichy and Barth 1992; Barth 2002a).

This chapter deals with the tactile sense of *Cupiennius salei*, a wandering spider mainly at home in Mexico and Central America (Barth 2002a; Barth and Cordes 1998, 2008), which has served our research for more than half a century now and found its way into many international laboratories. Research into the tactile sense of arthropods has been much neglected as compared to vision, hearing, and chemoreception, the senses appealing much more to many because of their dominant presence in our own human perceptions and consciousness (Barth 2012a). The tactile sense is a close-range sense par excellence. It seems to be particularly well developed in wandering spiders and prominently contrasts their lack of true long distance sensing. Although still far from a full understanding of the spider tactile sense, there are some interesting facets known already. These may justify the attempt of a review not meant to be exhaustive but pointing to the importance and refinement of the spider tactile sense, as well as to the gaps in our understanding and the challenges and promises of future research.

2.2 Numbers and Morphological Types

The sensilla of interest here are cuticular hairlike sensilla protruding from the exoskeleton, which respond to forces deflecting their hair shaft by direct contact. The exoskeleton of *Cupiennius* and many other spiders is densely covered by hairs. Their huge number amounts to several hundreds of thousands in an adult *Cupiennius* (Fig. 2.1a). Hair density is up to $400/\text{mm}^2$ (Eckweiler 1983; Friedrich

Fig. 2.1 (a) Ventral view of the proximal part of a walking leg of *Cupiennius salei*, showing the intriguingly large number of tactile hairs. *Fe* femur, *Tr* trochanter, *Co* coxa. (b) Reconstruction of fine structure of the basal part of a tactile hair (see TaD1 in Fig. 2.4a). CF connecting fibrils, *DS* dendrite sheath, *HB* hair base, *JM* joint membrane, *S* cuticular socket, *SS* socket septum, *TC* terminal connecting material, *1–3* tubular bodies of the three sensory cells innervating the hair (b from Barth et al. 2004)



1998), a number which exceeds that of the mechanoreceptors in the human glabrous skin by far (e.g., Meissner afferents on human fingertip ca. 150/cm²; Johnson et al. 2000). The large majority of the hairs are innervated (Foelix 1985; Friedrich 1998) and show a pronounced cuticular socket structure and a tubular body in their dendrites, indicating their mechanoreceptive function (Foelix 1985). The major exception is the short yellowish plume hairs of adult spiders; they are not innervated (Eckweiler 1983). Even the contact chemoreceptive hairs are supplied by two mechanoreceptive dendrites (in addition to 19 chemoreceptive ones), and some of the scopula hairs ventrally on the tarsus and metatarsus are innervated by one or two sensory cells as well (Foelix 1985; Friedrich 1998).

A pressing question posed by this richness in hair sensilla is whether we can safely distinguish morphological types and how these are distributed over the skeletal surface.

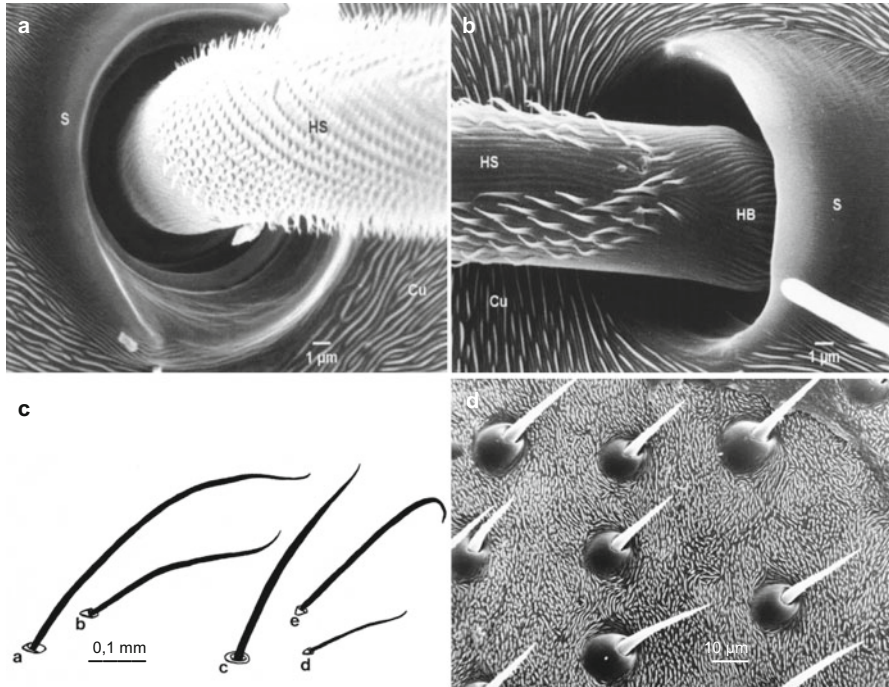


Fig. 2.2 Examples of mechanosensitive hair sensilla of *C. salei* differing morphologically. (a) “Open” round socket of a long tactile hair (1.5 mm) dorsally on the prosoma and forming a steep angle (ca. 82°) with the exoskeletal surface and showing largely isotropic directional properties; for abbreviations, see below. (b) Partly closed, slipper-like socket of tactile hair on the walking leg femur with a much smaller insertion angle and freedom of movement restricted in the direction toward the leg tip; *Cu* cuticle, *HB* hair base, *HS* hair shaft, *S* socket. (c) Variability of the shape of the hair shaft taking tactile hairs on the walking leg (*a*, *b*, *c*) and pedipalpal (*d*, *e*) tarsus as examples; note also differences in socket structure relevant for the mechanical directionality of the hairs and the angle they form with the cuticular surface. (d) Hair plate sensilla on the cheliceral basal segment (posterior side facing the labium) (*a*, *b* from Ullrich 2000, *c*, *d* from Friedrich 1998)

I do not consider the airflow-sensitive trichobothria here. They have received a lot of attention already (Humphrey and Barth 2008; Barth 2014). Nor the scopula hairs of which only a few are innervated and not the contact chemoreceptors. The tactile hairs treated here make up for the majority of all hair sensilla and, depending on their location, serve either exteroceptive or proprioceptive (e.g., hairs at a joint) functions. Like in other spiders, they are innervated by three sensory cells in *Cupiennius* (Foelix 1985; Friedrich 1998), the exception being the single sensory cell innervating the short and stout hairs of the coxal hair plates (Schaxel 1919; Seyfarth et al. 1990) and most likely also the more recently found hair plates on the chelicerae (about 100 sensilla proximally on the basal segment and facing the rostrum and about 45 sensilla in a group facing the midline of the body; Friedrich 1998) (Fig. 2.2d). The so-called long smooth hairs described by Eckweiler et al. (1989) and serving to measure the distance between neighboring coxae are

supplied by one neuron only as well. For details on both the hair plate sensilla and the long smooth hairs, the reader is also referred to the literature.

Assuming that the morphological diversity of tactile hairs is functionally significant, we may hypothesize that their respective patterns of distribution are constant but different on different body areas exposed to different stimulus patterns. To see what the variability is actually like and whether a classification into distinct hair types is possible at all, the following parameters were analyzed (Friedrich 1998): the shape of the hair socket, the hair length, the shape of the hair shaft, and the microtrichs found along its length. As it turns out the distribution pattern of hair types characterized by a certain combination of these parameters indeed is very conservative. However, intermediate forms of hair types are found as well. They render the distinction of clearly separable types more difficult or even doubtful. But what is the variation like?

Hair socket Its diameter varies between 3 and 15 μm , and there are big differences regarding its degree of openness, which affects the directional characteristics of hair shaft deflection (Fig. 2.2a, b). The socket of hairs with a steep insertion angle of 80–90° is round and “open,” whereas it is sunk into the exoskeleton in the direction of the hair shaft’s orientation in hairs with small insertion angles like 30°. As seen from above, this latter type is the “closed,” slipper-like socket type. There are intermediates between these two forms of sockets. Typically, the inner socket rim is smooth, but on the chelicerae, some sockets were found to bulge in a distinct way which strongly affects the hairs’ mechanical directionality.

Hair shaft length and shape The length of the hair shaft varies between ca. 60 μm for hairs with a diameter of ca. 3 μm at their base and ca. 500 μm for hairs with a diameter of ca. 10 μm at their base (measured right above the socket). Hair shaft shape varies greatly (Fig. 2.2c), affecting both a hair’s deflection and deformation under tactile load and its responsiveness for particular load directions. Some hairs are uniformly bent toward the exoskeletal surface, whereas others show s-shaped bends or a strong bend distally only. Another characteristic of *Cupiennius* tactile hairs is the variability of their surface structure (Friedrich 1998). With very few exceptions only, all these hairs are covered by some form of protuberances or microtrichs, which come as scales, may be thorn-like, or form fine pili (branchlets), reminding of the surface of trichobothria, where a fine coat of ‘branchlets’ is increasing the sensitivity to airflow (Barth et al. 1993; Humphrey and Barth 2008). The functional consequences of the surface structures of spider tactile hairs were not studied yet but are expected to affect the friction between the hair and the object touching it and thus the introduction of the tactile force into the hair. A pair of hairs opposing and deflecting each other in this way at the tibia-metatarsus joint is described below (Sect. 2.6.2.3).

Taking all kinds of tactile hairs together, one finds a linear correlation between the socket diameter and hair shaft diameter as well as between shaft diameter and the logarithm of hair length (Fig. 2.3a). Taking the socket diameter and the degree

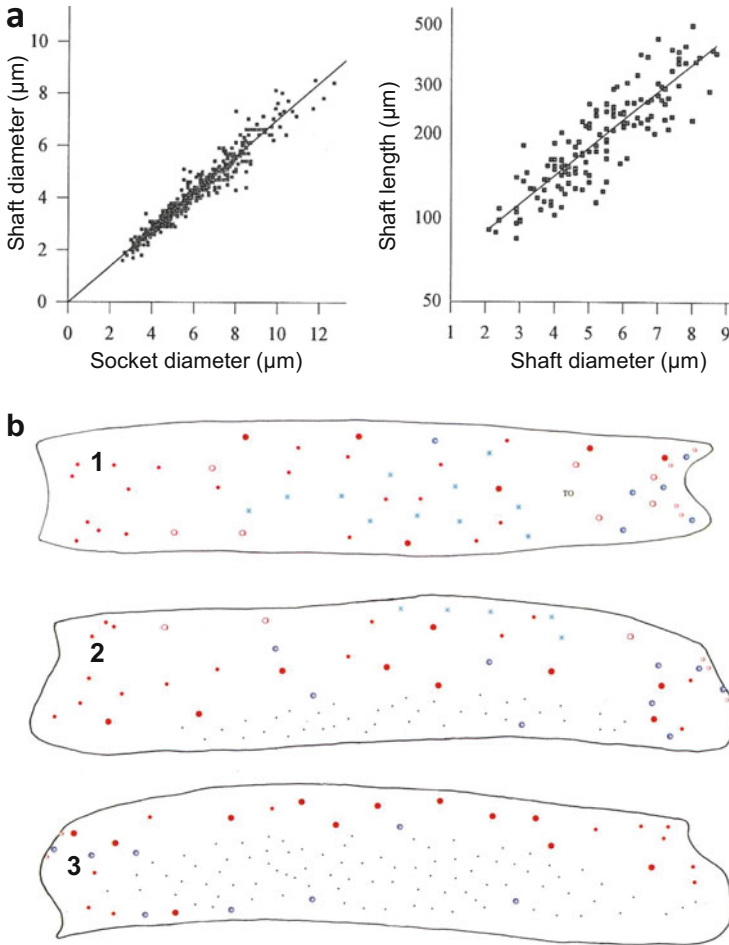


Fig. 2.3 Structural properties common to different tactile hairs on the sternum and the tarsi of walking legs and pedipalps of animals representing the seventh developmental stage. **(a)** Linear relationship between the diameters of the socket and the hair shaft (*left*; $n=640$, $r^2=0.93$, data from three animals) and the diameter of the hair shaft and the logarithm of its length (*right*; $n=143$, $r^2=0.77$, five animals). **(b)** Constant and stereotyped patterns of hair arrangement on different body parts, examples taken from the walking leg tarsus (seventh developmental stage). *1* dorsal, *2* anterior, and *3* posterior aspect. \circ long tactile hairs with open socket ($>250\ \mu\text{m}$); \bullet short hairs with open socket ($<250\ \mu\text{m}$); \bullet long hairs ($>250\ \mu\text{m}$) with closed socket; \bullet short hairs ($<250\ \mu\text{m}$) with closed socket; $*$ trichobothria; \odot contact chemoreceptors; \bullet scopula hairs; *TO* tarsal organ (**a**, **b** modified from Friedrich 1998)

of socket openness as the relevant parameters helps to compare the sensory inventory at different parts of the spider body (see below). Since socket diameter correlates with hair diameter and hair diameter with hair length, it also is a measure for the hair shaft's aspect ratio.

2.3 Distribution

According to careful mapping (using a scanning electron microscope, Jeol JSM-35SF, and light microscopical measurements aided by electronic image analysis, Lucia M/Comet 3.52; video camera Sony 3CCD), each of the body parts studied (walking leg tarsus, pedipalpal tarsus, sternum) had its own characteristic pattern of arrangement of the various types of hairs. Figure 2.3b exemplifies this finding for a juvenile spider (developmental stage 7). Presumably, the specificity and constancy of the patterns in different areas of the exoskeleton are functionally relevant, indicating an adaptation to different tactile stimulus patterns and potentially representing simplified templates of them (for arthropod visual orientation, see Wehner 1987). Unfortunately, we are still far from a sufficiently quantitative understanding of these stimulus patterns, although some of them seem to be simple (see Sect. 2.6 below).

Höger and Seyfarth (1995) studied the *development* of tactile hairs and tactile behavior during the entire lifetime of *Cupiennius salei*. The first tactile hairs appear before hatching (stage 2), when the spiderlings are still protected in their egg sac and a hair's stimulation only causes seemingly uncoordinated movements. After hatching from the egg sac, the next molt (stage 3), profound changes have occurred. The number of hairs has increased immensely. Höger and Seyfarth (1995) report an increase from ten hairs at stage 2 to >3000 tactile hairs per leg at stage 3, only counting those present in what they call the "tactile reflexive field" for body-raising behavior (see under Sect. 2.6.2.2). This receptive field comprises the ventrolateral coxa, the trochanter and proximal femur of the leg. The dramatic changes in hair number go along with a fivefold increase in hair density, which then remains roughly constant from stage 5 to adulthood. The hairs seem to occur just at the right time. At stage 3 (first complete stage; age ca. 30 days), the spiderlings do not rely on their yolk sac anymore but have to move around for prey now. Their reflective body raising (see Sect. 2.6.2.2), elicited by tactile stimulation of any and even a single hair in the "tactile reflexive field" (and mainly due to the activity of the hair's slowly adapting sensory cell), is now fully developed.

2.4 Coping with the Stimulus by Well-Matched Micromechanics

2.4.1 The "Clever" Hair Shaft

Computational biomechanics has helped a lot to reveal the refinement of tactile hair structure and its relevance for stimulus uptake and transmission and thus also to reveal the nature of the evolutionarily relevant fundamental physical constraints that must have contributed to shape the sensors (Dechant et al. 2001; Barth and Dechant 2003; Barth 2004; Fratzl and Barth 2009). The hairs examined in detail are

found dorsally on the walking leg tarsus and metatarsus. They are conspicuously long (e.g., hair TaD1: 2.6 ± 0.2 mm, $N = 7$, steep insertion angle of $58^\circ \pm 4^\circ$; Barth et al. 2004) and stick out of the carpet of other hairs, thus forming the outer boundary of the spider's tactile range (Fig. 2.4a). Only a few points will be raised here to highlight the biomechanical "cleverness" for dealing with the adequate stimulus. More details are found in the literature (see above).

The *stiffness of the articulation* of these hairs is larger by up to four powers of ten than that of the trichobothria, which are exquisitely sensitive to airflow (Humphrey and Barth 2008; McConney et al. 2009; Barth 2014). Like in fly macrochaetae (Theiß 1979), spring stiffness S is in the range between 10^{-8} and 10^{-9} Nm/rad. As a consequence the forces needed to overcome joint stiffness S , which are in the range of micronewtons, bend the hair shaft in addition to deflecting it. This fundamentally distinguishes them from the trichobothria, which respond to the frictional forces contained in airflows implying that they are much more sensitive. Different from the trichobothria case, the forces due to the inertia of the tactile hair shaft's mass may be neglected, not so Young's modulus E and the second moment of area J along the bending hair shaft. These parameters dominate the hair's mechanical behavior when loaded by a tactile force from above (as it happens when the spider is wandering around at night, see below). Due to its bending, the hair shaft's angle with the cuticular surface is never smaller than ca. 12° . This is seen by direct microscopical observation and numerical modeling based on finite element analysis, taking the cross-sectional heterogeneity of the hair shaft (diameter, curvature, wall thickness) along its length (with J , the axial moment of inertia, assuming values varying by almost four powers of ten) into account. With increasing load the point of contact of the stimulus from above is steadily moving toward the hair base. Thereby, the effective lever arm decreases and the bending moment increases. This increase slows down with increasing stimulus forces until it saturates at ca. 4×10^{-9} Nm (Dechant et al. 2001).

What does this mean in more general terms? The hair's micromechanical behavior implies both protection against breaking and a considerable enlargement of the working range as compared to that of a stiff, non-bending rod. It also tells us that the mechanical sensitivity of the hair is higher for small deflections than for large ones (forces needed to deflect the hair, ca. 5×10^{-5} N/° and ca. 1×10^{-4} N/°, respectively). This in turn implies a particular responsiveness to the initial phase of a stimulus. Like the majority of biological senses, the tactile hairs are more "interested" in changing than in static stimulus conditions.

The *axial stresses* in the hair shaft due to its bending measured up to about 3.2×10^5 N/m². Importantly, the hair shaft was found to be a structure of equal maximal strength, again pointing to its mechanical robustness and a nonnervous sensory periphery surprisingly well matched to and coping with the adequate stimulus. This conclusion is supported by the observation that joint restoring torques vary in individual hairs, whereas maximum stresses and bending do not. We conclude that Young's modulus varies in a way finely tuned to the stiffness of the joint (Dechant 2001; Dechant et al. 2001).

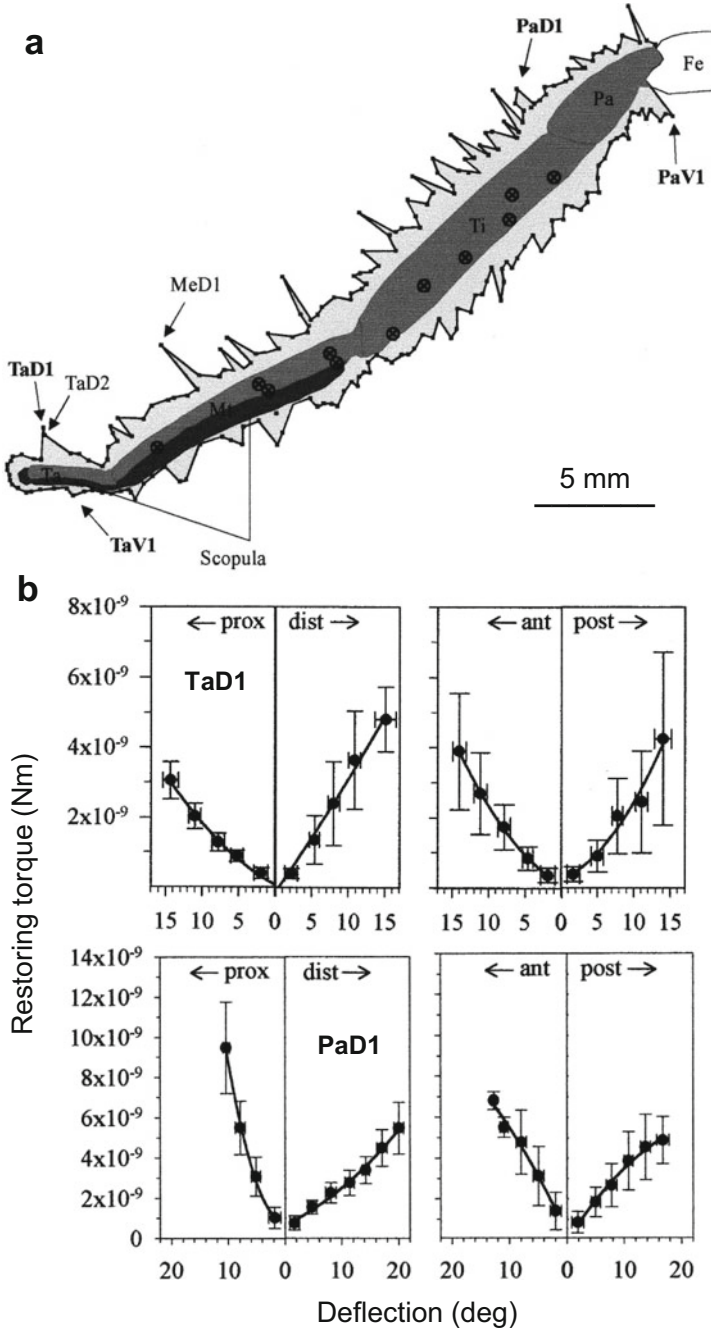


Fig. 2.4 (a) Tactile space of *C. salei*, taking its distal leg segments as example (*Fe* femur, *Pa* patella, *Ti* tibia, *Me* metatarsus, *Ta* tarsus). ● indicate tips of tactile hairs forming outer border of tactile space. *TaD1*, *TaD2*, *TaV1*, *MeD1*, *PaD1*, and *PaV1* indicate particularly long or steeply inserting well-studied tactile hairs. (b) Force (restoring torque) resisting hair deflection in different

An additional clever match of the tactile hair with the stimuli it is exposed to is that it also bends within the socket, even before the hair shaft touches it (Fig. 2.5). A quantitative description of this “*second joint*,” which can be directly seen in slice preparations of intact hairs and again increases the hair’s mechanical robustness, is found in Barth et al. (2004).

The micromechanical analyses now available may serve as a point of reference when studying other tactile hairs in search of overarching rules and big patterns of understanding their diversity.

2.4.2 The Coupling of the Sensory Dendrites

Like the hair shaft, the hair base proper appears to be “designed” for a combination of mechanical sensitivity and mechanical protection of the *dendritic endings*. The proximal part of the long tactile hair found dorsally on the tarsus has an anchor-like shape and connects to the joint membrane (Fig. 2.1b) (Foelix 1985; Barth et al. 2004).

As judged from transmission electron micrographs, the dendritic sheath is *not directly coupled* to the hair base as is the case in insect mechanoreceptive hairs (Keil 1997). Instead, there is a broad strand of material (looking homogeneous in the TEM) between the hair shaft and the dendritic sheath and the same material (according to TEM) within the distally open dendritic sheath and between the tubular bodies of the three dendrites (Fig. 2.1b) (Barth et al. 2004). A challenging question for future research concerns the mechanical properties of this material. Presumably these properties strongly affect stimulus transmission to the dendrites proper. The same structural phenomenon seems to be typical in spider tactile hairs in general. It was also found in tactile hairs on the prosoma and femur and at the femur/patella joint (Ullrich 2000) and similarly in tactile hairs on the legs of *Ciniflo*, a cribellate spider (Harris and Mill 1977). The fine structural details of the dendrite attachment sites look remarkably similar in the different tactile hairs of *Cupiennius*, as if they clearly were not a main source of hair diversity.

In slice preparations of intact hairs, the hair shaft’s *axis of rotation* can be pinpointed by identifying the area of no translational movement. It has a highly acentric position, lying on the proximal side of the shaft’s anchor-like base and right above the apical end of the dendritic sheath. From this the length of the inner lever arm of the hair shaft could be determined. It measures ca. 3.5 μm only, implying a length ratio of the outer versus the inner lever arm of 750 and more. This ratio in turn implies that the displacement of the hair tip is scaled down considerably and the force close to the dendrites amplified correspondingly. Deflection of the hair by



Fig. 2.4 (continued) directions. *Upper* row refers to hair *TaD1*, *lower* row to hair *PaD1* (for both hairs: $N=6$, $n=1$, $r > 0.95$). Note pronounced un-isotropic behavior of the resisting force for distal and proximal deflection of hair *PaD1* (**a**, **b** modified from Friedrich 2001)

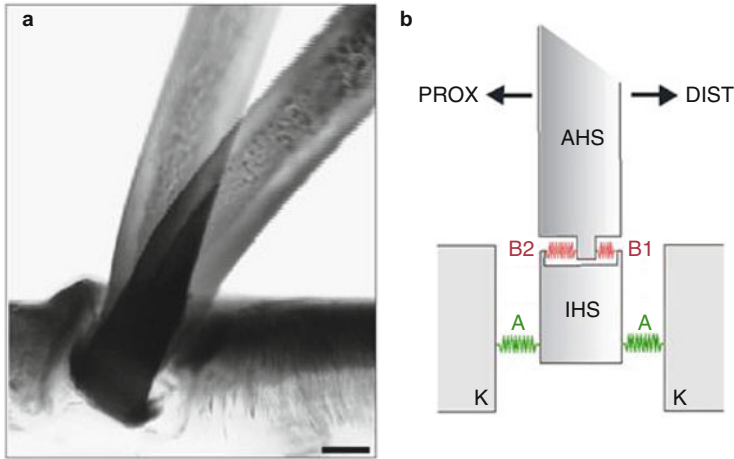


Fig. 2.5 (a) The second joint within the socket as seen in hair TaD1 (see Fig. 2.4a) when superimposing pictures of the hair shaft in resting and deflected (20°) position, respectively; note bending close to base of hair shaft. (b) Schematic representation of hair base of tarsal hair TaD1. Whereas *A* represents the elasticity of the hair suspension in the socket, *B1* and *B2* represent the hair's ability to bend close to its suspension. According to measurements of the restoring torques for proximal and distal hair deflection, *A* is equal in both directions, whereas the stiffness of *B* in proximal direction is larger than in distal direction. *AHS* outer hair shaft, *IHS* inner hair shaft, *K* cuticle (a, b from Barth et al. 2004)

10° is close to the maximum occurring under natural conditions (the hair then just does not touch the socket yet). The restoring torques counteracting such a stimulus are in the order of 10^{-8} – 10^{-9} Nm. They only moderately depend on the direction of the hair's deflection in the given case (see also below). The hair base closest to the dendrites is displaced by about $0.5 \mu\text{m}$ (toward the side opposing that of the outer lever arm movement). At the hair's physiologically determined threshold deflection of 1° (slow cell, see below), this value decreases to $0.05 \mu\text{m}$ (Albert et al. 2001). Considering (i) the shortness of the hair's inner lever arm, (ii) the presumed absorption of at least a fraction of its force and displacement by the deformation of the terminal connecting material, and (iii) the close proximity of the dendrite terminals to the axis of rotation again leaves us with the idea that the hair base, like the outer hair shaft and its "second joint" within the socket, is "designed" to protect the sensillum from being overloaded and damaged (Barth et al. 2004).

2.4.3 Forces, Torques, and Directionality

Taking both the diversity of the tactile sensilla of *Cupiennius* and the unflinching presence of identical modifications of the common Bauplan at the same location on its exoskeleton into account, it seems justified to assume that the hairs are adapted to different functions. One way to get a first idea about the differences implied in

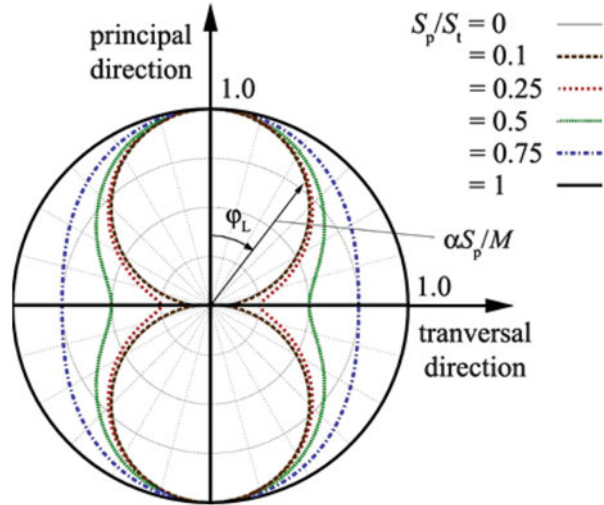
regard to the relevant stimulus patterns is the analysis of the sensors' mechanical properties. These might well reflect important aspects of stimulation under natural conditions.

The *restoring moments* opposing the deflection of a hair can be measured with high resolution (in the order of $1 \mu\text{N}$) by deflecting it with a glass capillary whose own deflection is proportional to the restoring torque and calibrated with a microbalance (Wiese 1976; Albert et al. 2001; Dechant et al. 2001). Such measurements are another way to characterize the diversity of the tactile hair sensilla. So far we have data on (i) four hairs located on the tarsus and patella of the walking legs known to be involved in active tactile behavior (see Sect. 2.6.1; Friedrich 2001) and tactile hairs (ii) on the prosoma, (iii) dorsally on the femur, (iv) at the femur/patella joint, (v) dorsally on the patella, and (vi) ventrally on the tarsus (Fuchs unpublished). All these hairs form the outer limit of the tactile space as shown in Fig. 2.4 a, standing out of the carpet of surrounding cuticular hairs. Interestingly, the tactile hair ventrally on the tarsus (length ca. 0.8 mm, insertion angle 70°) amidst a wealth of scopulate hairs was the most easily deflected, with elastic restoring constants S measuring $5.9 \times 10^{-11} \text{ Nm}^\circ$ and $9.1 \times 10^{-11} \text{ Nm}^\circ$ for distal and proximal deflection, respectively. We speculate that it may play a role not only during locomotion, providing sensory feedback, but also for prey capture (Melchers 1967; Klopsch et al. 2013; Barth 2014), the fine control of spinning the egg sac and holding it, and the highly refined copulatory behavior (see below under Sect. 2.6.2.4). The equivalent values for the long tactile hair dorsally on the tarsus (length ca. 2.6 mm, insertion angle ca. 60°) were $2.5 \times 10^{-10} \text{ Nm}^\circ$ and $1.7 \times 10^{-10} \text{ Nm}^\circ$. Apart from this, all other hairs behave similarly, sometimes with a moderately anisotropic mechanical behavior of their articulation. Examples are given in Fig. 2.4b. The most pronounced mechanical directionality is that of joint hairs, where easy deflectability coincides with the direction of the relevant stimulus load.

A strong *dependence on direction* of the torque resisting deflection is well documented for tactile hairs at the joint between tibia and metatarsus (see below under Sect. 2.6.2.3). The values of the torsional restoring constant S (elastic restoring force opposing hair deflection) for the natural direction of stimulation were smaller by one to two powers of ten compared to those for all other directions (between ca. 5×10^{-12} and $2 \times 10^{-11} \text{ Nm/deg}$; Schaber and Barth 2014). Similar differences, well matched to their behavioral role, were found for the hairs at the femur/patella joint (Barth and Fuchs unpublished). A quantitative mathematical description of the mechanical directional behavior of arthropod cuticular hair articulations in general is shown in Fig. 2.6 and detailed in Dechant et al. (2006).

In this study, a simple mathematical model is described which is applicable to any anisotropic articulation reacting with different joint stiffnesses to loads from different directions. Only a few parameters are needed to quantitatively describe the mechanical directionality. These parameters are S_p and S_r , the joint stiffnesses in the preferred direction of deflection and in a plane transversal to it and the stiffnesses for opposite directions. The equation derived in Dechant et al. (2006) well describes the directionality of a large range of structurally different arthropod hairs (with directionality curves ranging from isotropic to figure eight shaped) in good

Fig. 2.6 Directional characteristics of the joints of arthropod hair sensilla; polar plot derived from mathematical model for different ratios of joint stiffnesses in preferred direction (S_p) and the direction transversal to it (S_t). φ_L load direction, α actual deflection angle of hair under load; φ_α actual direction of deflection; M moment introduced to the joint (Modified from Dechant et al. 2006)



$$\alpha = \sqrt{\alpha_p^2 + \alpha_t^2} = M \sqrt{\frac{\cos^2(\varphi_L)}{S_p^2} + \frac{\sin^2(\varphi_L)}{S_t^2}}$$

agreement with experimental data. It also takes into account the discrepancy between the direction of the stimulus force and that of hair deflection.

As expected, the S values of the tactile hairs examined are all considerably higher (by up to ca. four powers of ten) than those determined for the airflow-sensitive trichobothria (Barth et al. 1993).

The most rewarding outcome of our studies aiming at a better understanding of the diversity of the seemingly innumerable mechanosensitive hairs on the exoskeleton may have been the appreciation of biomechanical details. These details to a large extent tell us how the basically simple Bauplan of a cuticular sensory hair can be adjusted to a variety of functions by the modification of only a few physical parameters. At the same time, the quantitative assessment of these details sheds light on the selection pressures contributing to the evolution of different hairs. We now more clearly see the keys of the piano evolution plays with. Similar to the complex visual systems involved in spatial orientation and highlighted as “matched filters” by Wehner (1987) as examples of sensory systems in general, individual mechanoreceptive hairs are highly selective and tuned to different types of stimulation, even way out in the sensory periphery by way of their nonnervous stimulus-transmitting structures.

2.5 Types of Physiological Responses and Information Encoding

The tactile hairs TaD1 and MeD1 of *Cupiennius* (s. Fig. 2.4a) were extensively studied electrophysiologically as well. They are the longest tactile hairs dorsally on the tarsus and metatarsus of the leg, respectively, protruding from the exoskeletal cuticle at an angle of $58 \pm 4^\circ$ (TaD1) and 73° (MeD1). They are 2.6 ± 0.2 mm (TaD1) and 3.2 ± 0.1 mm (MeD1) long (mean \pm SD; $N = 6$) (Albert et al. 2001). Like most other tactile hairs, they are supplied by three bipolar sensory cells (Foelix and Chu-Wang 1973; Harris and Mill 1977), one of these being substantially larger (53 ± 8 μm) than the others (23 ± 8 μm). For unknown reasons but in agreement with older studies (Harris and Mill 1977), only two of the three cells could be demonstrated unequivocally in extracellular electrophysiological recordings (Albert et al. 2001; but see Eckweiler and Seyfarth 1988 for hairs ventrally on the proximal leg). Notwithstanding this problem, which needs intracellular recordings to be solved, all studies available classify the nerve impulse response of the tactile hair sensory cells as phasic, with different rates of adaptation to maintained stimuli. The tactile hairs studied are all movement detectors. They respond to the dynamic phase of a stimulus, that is, to the hair deflection velocity. For the tactile hairs dorsally on the distal leg of *Cupiennius*, angular deflection thresholds are about 1° . When deflected with behaviorally relevant stimulus velocities (up to 11 cm/s; see Sect. 2.6.1), the maximum action potential frequency occurs already 1.2 ms after stimulus onset and is followed by a rapid decline. Both the fast cells (responding to the dynamic phase of the stimulus exclusively) and the slow cells do not provide detailed information on the time course of the stimulus or on the deflection angle but merely on its presence and onset (Albert et al. 2001). Note that this is in good agreement with the conclusions drawn from the analysis of the hair's micromechanical properties (see under Sect. 2.4.1).

Interestingly, the deflection velocity threshold is much lower for the "slow" than for the "fast" cell. To give an example for TaD1, whereas it is $30 \pm 9^\circ/\text{s}$ for the "fast" cell (response saturation at $\geq 650^\circ/\text{s}$), it is $< 0.1^\circ/\text{s}$ for the "slow" cell (saturation at ca. $250^\circ/\text{s}$) (Albert et al. 2001).

2.6 Matched to Specific Behaviors?

With the knowledge on the mechanical and physiological properties of individual tactile hairs at hand, one may proceed and ask for the behavioral significance of the spider tactile sense and the sensors' context-dependent adaptations. The task is difficult, in particular because the answers rely on a quantitative knowledge of the relevant pattern of tactile stimulation. The few pixels we have of a complex and multifaceted picture nevertheless reflect the refinement of a seemingly unspectacular sense and deepen the impression that arthropod tactile behavior needs much more attention than it so far received. We will first discuss (a) the tactile analysis of surfaces by active touch, then turn to (b) simple reflexes elicited by passive touch

and (c) to the measurement of joint movements by tactile hairs (proprioception), and finally summarize findings regarding (d) body raising initiated by tactile stimulation. This last behavior is a particularly well-studied tactile “simple behavior” of *Cupiennius* and other spiders. To conclude, a short paragraph (e) will point to the complexity of the tactile guidance of copulation behavior.

2.6.1 Actively Gained Contact Information for the Adaptive Control of Locomotion

In search of the functional logic of tactile hairs, one finds that, typically, tactile sensors in general show phasic response characteristics. The tactile analysis of surface structures therefore depends on active movement which largely determines the contribution of individual receptors. On the level of a single receptor hair, the texture of a surface (its profile) is represented as a sequence of hair shaft deflections. Thus, the mechanical limits of spatial resolution lie in the dynamics of the deflected hair shaft’s return to its resting position.

In complete darkness, *Cupiennius* uses its first pair of legs like antennae to intentionally probe its immediate surroundings while walking around on its dwelling or another plant during its nocturnal activity period. This near-range exploration behavior and tactile orientation first described by Schmid (1997) is referred to as “guide stick walk.” Upon the first contact with an object, the spider switches the mode of leg movements and starts to scan the surface with the dorsal aspects of the tarsi and/or metatarsi of its first two pairs of legs. According to video analyses (Friedrich 2001), the individual scanning movements are very regular with a velocity between 4 and 10 cm/s (6.4 ± 1.4 cm/s; $N = 12$). They differ from the pattern seen during locomotion. At a mean duration of 230 ± 82 ms ($N = 12$), the distance covered by the movement was 1.5 ± 0.8 cm ($N = 12$). The first contact with the substrate is mainly by the dorsal aspect of the tarsi. While scanning, the tarsi move at an average velocity of 10 cm/s (Fig. 2.5a).

This implies that it will take some 15 ms only until the hair touches the tarsal surface (provided movement is not slowed down). The action potential conduction velocity of tactile hair afferent fibers was estimated to be between 0.45 and 0.63 m/s (Eckweiler 1987). The distance of the tactile hair to the central nervous system (CNS) is about 6 cm in adult spiders, which implies a total conduction time of 95–133 ms. Obviously then the collision of the tarsal hair with the substrate is indeed not slowed down by efferent control, and a number of neighboring hairs will be stimulated together with the largest ones (Friedrich 2001).

Different from stereotyped tactile reflexes elicited by the stimulation of single hairs (see below Sect. 2.6.2.2), the motor pattern of active touch is variable and presumably depends on the activity of many hairs on correspondingly larger areas of the legs. For a nocturnal animal like *Cupiennius*, to probe its immediate environment using its tactile sense must be highly relevant.

When plotting the maximum impulse rate of the fast cell’s response against velocity of hair deflection (movement of cover glass from above), saturation is

reached between 100 and 200°/s for TaD1 and MeD1. Leg movement velocities during active touch are all within the saturation range of both impulse rate and threshold. Therefore, the fast cell functions like a quasi-digital indicator of a tactile event without providing any details about stimulus intensity and direction (Albert et al. 2001).

For an estimate of the *spatial resolution* possible with these movements, the distances between the tactile hairs located dorsally on the tarsus were determined. The average distance between one sensillum and its six nearest neighbors is remarkably constant for spiders of different age (measured from 2-month-old spiders to 1-year-old female adults). It measures $52 \pm 18 \mu\text{m}$ ($N = 4$; $n = 12$), corresponding to an average *density* of $370 \pm 90/\text{mm}^2$ (Höger and Seyfarth 1995; Albert 2001). This is a remarkably high density. It is hard not to assume that it reflects high spatial resolution and its corresponding behavioral importance.

An additional parameter to be considered is the velocity with which deflected hairs return to their resting position when released. When deflecting prominent tactile hairs dorsally on the tarsus and metatarsus (TaD1, TaD2, MeD1) in the distal direction, which is the biologically most relevant one, stroboscopic analyses showed that the velocity of the restoring movement amounts to some unexpected 25.000°/s for the tarsal hairs (TaD1 28.000°/s; TaD2 23.000°/s) and to even 130.000°/s for the metatarsal hair. A deflection of the hair shaft up to touching the socket was fully restored in only 1–2 ms. Such time periods are sufficiently short at the biologically relevant velocities of leg movements to resolve the surface structure in fine detail. The following experiment demonstrated this directly.

The movement of the spider's leg, when it probes and hits a surface, can be imitated by moving a plane object oriented in parallel to the exoskeletal surface toward the hair base (or leg surface). From the nonlinear increase of hair deflection (well represented by a hyperbolic function) with decreasing distance of the stimulating object (Dechant et al. 2001), it follows that a surface texture of constant depth will increasingly deflect the hair the closer it comes to the hair base. The threshold depth of a surface structure still detected by the hair will therefore decrease in the same way. Taking a threshold deflection of 1° needed to elicit an action potential and a distance of the hair tip to the cuticle surface of 1850 μm , threshold depth will be about 275 μm when touching the tip but only ca. 75 μm at a distance of 1000 μm . When mounting a surface profile of 340 μm height on a planar surface and drawing it over tarsal hair TaD1 in the distal direction (imitating the spider's scanning behavior) (Fig. 2.7a), the nervous response of the slow cell considerably increases when the distance between stimulus and tarsal surface is reduced. Spatial resolution therefore decreases dramatically with decreasing distance of the moving stimulus to the hair base or increasing pre-deflection of the hair (Albert 2001). To effectively probe a surface, the tarsi should just slightly touch it (Fig. 2.7b).

Whereas the *fast cell* innervating a spider tactile hair is interpreted as a quasi-digital indicator of touch as such (similar to a yes or no response), the *slow cell* is thought to be most relevant when the spider starts to scan the surface (Friedrich 2001) and to learn about its texture/structure with well-coordinated brushing

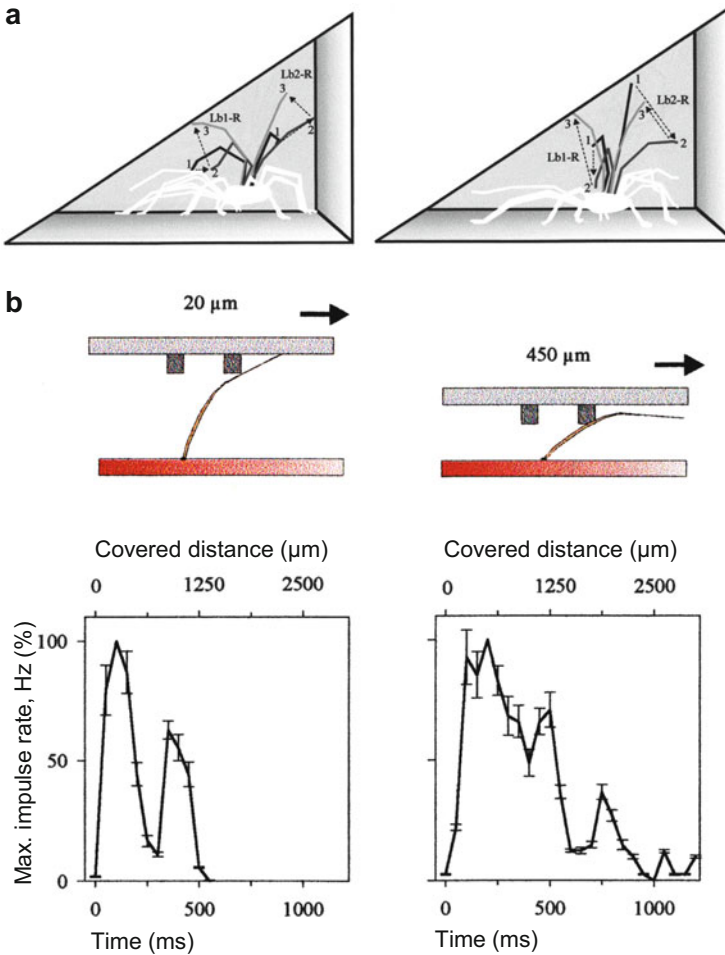


Fig. 2.7 (a) Active tactile behavior of *C. salei* under red light ($\lambda > 630$ nm) or blindfolded in a corridor with triangular cross section. Superposition of individual video frames shows movement of the first two pairs of legs (*Lb1* and *Lb2*; R right). Movement starts with the leg in position 1 in the direction indicated by arrow. Time span covered by drawings ca. 500 ms each. (b) Pre-deflection reduces the tactile contrast and spatial resolution. Electrophysiologically recorded response of slow sensory cell innervating hair TaD1 (see Fig. 2.4a) to a test stimulus consisting of two bars protruding 340 μm from a planar surface and separated by a gap of 750 μm ; left and right: pre-deflection 20 μm downward and 450 μm from hair tip, respectively. ($N = 2$, $n = 6$) (a from Friedrich 2001, b from Albert 2001)

movements (Albert et al. 2001; see also Sect. 2.6.2.4). The profile of a surface is then translated into a spatiotemporal pattern of hair shaft deflections and the nervous activity caused by them. Due to the leg's scanning movements, the surface profile is not only reflected by the simultaneous excitation of different receptors but additionally by the temporal sequence of activity of the individual receptor. The

“slow cell” seems to be better suited for this job than the “fast cell” for the following reasons: (i) no absolute velocity threshold, (ii) independence of its angular threshold deflection from the velocity of hair shaft deflection and thus constant spatial sensitivity for the entire range of leg movement velocities, and (iii) the potential of stronger modulation of the response due to its slower decrease (adaptation), which does not represent fatigue but goes along with unchanged excitability and sensitivity (Albert 2001). Remarkably, a similar role is attributed to the slowly adapting SAI tactile units in vertebrate glabrous skin (Johnson 2001).

2.6.2 Simple Stereotyped Behavior

The locomotion of spiders differs from that of other arthropods. Not only is hydraulic force used to extend the more distal joints of the legs but there are also many more muscles in the leg of a spider than in that of other arthropods. In addition the muscles are poly-neurally innervated by many more motor neurons (Sherman 1985). Possibly then spider leg movements are particularly subtle, and their fine control may rely on a particularly well-developed sensory periphery (Seyfarth 1985). And indeed three main types of sensors are found near the leg joints: slit sense organs, internal joint receptors, and large numbers of mechanosensitive hairs bridging the joints (see Sect. 2.6.2.3).

2.6.2.1 Synergic Withdrawal

As far as we know, resistance reflexes opposing an imposed joint movement are elicited by the internal joint receptors (Seyfarth and Pflüger 1984), whereas synergic reflexes acting in synergy with the imposed movement are due to the stimulation of strain-sensitive lyriform organs (Seyfarth 1985). The deflection of tactile hairs has been known to passively trigger withdrawal activity or turning away of the entire spider, moving the leg away from the stimulus (Seyfarth and Pflüger 1984). Apart from the (i) *withdrawal of a leg*, several other stereotyped reflex behaviors have been known in *Cupiennius* to be elicited by the stimulation of a single hair (Friedrich 1998). One of these is (ii) *raising the opisthosoma* elicited by the stimulation of long tactile hairs ventrally on the opisthosoma. If stimulated several times, the opisthosoma moves upward stepwise in an evasive way until it reaches the anatomical limit for that movement. The spider then continues to raise its opisthosoma by a tilting movement of the entire body, extending the hind legs only. Another reflex reaction following the stimulation of single hairs in their vicinity is the (iii) *withdrawal of the spinnerets* (Fig. 2.8a). Again, the reaction is stepwise and additive upon repeated stimulation. When stimulating long tactile hairs on the prosoma behind the eyes, *Cupiennius* shows (iv) *body lowering*, again in a stepwise additive manner upon repeated stimulation. This behavior is kind of the opposite of the (v) *body-raising reflex* (Eckweiler and Seyfarth 1988) described in more detail below (Fig. 2.8b). Presumably, all these reflexes serve a protective purpose and the avoidance of potential injuries by obstacles during the spiders' nightly activity. However, *raising the opisthosoma* may also play a role in

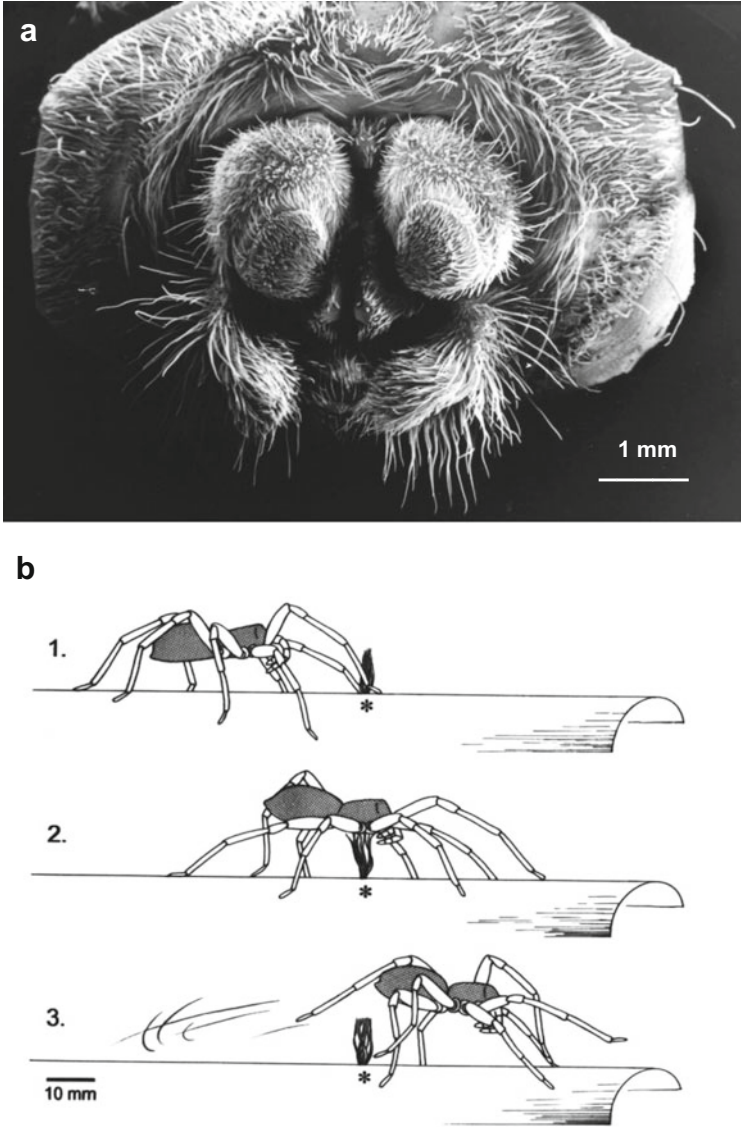


Fig. 2.8 (a) Spinnerets of *C. salei*; note large number of sensory hairs. (b) Tactile body raising: *C. salei* as it approaches (1) and walks across (2, 3) a 10 mm high wire obstacle (*). Neuronal correlates, including central nervous pathways, of this behavior are particularly well studied (see text) (b from Seyfarth 2000)

copulation behavior when the female has to raise its opisthosoma to permit the introduction of the male palpal embolus into the epigyne (see under Sect. 2.6.2.4). Likewise, the *withdrawal of the spinnerets* may serve the fine adjustment of the

spinning movements, e.g., when spinning the egg sac, attaching the safety thread on the plant, or properly carrying the egg sac (Melchers 1963; Barth 2002a).

2.6.2.2 Body Raising and a Spider's Mechanosensory Neuronal Circuit

Owing to the excellent neuroethological analysis by E.-A. Seyfarth and his associates, the “*body-raising*” behavior of *Cupiennius salei* (also found in four other species of *Cupiennius*, in the salticid *Phidippus regius* and the theraphosid *Brachypelma* sp.) now is the best understood tactile behavior in any spider. In addition to the behavior, neuronal mechanisms and the components responsible for the flow of sensory information could be identified at many levels, ranging from the sensory periphery to the central nervous system (Eckweiler and Seyfarth 1988; Milde and Seyfarth 1988; Seyfarth 2000). Although stereotyped and easy to elicit, the behavior is not a “simple reflex.”

The tactile stimulation (deflection) of long tactile hairs on the ventral aspect of the proximal leg segments and sternum first induces a local response only, activating the *coxa levator* muscle of the stimulated leg. This muscle pulls the coxa against the prosoma, while more distal leg joints are extended hydraulically by hemolymph pressure (Blickhan and Barth 1985). As a consequence, internal joint receptors located in the tergo-coxal joint are stimulated which in turn initiate a pluri-segmental response. Now the muscles in all remaining legs are contracting almost simultaneously and the legs are extended. Whereas the local reaction is seen ca. 30 ms after the onset of stimulation, the final body raising is observed after ca. 120 ms only. These delay times are very consistent indicating a rather stereotyped reflex pathway (Seyfarth 2000). Intracellular recordings from neurons in the central nervous system revealed the following neuronal correlates of the local and pluri-segmental response to tactile stimulation. (i) The primary afferent fibers of the tactile hairs project ventrally into the fused spider subesophageal ganglion (Babu and Barth 1984; Anton and Barth 1993; Ullrich 2000; Seyfarth 2000). Their many “local” branches mainly remain in the ipsilateral leg neuromer. (ii) The somata of the motor neurons, which activate the coxal muscles, are found in the dorsally located “motor area” of the neuromer, ca. 200 μm away from the hair afferents. Like the 30 ms delay time between stimulus onset and motor response, this is taken as an argument against rapid monosynaptic connections. (iii) Seyfarth and his associates identified both mono- (local) and pluri-segmental interneurons. In addition to spiking (short bursts) local interneurons, there were also interneurons responding to a tactile stimulus with a longer-lasting graded potential. These interneurons modulate the strength of muscle contraction as shown by experimental current injection. The pluri-segmental spiking interneurons extend into several leg neuromers. They respond to a tactile stimulus and their activity is instantly followed by body raising. Remarkably, the activity of such neurons can also be elicited by the experimental displacement of the coxo-trochanteral joint, which leads to a pluri-segmental motor response as well. Since these neurons are confined to the ventral part of the subesophageal ganglionic mass, they may well be connected to the motor neurons by the premotor non-spiking local interneurons, the only interneurons known to have the corresponding arborizations. Most likely, the afferent activity

of internal joint receptors is distributed to all legs by the spiking pluri-segmental neurons (which are assumed to be part of a “command system”; Seyfarth 2000), and the local circuitries are then activated as described.

2.6.2.3 Proprioception at a Leg Joint

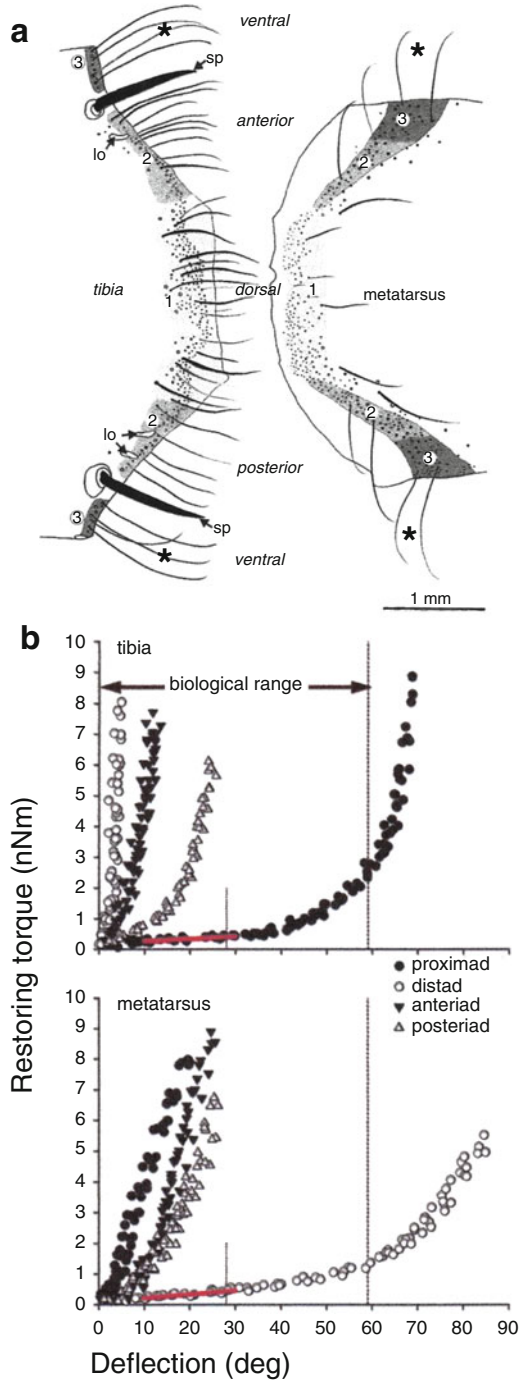
Considering the diligent and well-controlled movements seen in spiders, an important role of sensory feedback is likely. As mentioned before, there are long tactile hairs not only dorsally on the tarsus and metatarsus but also ventrally. These hairs might well play such a role during normal locomotion providing information about the contact with the substrate (Fig. 2.4a). Remember that among all tactile hairs tested so far (see Sect. 2.4.3), they are the most easily deflected. In a recent study, mechanosensitive hair sensilla ventrally at the tibia-metatarsus joint (Fig. 2.9a) were examined asking for their potential adaptedness to their presumed proprioceptive function in monitoring joint movement (Schaber and Barth 2014). Are these hairs indeed suited to this function as their specific location suggests?

Yes, they are. The changes of the joint angle during locomotion go along with their *deflection* in the distal (metatarsal hair) and proximal (tibial hair) direction, respectively. The hair shafts are covered by thousands of microtrichs arranged in regular rows, which reversibly interlock at their tips with the microtrichs of the hairs on the opposing leg segment. Thus, the opposing hairs deflect each other during joint flexion at each step by roughly the same amount (up to 60°). Note the similarity of their S values. Assisting the hairs' deflection in the relevant direction, the force resisting it, is smaller by one to two orders of magnitude in the direction of natural stimulation (torsional restoring constant S ca. 10^{-10} Nm rad⁻¹) as compared to the other directions (Fig. 2.9b) (where the hairs behave similar to the tactile hairs dorsally on tarsus and metatarsus; see Sect. 2.4.3). The torques for deflections in the proprioceptive direction measured less than 1 nNm for angles $\leq 30^\circ$ and up to 9 nNm at 70°, when the hair shaft already touched the socket wall. During normal locomotion, this does not happen even at maximum flexion of the joint (Fig. 2.9b).

Electrophysiological recordings from the sensory neurons supplying the joint hairs (neurons of the tibial and the metatarsal hairs) during quasi-natural stimulation corresponding to the pattern of joint flexion during locomotion revealed the following: (i) The hairs are pure movement detectors, and only deflection away from the resting position elicits a short burst of action potentials, whereas the return to it remains unanswered. (ii) The angular deflection threshold eliciting one action potential varied between 0.7 and 15°, depending on the frequency of the simulated stepping rate (0.1–5 Hz). The velocity of joint flexion was well resolved by the rate of action potentials, which saturates only at stepping rates higher than those occurring during walking.

All available evidence supports the idea of a role played by the hairs at the tibia-metatarsus joint and other joints in the fine control of joint movement during walking and other activities like spinning the egg sac. Ventrally at the most distal of the leg joints between metatarsus and tarsus, about 16 long hairs (up to 3 mm) bridging the joint were found to respond to dorsoventral displacement of the tarsus due to substrate vibration (Speck-Hergenröder and Barth 1988). These joint hairs

Fig. 2.9 Proprioceptive joint hairs of *C. salei*. **(a)** Distribution of hairs of different morphologies at the tibia-metatarsus joint of a walking leg in a flattened cuticle preparation. *Asterisks mark* hairs studied in some detail in regard to their presumed proprioceptive function. *sp* spine, *lo* lyriform organ. **(b)** Mechanical directionality seen from the restoring torques of hairs opposing each other on the tibia (Ti3 hair) and the metatarsus (NMe3 hair). *Dotted line* at 59° marks maximum hair deflection by joint flexion during moderate locomotion, and line at 28° gives the corresponding mean value. *Red* regression line used to determine torsional restoring constant *S*. Note opposite mechanical behavior of the two hairs in the proximal/distal plane of deflection (**a, b** modified from Schaber and Barth 2014)



are slightly bent with their tips touching the tarsus. According to recordings from interneurons in the leg ganglia onto which the hairs of the same joint converge, their absolute sensitivity is highest between 70 and 150 Hz and lower by at least two powers of ten than that of the spider's main vibration sensor, the metatarsal lyriform organ (Barth and Geethabali 1982; Barth 2002a).

2.6.2.4 Tactile Stimuli Guiding Copulation or Touching the Complexity of Haptic Perception

It is the courtship and copulatory behavior of *Cupiennius* and many other spiders with its intensive informational interaction which demonstrates both the subtleties and the limits of our knowledge of the sense of touch in spiders particularly well. After a chemical and a vibratory phase, courtship ends in a tactile phase where the mates are in direct contact and chemical communication is likely to play a role as well (Barth 1997, 2002a). As is typical for animals with internal fertilization, in general the sense of touch then becomes very important for mate selection and actual copulation. Although a lot is known about the sensors per se, our understanding of the sensory perception of entire tactile patterns still is in the dark. Analyses of input integration in the central nervous system and in-depth behavioral studies with a focus on sensory aspects are still badly needed.

In *Cupiennius*, copulation follows an elaborate sequence of courtship behaviors (Melchers 1963; Barth 1993; Hrcir et al. unpublished). It is of the lycosid type (Rovner 1971; von Helversen 1976) where the male approaches the female from in front, touches her legs and the dorsal pro- and opisthosoma, and then climbs over her prosoma until he reaches her opisthosoma (Fig. 2.10).

The male then gently strokes over the female's prosoma and opisthosoma with his pedipalps and legs. To insert his pedipalpal embolus into the female epigyne, the male glides down laterally on the female, strongly touching the female opisthosoma laterally and ventrally mainly with his first (72 % of touches) but also its second legs (21 %) and pedipalps (7 %). He either exhibits simple touches or brushing. The female then raises its opisthosoma by an average of 44° and, importantly, rotates it along its long axis by an average of 29° ($N=19$). She thereby exposes her opisthosomal underside and epigyne to the male. The male again brushes/scrapes over the female's underside with his pedipalps in search of and toward the copulatory pore of the duct leading to the receptaculum seminis (Fig. 2.10). Then its sperm is transferred which takes between 25 and 45 min. After finishing the sperm transfer with one of his pedipalps, the male assumes its initial position on the female prosoma again and, following the same sequence of events, inserts his other pedipalp into the second copulatory pore on the other side of the female's opisthosoma.

Whereas the duration of the different components of the copulation's tactile phase differs widely between individuals, their sequence is stereotyped and the tactile sense strongly involved in this complex sequence of events. Two questions may illustrate this. (i) Does the male need tactile cues to properly orient on the female and (ii) can the raising and swiveling of the female opisthosoma be related to tactile stimulation of the female by the male at particular areas (see also Rovner

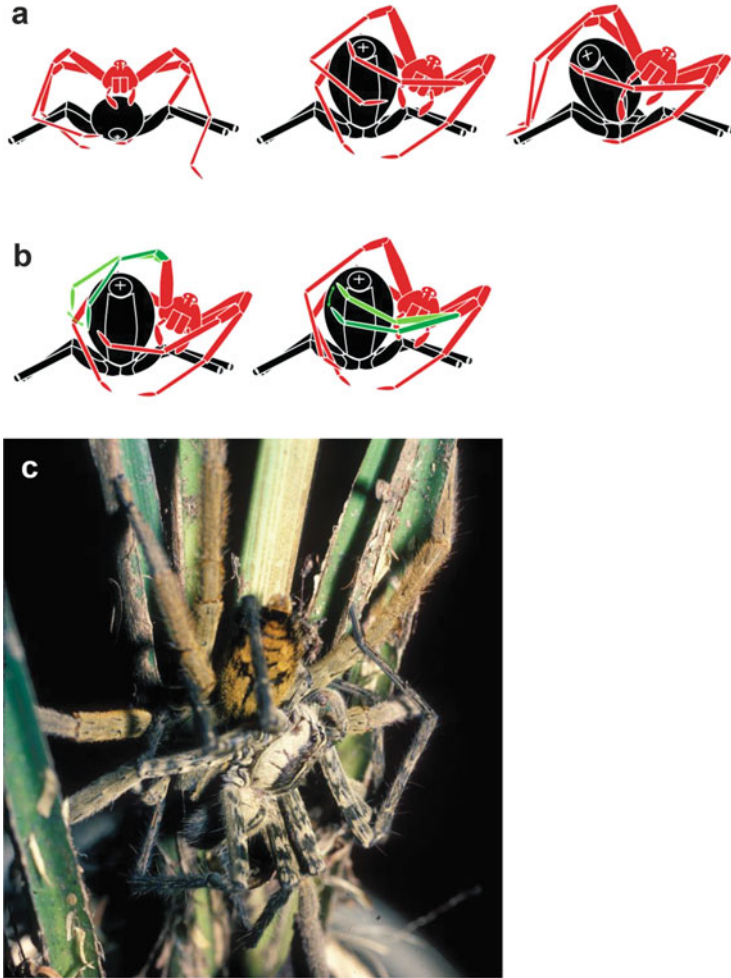


Fig. 2.10 Tactile stimulation during pre-copulatory behavior (*Cupiennius*). (a) Male (red) mounting a female (black) from in front (typical of the “lycosid type”) after having touched her legs and dorsal pro- and opisthosoma. He continues touching the female in typical ways until he finds the female copulatory pore (see text). (b) Two different ways of the male to touch the female: *left*, simple touch with the tarsus touching the female opisthosoma for some 50 ms only; *right*, brushing movement of tarsus without interrupting contact. (c) shows *C. coccineus* copulation (Hrnčir et al. unpublished data)

1971 for *Lycosa rabida*)? To answer such questions, first a quantitative description of the behavior is needed. Using video cameras we analyzed the raising and swiveling of the female opisthosoma in 55 pairs of *Cupiennius salei* (Hrnčir et al. unpublished).

The frequency of male tactile activity strongly increases toward the time of the female’s raising of the opisthosoma and then declines again toward its rotation and

the sperm transfer. Before the raising of the female opisthosoma, the male tactile stimuli focus on the ventro-anterior area of the opisthosoma close (posterior) to the epigyne and on the spinnerets. After shaving the tactile hairs ventrally and ventrolaterally in the posterior region of her opisthosoma (posterior to epigyne), the female never raised her opisthosoma, despite normal male behavior. Presumably then *she needs tactile stimulation of this region*. The rotation of her opisthosoma, however, was as usual. When stimulating artificially, it is just these areas where large raising angles are achieved. Rotation of the opisthosoma could be eliminated by shaving it ventrolaterally, anterior to the epigyne, which implies that *the male needs tactile sensory input to start his active rotation of the female opisthosoma*. The rotation could never be elicited by artificial tactile stimulation of the female opisthosoma. It is actively achieved by the male using his first pair of legs (as can also be shown in copulations with dead females). As seen from the many male touches, the presence of the female spinnerets is important for his correct orientation on his partner. Following the experimental removal of the spinnerets, the number of touches further increases significantly (Hrncir et al. unpublished).

Clearly, we are still a long way from recognizing the potential “template” of such complex stimulation in the arrangement and properties of the receiver’s arrays of tactile hairs.

In engineering, a “matched filter” is used to detect a particular known signal in the presence of noise and to maximize the signal to noise ratio. A commonly known application is for the detection of the reflected echo signal of a radar sender emitting electromagnetic pulses. The task is to detect the known signal or template in the unknown signal. As we have seen, particular mechanoreceptive hairs are tuned to different types of mechanical stimulation, and their properties may be considered kind of templates of the relevant stimulus patterns. Thinking in terms of evolution, this is trivial, the nontrivial part being the rigorous quantitative analysis of the details and the synthesis of the parts to form a whole. We have come some way along this path in regard to individual hairs. However, there is still an enormous lack of knowledge of potential “templates” to be applied to the many different behavioral situations a spider finds itself in and involving hundreds or thousands of sensory hairs exposed to complex spatiotemporal stimulus patterns. As a corollary of this, there is hardly any but a most superficial understanding of the spatial design of the tactile surface of spiders and other arthropods. It will not be an easy task to change this situation to the better, but certainly a lot can be achieved with the technologies now available.

2.7 Concluding Remarks

Impressed by the sheer number and density of the tactile hairs covering the exoskeleton of *Cupiennius* and other spiders, one is tempted to look for some simplifying overarching rules governing their role in touch reception. In the end, an organismal biologist would like to understand how all these sensory hairs

interact to construct the spider's subjective tactile reality. To this end we need careful quantitative analyses at many levels of organization.

A first general rule might be hidden in the morphology of the hairs. But are there clearly distinguishable modifications of the general Bauplan of the sensory hair? The detailed comparative analysis of hair morphology revealed the nonexistence of strictly separate types of tactile hairs (Friedrich 1998; Ullrich 2000). Instead there are graduations and intermediates between them. It is nevertheless possible, however, to distinguish large classes of hairs such as "long ($>250\ \mu\text{m}$) and with open socket" and "short ($<250\ \mu\text{m}$) and with closed socket." Thus, classified hairs form different stereotyped patterns typical of particular areas of the exoskeleton (Fig. 2.3). We therefore hypothesize that these patterns at least to some extent reflect features of the various tactile stimulus patterns relevant at different specific locations. A detailed analysis of such stimuli is still largely lacking. And it is demanding on a quantitative basis taking into account all relevant mechanical aspects (like contact forces, adhesion, friction, restoring torques, and hair deflections) for areas densely equipped with many tactile hairs.

Another prime focus of future interest must be the central nervous system. So far the study of "body raising" (Fig. 2.8b) (review by Seyfarth 2000) is the only one fully detailing a tactile behavior at different levels, from the touch receptors and primary afferents to interneurons, motor neurons, and behavior, thus revealing the entire information flow necessary. This study may well serve as an excellent example for similar studies which might also include data on the effects of the sense organs' efferent control. Whereas the fine structural and chemical basis of efferent control is well established in spiders, its functional implications are still far from being sufficiently understood (Foelix 1975; Albert and Barth 1999; Fabian-Fine et al. 2000; Panek et al. 2002). According to neuroanatomical studies (reviewed in Barth 2002a), the primary afferents of tactile hairs are organized in a somatotopic way, the terminal arborizations of sensilla situated proximally or more distally on the leg being represented in the dorsal and more ventral sensory longitudinal tracts (SLTs), respectively. The afferent fibers reach the subesophageal ganglionic mass along the main leg nerves. Their fine branches ramify in the corresponding leg neuromer, contacting interneurons and sending branches to the SLTs (which also are neuropils in addition to tracts). There a lot of convergence of the projections from different tactile hairs and other sensors is seen. Some branches of the primary afferents were also shown to reach the supraesophageal ganglion.

The examples of tactile hairs so far studied in detail amply demonstrate the fine-tuning of their micromechanical properties to particular tasks. For particularly long tactile hairs forming the outer borderline of the spider's tactile space (Fig. 2.4a) (not considering active touch), the structure and mechanical properties of the hair shaft together with the mechanics of its suspension were shown to be exquisitely adapted to both sufficient mechanical sensitivity and protection from breakage by overloads (Dechant et al. 2001; Fratzl and Barth 2009). Together with the phasic electrophysiological properties of the sensory cells, this also makes a perfect event detector particularly sensitive to the initial dynamic phase of a stimulus deflecting the hair

(Albert et al. 2001). Proprioceptive hairs opposing and deflecting each other, thereby monitoring joint movement, exhibit opposite mechanical directionality (Fig. 2.9). Apart from interactions with its abiotic environment, where the importance of small spaces serving the spider as retreats during the day may have strongly contributed to the evolution of a highly performing tactile sense, the tactile communication with the sexual partner during pre- and copulatory behavior (Fig. 2.10) deserves particular attention.

Sensory ecology has wide boundaries which should include principles of behavior and evolution in addition to studies mainly driven by the question of how a sensory system works. Nevertheless it may well be that the search for the overarching rules and general principles of organization is not the most adequate approach of research. As our knowledge presently stands, it may be more promising to search for the ways how the spider deals with different “tactile problems” inherent in its particular lifestyle. Such an approach also reflects the opportunistic character of natural selection, with no one designing “the” optimal system. In regard to the sense of touch, the comparison of spiders differing in lifestyle like wandering and web-building spiders, or nocturnal and diurnal spiders, might be particularly rewarding. As already pointed out, the same applies to a future focus on the quantitative analysis of complex mechanical stimulus patterns. Although the sensory periphery promises many more discoveries underlining its role in simplifying the flow of information by selecting, filtering, and preprocessing it, the central nervous integration of tactile input needs much more attention than it so far received. Using the tactile capabilities of their antennae, honeybees discriminate between different surface structures, forms, sizes, and locations of objects (Erber 2012). Regarding spiders, experimental data may eventually enable us to comment on questions like “Does the spider use information on form and surface structure (texture)? How is this information gained and which potential role do different modes of active touch, like tapping or brushing, and the timing of tactile sampling play?”

Acknowledgments Research in the author’s laboratories reported here was generously supported by the Austrian Science Fund FWF (grant P 12192-Bio to FGB). I am grateful to all my former students and associates for their contributions and to Prof. FG Rammerstorfer of the Vienna University of Technology for his invaluable input from the engineering side. JT Albert, OC Friedrich, M Hrnčir, S Jarau, and N Ullrich gave permission to use unpublished figures. I also thank E.-A. Seyfarth and Aarhus University Press for the permission to use Fig. 2.8b and Springer-Verlag for the permission to use Figs. 2.1b, 2.5, 2.6, and 2.9 from our own previous publications.

References

- Albert JT (2001) Zur Physiologie des Berührungssinnes von Spinnen. Doctoral thesis, Faculty of Life Sciences, University of Vienna
- Albert JT, Barth FG (1999) Tactile hairs of a spider. III. GABA and circadian modulation of sensitivity. *Zoology* 102:48
- Albert JT, Friedrich OC, Dechant H-E, Barth FG (2001) Arthropod touch reception: spider hair sensilla as rapid touch detectors. *J Comp Physiol A* 187:303–312

- Anton S, Barth FG (1993) Central nervous projection patterns of trichobothria and other cuticular sensilla in the wandering spider *Cupiennius salei* (Arachnida, Araneae). *Zoomorphology* 113:21–32
- Babu SK, Barth FG (1984) Neuroanatomy of the central nervous system of a wandering spider, *Cupiennius salei* (Arachnida, Araneae). *Zoomorphology* 104:344–359
- Barth FG (1993) Sensory guidance in spider pre-copulatory behavior. *Comp Biochem Physiol* 104 (A):717–733
- Barth FG (1997) Vibratory communication in spiders: adaptation and compromise at many levels. In: Lehrer M (ed) *Orientation and communication in arthropods*. Birkhäuser, Basel, pp 247–272
- Barth FG (2002a) A spider's world: senses and behavior. Springer, Berlin, 394 p
- Barth FG (2002b) Spider senses – technical perfection and biology. Karl von Frisch lecture. *Zoology* 105:271–285
- Barth FG (2004) Spider mechanoreceptors. *Curr Opin Neurobiol* 14:415–422
- Barth FG (2012a) Sensory perception: adaptation to life style and habitat. In: Barth FG, Giampieri-Deutsch P, Klein H-D (eds) *Sensory perception – mind and matter*. Springer, Wien, pp 88–107
- Barth FG (2012b) Spider strain detection. In: Barth FG, Humphrey JAC, Srinivasan MV (eds) *Frontiers in sensing: from biology to engineering*. Springer, Wien, pp 251–273
- Barth FG (2014) The slightest whiff of air: airflow sensing in arthropods. In: Bleckmann H, Mogdans J, Coombs SL (eds) *Flow sensing in air and water – behavioral, neural and engineering principles of operation*. Springer, Berlin, pp 169–196
- Barth FG, Cordes D (1998) *Cupiennius remediatus* (Araneae, Ctenidae), a new species in Central America, and a key for the genus *Cupiennius*. *J Arachnol* 26:133–141
- Barth FG, Cordes D (2008) Key to the genus *Cupiennius* (Araneae, Ctenidae). In: Weissenhofer et al. (eds) *Natural and cultural history of the Golfo Dulce region*. Spapfia 88, zugleich Kataloge der oberösterreichischen Landesmuseen, Neue Serie 80:225–228
- Barth FG, Dechant H-E (2003) Arthropod cuticular hairs: tactile sensors and the refinement of stimulus transformation. In: Barth FG, Humphrey JAC, Secomb TW (eds) *Sensors and sensing in biology and engineering*. Springer, Wien, pp 159–171
- Barth FG, Geethabali (1982) Spider vibration receptors. Threshold curves of individual slits in the metatarsal lyriform organ. *J Comp Physiol* 148:175–185
- Barth FG, Höller A (1999) Dynamics of arthropod filiform hairs. V. The response of spider trichobothria to natural stimuli. *Phil Trans R Soc Lond B* 354:183–192
- Barth FG, Schmid A (eds) (2001) *Ecology of sensing*. Springer, Berlin, 341 p
- Barth FG, Wastl U, Humphrey JAC, Devarakonda R (1993) Dynamics of arthropod filiform hairs. II- Mechanical properties of spider trichobothria (*Cupiennius salei* KEYS). *Phil Trans R Soc Lond B* 340:445–461
- Barth FG, Nemeth SS, Friedrich OC (2004) Arthropod touch reception: structure and mechanics of the basal part of a spider tactile hair. *J Comp Physiol A* 190:523–530
- Bathellier B, Barth FG, Albert JT, Humphrey JAC (2005) Viscosity-mediated motion coupling between pairs of trichobothria on the leg of the spider *Cupiennius salei*. *J Comp Physiol A* 191:733–746, see also Erratum: *J Comp Physiol A* 196:89
- Bathellier B, Steinmann T, Barth FG, Casas J (2012) Air motion sensing hairs of arthropods detect high frequencies at near maximal mechanical efficiency. *J R Soc Interface* 9:1131–1143
- Blickhan R, Barth FG (1985) Strains in the exoskeleton of spiders. *J Comp Physiol A* 157:115–147
- Dechant H-E (2001) *Mechanical properties and finite element simulation of spider tactile hairs*. Doctoral thesis, Vienna University of Technology, Vienna
- Dechant H-E, Rammerstorfer FG, Barth FG (2001) Arthropod touch reception: stimulus transformation and finite element model of spider tactile hairs. *J Comp Physiol A* 187:313–322, see also Erratum *J Comp Physiol A* 187:851
- Dechant H-E, Hößl B, Rammerstorfer FG, Barth FG (2006) Arthropod mechanoreceptive hairs: modeling the directionality of the joint. *J Comp Physiol A* 192:1271–1278
- Dusenbery DB (1992) *Sensory ecology. How organisms acquire and respond to information*. WH Freeman and Co., New York

- Eckweiler (1983) Topographie von Proprioceptoren, Muskeln und Nerven im Patella-Tibia- und Metatarsus-Tarsus –Gelenk des Spinnenbeins. Diploma thesis, Biology, JW Goethe University, Frankfurt am Main
- Eckweiler W (1987) Tasthaare, Beinmuskelreflexe und Einstellung der Körperhöhe bei Jagdspinnen. Doctoral thesis, Biology, JW Goethe University, Frankfurt am Main
- Eckweiler W, Seyfarth E-A (1988) Tactile hairs and the adjustment of body height in wandering spiders: behavior, leg reflexes, and afferent projections in the leg ganglia. *J Comp Physiol A* 162:611–621
- Eckweiler W, Hammer K, Seyfarth E-A (1989) Long smooth hair sensilla on the spider leg coxa: sensory physiology, central projection pattern, and proprioceptive function. *Zoomorphology* 109:97–102
- Erber J (2012) Tactile antennal learning in the honey bee. In: Galizia GC, Eisenhardt D, Giurfa M (eds) *Honeybee neurobiology and behavior*. Springer Science and Business, Dordrecht, pp 439–455
- Fabian-Fine R, Meinertzhagen IA, Seyfarth E-A (2000) Organization of efferent peripheral synapses at mechanosensory neurons in spiders. *J Comp Neurol* 420:195–210
- Foelix RF (1975) Occurrence of synapses in peripheral sensory nerves of arachnids. *Nature* 254:146–148
- Foelix R (1985) Mechano- and chemoreceptive sensilla. In: Barth FG (ed) *Neurobiology of arachnids*. Springer, Berlin, pp 118–137
- Foelix R, Chu-Wang I-W (1973) The morphology of spider sensilla. I. Mechanoreceptors. *Tissue Cell* 5:451–460
- Fratzl P, Barth FG (2009) Biomaterial systems for mechanosensing and actuation. *Nature* 462:442–448
- Friedrich OC (1998) Tasthaare bei Spinnen: Zur äußeren Morphologie, Biomechanik und Innervierung mechanorezeptiver Haarsensillen bei der Jagdspinne *Cupiennius salei* Keys. (Ctenidae). Diploma thesis, Faculty of Life Sciences, University of Vienna, Vienna
- Friedrich OC (2001) Zum Berührungssinn von Spinnen. Doctoral thesis, Faculty of Life Sciences, University of Vienna, Vienna
- Harris DJ, Mill PJ (1977) Observations on the leg receptors of *Ciniflo* (Araneidae, Dictynidae) I. External mechanoreceptors. *J Comp Physiol* 119:37–54
- Höger U, Seyfarth E-A (1995) Just in the nick of time: postembryonic development of tactile hairs and of tactile behavior in spiders. *Zoology (ZACS)* 99:49–57
- Höbl B, Böhm HJ, Rammerstorfer FG, Müllan R, Barth FG (2006) Studying the deformation of arachnid slit sensilla by a fracture mechanical approach. *J Biomech* 39:1761–1768
- Höbl B, Böhm HJ, Rammerstorfer FG, Barth FG (2007) Finite element modeling of arachnid slit sensilla. I: The mechanical significance of different slit arrays. *J Comp Physiol A* 193:445–459, see also Erratum *J Comp Physiol A* 193:575
- Höbl B, Böhm HJ, Schaber CF, Rammerstorfer FG, Barth FG (2009) Finite element modeling of arachnid slit sensilla. II. Actual lyriform organs and the face deformations of the individual slits. *J Comp Physiol A* 195:881–894
- Höbl B, Böhm HJ, Rammerstorfer FG, Barth FG (2014) Finite element modeling of arachnid slit sensilla. III. 3D morphology and embedding (submitted)
- Humphrey JAC, Barth FG (2008) Medium flow-sensing hairs: biomechanics and models. In: Casas J, Simpson SJ (eds) *Adv Ins Physiol*. 34. Insect mechanics and control, 1–80
- Johnson KO (2001) The roles and functions of cutaneous mechanoreceptors. *Curr Opin Neurobiol* 11:455–461
- Johnson KO, Yoshioka T, Vega-Bermudez F (2000) Tactile functions of mechanoreceptive afferents innervating the hand. *J Clin Neurophysiol* 17:539–558
- Keil TA (1997) Functional morphology of insect mechanoreceptors. *Microsc Res Tech* 39:506–531
- Klopsch C, Kuhlmann HC, Barth FG (2013) Airflow elicits a spider's jump towards airborne prey. II. Flow characteristics guiding behaviour. *J R Soc Interface* 10:82, 10.20120820

- McConney ME, Schaber CF, Julian MD, Eberhardt WC, Humphrey JAC, Barth FG, Tsukruk VV (2009) Surface force spectroscopic point load measurements and viscoelastic modelling of the micromechanical properties of air flow sensitive hairs of a spider (*Cupiennius salei*). *J R Soc Interface* 6:681–694
- Melchers M (1963) Zur Biologie und zum Verhalten von *Cupiennius salei* (Keyserling), einer amerikanischen Ctenide. *Zool Jb Syst* 91:1–90
- Melchers M (1967) Der Beutefang von *Cupiennius salei* Keyserling (Ctenidae). *Z Morph Ökol Tiere* 58:321–346
- Milde JJ, Seyfarth E-A (1988) Tactile hairs and leg reflexes in wandering spiders: physiological and anatomical correlates of reflex activity in the leg ganglia. *J Comp Physiol A* 162:623–631
- Panek I, French AS, Seyfarth E-A, Sekizawa SI, Torkkeli PH (2002) Peripheral GABAergic inhibition of spider mechanosensory afferents. *Eur J Neurosci* 16:96–104
- Rovner JS (1971) Mechanisms controlling copulatory behavior in wolf spiders (Araneae: Lycosidae). *Psyche* 78(3):150–165
- Schaber CF, Barth FG (2014) Spider joint hairs: adaptation to proprioceptive stimulation. *J Comp Physiol A* 201(2):235–248
- Schaber CF, Gorb S, Barth FG (2012) Force transformation in spider strain sensors: white light interferometry. *J R Soc Interface* 9:1254–1264
- Schaxel J (1919) Die Tastsinnesorgane der Spinnen. *Jena Z Nat* 56:13–20
- Schmid A (1997) A visually induced switch in mode of locomotion of a spider. *Z Naturforsch* 52c:124–128
- Seyfarth E-A (1985) Spider proprioception: receptors, reflexes and control of locomotion. In: Barth FG (ed) *Neurobiology of arachnids*. Springer, Berlin, pp 230–248
- Seyfarth E-A (2000) Tactile body raising: neuronal correlates of a 'simple' behavior in spiders. *Proc 19th Eur Coll Arachnol*. In: Toft S, Scharff N (eds) *Europ Arachnol 2000*:19–32. Aarhus University Press, Aarhus 2002
- Seyfarth E-A, Pflüger H-J (1984) Proprioceptor distribution and control of a muscle reflex in the tibia of spider legs. *J Neurobiol* 15:365–374
- Seyfarth E-A, Gnatzy W, Hammer K (1990) Coxal hair plates in spiders: physiology, fine structure, and specific central projections. *J Comp Physiol A* 166:633–642
- Sherman RG (1985) Neural control of the heartbeat and skeletal muscle in spiders and scorpions. In: Barth FG (ed) *Neurobiology of arachnids*. Springer, Berlin, pp 319–336
- Speck-Hergenröder J, Barth FG (1988) Vibration sensitive hairs on the spider leg. *Experientia* 44(1):13–14
- Theiß J (1979) Mechanoreceptive bristles on the head of the blowfly: mechanics and electrophysiology of the macrochaetae. *J Comp Physiol* 32:55–68
- Tichy H, Barth FG (1992) Fine structure of olfactory sensilla in myriapods and arachnids. *Microsc Res Tech* 22(4):372–391
- Ullrich ND (2000) Zum Berührungssinn von Spinnen: Feinstruktur und zentrale Projektion von Tasthaaren bei *Cupiennius salei* Keys. (Ctenidae). Diploma thesis, Faculty of Life Sciences, University of Vienna, Vienna
- von Frisch K (1965) *Tanzsprache und Orientierung der Bienen*. Springer, Berlin
- von Helversen O (1976) Gedanken zur Evolution der Paarungsstellung bei den Spinnen (Arachnida: Araneae). *Entomol Ger* 3(1/2):13–28
- von Uexküll J (1909) *Umwelt und Innenwelt der Tiere*. Springer, Berlin
- von Uexküll J (1920) *Theoretische Biologie*. Springer, Berlin
- Wehner R (1987) 'Matched filters'- neural models of the external world. *J Comp Physiol A* 161:511–531
- Wiese K (1976) The mechanosensitive system of prey localization in *Notonecta*. *J Comp Physiol A* 92:317–325
- Wilson OE (1984) *Biophilia. The human bond with other species*. Harvard University Press, Cambridge, MA

Robyn A. Grant and Kendra P. Arkley

Contents

3.1	Introduction	60
3.2	Matched Sensors	62
3.2.1	Layout of the Mystacial Pad and Design of the Whisker Field	62
3.2.2	Individual Whiskers	64
3.2.3	Microvibrissae	65
3.2.4	Matched Sensor Conclusions	65
3.3	Neural Control and Maps	66
3.3.1	Neural Maps	66
3.3.2	Sensory Pathways	67
3.3.3	Motor Control	68
3.3.4	Neural Control and Maps Conclusions	68
3.4	Whisker Behaviour in Rats	69
3.4.1	Whisking	69
3.4.2	Exploratory Whisking During Object Contact	70
3.4.3	Mystacial Musculature	70
3.4.4	Behavioural Conclusions	71
3.5	Ecology and Evolution of Active Touch	72
3.5.1	Vibrissal Function in Rats	72
3.5.2	Vibrissal Function in Other Mammals	75
3.5.3	Evolution	76
3.5.4	Conclusions of Ecology and Evolution of Active Touch	76
3.6	Active Touch Sensing as a Matched Filter Design	77
3.7	Conclusions	78
	References	78

R.A. Grant (✉)

Conservation, Evolution and Behaviour Research Group, Manchester Metropolitan University,
Manchester, UK

e-mail: Robyn.grant@mmu.ac.uk

K.P. Arkley

Active Touch Laboratory, University of Sheffield, Sheffield, UK

Abstract

Whiskers are present on most mammals, and whisker specialists, such as rodents, pinnipeds and insectivores, can actively position their whiskers to efficiently guide navigation, locomotion and exploration. That only a small number of whiskers give enough information about the local environment to be the primary tactile sense in many mammals has prompted researchers to explore how well adapted the whisker system is and how “matched” these sensors are to their function. In this chapter, we suggest that whisker touch systems have a matched filter design by arguing that (i) the layout of the vibrissae and their mechanical properties provide a computationally cheap way to gather tactile and spatial information; (ii) this layout is topographically mapped throughout the brain, enabling temporal and spatial information to be preserved easily during processing, freeing up other areas of the brain; and (iii) movement of the whiskers can focus the sensors onto salient regions of space and also control the amount, type and quality of information gathered from an environment. That anatomical and behavioural characteristics are maintained throughout many different mammalian orders indicates the importance of vibrissal touch sensing in arboreal, nocturnal animals, hence its conservation throughout mammalian evolution.

3.1 Introduction

One of the most striking facial features of mammals is the presence of whiskers or vibrissae—tactile hairs that are only truly absent in humans and higher primates (Ahl 1986). The “whisker specialists”, namely, rodents (e.g. rats and mice), insectivores (e.g. shrews) and pinnipeds (e.g. seals and walruses), are animals that actively employ their whiskers to guide activities, ranging from exploration and navigation (Dehnhardt and Kaminski 1995; Dehnhardt et al. 2001) to feeding (Anjum et al. 2006; Dehnhardt and Kaminski 1995; Dehnhardt et al. 2001) and social behaviours (Ahl 1986; Bugbee and Eichelman 1972; Dehnhardt and Kaminski 1995; Reep et al. 2001). Much like humans move their hands over surfaces and objects to feel for certain properties, whisker specialists move their whiskers to extract information such as size, texture, shape and position.

Perhaps the most researched and well understood of these specialists is the rat (*Rattus norvegicus*), the animal that will be the main focus of this chapter. Rats have two sets of facial whiskers, the microvibrissae and the macrovibrissae (Fig. 3.1b). The macrovibrissae are the longer facial whiskers, which can be moved in regular and rapid bouts of sweeping movements known as “whisking” (the word vibrissa, itself, comes from the Latin “vibrio”, meaning “to vibrate”). This sweeping whisking movement is not greatly dissimilar from how humans might scan in front of them with their hands as they navigate in the dark. However, whiskers do not just make simple scanning movements; whisker behaviours are

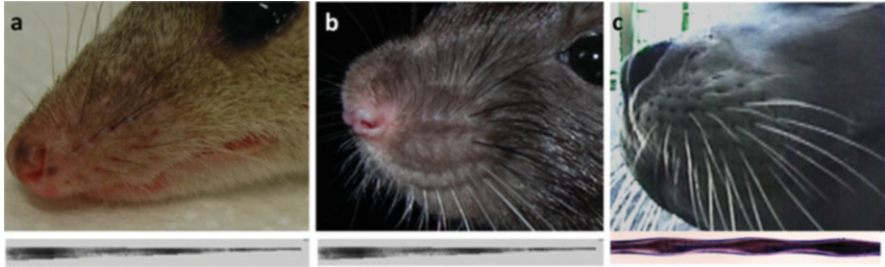


Fig. 3.1 Whisker layout and shape in the (a) opossum, *Monodelphis domestica*; (b) rat, *Rattus norvegicus*; and (c) harbour seal, *Phoca vitulina*. Below each photograph of their whisker layout are representations of their whisker shapes. The opossum and rat have smooth tapered whiskers while the harbour seal has rippling (undulating) whiskers

much more variable in, for instance, locomoting animals (Arkley et al. 2014) and those exploring objects or surfaces (Mitchinson et al. 2007; Sachdev et al. 2002; Towal and Hartmann 2006). Further, as we will demonstrate, despite there being a huge variation in whisker use (be that using whiskers for texture discrimination or something as complex as tree climbing), whisker sensing provides detailed and accurate information about the environment, albeit that which can be *directly* touched and sensed (in comparison to visual, auditory or olfactory senses). This is possible as whisker movements are not just passive palpations but are actively and quickly modified in response to environmental contact and sensory input (Towal and Hartmann 2006; Mitchinson et al. 2007; Grant et al. 2009). It is therefore thought that whisker sensing is an *active* sensory system (Grant et al. 2014; Prescott et al. 2011).

The vibrissae play a key role in locomotion, object discrimination and navigation in mammals that live in the dark, be that underwater or underground. The whisker system has only a relatively small numbers of modular sensory elements—approximately 70 tactile hairs in rats. This means that mammals gather information to complete complex tasks by processing information from only a limited amount of sensors. Compare this, for example, to the number of mechanoreceptors in each human fingertip, which is approximately 241 u/cm^2 low-threshold mechanoreceptive units (Johansson and Vallbo 1979). Owing to the fact that the sensory array has finite and measureable units and is computationally “cheap” to process information about object shape, texture and position, the rat whisker system is a suitable candidate from which to discuss matched filtering.

Studies in neuroscience have made use of the ability to stimulate individual rat vibrissae in a precise and repeatable manner while tracing sensory processing pathways from the primary afferent nerves through to the cortex (Deschenes et al. 2003; Diamond et al. 2003; Welker 1964; Woolsey and Van der Loos 1970) (See Sect. 3.3 for more information). Due to these useful properties, many studies have investigated the whisker system from a neuronal, physiological or anatomical perspective (Ahl 1986; Dyck 2005). While research exploring the vibrissal sensing system has deep roots in the neurosciences, recent behavioural studies have also

discovered important implications for behavioural ecology and evolution. This chapter will focus on these behavioural findings and examine the role of the vibrissae as matched filters.

To begin, we will first examine the layout of the whisker pad and consider, for instance, how the properties of the whiskers and their layout make them matched filters. Secondly, the neural structures of the whisker system will be considered, including the barrel-like structures that increase computational efficiency, freeing up other areas for more complex sensory processing. Thirdly, basic principles of behavioural control will be introduced, to show that the sensors can be actively positioned to focus on areas of interest in the environment. Finally, we will consider whisker function more closely, discussing its implications for mammalian ecology and evolution. While this chapter focusses on the rodent vibrissal system, examples from pinnipeds, insectivores and marsupials will also be incorporated.

3.2 Matched Sensors

Wehner (1987) suggested that much sensory processing is conducted at the periphery, at the sensor level itself, and that the spatial layout and properties of the sensor are matched to the problem at hand. The mystacial whiskers are positioned on each side of the face so as to sample around the head of the animal, making them ideal touch sensors from which to explore a large area of space. In addition, in mammals with more upward- and forward-facing eyes, the whiskers might also be able to sample an area that is not covered by the visual system (e.g. below the snout; Wallace et al. 2013). In this section, we will describe the layout of the whisker pad and move on to a discussion at the level of the individual whisker.

3.2.1 Layout of the Mystacial Pad and Design of the Whisker Field

While prominent vibrissal hairs can be positioned on the upper lip (mystacial pad), lower lip, brow, cheeks and forelegs of mammals (Vincent 1913), it is the mystacial macrovibrissae that have excited the most interest, as they are predominantly larger and movable. The mystacial whiskers (macrovibrissae) of all mammals are arranged in a grid-like system, with rows and columns on each side of the face, much like a map. The exact number of whiskers and their arrangement varies between species; however, the grid-like pattern itself is maintained (see Fig. 3.1—the mystacial pad in a marsupial, rodent and pinniped). In the rat, the macrovibrissae are arranged in distinct caudal-rostral columns (0–7) and dorsoventral rows (A–E); there are also “straddlers” (often referred to as column 0) that do not align with the rows and are assigned the labels α , β , γ and δ (Figs. 3.1b and 3.2).

Whiskers in the same column tend to be of similar sizes (Brecht et al. 1997; Dyck 2005), with rows C, D and E being slightly longer than A and B (Haidarliu and Ahissar 2001). Whiskers in the same row have a clear pattern, increasing in length exponentially in the rostro-caudal direction, by a factor of 1.2–1.6, making

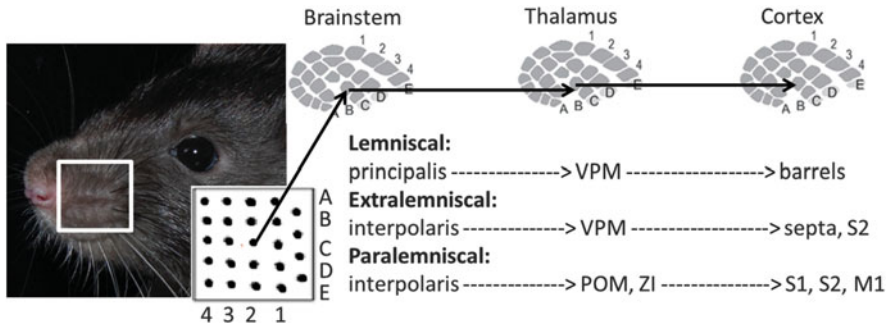


Fig. 3.2 Whisker layout and neural maps in the rat vibrissal system. Topographic maps in the brainstem (barrelettes), thalamus (barreloids) and cortex (barrels in layer iv of primary sensory cortex (*S1*)). Three pathways pass whisker information from brainstem, via the thalamus (VPM and POM) to the cortex, including other structures such as the zona incerta (*ZI*), secondary somatosensory cortex (*S2*) and motor cortex (*M1*)

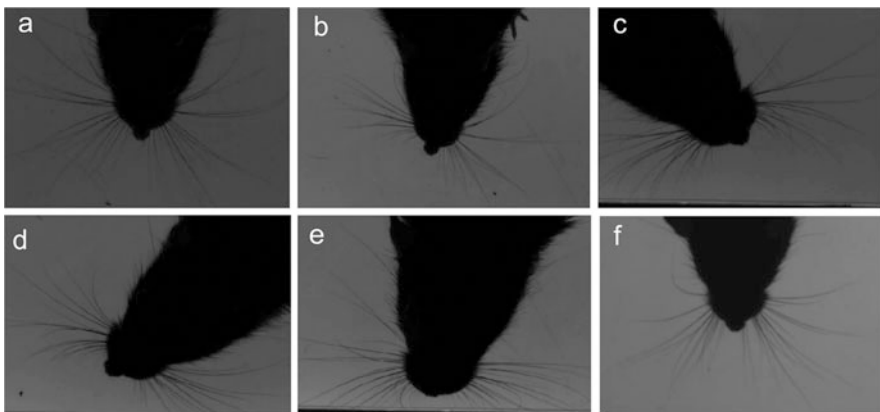


Fig. 3.3 Exploratory whisker behaviours. (a) Normal whisker positions during non-contact protraction. (b) Head-turning asymmetry, as the head is rotating rightwards, the ipsilateral whiskers are retracting, while the contralateral whiskers are positioned forwards. (c) Rapid cessation of protraction, showing a retraction on the ipsilateral *right* side and a continued protraction on the *left* side. (d) Contact-induced asymmetry, where the ipsilateral left whiskers are positioned backwards with small-amplitude movements and the contralateral right whiskers are positioned forwards with large amplitude movements. (e) Spread reduction of the whiskers following a contact (e.g. compare the whisker spread to (a)). (f) Protracting whiskers during running, increasing lookahead time

the outlying whiskers the longest (Brecht et al. 1997; Haidarliu and Ahissar 2001; Ibrahim and Wright 1975). The increasing lengths in the rostro-caudal direction allow more whiskers to touch an object, as the longer whiskers can be brought forwards to contact, even though they are more caudally positioned in the pad (e.g. see Fig. 3.3e).

As well as aiding in maximising the number of contacts on a surface, the length of the whisker also influences its resonance properties (Moore and Andermann 2005), which is the degree of vibration that occurs as a whisker is swept along a textured surface. As the length of the whisker is strongly proportional to the radius of its base, the resonance frequency is inversely proportional to whisker length, resulting in the longer, thicker, caudal vibrissae having lower vibration frequencies than the thinner, shorter whiskers (Moore and Andermann 2005). As a result, there is a frequency map along the whisker grid, dependent on whisker length, which aids the identification of frequency-dependent stimuli, such as surface roughness (Moore and Andermann 2005). This means that whiskers, as a function of their length, can passively discriminate between 35 different textures. The layout of the mystacial pad and design of the whisker field is one way in which necessary information can be quickly *filtered* from the local environment.

3.2.2 Individual Whiskers

Not only does the gross structure of the whisker field allow quick estimations of the local environment, but the fine structure of each whisker may also help to provide information about relevant aspects of the environment. Whiskers are tapered and curved and can be up to 50 mm in length in rats (*Rattus norvegicus*) and 200 mm in California sea lions (*Zalophus californianus*). As well as the variation in size and therefore resonance properties between whiskers, curvature and taper also vary. Tapering of the whisker shaft causes differences in force and moment at the base of the whisker; therefore, it is possible to identify the point of object contact along the shaft (radial distance) by incorporating taper into mechanical beam equations (Birdwell et al. 2007; Szwed et al. 2006). Whiskers tend to be more curved at their thinner tip than the base, and most object contacts occur at the tip. The direction and extent of the curvature significantly affect the force and moment at the whisker base; however, whiskers are often bent during an object contact and curvature can also be affected during whisking (see Sect. 3.4); therefore, curvature plays a more complex role in whisker signalling, which is not altogether understood but is likely to provide the animal with important information about contact location.

The overall shape of the whiskers varies greatly between different species. Pinnipeds, including sea lions, walruses and seals, use their whiskers for both hydrodynamic sensing and active touch sensing underwater (Dehnhardt et al. 2001; Dehnhardt and Mauck 2008; Glaser et al. 2011; Wieskotten et al. 2010a, b). Sea lion whiskers are smooth and oval, walrus whiskers are smooth and circular, and harbour seal whiskers are undulating and oval (Fig. 3.1c). The undulations along the shaft of the harbour seal whiskers are thought to stabilise the whiskers in a turbulent underwater environment (Hanke et al. 2010), playing much the same role as the dimples on a golf ball and tubercles on humpback whale flippers. The function of the oval and circular shapes is not yet known; however, walruses are thought to use their whiskers more for touch than the sea lion and the

harbour seal. Indeed, other touch specialists like the rat also have round, smooth whiskers (Fig. 3.1b), although they are much smaller and thinner than those of the walrus.

While the layout, shape and size of the whiskers can be thought of as being well matched to their task, it must be emphasised that the design itself is quite flexible. The whiskers themselves change in length and calibre, with a moult every 4 weeks in the rat and yearly in pinnipeds. Two whiskers can even emerge from the same follicle. Head and body movements also affect whisker position and movement (e.g. Towal and Hartmann 2006) and cause various degrees of bending of the shaft. These relative changes will impact the geometry of the whisker field, meaning it is not a fixed coordinate system (Carvell and Simons 1990). Therefore, although the individual whisker shapes and their layout conform to a matched filter design, it is worth bearing in mind that the area is continually changing and makes environmental inspections by moving and shifting reference points. This is consistent with the description of the whisker system as an active touch system, whereby the whiskers are purposely moved into salient and relevant areas of the environment to compensate for head and body movements.

3.2.3 Microvibrissae

The microvibrissae are much smaller than the macrovibrissae (<7 mm in rats) and more numerous. They are not only constrained to the mystacial pad but can also be seen on the lower jaw and upper lip (Fig. 3.1b) (Brecht et al. 1997; Welker 1964). Due to their high density of whisker sensors (87/cm² microvibrissae, compared to 2/cm² macrovibrissae in the rat), the microvibrissae are often thought of as the tactile “fovea” (Brecht et al. 1997; Grant et al. 2012). Indeed, following a macrovibrissal contact, rats tend to orient subsequent contacts onto the microvibrissae, which is a higher resolution sampling space (Grant et al. 2012). While not all mammals have microvibrissae, many, such as harbour seals and sea lions, use their denser, smaller, rostral whiskers in much the same way (Dehnhardt 1994; Dehnhardt and Dücker 1996; Grant et al. 2013a). Not only do microvibrissae allow for higher resolution tactile sampling, but their positioning on the face allows animals to also sample simultaneously with their nose (smell) and tongue (taste). Therefore, the small numbers of macrovibrissae samples are enhanced both by the density of the microvibrissae and the ability to perform simultaneous multisensory sampling of an object.

3.2.4 Matched Sensor Conclusions

The whiskers are discrete sensors that can sample from approximately 70 different points in the environment. Their increasing length caudally has evolved such that they enable as many whiskers as possible to contact a surface and, as they are tuned to resonate at specific frequencies, allows quick access to contact information. The

correspondence of the whisker shaft to its function provides a good example of matched filter design. Furthermore, the function of this system is enhanced by the presence of high-resolution microvibrissae. While the larger macrovibrissae sample areas of the local environment that may not be directly accessible to the visual system, orienting the microvibrissae to the surface of investigation allows the animal to sample at high resolution simultaneously with touch, smell and taste.

3.3 Neural Control and Maps

Despite the complexity of the resonance properties of whiskers, they are essentially “dead” cells. However, they sit within intricate and strongly innervated follicles that receive and transmit vital sensory information from the shaft, including information on force and direction (Vincent 1913). This information is then passed through multiple neural pathways to the cortex. The whisker system has received much attention in the neurosciences due to the presence of topographic maps (Fig. 3.2), which allows the sensory responses of individual whiskers to be traced precisely throughout the brain (Deschenes et al. 2003; Diamond et al. 2003; Welker 1964; Woolsey and Van der Loos 1970). The cognitive representation of the whiskers in cortex is unique as it has a direct one-to-one mapping with the layout of the mystacial pad.

3.3.1 Neural Maps

First observed by Woolsey and Van der Loos (1970), the grid-like arrangement of the whiskers can be seen in topographic maps throughout the cortex in rodents. Due to the shape of each representation of a whisker being barrel-like, these structures were termed *barrels*, and the area they were found in (layer IV of primary somatosensory cortex), the barrel cortex (Fig. 3.2). Since then, related barreloids have been found in the thalamus and barrelettes in the brainstem. Much like the visual system, the vibrissal system is bilateral and whiskers on the right-hand side project to the left-hand side of the cortex and vice versa. This means that if the left-hand whisker C2, for instance, contacted a surface, responses would be observed in the C2 equivalent area in the left-hand barrelettes, the right-hand barreloids and the right-hand barrels (Fig. 3.2). In this way, spatial and temporal information from whisker contacts can be preserved in the brain, from brainstem to cortex. Therefore, not only do the whiskers themselves conform to a matched sensor design, collecting data from ~70 contact points, but physical structures in the brain can also efficiently process temporal and spatial information from these points.

The barrel structures are relatively plastic and rely on whisker inputs in development to take shape. For instance, if some whiskers were plucked from birth, the corresponding barrels would be smaller, and neighbouring whisker barrels would be enlarged (Feldman and Brecht 2005). If a whisker is implanted at birth, then an additional barrel will appear in the corresponding place in the map (Feldman and

Brecht 2005). However, while the topographic maps are plastic and flexible to some extent, they are not able to compensate for changes in whisker shape during growth, movement and contact. Rather, these are processed by a number of pathways in the brain, which connect the barrelettes, barreloids and barrels to other important structures. This is in keeping with the suggestion by Wehner (1987) that a matched filter sense frees up the brain for more complex calculations. The main pathways involved in whisker sensing will be introduced briefly below.

3.3.2 Sensory Pathways

The base of each whisker is enclosed by a follicle within the mystacial pad where mechanoreceptors translate whisker stimulation (force and direction) into neural signals (Baumann et al. 1996; Mitchinson et al. 2004). The follicle itself is surrounded by a blood sinus (Vincent 1913), forming the follicle sinus complex (FSC) that is well endowed with a variety of nerve terminals (Baumann et al. 1996; Rice et al. 1986). Signals from the follicle are sent to the trigeminal ganglion and the trigeminal nuclei. The subnuclei *principalis*, *interpolaris* and *caudalis* all have barrelette maps, while the subnucleus *oralis* does not contain barrelettes (Waite and Tracey 1995). The trigeminal nuclei then project via three different pathways, the *lemniscal*, *paralemniscal* and *extralemniscal*, to the cortex (Fig. 3.2). In the lemniscal pathway, neurons in *principalis* project to the barreloids in the dorsomedial section of the ventral posteromedial thalamus (VPM), which projects to the barrels in barrel cortex. In the extralemniscal pathway, *interpolaris* projects to barreloids in the ventrolateral section of VPM, which projects to the septa (the area in between the barrels in barrel cortex) and the secondary somatosensory cortex (Diamond et al. 2008). In the paralemniscal pathway, the rostral area of *interpolaris* that does not contain barrelettes projects to the medial sector of the posterior nucleus (POm) of the thalamus and the zona incerta and then onto layer 5a of primary somatosensory cortex, secondary somatosensory cortex and the motor cortex. It is unlikely that this paralemniscal pathway carries any spatial information, as it does not have barrelettes; rather, it integrates information from multiple whiskers.

The exact function of each of these pathways is unknown (Diamond et al. 2008) and hypotheses vary. One hypothesis is that the paralemniscal pathway carries information about whisker movements, the extralemniscal pathway about contacts and timing, and the lemniscal pathway about whisker movements, contact and timing. However, many of the structures along these pathways project to other important brain areas, indicating that the overall system is much more interconnected and complex than once thought. One such important structure is that of the superior colliculus, which is thought to play a role in orienting (i.e. to the microvibrissae following an object contact). The superior colliculus responds quickly to vibrissal contacts and receives inputs directly from the trigeminal nuclei (Hemelt and Keller 2007). There is a topographic whisker map in the superior colliculus, but it is not as distinct as the barrel map; rather, there are overlapping organisations of the whiskers, with dorsal whiskers represented on the medial side

and ventral whiskers on the lateral side (Benedetti 1991; Dräger and Hubel 1976). The organisation of the collicular somatosensory map relies heavily on the visual map, given that whiskers more central to the visual field will project to larger areas, irrespective of their size or pad position. Indeed, perception is a multisensory experience, and rats are touching, smelling, tasting and seeing an object all at once; therefore, structures that can integrate information easily from a number of senses in a simple way help reduce computational demands.

3.3.3 Motor Control

The interactions between sensory and motor pathways are crucial to the neural control of whisker movements. Due to the emphasis in the neurosciences on tracing sensory inputs from whisker deflections, less is known about the motor pathways recruited during whisker movements. The mechanisms that drive precise whisker movement strategies during object exploration are unknown, and more is known about what drives the simple back and forth, rhythmic whisking of the whiskers.

The vibrissal motor cortex is not entirely essential for whisking (Gao et al. 2001); rather, it initiates whisking rhythms on a cycle-by-cycle basis (Berg and Kleinfeld 2003b; Friedman et al. 2006). There is evidence that the vibrissal motor cortex regulates whisking through a subcortical central pattern generator (CPG), rather than influencing whisker movements directly (Cramer and Keller 2006). Indeed, a whisking pattern generator is thought to exist in the pre-Bötzinger complex in the ventrolateral medulla of brainstem (Moore et al. 2013), an area that controls both whisking and sniffing. Therefore, not only do rats touch objects with their whiskers that are close to their nose, but they systematically touch and sniff at the same time (Cao et al. 2012; Deschênes et al. 2012; Welker 1964). Conceptually, CPG theory states that motor patterns may be produced in the absence of sensory feedback, and in reality, removal of whisking reafference (unilateral and bilateral sectioning of the infraorbital nerve) does not significantly affect whisker movements (Gao et al. 2001). That right and left whisker fields can move independently, causing whisker asymmetry, provides evidence that there are probably two distinct (right and left) CPGs that are closely coupled. On the whole, multiple mechanisms are probably responsible for generating the full movements of the vibrissae, as it is unlikely that one system or circuit could account for all the changes of behaviour that are observed in complex exploratory whisking (Cramer et al. 2007).

3.3.4 Neural Control and Maps Conclusions

We have concluded that the shape of the vibrissae and their discrete arrangement contribute to the animal's ability to sense efficiently. In addition, the mirroring of this arrangement in cortex allows for reliable spatial and temporal integration. We can see that the neural architecture has the capacity to efficiently integrate touch,

smell and sight information, which could be used to enhance tactile information from a small number of macrovibrissae sensors. That the architecture of the system involves a number of different brain structures allows the system to both sense and control changes in the positioning of the whiskers, which leads to the range of sensory behaviours that are observed.

3.4 Whisker Behaviour in Rats

So far, we have discussed the role of the whiskers as matched filters—70 discrete sensors that collect information from the environment, transmitting tactile information via mechanoreceptors at the base of the whisker follicle, and through distinct neural pathways into cortical topographic maps. Any body and head movements we have discussed thus far alter the arrangement of the whisker fields and make processing tactile sensory information more complex. However, the brain carries information about whisker movements, timings and contacts to therefore compensate and incorporate these movements. Moreover, movement is an inherent characteristic of an active sensing system; and it is the quick and precise alteration of whisker position that enables the animal to collect salient and relevant information from areas in the environment. We will explore the range and type of movements that rat whiskers can make and consider the musculature—the driving force behind the whisker's movements.

3.4.1 Whisking

When a sensory system has a limited number of sensors, it is imperative that these sensors are positioned in an efficient manner so as to maximise relevant information from a region of interest. During normal non-contact protraction, the whisker tips scan a large area right in front of the face. This is caused by (i) the changeable spread of the whisker array and (ii) the effect of torsion rotating the whisker tips forwards. As whiskers protract forwards, they become more spread out (Fig. 3.3a) and they bunch together in the retraction stage (Sachdev et al. 2001). This enables the sensors to sample from a wider area in front of the face, due to being more spread out when they are positioned forwards. At the same time, torsion on the whiskers enables the whisker tips to face forwards during protraction and downwards during retraction. The ability to increase the scanning area by directing the whisker tips to the front of the face might be especially useful during forward locomotion, for example.

Scanning the area around the head is an important function of the vibrissae and is suggestive that whiskers play a key role in guiding locomotion and navigation. Another example of this is head-turning asymmetry (Fig. 3.3b), whereby asymmetric positioning of the whiskers allows whiskers to scan ahead of the area that the head is moving into, a behaviour comparable to a saccade in the visual system (Towal and Hartmann 2006).

3.4.2 Exploratory Whisking During Object Contact

Whisking without contact has given us good insights into some components of whisker kinematics; however, it was only by observing rats exploring objects that the range of behavioural control came to light. During object exploration, whisker movements alter substantially in terms of velocity, frequency, bilateral coupling, spread and torsion. Changes in these parameters can be described using a control strategy termed *minimal impingement maximal contact*: the whiskers make light, gentle touches while at the same time maximising the number of whisker contacts and the amount of time in contact with the surface. For example, when the whiskers contact an object, a rat may increase their whisker frequency to increase the sampling rate of the object (maximal contact). They will reduce the angular position of the whisker, to enable a gentle touch against the surface (minimal impingement), and the retraction velocity will also reduce significantly, allowing the whiskers to spend more time in contact with the surface during the retraction stage of the whisk (maximal contact) (Grant et al. 2009). Whisker spread will also be reduced substantially (Fig. 3.3e), so that more whiskers are “bunched up” and contact a surface (Grant et al. 2009). This simple strategy alone gives a perfect example of a sensory filter, whereby the position and movement of the tactile sensors are altered in order to manipulate the amount and type of information they collect.

Whisker movements can become bilaterally decoupled following an object contact, in terms of both symmetry (angular position) and synchrony (timing). *Contact-induced asymmetry* occurs following a unilateral contact, whereupon the whiskers on the side furthest from the contact (contralateral side) increase in amplitude, maximising the number of whisker contacts, while those closest to the contact (ipsilateral side) reduce their amplitude to enable a light touch (Mitchinson et al. 2007) (Fig. 3.3d). Asynchrony can also occur at very fast timescales; this is termed *rapid cessation of protraction* (RCP). RCP occurs at around 13 ms following a contact. During RCP, the ipsilateral whiskers stop protracting soon after they have contacted an object while the contralateral whiskers continue to complete their protraction trajectory (Mitchinson et al. 2007) (Fig. 3.3c). Allowing a light touch on the ipsilateral side is thought to enable clearer signals at the whisker bases and complies with the minimal impingement aspect of control. The quick timescale of RCP suggests that it might be initiated by lower level brain areas such as the brainstem or superior colliculus (Mitchinson et al. 2007).

3.4.3 Mystacial Musculature

Whisking movements and contact-related behaviours are driven by specialised muscle architecture. During whisking, whiskers are moved forwards (protracted) by intrinsic muscles that form a sling around each follicle (Berg and Kleinfeld 2003a; Dorfl 1982). Each individual whisker has its own intrinsic muscle looped around its base and attached to the adjacent caudal whisker in the same row. As the intrinsic muscle contracts, the follicle is moved backwards and the whiskers are

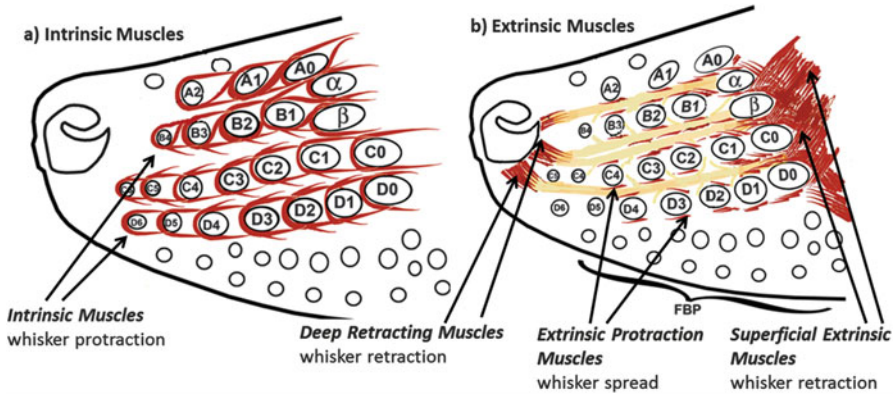


Fig. 3.4 Mystacial musculature in small mammals. Based on work in the opossum *Monodelphis domestica* (Grant et al. 2013b), this figure shows the general intrinsic (a) and extrinsic (b) musculature found in whisking animals, including opossums, rats and guinea pigs

protracted forwards (Dörfl 1982). Due to the chain-like architecture of the intrinsic muscles, meaning that each whisker is attached to another in the same row, whiskers tend to move forwards together. This design of intrinsic muscles causes the change in spread and torsional forces during non-contact whisking.

As well as the intrinsic muscles, thus named because they are attached within the mystacial pad, there are also three sets of extrinsic muscles that are attached externally to the pad—and only recently fully described in rodents (Haidarliu et al. 2010) and marsupials (Grant et al. 2013b). Both slow and fast muscle fibres can be found in intrinsic and extrinsic muscles. The *deep retracting muscles* of the extrinsics attach near the nose, and contractions of these muscles deep below the mystacial pad cause the whiskers to retract. These muscles are thought to control retraction velocity during object exploration (Grant et al. 2013b). The *superficial extrinsic muscles* are attached caudal to the mystacial pad, and their contraction pulls the mystacial pad back resulting in whisker retractions. These muscles are thought to control retraction velocity during non-contact whisking (Grant et al. 2013c). The *extrinsic protraction muscles* are inserted throughout the pad but are attached towards the nose. Their contraction causes whiskers to “bunch up” during protraction and controls the reduction in spread during object exploration (Grant et al. 2009, 2013b; Haidarliu et al. 2010) (Fig. 3.4).

3.4.4 Behavioural Conclusions

Whisker touch sensors are moved in a precise manner to control the quality and amount of information that can be gathered from the environment. The ability to move these discrete sensors quickly and accurately justifies why the 70 sensors are sufficient for tactile sensing, as they are able to focus on important regions of interest in the sample space.

3.5 Ecology and Evolution of Active Touch

By observing the large variation in whisker movements, it is clear that the rat has vast control over its whiskers and recruits different strategies in order to successfully complete individual tasks (Berg and Kleinfeld 2003a; Carvell and Simons 1990; Harvey et al. 2001). Whiskers are moved and positioned differently on salient areas of the environment, depending on the task at hand. For instance, they will be positioned on object surfaces to gauge texture information and on object edges to judge shape. Early studies in vibrissal sensing, although not measuring whisker movements or control strategies, focussed on the function of whiskers (Vincent 1912), usually by trimming or removing all or some of the whiskers and analysing the resulting effect on overall behaviour. These studies discovered that vibrissae have a range of functions that includes guiding locomotion, swimming, wall-following and gap crossing, as well as playing a large role in social, feeding and predatory behaviours.

3.5.1 Vibrissal Function in Rats

The whiskers are thought to play a role in locomotion during walking, running and climbing. While walking, the head of the rat is often angled downwards, the more ventral whiskers being frequently in contact with the floor and often dragging along it relatively passively. As the rat whisks, torsional forces will enable the more dorsal whiskers to touch the floor and the more ventral whiskers to touch the ceiling (Knutsen et al. 2008). This enables them to continually sample the position just ahead of the body, guiding a safe passage through the environment. Rats show a shift in whisking strategy according to the speed at which they are locomoting. As they gain speed and locomote more quickly (at speeds as high as 150 cm/s), they alter the position and movement of their whiskers from sampling a wide area surrounding the snout (so as to explore and make contacts with many surfaces) to focussing the whiskers on the salient area in front of the snout (see Figs. 3.5 and 3.3f) (Arkley et al. 2014). This increase in whisker protraction and decrease in whisk amplitude provide the function of protecting the delicate snout area by attending to the direction of travel and, importantly, any potential obstacles in the path of the locomoting animal.

Rats also commonly wall-follow by sampling a surface with the ipsilateral whisker field relatively passively while still actively sampling the immediate environment as they pass by with the contralateral whisker field (Barnett 2007) (Fig. 3.5). Rats use this “thigmotaxis” behaviour in order to remain in contact with vertical walls, enabling the rat to travel adjacent to them and navigate in dark burrows (Barnett 2007)—a key behaviour for finding quality habitats.

Macrovibrissae can judge both size and shape. An example can be found in a study by Brecht et al. (1997) who tested whether the rat could find sweet-tasting small triangles amongst distractor cookies of different sizes and shapes. The rats employed both their macro- and microvibrissae to complete the task successfully,

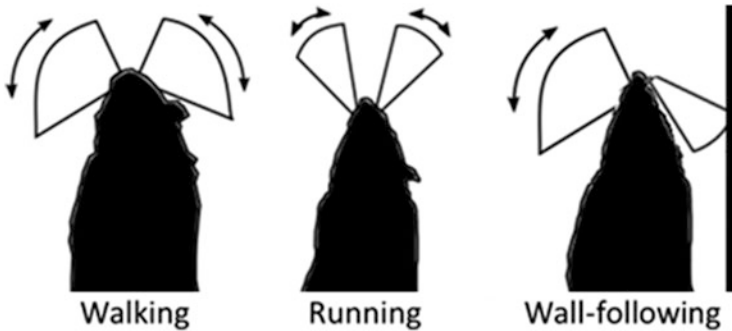


Fig. 3.5 Whisker behaviour during forward locomotion. Rats engage in exploratory whisking during walking, focussed positioning during running and asymmetric whisking during wall-following

and the authors proposed from their findings that the macrovibrissae performed the task of distance detectors, with the longest, most caudal whiskers decoding the minimal distance to a contact with a cookie shape. The microvibrissae, on the other hand, seemed to assist in tactile object recognition at a smaller scale, perhaps being employed to judge differences in cookie shape or texture. Harvey et al. (2001) went on to show that the macrovibrissae alone have the ability to judge between object size, shape and texture, by devising an experiment allowing only the macrovibrissae to touch different objects.

Texture discrimination is important to rats as they judge their food in terms of taste and texture (Barnett 2007). They prefer soft, finely divided foods to hard coarse ones (Barnett 2007). Indeed, laboratory rats will eat softer grains and leave harder ones, yet will consume either when soaked in water (Carlson and Hoelzel 1949). Texture differentiation using the whiskers is a widely studied area in tactile sensing, with many experiments being carried out to investigate its neuronal underpinnings. However, behavioural studies also exist and date back as long ago as Vincent's observations in 1912. In her study, rats were rewarded by selecting to run down a pathway with corrugated walls rather than one of two smooth pathways. The rats varied their approaches to gauging the texture of the passage greatly; some used their whiskers lightly to touch the walls, whereas others used their microvibrissae and macrovibrissae. Furthermore, texture discrimination is linked to the resonance properties of the whiskers; while rats can judge texture with only one whisker, they are much more efficient with multiple whiskers.

As well as observing the ability of the whiskers to discriminate between small-scale object properties, larger scale environmental tasks have also been conducted, such as distance and location detection. It has been found, for instance, that rats use their whiskers to judge a safe gap size to cross (Jenkinson and Glickstein 2000). They can also discriminate between different-sized apertures (Krupa et al. 2001) and have the ability to compare distance information from the whiskers on both the left- and right-hand side of the face (Shuler et al. 2001). The ability to judge

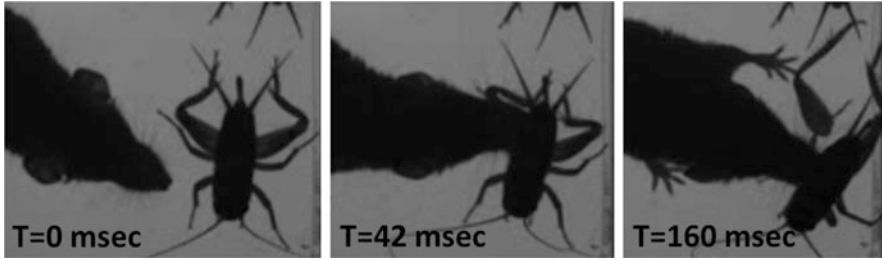


Fig. 3.6 Etruscan shrew hunting for crickets in the dark. The whiskers contact a hind leg (0 ms) and prompt the shrew to bite it (42 ms), the leg is removed and the shrew then targets the thorax in further attacks (160 ms)

distance and position is key in prey capture. Rats will catch and consume insects, such as locusts (Christie et al. 1990) and crickets (Ivanco et al. 1996). Although no data exists for rats, Etruscan shrews have been found to primarily use their whiskers to guide attacks on crickets, targeting certain areas on the legs and trunk (Fig. 3.6) (Anjum et al. 2006).

Whiskers are also involved in social interactions; they are used in facial touch and guide the orientation of one animal to another (Wolfe et al. 2011). Rats tend to touch their whiskers together when they first encounter one another. When rats “box”, a form of upright aggressive behaviour, the defending rat appears to attempt to keep whisker-whisker contact, in order to prevent or detect a lunge from its opponent (Ahl 1986; Barnett 2007). Boxing does not usually occur in animals that have had their whiskers removed, and the behaviour is usually replaced by “freezing” in these animals, which causes greater wounds (Ahl 1986; Wolfe et al. 2011). Vibrissal removal has been associated with an emotional component and can cause a decrease in motivation in the laboratory rat (Ahl 1986; Vincent 1912). Some rats even engage in barbing, where they remove another’s whiskers, usually from an animal lower in the dominance hierarchy.

Rat’s vibrissae have also been suggested to be associated with balance, although balance in the rat is mainly attributed to the tail (Barnett 2007). Following whisker removal, rats alter their postures and perform badly in edge-following tasks, often losing their balance as if they were unable to locate the edge successfully (Gustafson and Felbain-Keramidas 1977; Vincent 1912). That the rat tends to sample using both olfactory and tactile stimuli during environmental explorations (Welker 1964) has led to the suspicion that the vibrissae might also act as a funnel of olfactory cues to the nostrils. Indeed, protraction of the whiskers coincides with inhalation, which lends support to this hypothesis (Cao et al. 2012; Deschênes et al. 2012; Welker 1964); however, only circumstantial evidence exists for this function.

3.5.2 Vibrissal Function in Other Mammals

The majority of vibrissal research has focussed on rodent vibrissae, in particular the rat, due to the ease of studying them in the laboratory. However, some studies have considered aspects of vibrissal behaviour and function in other mammals. Small mammals including opossums, hamsters, guinea pigs and shrews have had their whisker movements measured, showing that they also move their whiskers (Anjum et al. 2006; Grant et al. 2013b; Haidarliu and Ahissar 1997); however, they move them less often and without the same level of control as the rat. The Etruscan shrew has been studied extensively in terms of vibrissal-guided prey capture, and (as discussed above) their whiskers are thought to guide the location of attacks on prey items (Anjum et al. 2006).

Marine mammals' vibrissae, such as pinnipeds, have also excited a lot of interest. The pinniped whisker system is said to be even more efficient than that of terrestrial mammals, owing to the fact that their whiskers have ten times more nerve fibres and are unaffected by temperature changes in the water (Dehnhardt et al. 1998; Hyvärinen 1989; Mauck et al. 2000; Rice et al. 1986). Pinnipeds do not continually move their whiskers back and forth but can protract them and position them onto surfaces (Grant et al. 2013a; Milne and Grant 2014). Walruses, sea lions and seals have all been found to use their whiskers to judge size, shape and texture (Dehnhardt 1994; Dehnhardt et al. 2001; Hyvärinen 1989). Seals and sea lions also use their whiskers as hydrodynamic sensors, to sense and follow the wakes given off by fish as they swim through the water (Dehnhardt and Mauck 2008; Glaser et al. 2011; Wieskotten et al. 2010a, b), aiding in prey localisation and capture. Sirenians, such as manatees, can also use their whiskers to judge size, shape and texture (Reep et al. 2001) and, in addition, employs their facial whiskers to grasp food and move it towards their mouth (Reep et al. 2001), much like how we use our hands. Another interesting marine mammal is the bottlenose dolphin, which is born with vibrissae; however, these fall out within the first week of life and the follicles that remain are used for electrosensing (Czech-Damal et al. 2011).

Moveable whiskers have been documented in many orders, including Marsupialia (grey short-tailed opossum), Insectivora (Etruscan shrew), Rodentia (rat, mice, hamsters) and Carnivora (pinnipeds). There have been no observations of moveable whiskers in the primates; however, nocturnal, arboreal primates do have the muscle structures, including the intrinsic muscles, that could enable whisker movements, even though they choose not to employ them in this manner (Muchlinski et al. 2013). Moreover, both barrelettes and barreloids have been found in the nocturnal primate *Otolemur garnettii* (Sawyer et al. 2015). Indeed, that so many mammalian orders have facial vibrissae, and that they also have a common muscle and neural architecture, has important implications for mammalian evolution.

3.5.3 Evolution

The evolution of mammals can be defined by a number of stages, including the ability to thermoregulate and the restructuring of the inner ear and cortex. Hair was thought to play a significant role in tactile sensing prior to thermoregulation in the first mammals (Maderson 1972, 2003) and was an important driver in mammalian brain evolution, specifically in the cortex (Rowe et al. 2011). Fossil evidence suggests that the first eutherian (placental) mammals were nocturnal and arboreal (Ji et al. 2002; Rowe et al. 2011) and tactile hairs might well have played a key role in guiding locomotion as these animals travelled through the trees in the dark, much like the role whiskers play in present-day nocturnal, arboreal mammals.

Studies using the model primitive mammal, the opossum (*Monodelphis domestica*), have found that they move their whiskers in a very similar way to rodents, even though their last common ancestor was an early mammal of the Triassic period living more than 160 million years ago (Luo et al. 2011; Mitchinson et al. 2011). It has been found that the opossum has intrinsic whisker muscles much like that of the rodents; however, reductions in certain sets of extrinsic muscles (the deep retracting and extrinsic protracting muscles) cause an absence of spread and retraction control during object exploration (Grant et al. 2013b). The presence of a similar muscle architecture in marsupials and rodents suggests that a common mammalian ancestor might have exploited their sense of whisker touch, even having moveable whiskers. Indeed, small, nocturnal and arboreal mammals have been found to have longer vibrissae with a more densely packed vibrissal field than that of ground-dwelling and burrowing mammals (Ahl 1986; Lyne 1959; Pocock 1914). This suggests that vibrissae are important in tree-climbing, nocturnal mammals. While vibrissal morphology might vary between different species, the grid-like layout of the whiskers is conserved in mammals, even in those that do not have moveable whiskers.

3.5.4 Conclusions of Ecology and Evolution of Active Touch

The ability of whiskers to quickly and precisely alter their position and movement allows them to fulfil many functions. In particular, the area of interest that the whiskers are directed towards can increase in focus and change in position, depending on whether an animal is locomoting forwards, following a wall, exploring an object or hunting for prey. Whiskers play a primary role in guiding movements of nocturnal, arboreal mammals, including marsupials, insectivores, rodents and even primates. That the spatial arrangement and musculature of the whiskers are preserved from marsupials to primates suggests that the first mammals may have had whiskers. In addition, because the early mammals were thought to be nocturnal climbers, they may also have had moveable whiskers. Indeed, the ability for the sensor to move is key to them being a successful matched filter. That the 70 sensors can be focussed in front of the face during forward motion, while also

taking quick samples around the side of the animal, enables them to be the primary sense in mammals that live in dark environments.

3.6 Active Touch Sensing as a Matched Filter Design

It is astonishing that mammals can use a discrete number of only around 70 sensors (in rat) to do so many different tasks, including discriminating object textures, sizes, shapes and positions with implications for social, predatory, locomotor and navigation behaviours. Primarily, these sensors act as matched filters, in that their layout, shape and length are well adapted for positioning onto surfaces. Secondly, physical structures in the brain can efficiently process temporal and spatial information from these sensors as they have the same topography. Thirdly, these sensors are able to be quickly and precisely positioned so as to maximise information from a surface, using a specific set of muscles and strategic behaviours. Without the active positioning of these sensors, they would be unable to gather sufficient amounts of information from the environment to complete all these tasks competently, and furthermore, they would waste much energy in collecting unnecessary information.

The position of the whiskers on the head enables tactile sampling during head rotations and locomotion. Forward locomotion is a good example of the region of whisker interest being manipulated (Fig. 3.5). While moving forwards in an area of space, the slowly moving, exploring rat spreads its whisker tips out in front of the face (Fig. 3.5); during fast-paced locomotion, the rat will focus the whisker field to a narrow area of salience directly in front of the snout to detect obstacles. Similarly, if the animal is wall-following and moving forwards, ipsilateral whiskers will be fairly passive against the wall while contralateral whiskers actively explore the area in front and to the contralateral side of the face, in a behaviour termed contact-induced asymmetry (Fig. 3.5). These shifts in the positioning of the sensors is task dependent and thought to correspond to the *zone of attention*, or the region of space that the animal is attending to (Mitchinson and Prescott 2013). During object contact, whiskers bunch up onto a surface, enabling the maximum number of surface contacts to focus on certain areas of interest, such as the edge of an object during shape discrimination, or a cricket's thorax during prey localisation.

It is worth bearing in mind, however, that these 70 whiskers do not act alone in sensory processing. As well as the ~70 macrovibrissae, the numerous, denser microvibrissae are also used during object exploration, giving a higher resolution sampling area for texture and shape tasks. In addition, the position of the whiskers allows for simultaneous multisensory sampling of the same region of the environment with vision, smell and taste. Related brain regions then efficiently process these senses by integrating spatial maps, such as in the superior colliculus, or entraining rhythms, such as in the brainstem pattern generator.

While animals do actively position their sensors onto areas of interest, it is impossible for a limited number of sensors to be everywhere. Indeed, it has been observed that rats can collide with small objects, such as sharp corners or poles that fall outside of the whisker field. Collisions usually occur right on the nose, where

the two whisker fields do not overlap. This region in particular does not feature in the rat visual map (Wallace et al. 2013) and the microvibrissae are too small to detect contact prior to a collision. However, in a realistic environment, these collisions are rarely seen. Wehner (1987) acknowledged that matched filters cannot include every variation in the world but that they work well enough that these errors are not eradicated through natural selection.

3.7 Conclusions

The whisker system is an elegant example of a matched filter design. The spatial arrangement of a number of discrete sensors on either side of an animal's face has been preserved from the first mammals and can be seen in extant mammals from marsupials to primates. The positioning of the whiskers also places them in a prime area to sample ahead during locomotion and head movements. Whisker specialists such as the rat have areas of the brain that are topologically mapped to the same arrangement of the whiskers, improving the neural processing efficiency of temporal and spatial information. The rat can also actively move these sensors to position them in their local environment in order to maximise their sensory potential. In this way, whiskers have become a primary sense in mammals that navigate in dark and complex environments, including insectivores, rodents and pinnipeds.

References

- Ahl AS (1986) The role of vibrissae in behavior – a status review. *Vet Res Commun* 10:245–268
- Anjum F, Turni H, Mulder PG, van der Burg J, Brecht M (2006) Tactile guidance of prey capture in Etruscan shrews. *Proc Natl Acad Sci U S A* 103:16544–16549
- Arkley K, Grant RA, Mitchinson B, Prescott TJ (2014) Strategy change in vibrissal active sensing during rat locomotion. *Curr Biol* 24(13):1507–1512
- Barnett SA (2007) *The rat: a study in behaviour*. Aldine Transaction, London
- Baumann KI, Chan E, Halata Z, Senok SS, Yung WH (1996) An isolated rat vibrissal preparation with stable responses of slowly adapting mechanoreceptors. *Neurosci Lett* 213:1–4
- Benedetti F (1991) The postnatal emergence of a functional somatosensory representation in the superior colliculus of the mouse. *Dev Brain Res* 60(1):51–57
- Berg RW, Kleinfeld D (2003a) Rhythmic whisking by rat: retraction as well as protraction of the vibrissae is under active muscular control. *J Neurophysiol* 89:104–117
- Berg RW, Kleinfeld D (2003b) Vibrissa movement elicited by rhythmic electrical microstimulation to motor cortex in the aroused rat mimics exploratory whisking. *J Neurophysiol* 90:2950–2963
- Birdwell JA, Solomon JH, Thajchayapong M, Taylor MA, Cheely M, Towal RB, Conradt J, Hartmann MJZ (2007) Biomechanical models for radial distance determination by the rat vibrissal system. *J Neurophysiol* 98:2439–2455
- Brecht M, Preilowski B, Merzenich MM (1997) Functional architecture of the mystacial vibrissae. *Behav Brain Res* 84(1–2):81–97
- Bugbee NM, Eichelman BS (1972) Sensory alterations and aggressive behaviour in the rat. *Physiol Behav* 8:981–985
- Cao Y, Roy S, Sachdev RN, Heck DH (2012) Dynamic correlation between whisking and breathing rhythms in mice. *J Neurosci* 32:1653–1659

- Carlson AJ, Hoelzel F (1949) Influence of texture of food on its acceptance by rats. *Science* 109:63–64
- Carvell GE, Simons DJ (1990) Biometric analyses of vibrissal tactile discrimination in the rat. *J Neurosci* 10(8):2638–2648
- Christie D, Terry P, Oakley DA (1990) The effect of unilateral anteromedial cortex lesions on prey-catching and spatio-motor behaviour in the rat. *Behav Brain Res* 37:263–268
- Cramer NP, Keller A (2006) Cortical control of a whisking central pattern generator. *J Neurophysiol* 96:209–217
- Cramer N, Li Y, Keller A (2007) The whisking rhythm generator: a novel mammalian network for the generation of movement. *J Neurophysiol* 97(3):2148–2158
- Czech-Damal NU, Liebschner A, Miersch L, Klauer G, Hanke FD, Marshall C, Dehnhardt G, Hanke W (2011) Electroreception in the Guiana dolphin (*Sotalia guianensis*). *Proc R Soc B* 279(1729):663–668
- Dehnhardt G (1994) Tactile size discrimination by a California sea lion (*Zalophus californianus*) using its mystacial vibrissae. *J Comp Physiol A* 175:791–800
- Dehnhardt G, Dücker G (1996) Tactual discrimination of size and shape by a California sea lion (*Zalophus californianus*). *Anim Learn Behav* 24(4):366–374
- Dehnhardt G, Kaminski A (1995) Sensitivity of the mystacial vibrissae of harbor seals (*Phoca vitulina*) for size differences of actively touched objects. *J Exp Biol* 198:2317
- Dehnhardt G, Mauck B, Bleckmann H (1998) Seal whiskers detect water movements. *Nature* 394(6690):235–236
- Dehnhardt G, Mauck B (2008) Mechanoreception in secondarily aquatic vertebrates. In: Thewissen JGM, Nummela S (eds) *Sensory evolution on the threshold—adaptations in secondarily aquatic vertebrates*. University of California Press, Berkeley, pp 295–314
- Dehnhardt G, Mauck B, Hanke W, Bleckmann H (2001) Hydrodynamic trail-following in harbor seals (*Phoca vitulina*). *Science* 293:102–104
- Deschenes M, Timofeeva E, Lavallee P (2003) The relay of high-frequency sensory signals in the Whisker-to-barreloid pathway. *J Neurosci* 23:6778–6787
- Deschênes M, Moore J, Kleinfeld D (2012) Sniffing and whisking in rodents. *Curr Opin Neurobiol* 22(2):243–250
- Diamond ME, Petersen RS, Harris JA, Panzeri S (2003) Investigations into the organization of information in sensory cortex. *J Physiol Paris* 97:529–536
- Diamond ME, von Heimendahl M, Knutsen PM, Kleinfeld D, Ahissar E (2008) ‘Where’ and ‘what’ in the whisker sensorimotor system. *Nat Rev Neurosci* 9:601–612
- Dorfl J (1982) The musculature of the mystacial vibrissae of the white-mouse. *J Anat* 135:147–154
- Dräger UC, Hubel DH (1976) Topography of visual and somatosensory projections to mouse superior colliculus. *J Neurophysiol* 39(1):91–101
- Dyck RH (2005) Vibrissae. In: Wishaw IQ, Kolb B (eds) *The behavior of the laboratory rat: a handbook with tests*. Oxford University Press, Oxford, pp 81–89
- Feldman DE, Brecht M (2005) Map plasticity in somatosensory cortex. *Science* 310(5749):81
- Friedman WA, Jones LM, Cramer NP, Kwegyir-Afful EE, Zeigler HP, Keller A (2006). Anticipatory activity of motor cortex in relation to rhythmic whisking. *J Neurophysiol*, 95(2):1274–1277
- Gao P, Bermejo R, Zeigler HP (2001) Whisker deafferentation and rodent whisking patterns: behavioral evidence for a central pattern generator. *J Neurosci* 21:5374–5380
- Glaser N, Wieskotten S, Otter C, Dehnhardt G, Hanke W (2011) Hydrodynamic trail following in a California sea lion (*Zalophus Californianus*). *J Comp Physiol A* 197:141–151
- Grant R, Mitchinson B, Fox C, Prescott TJ (2009) Active touch sensing in the rat: anticipatory and regulatory control of whisker movements during surface exploration. *J Neurophysiol* 101:862–874
- Grant RA, Sperber A, Prescott TJ (2012) The role of orienting in vibrissal touch sensing. *Front Behav Neurosci* 6:39

- Grant RA, Weiskotten S, Wengst N, Prescott TJ, Dehnhardt G (2013a) Vibrissal touch sensing in the harbour seal (*Phoca vitulina*): how do seals judge size? *J Comp Physiol A* 199(6):521–533, In Special Issue on the Sensory Biology of Aquatic Mammals
- Grant RA, Haidarliu S, Kennerley NJ, Prescott TJ (2013b) The evolution of active vibrissal sensing in mammals: evidence from vibrissal musculature and function in the marsupial opossum *Monodelphis domestica*. *J Exp Biol* 216(18):3483–3494
- Grant RA, Sharp PS, Kennerley AJ, Berwick J, Grierson A, Ramesh T, Prescott TJ (2013c) Abnormalities in whisking behaviour are associated with lesions in brain stem nuclei in a mouse model of amyotrophic lateral sclerosis. *Behav Brain Res* 259:274–283
- Grant R, Itskov PM, Towal B, Prescott TJ (eds) (2014) Active touch sensing. *Frontiers E-books*
- Gustafson JW, Felbain-Keramidas SL (1977) Behavioral and neural approaches to the function of the mystacial vibrissae. *Psychol Bull* 84:477–488
- Haidarliu S, Ahissar E (1997) Spatial organization of facial vibrissae and cortical barrels in the guinea pig and golden hamster. *J Comp Neurol* 385:515–527
- Haidarliu S, Ahissar E (2001) Size gradients in the barreloids in the rat thalamus. *J Comp Neurol* 429:372–387
- Haidarliu S, Simony E, Golomb D, Ahissar E (2010) Muscle architecture in the mystacial pad of the rat. *Anat Rec* 293:1192–1206
- Hanke W, Witte M, Miersch L, Brede M, Oeffner J, Michael M, Hanke F, Leder A, Dehnhardt G (2010) Harbor seal vibrissa morphology suppresses vortex-induced vibrations. *J Exp Biol* 213:2665–2672
- Harvey MA, Bermejo R, Zeigler HP (2001) Discriminative whisking in the head-fixed rat: optoelectronic monitoring during tactile detection and discrimination tasks. *Somatosens Mot Res* 18:211–222
- Hemelt ME, Keller A (2007) Superior sensation: superior colliculus participation in rat vibrissa system. *BMC Neurosci* 8(1):12
- Hyvärinen H (1989) Diving in darkness: whiskers as sense organs of the Ringed seal (*Phoca hispida*). *J Zool* 238:663–678 system. *BMC Neurosci* 8:12
- Ibrahim L, Wright EA (1975) The growth of rats and mice vibrissae under normal and some abnormal conditions. *J Embryol Exp Morphol* 33:831–844
- Ivanco TL, Pellis SM, Whishaw IQ (1996) Skilled forelimb movements in prey catching and in reaching by rats (*Rattus norvegicus*) and opossums (*Monodelphis domestica*): relations to anatomical differences in motor systems. *Behav Brain Res* 79:163–181
- Jenkinson EW, Glickstein M (2000) Whiskers, barrels, and cortical efferent pathways in gap crossing by rats. *J Neurophysiol* 84:1781–1789
- Ji Q, Luo Z-X, Yuan C-X, Wible JR, Zhang J-P, Georgi JA (2002) The earliest known eutherian mammal. *Nature* 416:816–822
- Johansson RS, Vallbo AB (1979) Tactile sensibility in the human hand: relative and absolute densities of four types of mechanoreceptive units in glabrous skin. *J Physiol* 286:283–300
- Knutsen PM, Biess A, Ahissar E (2008) Vibrissal kinematics in 3D: tight coupling of azimuth, elevation, and torsion across different whisking modes. *Neuron* 59:35–42
- Krupa DJ, Brisben AJ, Nicolelis MA (2001) A multi-channel whisker stimulator for producing spatiotemporally complex tactile stimuli. *J Neurosci Methods* 104:199–208
- Luo Z-X, Yuan C-X, Meng Q-J, Ji Q (2011) A Jurassic eutherian mammal and divergence of marsupials and placentals. *Nature* 476:442–445
- Lyne AG (1959) The systematic and adaptive significance of the vibrissae in the Marsupialia. *Proc Zool Soc Lond* 133:79–133
- Maderson PFA (1972) When? Why? And how? Some speculations on the evolution of the vertebrate integument. *Am Zool* 12:159–171
- Maderson PFA (2003) Mammalian skin evolution: a re-evaluation. *Exp Dermatol* 12:233–236
- Mauck B, Eysel U, Dehnhardt G (2000) Selective heating of vibrissal follicles in seals (*Phoca vitulina*) and dolphins (*Sotalia fluviatilis guianensis*). *J Exp Biol* 203(14):2125–2131

- Milne AO, Grant RA (2014) Characterisation of whisker control in the California sea lion (*Zalophus californianus*) during a complex, dynamic sensorimotor task. *J Comp Physiol A* 200(10):871–879
- Mitchinson B, Prescott TJ (2013) Whisker movements reveal spatial attention: a unified computational model of active sensing control in the rat. *PLoS Comput Biol* 9(9):e1003236
- Mitchinson B, Gurney KN, Redgrave P, Melhuish C, Pipe AG, Pearson M, Gilhespy I, Prescott TJ (2004) Empirically inspired simulated electro-mechanical model of the rat mystacial follicle-sinus complex. *Proc Biol Sci* 271:2509–2516
- Mitchinson B, Martin CJ, Grant RA, Prescott TJ (2007) Feedback control in active sensing: rat exploratory whisking is modulated by environmental contact. *Proc Biol Sci* 274:1035–1041
- Mitchinson B, Grant RA, Arkley KP, Perkon I, Prescott TJ (2011) Active vibrissal sensing in rodents and marsupials. *Phil Trans B* 366(1581):3037–3048
- Moore CI, Andermann ML (2005) The vibrissa resonance hypothesis. In: Somatosensory plasticity, Ebner FF (ed) CRC Press, Taylor & Francis, London, pp 21–60
- Moore JD, Deschenes M, Furuta T, Huber D, Smear MC, Demers M, Kleinfeld D (2013) Hierarchy of orofacial rhythms revealed through whisking and breathing. *Nature* 497:205–210
- Muchlinski MN, Durham EL, Smith TD, Burrows AM (2013) Comparative histomorphology of intrinsic vibrissa musculature among primates: implications for the evolution of sensory ecology and “face touch”. *Am J Phys Anthropol* 150(2):301–312
- Pocock RI (1914) On the facial vibrissae of mammalia. *Proc Zool Soc Lond* 84:889–912
- Prescott TJ, Diamond ME, Wing AM (2011) Active touch sensing. *Phil Trans R Soc Lond B: Biol Sci* 366(1581):2989–2995
- Reep RL, Stoll ML, Marshall CD, Homer BL, Samuelson DA (2001) Microanatomy of facial vibrissae in the Florida manatee: the basis for specialized sensory function and oripulation. *Brain Behav Evol* 58:1–14
- Rice FL, Mance A, Munger BL (1986) A comparative light microscopic analysis of the sensory innervation of the mystacial pad. I. Innervation of the vibrissal follicle-sinus complexes. *J Comp Neurol* 252:154–174
- Rowe TB, Macrini TE, Luo Z-X (2011) Fossil evidence on origin of the mammalian brain. *Science* 332(6032):955–957
- Sachdev RN, Sellien H, Ebner F (2001) Temporal organization of multi-whisker contact in rats. *Somatosens Mot Res* 18:91–100
- Sachdev RNS, Sato T, Ebner FF (2002) Divergent movement of adjacent whiskers. *J Neurophysiol* 87:1440–1448
- Sawyer EK, Liao CC, Qi HX, Balaram P, Matrov D, Kaas JH (2015) Subcortical barrelette-like and barreloid-like structures in the prosimian galago (*Otolemur garnettii*). *Proc Natl Acad Sci* 112(22):7079–7084
- Shuler MG, Krupa DJ, Nicolelis MA (2001) Integration of bilateral whisker stimuli in rats: role of the whisker barrel cortices. *Cereb Cortex* 12:86–97
- Szwed M, Bagdasarian K, Blumenfeld B, Barak O, Derdikman D, Ahissar E (2006) Responses of trigeminal ganglion neurons to the radial distance of contact during active vibrissal touch. *J Neurophysiol* 95:791–802
- Towal RB, Hartmann MJ (2006) Right-left asymmetries in the whisking behavior of rats anticipate head movements. *J Neurosci* 26:8838–8846
- Vincent SB (1912) The function of the vibrissae in the behaviour of the white rat. *Behav Monogr* 1:1–82
- Vincent SB (1913) The tactile hair of the white rat. *J Comp Neurol* 23:1–36
- Waite PME, Tracey DJ (1995) Trigeminal sensory system. In: Paxinos G (ed) *The rat nervous system*. Academic, Sydney, pp 705–724
- Wallace DJ, Greenberg DS, Sawinski J, Rulla S, Notaro G, Kerr JND (2013) Rats maintain an overhead binocular field at the expense of constant fusion. *Nature* 498:65–69
- Wehner R (1987) ‘Matched filters’ – neural models of the external world. *J Comp Physiol A* 161:511–531

- Welker WI (1964) Analysis of sniffing in the albino rat. *Behavior* 22:223–224
- Wieskotten S, Dehnhardt G, Mauck B, Miersch L, Hanke W (2010a) Hydrodynamic determination of the moving direction of an artificial fin by a harbor seal (*Phoca vitulina*). *J Exp Biol* 213:2194–2200
- Wieskotten S, Dehnhardt G, Mauck B, Miersch L, Hanke W (2010b) The impact of glide phases on the trackability of hydrodynamic trials in harbor seals (*Phoca vitulina*). *J Exp Biol* 213:3734–3740
- Wolfe J, Mende C, Brecht M (2011) Social facial touch in rats. *Behav Neurosci* 125(6):900
- Woolsey TA, Van der Loos H (1970) The structural organization of layer IV in the somatosensory region (SI) of the mouse cerebral cortex: the description of a cortical field composed of discrete cytoarchitectonic units. *Brain Res* 17:205–242

Matched Filters in Insect Audition: Tuning Curves and Beyond

4

Heiner Römer

Contents

4.1	Introduction	84
4.2	Matched Filters for “Good” and “Bad”: The Cricket Case	85
4.2.1	Variable CFs and Matched Filters?	87
4.2.2	The Problem of Matching Two “Matched Filters”	87
4.3	Mismatched Filters or Result of Complex Sensory Drive?	89
4.4	Passive and Active Frequency Filters in Insect Ears	92
4.4.1	The “Simple” Ear of a Moth and Its Adaptive Shift in Tuning	92
4.4.2	Antennal Ears of Mosquitoes and Flies: Mechanical Feedback Amplification and Tuning	94
4.5	The Tuned Frequency-Filter Paradox in Katydid	95
4.5.1	Distance Estimation: <i>Odotopic</i> Rather Than <i>Tonotopic</i> Maps?	96
4.5.2	Intensity Discrimination	96
4.5.3	Noise Filtering Through Novelty Detection	97
4.5.4	Improving the Signal-to-Noise Ratio for Temporal Processing	98
4.6	Filters in the Time Domain	99
4.6.1	Filter for Species-Specific Temporal Call PatternTemporal call pattern	99
4.6.2	Time Windows: A Most Efficient and Economical Filter in the Temporal Domain	100
4.7	Filters for Sound Amplitude	101
4.7.1	Gain Control Is an Effective Filter Matched for Eliminating Low-Intensity Sound	101
4.7.2	Reduced Sensitivity as a Matched Filter for Irrelevant Sound?	102
	References	103

H. Römer (✉)

Institute of Zoology, Karl-Franzens University Graz, Universitätsplatz 2, Graz 8010, Austria

e-mail: heinrich.roemer@uni-graz.at

Abstract

The sense of hearing evolved in insects many times independently, and different groups use sound for intraspecific communication, predator detection, and host finding. Although it can be generally assumed that ears and associated auditory pathways are matched to the relevant properties of acoustic signals and cues, the behavioral contexts, environmental conditions, and selection pressures for hearing may differ strongly between insects. Given the diversity in ear structure, active range of hearing, and the behavioral and ecological context under which hearing evolved, it is probably not surprising to find cases of sensory systems apparently mismatched to relevant parameters of the physical world. Indeed, such cases may be equally instructive for the principle of matching as the perfectly matched ones, since they may tell us something about the conflicting selection pressures and trade-offs associated with a given solution. The examples I have chosen cover the most traditional aspect of matching in the acoustic domain, namely, how the carrier frequency of the relevant sound is matched to the tuning of receivers and how central nervous processing allows species-specific responses to the temporal parameters of song. However, economical filtering also occurs in the intensity domain, starting as early as in the receptors and continuing at the first synapse of central processing. All examples serve to illustrate the similarities and differences between the sensory systems; both may help to define the conditions under which matching operates and may have evolved.

Abbreviations

BF	Best frequency
CF	Carrier frequency
HF	High frequency
IID	Interaural intensity difference
IPI	Inter-pulse interval
ITD	Interaural time difference
SPL	Sound pressure level

4.1 Introduction

This book makes a case for one of the most common principles governing sensory processing in functionally and phylogenetically diverse systems: the matching of sensory cells or whole sensory organs with properties of a signal. The selectivity of sensory systems is the result of selective forces to concentrate on only some aspects of the physical world while ignoring the rest. It is almost trivial to say that this selectivity is for biologically relevant aspects of the physical world, i.e., those

which are important for survival and reproduction. If we take a closer look at such matching, however, it is not at all trivial how exactly such a match is realized or why it is not perfect for a given task.

Both the taxon and the sensory modality of the current chapter offer a rich source of new discoveries concerning sensory matching. One reason is the multiple and independent evolutionary origin of insect ears, perhaps 19 times in 7 insect orders, and they can be found on almost any body part in different insect groups (Yack and Fullard 1993; Hoy and Robert 1996). Another reason may be the different context under which hearing has originally evolved: predator detection (such as in moths, mantises, lacewings, and grasshoppers), intraspecific communication (katydids, crickets, cicadas), or the detection and localization of hosts (parasitoid flies). Furthermore, insect hearing is mediated by two different kinds of sound receivers: one type responds to the particle velocity component of the sound field, such as the filiform hairs on the body wall or the cerci (Gnatzy and Tautz 1980) or the antennae of mosquitoes (Johnson 1855). The other type are tympanal ears, responding to the pressure component (for various aspects of the anatomy, neurobiology, or sensory ecology of insects hearing, find reviews in Hoy et al. 1998; Römer 1998; Yager 1999; Yack 2004; Hennig et al. 2004; Hedwig and Pollack 2008). Given the diversity in ear structure, active range of hearing, and the behavioral and ecological context under which hearing evolved, it is probably not surprising to find cases of sensory systems apparently mismatched to relevant parameters of the physical world. Indeed, such cases may be equally instructive for the principle of matching as the perfectly matched ones, since they may tell us something about the conflicting selection pressures and trade-offs associated with a given solution. The examples I have chosen serve to illustrate the similarities and differences between the sensory systems; both may help to define the conditions under which matching operates and may have evolved.

4.2 Matched Filters for “Good” and “Bad”: The Cricket Case

The communication system of crickets probably comes closest to what we imagine immediately in the context of matched filtering. Males produce an almost pure-tone calling song with modified forewings (tegmina), and an area of the tegmina (harp) is set into vibration at its resonant frequency when the plectrum of the left tegmen acts against the file of the right one (Elliott and Koch 1985; Bennet-Clark 1989; Montealegre-Z et al. 2011). As a result of environmental selection on the acoustic communication channel, one would expect to find a correlation between the sound spectrum produced by the sender and the tuning properties of receivers (Endler 1992; Ryan and Keddy-Hector 1992; Meyer and Elsner 1996). Not surprisingly, most auditory receptors in the ears are tuned to the carrier frequency of the song. A subset of receptors is sensitive to frequencies up to 100 kHz (Imaizumi and Pollack 1999); the hearing of these ultrasonic frequencies indicates the second major function in cricket audition, namely, predator detection and avoidance (Moiseff et al. 1978; Hoy 1992; Fullard 1998). Behavioral experiments with tethered flying

crickets (*Teleogryllus oceanicus*) indicate that they perform initial frequency discrimination, by dividing the entire range of frequencies into only two categories of low and high frequencies, with a sharp border in between at about 15 kHz (Wytttenbach et al. 1996). Such categorical perception allows matching the huge range of frequencies in the outside world into just two categories of sound important for reproduction and survival: “good”=cricket-like and “bad”=bat-like. There is no evidence of further frequency discrimination ability within the high-frequency range (Ehret et al. 1982; Wytttenbach and Farris 2004). These two categories of frequency are represented in two behaviorally relevant interneurons in the afferent auditory pathway: auditory responses to the male song are forwarded toward the brain via a single ascending interneuron AN1 (Schildberger and Hörner 1988; Schildberger et al. 1989; Kostarakos and Hedwig 2014), whereas AN2 is tuned to ultrasonic frequencies, and its activity has been shown to be necessary and sufficient for eliciting steering away from ultrasound in flight (Nolen and Hoy 1984; Pollack and Hoy 1989; Pollack 2014).

In a world with several species of bats echolocating at various ultrasonic frequencies, and only one (conspecific) species of cricket with a calling song below 15 kHz, the detection and identification of the cricket signal would be no problem, since it could be simply based on a separation of these two frequency ranges. In real worlds, however, background noise by other species competing for the same transmission channel is a selection pressure demanding for more sophisticated solutions (Römer 2014). One obvious sensory adaptation is the tuning of the ear around the species-specific CF. Thus, any sound outside the sensitivity range of the filter will play a reduced role in masking of the signals. In this way, the peripheral filter frees the central nervous system from the complicated task to distinguish between afferent activity resulting from background noise and relevant signals. This is the core of the matched filter hypothesis (Capranica and Moffat 1983; Wehner 1987).

We would expect that such filters are shaped by natural selection in their selectivity, with more sharply tuned receivers evolving when the potential for call frequency overlaps and masking interference is higher. This has been studied in a comparison of a rainforest cricket, suffering from strong competition for call frequencies with other crickets, and two species of European field crickets, where such competition does not exist (Schmidt et al. 2011). As predicted, the rainforest species exhibited a more selective tuning compared with the European counterparts. The filter reduced background nocturnal noise levels by 26 dB, compared with only 16 and 10 dB in the two European species. As a result, the representation of the species-specific amplitude modulation of the male calling song in the afferent auditory pathway was provided even in high-background noise levels.

In a choice between two males, one calling at the BF of the female receiver and the other at a higher or lower CF, a female should consistently prefer the first one, since the signal provides a stimulation which is more intense relative to the alternative. Kostarakos et al. (2008) followed this prediction from the “matched filter hypothesis” by studying the tuning of AN1 in a field cricket, known for its function in phonotaxis, and correlating this with the preference of the same individuals in two-choice trials. Females vary in their neuronal frequency tuning,

which strongly predicted their preference in a choice situation between two songs differing in CF. Thus, the tuning of a female receiver is not only important for reducing the amount of irrelevant information but has also direct consequences for mate choice. These findings are different from those in the inferior colliculus in mice where the tuning curves of neurons were not good predictors of the actual neural responses to the vocalizations (Portfors and Roberts 2014).

4.2.1 Variable CFs and Matched Filters?

The frequency filter outlined above represents a reliable solution for receivers in noisy worlds reducing the representation of biologically irrelevant sound (heterospecific songs) outside the filter frequencies. But what if the CF of the signal does vary with environmental conditions and receivers are tuned to a fixed best frequency? This is the case in tree crickets, where the CF of the calling songs changes with temperature (Metrani and Balakrishnan 2005). A sender–receiver match under these conditions would be possible if either the receiver shifts its tuning according to the changing signal (temperature coupling; Gerhardt and Huber 2002) or the tuning of receivers is less selective, allowing equal perception of the entire variation in the CF of the signal (with the trade-off of increased signal masking).

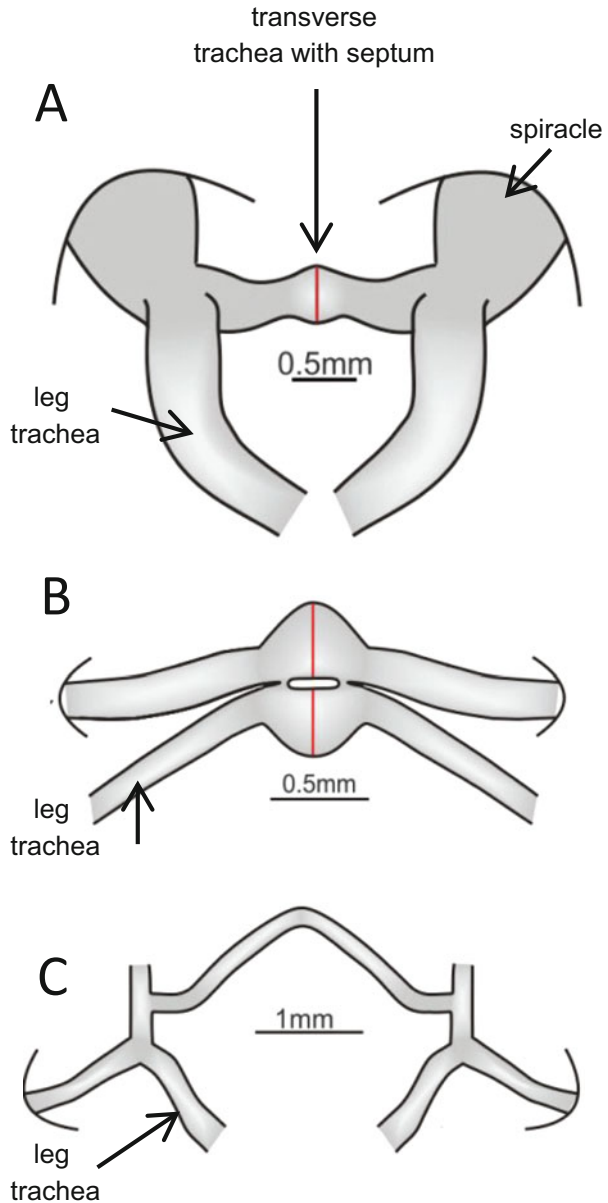
The tree cricket *Oecanthus henryi* is acoustically active from 18 to 28 °C; within this temperature range, its CF changes from 2.4 to 3.3 kHz. Mhatre et al. (2011) investigated the behavioral response of females to songs with different CFs and the mechanical frequency response of their tympanum. They found that songs with a CF from 2.5 to 4.5 kHz were equally attractive across all temperatures. Remarkably, and different from field crickets, the displacement transfer function of the anterior tympanum in the ear showed very little change in amplitude in response to a wide range of frequencies from 1.75 to about 12 kHz. Thus, *O. henryi* females appear to solve the problem of sender–receiver matching in the spectral domain by being broadly tuned both mechanically and behaviorally, consistent with results on other *Oecanthus* species (Walker 1957; Brown et al. 1996). However, as discussed by Mhatre et al. (2011), choice experiments would probably provide better answers on the preferences for particular CFs by females without any tympanal tuning. The discriminatory potential of receivers from preference functions obtained in no-choice trials is potentially misleading, since females will track a male calling song for a large range of CF, given that the sound pressure level is well above the behavioral threshold for phonotaxis (Kostarakos et al. 2008), whereas in a choice situation, the relative intensities of the two signals become highly relevant, if the neuronal elements responsible for the behavior are tuned.

4.2.2 The Problem of Matching Two “Matched Filters”

In addition to the task of detecting and identifying a male signal, female crickets also need to localize the sound source. In order to exploit interaural intensity

differences (IIDs), they cannot rely on diffractive mechanisms due to the unfavorable ratio $l:\lambda$ (body size to the wavelength of sound). Instead, the necessary IIDs result from a pressure difference receiver with a functional three-input system for the sound, provided by a complicated anatomical arrangement of connecting trachea between the ears in the forelegs (Fig. 4.1), and a phase delay mechanism

Fig. 4.1 The morphological basis for the pressure difference receiver in cricket ears. Shown are three types of acoustic tracheal systems: (A) *Gryllus bimaculatus* (Gryllidae: Gryllinae), (B) *Paroecanthus podagrosus* (Gryllidae: Eneopterinae), and (C) a member of the subfamily Gryllacridinae (Gryllacrididae) considered as primarily non-hearing, with an unspecialized connecting trachea without a septum, which appears to be the most basic form. One of the most conspicuous features concerns modifications of the transverse acoustic trachea providing the anatomical basis for the contralateral input to the ear. Within the Gryllidae, the simplest structural modification in the midline of the transverse trachea is a single, small-sized vesicle as in *G. bimaculatus*, whereas in other cricket species, the acoustic vesicle can be enlarged or structurally modified into a double acoustic vesicle as in *P. podagrosus* (Modified from Schmidt and Römer 2013)



(Hill and Boyan 1976; Wendler and Löhle 1993; Michelsen 1998; Michelsen and Löhle 1995; Robert 2005). However, the directionality of the ear is strongly frequency dependent, so that reasonable IIDs are only provided for a narrow range of frequencies. Thus, there exists a second “matched filter” for directional hearing in the receiver, depending on sound frequency as well.

In an ideal receiver, the sensitivity filter and the directionality filter should both be tuned to the same frequency, so that the CF of a male call can be perceived with highest sensitivity *and* localized with maximal IIDs. However, by examining both “matched filters” in the same individuals, Kostarakos et al. (2008) could show that the frequency providing strongest stimulation for the auditory system may provide only poor directional cues and vice versa. For *Gryllus bimaculatus*, they reported on average a discrepancy of 400 Hz between the two frequency optima. A comparison with three further species of field crickets (*G. campestris*, *Teleogryllus oceanicus*, and *T. commodus*) confirmed such mismatch (with the exception of *T. commodus*), which can amount to 1.2 kHz (Kostarakos et al. 2009). In *G. campestris* and *T. oceanicus*, the tuned directionality may even peak at frequencies outside the range of carrier frequencies of males. These results show that a mismatch between the sensitivity and directionality tuning is not uncommon in crickets.

Sensory tuning may impose stabilizing sexual selection on the male signal (Brooks et al. 2005; Bentsen et al. 2006; Ryan and Keddy-Hector 1992). In *G. bimaculatus*, the afferent sensitivity is tuned on average at 4.9 kHz, whereas the directional tuning is best at 4.5 kHz. Thus, there are two different preference peaks, which may exert selection on male signals. The fact that the average CF of male calls in a population is close to 4.7 kHz, and thus right between both receiver optima, would indicate that sexual selection is stabilizing, with both filters probably contributing to the evolution of the CF in the male signal (Kostarakos et al. 2008).

4.3 Mismatched Filters or Result of Complex Sensory Drive?

As we have seen in the above examples, for most animals that use sound to communicate between the sexes, there is a match between the carrier frequency of the signal and the hearing sensitivity of the receiver. It has been argued that stimulus filtering, i.e., the ability of sense organs and associated neural networks to ignore vast amounts of information in the outside physical world, is highly adaptive to focus on biologically relevant information. There are, however, a number of exceptions to this general rule among the insects which might tell us more about adaptive filtering. On the one hand, we find obvious cases of mismatch between the social signal and tuning of the ear, as in the primitive ensiferan insect *Cyphoderris monstrosa* (Mason 1991; Mason et al. 1999). The frequency spectrum of the calling song is narrowly centered at 12 kHz, whereas best hearing is at 2 kHz, resulting in reduced sensitivity to 12 kHz by 30 dB. No plausible explanation for this discrepancy could be offered by the authors, except for the possibility that the auditory system appears to be adapted to a function different from intraspecific

communication. A number of cases of sender–receiver mismatch have also been reported for cicadas (Popov 1981; Huber et al. 1990). In two species of 17-year cicadas, a perfect match between call frequency at 1.4 kHz and auditory nerve responses exists only in *Magicicada septendecim*, whereas in *M. cassini*, a sender–receiver mismatch was found (Huber et al. 1990). During the short period of emergence and reproductive activity, they overlap in their daily singing time and may chorus together. Due to the mismatch, the ear in *M. cassini* responds better to calls of the heterospecific cicada compared to the conspecific one. How the species solves this problem is currently unknown. In another cicada species (*Cicadetta sinuatifennis*), auditory nerve responses are completely mismatched to the spectrum of the tymbal sound usual for cicadas but match quite well with sound produced by wing flicking (Popov 1981). Notably, a mismatch can also occur between the hearing sensitivity of parasitoid flies and their host (Lakes-Harlan et al. 1999), although in all other reported cases of parasitoid/host interactions, the flies' hearing is well matched to the host calls (Robert et al. 1992; Lehmann 2003; for review on such interactions, see Lakes-Harlan and Lehmann 2014).

The example of the atympanate bladder grasshopper *Bullacris membracioides* with no less than six pairs of ears demonstrates that responses to biologically significant sound may not depend on sender–receiver matching, given that some conditions are met (van Staaden and Römer 1998; van Staaden et al. 2003). These insects possess six pairs of ears: one in abdominal segment 1, homologous to the single pair of tympanate ears found in “modern” grasshoppers, and in addition, five posterior pairs of ears in abdominal segments 2–6, resembling pleural chordotonal organs (pICOs) in other grasshoppers. All six pairs of pICOs respond to acoustic stimulation within a biologically meaningful intensity and frequency range, although only the organs in the posterior segments matched with their tuning to the male call at 1.7 kHz. By contrast, the organ in the first abdominal segment is tuned to 4 kHz, but since it is extremely sensitive (absolute threshold 13 dB SPL), the active range of the signal achieved with this “mismatched organ” is much higher than the corresponding value of the matched pairs of ears (van Staaden et al. 2003).

We can assume that sensory matching has been arrived at by selection on both signalers and receivers (Endler 1992), with four major sources of selection: (i) mate choice (Andersson 1994), (ii) predator detection and avoidance (Endler 1992), (iii) prey detection by acoustically orienting predators (Cade 1975), (iv) and the transmission channel for sound (Römer 1998). Thus, call frequency and the tuning of the ear may be under selection from potentially conflicting forces, and Endler (1992) refers to the complex evolutionary processes that shape the sensory systems as “sensory drive.” I argue here that such processes may have shaped the following example of mismatch and probably more yet undiscovered ones.

The CF at 5 kHz in the call of the Australian katydid *Sciarasaga quadrata* is unusually low for tettigoniids (Römer and Bailey 1998). The hearing system is most sensitive to frequencies of 15–20 kHz, an effective mismatch resulting in a reduced sensitivity of approximately 15–20 dB for the conspecific signal (Fig. 4.2A). One likely source of selection for shifting the call CF away from best hearing is the parasitoid fly *Homotrixa allenii*, which detects and orients toward the male host

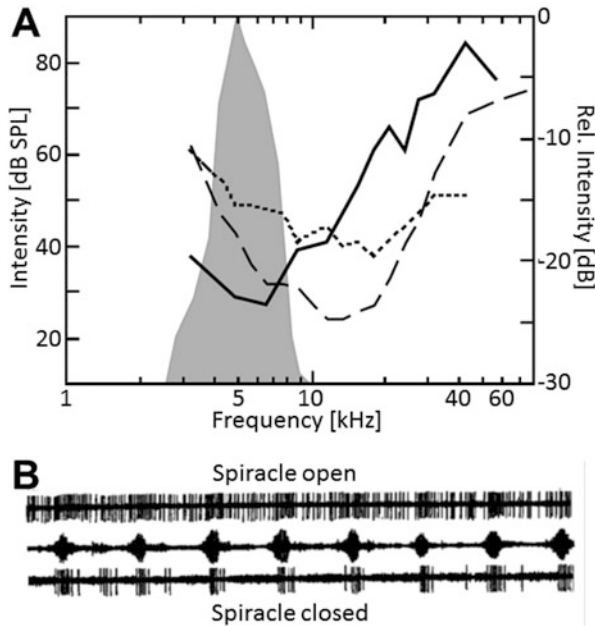


Fig. 4.2 (A) Hearing sensitivity of *Sciarasaga quadrata* in the open (dashed line) and partially blocked (solid line) spiracle condition compared with the sensitivity of the ear of its most common predator, the parasitoid fly *Homotrixa allenii* (dotted line; after Lakes-Harlan et al. 1995). Note the selective advantage to *S. quadrata* of hearing conspecifics by shifting the carrier frequency of the call to 5 kHz relative to the ability of the fly to detect its prey at this low frequency. The shaded area represents the spectrum of the calling song of *S. quadrata*. (B) Activity of the omega neuron in response to sound recordings with a conspecific male and a number of heterospecifics calling in the background. The amplitude of the heterospecific calls was approximately 20 dB lower than that of the conspecific. Note that in the open spiracle condition (upper recording), the neuronal response to the species-specific call is strongly masked by the less intense background whereas in the blocked condition (lower recording), there is a clearly detectable response pattern to the species-specific call (From Römer and Bailey 1998)

using the host call. The flies' hearing system is most sensitive between 10 and 20 kHz (Stumpner et al. 2007); thus, shifting the call CF toward low frequencies results in a partial sensory escape from the parasitoid. Nevertheless, since the shift also reduces the sensitivity to the own call, these katydids have evolved an intriguing flexible mechanism to change the tuning of the ear: by partial occlusion of the acoustic spiracle in the foreleg, they reduce the high-frequency input to the inner tympanum. Under these conditions, the ear is tuned to the call at 5 kHz (solid line in Fig. 4.2A). At the same time, they avoid the strong masking due to the singing activity of other species at frequencies higher than 10 kHz (Fig. 4.2B). Finally, the low-frequency call is well transmitted in the habitat of the katydid, almost without excess attenuation. Thus, this insect may show all components of sensory drive: sexual selection and natural selection acting on the male signal and female receiver, including selection through properties of the transmission channel

for sound. The outcome may be a matched or mismatched system depending on the ability of species to flexibly modify components in the hearing system.

4.4 Passive and Active Frequency Filters in Insect Ears

Insect ears have evolved many times independently, they can be located on almost any part of the body, and the external anatomy of the sound receiving structures varies strongly between antennal and tympanal receivers (Hoy and Robert 1996; Yager 1999; Göpfert and Robert 2008). Despite this anatomical diversity, the cellular basis of all these ears is rather uniform, comprising single or grouped chordotonal sensilla (scopodia; Field and Matheson 1998; Yack 2004). For decades, the observation that mechanosensory organs are more or less finely tuned to signals of biological relevance has been attributed to the structural biomechanics and material architecture of the respective sound receivers, although vertebrate ears were known to employ positive mechanical feedback to actively amplify their sensitivity to sound, a process known as the cochlear amplifier (Ashmore and Gale 2004; Hudspeth 1997, 2008 for review). First experimental evidence for active mechanical processes in insect ears has been the discovery of distortion product otoacoustic emissions in tympanal ears (Kössl and Boyan 1998), whereas such active processes have been more thoroughly studied in antennal ears of mosquitoes and flies.

Ignoring the chronological sequence of discoveries on active hearing processes in insects, I start with a case study on a tympanal ear of a moth, before turning to the best studied cases of antennal hearing in mosquitoes and drosophilid flies. More detailed information on all aspects of active mechanisms, including its molecular basis, can be found in Göpfert and Robert (2008), Göpfert (2008), Kavlie et al. (2014), and a recent review by Mhatre (2014).

4.4.1 The “Simple” Ear of a Moth and Its Adaptive Shift in Tuning

Insectivorous bats constitute a strong selection pressure on their prey, which favored the evolution of sensory mechanisms to detect them (Fullard 1998; ter Hofstede et al. 2013). The effect of this selection pressure has been demonstrated for many nocturnal insects in different taxa, including moths, where most species developed simple ears with the sole purpose of detecting bats (Roeder and Treat 1957). Although there is an association between the tuning of moth ears and the cues provided by sympatric bat predators (ter Hofstede et al. 2013). Windmill et al. 2006 were puzzled by the finding that in these moth, the ears are most sensitive between 20 and 40 kHz and thus somewhat mistuned to the higher echolocation calls shortly before prey capture. When they analyzed the vibrational response of the moth’s tympanum, they found a conspicuous nonlinearity and a strong shift in the resonant frequency with stimulus intensity: at low SPL, the resonant peak was at

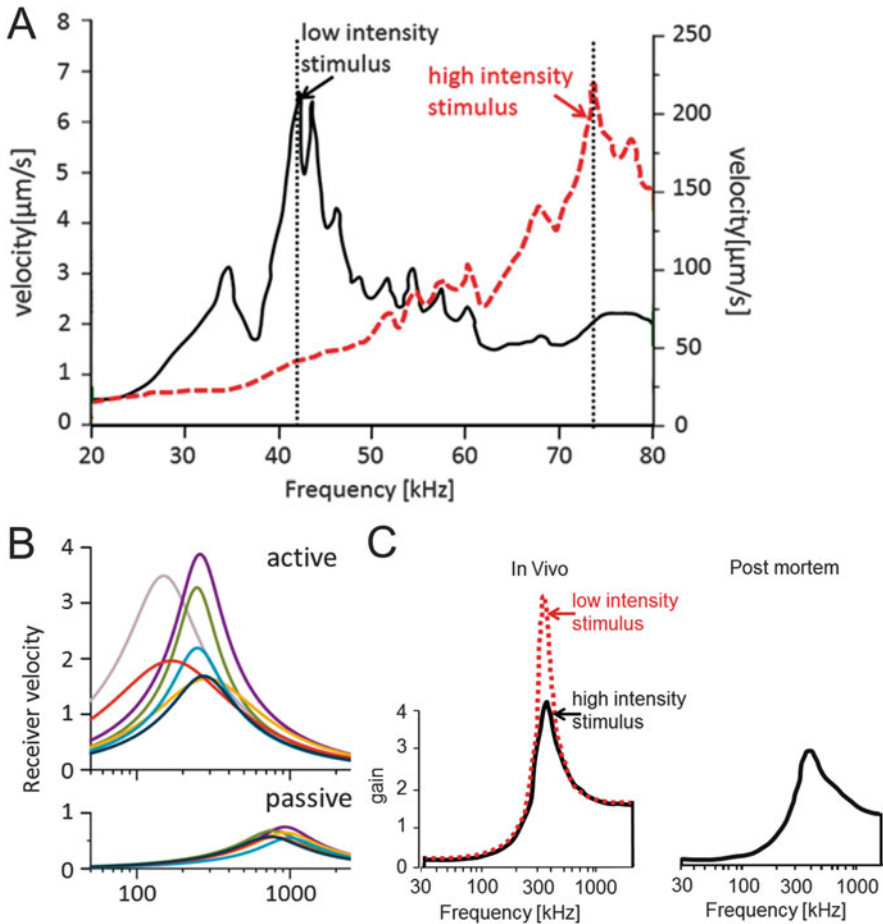


Fig. 4.3 (A) Frequency spectrum of the mechanical response of the tympanum in the moth *Noctua pronuba*. The black continuous curve depicts the response to stimulation at low stimulus intensity (left ordinate), and the red stippled curve depicts the response at high stimulus intensity (+35 dB; right ordinate) (Modified from Windmill et al. 2006). (B) Species-specific frequency tuning of antennal ears in seven species of *Drosophila*. The free mechanical fluctuations of the antennae are well described by a simple harmonic oscillator model both in the active receivers of awake (top) and in the passive receivers of CO₂-anesthetized (bottom) flies. Note the shift in frequency tuning with active hearing (From Riabinia et al. 2011). (C) Mechanical sensitivity of the mosquito antenna in response to sound. The dimensionless quantity df/dp represents the gain of the response, with df the antennal vibration velocity (the mechanical output) and dp the acoustic particle velocity (the acoustical input). The mechanical response is nonlinear at resonance frequency: gain increases as stimulus intensity decreases (Modified from Robert and Göpfert 2002)

42 kHz, and at higher SPL, the peak shifted to 74 kHz (Fig. 4.3A). In dead animals and those under CO₂ hypoxia, the shift never occurred, which is one of several indications that active processes cause this shift. Further experiments revealed that

at an SPL of 87 dB, equivalent to a bat about 3 m away, the moth ear tuned up to the higher frequency within 0.75 s, but the return to the low-frequency state may take several minutes, i.e., the tuning is hysteretic. This is highly adaptive, keeping the ear tuned up for a possible return of the bat.

Such findings are remarkable, since they demonstrate that the most peripheral filter in an auditory system is variable and strongly dependent on the active state of the sensory cells. In the case of the studied moth, there are only two sensory cells and another one (the B cell) of unknown function. Earlier work on tympanal ears of locusts and other moths had already provided evidence for active hearing mechanics (Kössl and Boyan 1998; Coro and Kössl 1998, 2001). The distortion product otoacoustic emissions (DPOAEs) recorded with two-tone stimulation showed characteristics quite similar to those from vertebrate ears, including physiological lability.

4.4.2 Antennal Ears of Mosquitoes and Flies: Mechanical Feedback Amplification and Tuning

Although the above studies had demonstrated that the mechanics of insect tympana are nonlinearly improved by physiological processes, the remarkable antennal receivers of both mosquitoes and drosophilid flies provided more in-depth results on various aspects of the active processes. The antennal ear of *Drosophila* consists of the funiculus and arista, which together act as the sound receiver, and the pedicellus, harboring the Johnston's organ with about 150–200 chordotonal sensilla (with two to three sensory neurons each; Caldwell and Eberl 2002). In response to near-field sound, the entire third segment twists around its longitudinal axis, which is the adequate stimulus for the Johnston's organ in the pedicellus (Göpfert and Robert 2001b). This antennal receiver demonstrates strong nonlinearity and frequency-specific amplification: in dead animals and those under anesthesia, the mechanical response is linear and tuned to around 800 Hz similar to a moderately damped harmonic oscillator. The same is true in live animals at high stimulus intensities, but with decreasing intensity, the tuning is shifted toward lower frequencies around 200 Hz and the sensitivity at resonance is increased (Göpfert and Robert 2002). The shift to lower frequencies is one of two highly adaptive processes mediated by active hearing, since it matches the receiver frequency rather precisely with the spectral composition of *Drosophila* courtship song pulses. This has been demonstrated in a comparative study on seven members of the *D. melanogaster* species group by Riabinia et al. (2011). The authors used CO₂ anesthesia as a tool to distinguish between active and passive tuning mechanisms, since it reversibly eliminates the active feedback from sensory neurons (Göpfert and Robert 2003). They found a species-specific tuning with best frequencies ranging between about 150 and 300 Hz, whereas in CO₂-sedated flies, the passive tuning shifted strongly in all fly species toward 800–1000 Hz (Fig. 4.3B).

The second adaptive process mediated by active hearing plays a role in the intimate link between acoustic communication and flight in Diptera and in the dual

role the antennae have as sensors in the courtship behavior and for flight control (Budick et al. 2007). For the seven members of the *D. melanogaster* species group, Riabinia et al. (2011) also measured the wing beat frequencies and the peak-to-peak antennal displacement amplitudes during tethered flight. The wing beat frequencies ranged between 145 and 213 Hz and thus close to the range of CFs of the sine songs. However, the displacement amplitudes were several orders of magnitude higher than those resulting in mechanical feedback amplification. As a result, the authors found high displacement gains ($\text{displacement}_{\text{active}}/\text{displacement}_{\text{passive}}$) of about 8 for deflections <300 nm, but a gain of only 1 for deflections >10 μm , so that these deflections drive the antenna into the passive regime during flight, tuned at about 800 Hz. Taken together, the mechanical feedback amplification and its level dependency is an excellent mechanism to enable the detection of the subtle stimuli to which the antenna is exposed during courtship, whereas the much larger stimuli during the animals own flight become negligible.

Combined laser Doppler vibrometry and electrophysiological recordings revealed the extraordinary sensitivity of the chordotonal sensilla in the Johnston's organ of mosquitoes (Göpfert and Robert 2001a). The organ in the second segment of the antenna contains about 15,000 sensilla in the male, which connect to the third segment, a long flagellum representing the sound receiver proper (Göpfert et al. 1999). At the threshold of hearing, the flagellum is deflected by only 0.1 millidegree, and at the location of the sensory neurons in the Johnston's organ, displacement amplitudes as small as 0.3 nm can be calculated. This extraordinary sensitivity is again the result of active auditory mechanics with an intensity-dependent non-linearity (Göpfert and Robert 2001a). The antenna shows a moderately damped resonance at 430 Hz in dead males, and in live animals, the tuning was similar when the stimulus intensity was high (Fig. 4.3C). At low intensities, however, the response increased and sharpened at the resonant frequency. The gain in sensitivity at resonance was between 1.5 and 2. This boost in sensitivity allows male mosquitoes to hear the faint sound of their females as a result of the wing strokes. Thus, unlike the antennal receiver in drosophilid flies, the nonlinear active process in mosquitoes operates to amplify rather than to tune the receiver.

4.5 The Tuned Frequency-Filter Paradox in Katydid

The ears of many insect species are capable of at least some basic peripheral spectral analysis (crickets: Imaizumi and Pollack 1999; grasshoppers: Michelsen 1968; Römer 1976; Jacobs et al. 1999; cicadas: Fonseca et al. 2000). For the best studied ears of katydids, two recent studies (Palghat Udayashankar et al. 2012; Montealegre-Z et al. 2012) have shown that impedance conversion and dispersive wave propagation underlie the tonotopic representation of frequencies previously reported in the crista acustica (the linear arrangement of receptors) in the ear (Oldfield 1982; Stumpner 1996; Stölting and Stumpner 1998). The tonotopic arrangement in the periphery is also reflected in their central projections within

the auditory neuropile (Römer 1983; Römer et al. 1988; Stölting and Stumpner 1998), and the frequency tuning of the first-order interneurons can be predicted from their dendritic branching pattern within the neuropile (Römer 1985; Römer et al. 1988). Surprisingly, however, most of the detailed frequency representation of the periphery is lost centrally due to strong neuronal convergence (for rare exceptions, see Stumpner 1998). So we may ask what the tonotopic arrangement of the periphery is good for (Hildebrandt 2014). Here, I suggest four cases of auditory processing in ecologically important contexts, where spectral information through the series of frequency filters in the ear can be used: (1) estimation of distance to signalers, (2) intensity discrimination, (3) novelty detection, and (4) improvement of SNR for temporal processing (see also Pollack and Imaizumi 1999; Hennig et al. 2004; Hildebrandt et al. 2014).

4.5.1 Distance Estimation: *Odotopic* Rather Than *Tonotopic* Maps?

When female katydids make phonotactic decisions between several potential mates based on long-distance acoustic cues, it should be highly adaptive to estimate the distance to the sound sources. The same holds for males spacing out in a population, where they maintain a mean acoustic distance to each other (Thiele and Bailey 1980; Römer and Bailey 1986). For this task, they could use spectral information provided by the series of frequency analyzers in the crista acustica. As sound propagates through the environment, the broad spectrum of a male katydid calling song suffers frequency-dependent excess attenuation over distance (Keuper and Kühne 1983; Römer and Lewald 1992). Individual receptors have different tuning and absolute sensitivity; in combination with the frequency filtering effect of the transmission channel, each receptor differs in the distance at which it starts to respond (threshold distance). In this way, spectral information can be used for a range fractionation in the coding of distance to a signaler (Römer 1987). Moreover, the tonotopic arrangement of axonal endings of these receptors and their range fractionation results in a specific spatial distribution of afferent activity which can also be interpreted as an *odotopic map* (Pollack and Imaizumi 1999): a systematic relationship between distance to the sound source and spatial distribution of activity in the auditory neuropile.

4.5.2 Intensity Discrimination

The series of frequency analyzers in the crista acustica of katydids provides a frequency hearing range from about 1 kHz up to 100 kHz; yet, the species-specific calling song is often restricted to a mid-frequency range. Thus, receptors outside the frequency range of the calling song appear to be mismatched to the song. The consequences for intensity discrimination have been studied in the katydid *Requena verticalis*, with only 22 receptors in each ear (Römer et al. 1998; see also Stumpner and Nowotny 2014). However, as a result of such mismatch, the threshold to the

conspecific signal varies from about 40 dB SPL for those afferents tuned to the song spectrum up to 90 dB SPL for the mismatched ones, allowing for a range fractionation within the hearing organ. Thus, an important function of these mismatched afferents is the extension of a detailed intensity coding over the complete intensity range, since the intensity-response function of each single afferent is sigmoid and saturates after only about 15–20 dB above threshold, providing a rather limited range for detailed intensity coding. For *R. verticalis*, it has been shown that at low stimulus intensities (50 dB SPL), only the mid-frequency afferents (the matched ones) provide large and reliable discharge differences with IIDs, whereas the mismatched ones remain subthreshold. By contrast, at high sound pressure levels (80 dB SPL), the mid-frequency afferents are completely saturated, so that only a few very low- and high-frequency tuned receptors provide the necessary information about IIDs (Römer et al. 1998). Hardt (1988) pointed to the importance of such range fractionation for those species with extremely short communication signals, as in the Phaneropterine katydid *Leptophyes punctatissima*, where the female response to the male call is less than 1 ms in duration. In response to this signal, a single receptor response shows no dependence to the SPL and is activated with only one action potential at suprathreshold intensities. Hence, the only information about intensity is provided by the increased recruitment of differently tuned receptors in each ear.

Future work on this topic may concentrate on those species of katydid where the frequency spectrum of the song is narrowly tuned, often at high sonic or ultrasonic frequencies (Morris et al. 1994; Montealegre-Z and Morris 1999; Montealegre-Z et al. 2006). If these species have a similar representation of frequencies in the crista acustica of the ear as outlined above, most of these receptors would be really mismatched and could not be recruited by the conspecific signal even at high SPLs. It is quite possible that we may find an interesting adaptive modification of the frequency representation, analogous to an “acoustic fovea,” in that several receptors are concentrated at the point along the crista where the relevant frequency in the traveling wave is represented (Montealegre-Z et al. 2012). Strauss et al. (2012) have provided some morphological evidence that receptors in the crista acustica are not always arranged linearly.

4.5.3 Noise Filtering Through Novelty Detection

Acoustic insects often communicate in choruses of many conspecific and heterospecific signalers, which produce a more or less constant acoustic background, so that the detection of relevant signals is problematic. In this context, a series of frequency analyzers in the ear can be advantageous, as shown by Schul et al. (2012). They described the selective coding of a biologically important sound (the echolocation pulse of a bat) by an auditory interneuron, under the simultaneous playback of a highly repetitive series of conspecific call pulses.

Responses to the bat pulses in this interneuron occurred only when its carrier frequency was sufficiently different from the standard pulses, both when the bat

pulses had a higher or lower carrier frequency than the standard. They called the phenomenon “novelty detection” because it relies on the detection of a sudden change in the acoustic scene, indicated by a frequency difference between the signal and background. The ability to detect such changes is also of relevance for the detection of conspecific stimuli. Siegert et al. (2013) examined acoustic masking in a chirping katydid species of the *Mecopoda elongata* complex due to interference with a sympatric species where males produce continuous trills at high amplitudes. Strong masking of chirps under the continuous trill could be expected, since the frequency spectra of both songs range from 1 to 80 kHz and strongly overlap. However, the chirper species has some more energy in a narrow frequency band at 2 kHz. Behaviorally, chirper males detect conspecific chirps under masking conditions at signal-to-noise ratios (SNRs) of -8 dB, but when the 2 kHz band in the chirp had been equalized to the level in the masking trill, detection was only possible at an SNR of $+7$ dB. Apparently, this species uses its potential for frequency analysis in the ear to detect the small spectral difference between the conspecific and a heterospecific signal to avoid strong masking. Intracellular recordings of identified interneurons revealed two mechanisms providing response selectivity to the chirp (Kostarakos and Römer 2015). Several identified interneurons exhibit remarkably selective responses to the chirps, even at signal-to-noise ratios of -21 dB, since they are sharply tuned to 2 kHz. Another group of interneurons is broadly tuned and thus responds strongly to the masker. However, because of strong stimulus-specific adaptation to the masker spectrum and “novelty detection” to the 2 kHz band present only in the conspecific signal, these interneurons respond selectively to the chirp shortly after the onset of the continuous masker. Both mechanisms rely on the selective tuning of receptors to the 2 kHz component in the signal; they provide the sensory basis for hearing at unfavorable signal-to-noise ratios.

4.5.4 Improving the Signal-to-Noise Ratio for Temporal Processing

A series of frequency analyzers in the ear may also be advantageous for the coding of the temporal song pattern. In their outdoor approach, Römer and Lewald (1992) modified the spectral content of a stimulus from a pure tone (CF 20 kHz) to a broadband signal and studied the response of an auditory neuron at some distance from the source. They reported a decreasing variability of responses with increasing bandwidth of the signal, i.e., the temporal pattern was more reliably encoded in the afferent activity. With increasing bandwidth, more and more independent frequency channels in the ear are being activated, which increases the reliability of coding more efficiently as compared to a system where all elements are equally tuned (Klump 1996).

4.6 Filters in the Time Domain

4.6.1 Filter for Species-Specific Temporal Call Pattern

A distinctive feature of insect sound signals is their pattern of amplitude modulation (the sound envelope), varying from simple repetitions of single sound pulses to more complex grouping of pulses into chirps (Alexander 1962; Hennig et al. 2004). The amplitude modulation provides the most crucial cue for song recognition and allows crickets and grasshoppers to respond adaptively only to signals of their own species. “Innate releasing mechanism” was the term created by the early ethologists to describe an unknown filter in the brain of receivers to explain these selective behavioral responses. In the following section, I shortly describe two recent approaches to identify this temporal filter in the brain of insects.

4.6.1.1 A Modeling Approach for Grasshoppers and Crickets

One approach was to describe behavioral preference functions of females in response to male signals using a modeling framework (Clemens and Ronacher 2013; Clemens and Hennig 2013; review in Ronacher et al. 2014). The model consists of three processing steps: (1) feature extraction with a bank of “LN models,” each with a Linear filter followed by a Nonlinearity, (2) temporal integration, and (3) linear combination. The specific properties of the filters and nonlinearities were determined using a genetic learning algorithm trained on a large dataset of song features and the corresponding behavioral response scores. The model showed an excellent prediction of the behavioral responses to the song models tested. Surprisingly, the genetic algorithm found Gabor-like functions as the optimal filter shapes for both crickets and grasshoppers, although these two taxa differ considerably in the organization of their auditory pathways and in the complexity of their songs.

These findings shed new light on the black box “innate releasing mechanism” in the brain of female receivers, but since insects provide the advantage to analyze auditory processing at the level of identified neurons, we would also like to know how the neuronal network tuned to the species-specific temporal pattern of song looks like. Cross-correlation (Hennig 2003), internal template matching (Hoy 1978), or oscillatory responses of individual neurons (Bush and Schul 2006) have been proposed to explain the neural basis of temporal selectivity, and Schildberger (1984) provided evidence for sequential processing in low-pass and high-pass filter neurons shaping the band-pass response properties of brain neurons.

4.6.1.2 The Neuronal Network in Crickets

Kostarakos and Hedwig (2012, 2014) and Schöneich et al. (2015) characterized the temporal filtering of auditory neurons in the cricket brain and compared it with the phonotactic responses of females. They described an area in the anterior protocerebrum where the neurites of four newly identified local brain neurons overlap with the axonal arborizations of an ascending interneuron (TH1-AC1, formerly known as AN1) which forward the information about the calling song to the brain.

Whereas the spike activity of TH1-AC1 and one local interneuron copy different auditory patterns regardless of their temporal structure, two other neurons match the temporal selectivity as seen in behavior, but they also responded to some non-attractive temporal patterns. One local brain neuron (B-LI4), however, exhibits band-pass response properties; its different auditory response functions match the behavioral tuning almost perfectly. The selectivity of this neuron is based on fast interactions of inhibitory and excitatory synaptic inputs. The authors also demonstrated that selective processing requires only one specific pulse interval to elicit an enhanced response to the next sound pulse, a property which is very different from band-pass filtering by low-pass and high-pass neurons as suggested by Schildberger (1984).

4.6.1.3 The Neuronal Network for Pulse Song Intervals in *Drosophila*

The courtship song in *Drosophila* is composed of the sine song and pulse song, with a distinct temporal pulse pattern in the latter. In *D. melanogaster*, this part of song is a series of pulses with inter-pulse intervals (IPI) of about 35 ms (Shorey 1962); other species differ in their mean IPI and other aspects of courtship song. Although the importance of IPI for reproductive isolation between sympatric species is known for a long time, the neuronal pathways necessary for processing and discriminating conspecific song were unknown until recently. Vaughan et al. (2014) identified the circuitry underlying courtship song responses in males and females. They distinguished seven major classes of auditory projection neurons (aPNs) and five classes of auditory local neurons, with arborizations in the antennal mechanosensory and motor center and projections to a variety of downstream regions. The authors tested each class of interneuron for its role in courtship hearing, using shibire^{TS}-mediated silencing and dTrpA1-mediated hyperactivation. Surprisingly, only one class of projection neurons and one class of local interneurons are necessary for behavioral responses to song in either sex. Direct recordings of this specific class of projection neurons revealed an intracellular band-pass filter favoring IPIs of conspecific song.

4.6.2 Time Windows: A Most Efficient and Economical Filter in the Temporal Domain

The signaling of most acoustic insects is rather “speculative” (Zimmermann et al. 1989), since males producing a calling song do not know the effectiveness of their signaling until the moment of arrival of a female. This is not the case for some short-horned grasshoppers and katydids, where pair formation is achieved by duetting; the male song elicits an acoustic reply from the female, so that the male (in most species) then responds phonotactically (von Helversen 1972; Heller and von Helversen 1986; review in Bailey 2003). Remarkably, however, the female reply is extremely short in the order of a few milliseconds: in *Leptophyes punctatissima*, a click of less than 0.5 ms in duration. This creates a problem for signal recognition since such a short click does not provide the species-specific

amplitude modulation usually necessary to distinguish between songs of species (see Sect. 4.6.1).

The solution is a female response which occurs after a very short delay time (28 ms in *L. punctatissima*; Robinson et al. 1986), and the female reply has to occur within a time window after onset of the male song in order to elicit phonotaxis in the male. The delay time of the female is a very precise and species-specific characteristic, varying between species from less than 20 ms up to 450 ms and could be used by the male as a temporal feature for species recognition (Heller and von Helversen 1986). The combination of extremely brief signals, a narrow time window of the male, and the corresponding delay time of the female may be particularly advantageous under noisy field conditions. Indeed, by listening for and only accepting a signal in a narrow time window of about 50 ms, while completely ignoring the rest of the time, may reduce many false alarms. It would be even more economic than the more or less selective filters for CF as outlined in Sect. 4.2. This has, however, never been tested under realistic outdoor conditions and awaits further experimental proof. We also do not know yet how these time windows are implemented in the nervous system of an insect.

4.7 Filters for Sound Amplitude

4.7.1 Gain Control Is an Effective Filter Matched for Eliminating Low-Intensity Sound

The more or less sharply tuned frequency filter outlined for crickets (see Sect. 4.2) works sufficiently well in species with tonal carrier frequencies, to free the CNS from computational processing for separating relevant from irrelevant sound. However, many insects communicate acoustically in aggregations, where a receiver is within earshot of several conspecific signalers (Römer and Bailey 1986; Greenfield 1994). The temporal overlap of several conspecific signals arriving from different directions and distances may result in a severe masking of the temporal song pattern at the position of the receiver, which is so important both for species identification and female choice (see Sect. 4.6.1). Pollack (1988) for crickets and Römer and Krusch (2000) for katydids discovered a neuronal gain control mechanism in first-order interneurons that could selectively code the more intense of two simultaneously presented sound signals, analogous to the “cocktail party phenomenon” familiar to humans (Cherry 1953). For example, a low-intensity signal at 45 dB SPL was quite effective when presented alone but completely suppressed when given simultaneously with another signal at 60 dB SPL. In rainforest crickets, the same membrane characteristic is also efficient to suppress activity resulting from background noise at various SNRs, thereby increasing the contrast between the relevant signal and background (Schmidt and Römer 2011). In this way, an effective intensity filter is established, again at a rather early point of the auditory

pathway, so that the central nervous temporal filter in the brain can deal with clear representations of the temporal pattern.

4.7.2 Reduced Sensitivity as a Matched Filter for Irrelevant Sound?

If we agree with the gain control mechanism as an efficient filter for some irrelevant sound, we should further develop the argument and consider that a reduced peripheral hearing sensitivity may represent such a filter as well, following the notion made by Wehner (1987; see also Wehner, this volume) that “. . . perceiving the world through such a ‘matched filter’ severely limits the amount of information the brain can pick up from the outside world, but it frees the brain from the need to perform more intricate computations to extract the information finally needed for fulfilling a particular task.” In the context of detection of acoustic predator cues, this argument seems to be intuitively wrong, because it is generally accepted that in the sensory arms race between predator and prey, the detection distance is of crucial importance for both (Surlykke and Filskov 1999; see Schul et al. 2000 for an experimental approach). Hence, by reducing the hearing sensitivity of a nocturnal flying insect to the ultrasonic calls of a bat, it would reduce the distance over which the insect gets aware of the predator and can initiate appropriate escape responses. However, for the insect, it is not relevant to achieve the *maximal possible* detection distance through high sensitivity, but a detection distance *just sufficient* for escape. Even more important, there is a trade-off between increased sensitivity of a sensory system and the potential for confounding high-frequency calls from other sources in the background (e.g., katydid calls) with bat predators, thus producing “false alarms.” In an environment with a high incidence of misleading sound, it would likely be adaptive that the threshold for eliciting either an escape behavior or neuronal responses is rather high. This is indeed a property of the HF channel which holds for insect taxa as diverse as crickets, praying mantis, lacewings, tiger beetles, butterflies, and moth (Yager and Hoy 1989; Yager et al. 2000; Yack and Fullard 2000). With the exception of arctiid moths with reported thresholds close to 40 dB SPL, those of the other insect groups are considerably higher and range between 50 and 80 dB SPL. Corresponding thresholds of many rainforest cricket species are consistently between 70 and 80 dB SPL (M. H. Brunnhofer, 2015, personal communication). Since background noise levels between 60 and 70 dB SPL have been reported in the same environment (Lang et al. 2005), the reduced sensitivity in the HF channel may release the central nervous system from the difficult task to distinguish between irrelevant HF events and those indicating real danger.

Thus, with respect to filters for the intensity domain, we find the interesting situation that in some cases, exquisite active mechanisms have evolved to boost up the sensitivity in response to very faint sound, and at the same time reducing the effect of higher amplitudes. It is probably not by chance that this is found in particular in the context of flies hearing near-field sound, where relevant stimulus amplitudes can be minute. On the other hand, gain control mechanisms and reduced

general sensitivities filter stimulus levels in the opposite direction, favoring larger stimulus levels. In any case, it is obvious that these different solutions are highly adaptive in the particular ecological context.

Acknowledgments Own research mentioned in this review was funded by the Austrian Science Fund (FWF) through grants P17986-B06, P20882-B09, P23896-B24, and P26072-B25 to HR.

References

- Alexander RD (1962) Evolutionary change in cricket acoustical communication. *Evolution* 16:443–467
- Andersson M (1994) Sexual selection. Princeton University Press, Princeton
- Ashmore J, Gale J (2004) The cochlear amplifier. *Curr Biol* 14:R404
- Bailey WJ (2003) Insect duets: their mechanisms and underlying evolution. *Physiol Entomol* 28:157–174
- Bailey WJ, Römer H (1991) Sexual differences in auditory sensitivity: mismatch of hearing threshold and call frequency in a tettigoniid (Orthoptera, Tettigoniidae: Zaprochilinae). *J Comp Physiol A* 169:349–353
- Bennet-Clark HC (1989) Songs and the physics of sound production. In: Huber F, Moore TE, Loher W (eds) Cricket behavior and neurobiology. Cornell University Press, Ithaca, pp 227–261
- Bentsen CL, Hunt J, Jennions MD, Brooks R (2006) Complex multivariate sexual selection on male acoustic signaling in a wild population of *Teleogryllus commodus*. *Am Nat* 167(4):E102–E116
- Brooks R, Hunt J, Blows MW, Smith MJ, Bussière LF, Jennions MD (2005) Experimental evidence for multivariate stabilizing sexual selection. *Evolution* 59:871–880
- Brown WD, Wideman J, Andrade MCB, Mason AC, Gwynne DT (1996) Female choice for an indicator of male size in the song of the black-horned tree cricket, *Oecanthus nigricornis* (Orthoptera: Gryllidae: Oecanthinae). *Evolution* 50:2400–2411
- Budick SA, Reiser MB, Dickinson MH (2007) The role of visual and mechanosensory cues in structuring forward flight in *Drosophila melanogaster*. *J Exp Biol* 210:4092–4103
- Bush SL, Schul J (2006) Pulse-rate recognition in an insect: evidence of a role for oscillatory neurons. *J Comp Physiol A* 192:113–121
- Cade WH (1975) Acoustically orienting parasitoids: fly phonotaxis to cricket song. *Science* 190:1312–1313
- Caldwell J, Eberl DF (2002) Towards a molecular understanding of *Drosophila* hearing. *J Neurobiol* 53:172–189
- Capranica RR, Moffat AJM (1983) Neurobehavioral correlates of sound communication in anurans. In: Capranica RR, Ingle D, Ewert JP (eds) Vertebrate neuroethology. Plenum, New York, pp 701–730
- Cherry EC (1953) Some experiments on the recognition of speech with one and with two ears. *J Acoust Soc Am* 25:975–979
- Clemens J, Hennig RM (2013) Computational principles underlying the recognition of acoustic signals in insects. *J Comput Neurosci* 35:75–85
- Clemens J, Ronacher B (2013) Feature extraction and integration underlying perceptual decision making during courtship in grasshoppers. *J Neurosci* 33:12136–12145
- Coro F, Kössl M (1998) Distortion-product otoacoustic emissions from the tympanic organ in two noctuid moths. *J Comp Physiol A* 183:525–531
- Coro F, Kössl M (2001) Components of the 2f(1)-2f(2) distortion-product otoacoustic emission in a moth. *Hear Res* 162:126–133

- Ehret G, Moffat AJM, Tautz J (1982) Behavioral determination of frequency resolution in the ear of the cricket, *Teleogryllus oceanicus*. *J Comp Physiol* 148:237–244
- Elliott CJH, Koch UT (1985) The clockwork cricket. *Naturwissenschaften* 72:150–153
- Endler JA (1992) Signals, signal conditions, and the direction of evolution. *Am Nat* 139:125–153
- Field LH, Matheson T (1998) Chordotonal organs in insects. *Adv Insect Physiol* 27:1–28
- Fonseca PJ, Münch D, Hennig RM (2000) How cicadas interpret acoustic signals. *Nature* 405:297–298
- Fullard JH (1998) The sensory coevolution of moths and bats. In: Hoy RR, Popper AN, Fay RR (eds) *Comparative hearing: insects*. Springer, New York, pp 279–326
- Gerhardt HC, Huber F (2002) Acoustic communication in insects and anurans: common problems and diverse solutions. University of Chicago Press, Chicago
- Gnatzy W, Tautz J (1980) Ultrastructure and mechanical properties of an insect mechanoreceptor: stimulus-transmitting structures and sensory apparatus of the cercal filiform hairs of *Gryllus*. *Cell Tissue Res* 213:441–463
- Göpfert MC (2008) Amplification and feedback in invertebrates. In: Dallos P, Oertel D (eds) *Audition, vol 3, The senses: a comprehensive reference*. Elsevier, Amsterdam, pp 293–299
- Göpfert MC, Robert D (2001a) Active auditory mechanics in mosquitoes. *Proc R Soc Lond B* 268:333–339
- Göpfert MC, Robert D (2001b) Turning the key on *Drosophila* audition. *Nature* 411:908
- Göpfert MC, Robert D (2002) The mechanical basis of *Drosophila* audition. *J Exp Biol* 205:1199–1208
- Göpfert MC, Robert D (2003) Motion generation by *Drosophila* mechanosensory neurons. *Proc Natl Acad Sci U S A* 100:5514–5519
- Göpfert MC, Robert D (2008) Active processes in insect hearing. In: Manley GA, Fay RR, Popper AN (eds) *Active mechanics and otoacoustic emissions, vol 30, Springer handbook of auditory research*. Springer, Heidelberg, pp 191–210
- Göpfert MC, Briegel H, Robert D (1999) Mosquito hearing: sound-induced antennal vibrations in male and female *Aedes aegypti*. *J Exp Biol* 202:2727–2738
- Greenfield MD (1994) Synchronous and alternating choruses in insects and anurans: common mechanisms and diverse functions. *Ann Rev Ecol Evol Syst* 25:97–126
- Hardt M (1988) Zur Phonotaxis von Laubheuschrecken: Eine vergleichende verhaltensphysiologische und neurophysiologisch-anatomische Untersuchung. PhD thesis, University of Bochum
- Hedwig B, Pollack GS (2008) Invertebrate auditory pathways. In: Basbaum AI, Akimichi K, Shepard GM, Westheiner G, Dallos P, Oertel D (eds) *Invertebrate auditory pathways. The senses: a comprehensive reference*. Academic, San Diego, pp 525–564
- Heller K-G, von Helversen D (1986) Acoustic communication in phaneropterid bushcrickets: species-specific delay of female stridulatory response and matching male sensory time window. *Behav Ecol Sociobiol* 18:189–198
- Hennig RM (2003) Acoustic feature extraction by cross-correlation in crickets? *J Comp Physiol A* 189:589–598
- Hennig RM, Franz A, Stumpner A (2004) Processing of auditory information in insects. *Microsc Res Tech* 63:351–374
- Hildebrandt KJ (2014) Neural maps in insect versus vertebrate auditory systems. *Curr Opin Neurobiol* 24:82–87
- Hildebrandt KJ, Benda J, Hennig RM (2014) Computational themes of peripheral processing in the auditory pathway of insects. *J Comp Physiol A*. doi:10.1007/s00359-014-0956-5
- Hill KG, Boyan GS (1976) Directional hearing in crickets. *Nature* 262:390–391
- Hoy RR (1978) Acoustic communication in cricket: a model system for the study of feature detection. *Fed Proc* 37:2316–2323
- Hoy RR (1992) The evolution of hearing in insects as an adaptation to predation from bats. In: Webster DG, Popper AN, Fay RR (eds) *The evolutionary biology of hearing*. Springer, New York, pp 115–130

- Hoy RR, Robert D (1996) Tympanal hearing in insects. *Annu Rev Entomol* 41:433–450
- Hoy RR, Popper AN, Fay RR (eds) (1998) *Comparative hearing: insects*. Springer, New York
- Huber F, Kleindienst HU, Moore TH, Schildberger K, Weber TH (1990) Acoustic communication in periodical cicadas: neuronal responses to songs of sympatric species. In: Gribakin FG, Wiese K, Popov AV (eds) *Sensory systems and communication in arthropods; advances in life sciences*. Birkhäuser Verlag, Basel, pp 217–228
- Hudspeth AJ (1997) Mechanical amplification by hair cells. *Curr Opin Neurobiol* 7:480–486
- Hudspeth AJ (2008) Making an effort to listen: mechanical amplification in the ear. *Neuron* 59:530–545
- Imaizumi K, Pollack GS (1999) Neural coding of sound frequency by cricket auditory receptors. *J Neurosci* 19:1508–1516
- Jacobs K, Otte B, Lakes-Harlan R (1999) Tympanal receptor cells of *Schistocerca gregaria*: correlation of soma positions and dendrite attachment sites, central projections and physiologies. *J Exp Zool* 283:270–285
- Johnson C (1855) Auditory apparatus of the *Culex* mosquito. *Q J Microsc Sci* 3:97–102
- Kavlie RG, Fritz JL, Nies F, Göpfert MC, Oliver D, Albert JT, Eberl DF (2014) Prestin is an anion transporter dispensable for mechanical feedback amplification in *Drosophila* hearing. *J Comp Physiol A*. doi:10.1007/s00359-014-0960-9
- Keuper A, Kühne R (1983) The acoustic behavior of the bushcricket *Tettigonia cantans*. II. Transmission of airborne sound and vibration signals in the biotope. *Behav Processes* 8:125–145
- Klump GM (1996) Bird communication in a noisy world. In: Miller EH, Kroodsma DE (eds) *Ecology and evolution of acoustic communication in birds*. Cornell University Press, Ithaca, pp 321–338
- Kössl M, Boyan GS (1998) Distortion-product otoacoustic emissions from the ear of a grasshopper. *J Acoust Soc Am* 104:326–335
- Kostarakos K, Hedwig B (2012) Calling song recognition in female crickets: temporal tuning of identified brain neurons matches behavior. *J Neurosci* 32(28):9601–9961
- Kostarakos K, Hedwig B (2014) Pattern recognition in field crickets: concepts and neural evidence. *J Comp Physiol A*. doi:10.1007/s00359-014-0949-4
- Kostarakos K, Römer H (2015) Neural mechanisms for acoustic signal detection under strong masking in an insect. *J Neurosci* 35(29):10562–10571
- Kostarakos K, Hartbauer M, Römer H (2008) Matched filters, mate choice and the evolution of sexually selected traits. *PLoS One* 3:e3005
- Kostarakos K, Hennig MR, Römer H (2009) Two matched filters and the evolution of mating signals in four species of cricket. *Front Zool* 6:22
- Lakes-Harlan R, Lehmann GUC (2014) Parasitoid flies exploiting acoustic communication of insects – comparative aspects of independent functional adaptations. In: Römer H, Ronacher B (eds) *Insect hearing: from physics to ecology*. *J Comp Physiol*. doi:10.1007/s00359-014-0958-3
- Lakes-Harlan R, Stumpner A, Allen G (1995) Functional adaptations of the auditory system of two parasitoid fly species, *Therobia leonidei* and *Homotrixia spec.* In: Burrows M, Matheson T, Newland P, Schuppe H (eds) *Nervous systems and behavior*. ThiemeVerlag Stuttgart, New York, p 358
- Lakes-Harlan R, Stölting H, Stumpner A (1999) Convergent evolution of insect hearing organs from a preadaptive structure. *Proc R Soc Lond B* 266:1161–1167
- Lang A, Teppner I, Hartbauer M, Römer H (2005) Predation and noise in communication networks of neotropical katydids. In: McGregor P (ed) *Animal communication networks*. Cambridge University Press, Cambridge, pp 152–169
- Lehmann GUC (2003) Review of biogeography, host range and evolution of acoustic hunting in Ormiini (Insecta, Diptera, Tachinidae), parasitoids of night-calling bushcrickets and crickets (Insecta, Orthoptera, Ensifera). *Zool Anz* 242:107–120

- Mason AC (1991) Hearing in a primitive ensiferan: the auditory system of *Cyphoderris mostrosa* (Orthoptera: Haglidae). *J Comp Physiol* 168:351–363
- Mason AC, Morris GK, Hoy RR (1999) Peripheral frequency mis-match in the primitive ensiferan *Cyphoderris mostrosa* (Orthoptera: Haglidae). *J Comp Physiol A* 184:543–551
- Metrani S, Balakrishnan R (2005) The utility of song and morphological characters in delineating species boundaries among sympatric tree crickets of the genus *Oecanthus* (Orthoptera: Gryllidae: Oecanthinae): a numerical taxonomic approach. *J Orthoptera Res* 14:1–16
- Meyer J, Elsner N (1996) How well are frequency sensitivities of grasshopper ears tuned to species-specific song spectra? *J Exp Biol* 199:1631–1642
- Mhatre N (2014) Active amplification in insect ears: mechanics, models and molecules. *J Comp Physiol A*. doi:[10.1007/s00359-014-0969-0](https://doi.org/10.1007/s00359-014-0969-0)
- Mhatre N, Bhattacharya M, Robert D, Balakrishnan R (2011) Matching sender and receiver: poikilothermy and frequency tuning in a tree cricket. *J Exp Biol* 214:2569–2578
- Michelsen A (1968) Frequency discrimination in the locust ear by means of four groups of receptor cells. *Nature* 220:585–586
- Michelsen A (1998) The tuned cricket. *News Physiol Sci* 13:32–38
- Michelsen A, Löhe G (1995) Tuned directionality in cricket ears. *Nature* 375:639
- Moiseff A, Pollack GS, Hoy RR (1978) Steering response of flying crickets to sound and ultrasound: mate attraction and predator avoidance. *Proc Natl Acad Sci U S A* 75:4052–4056
- Montealegre-Z F, Morris GK (1999) Songs and systematics of some Tettigoniidae from Columbia and Ecuador I. Pseudophyllinae (Orthoptera). *J Orthoptera Res* 8:163–236
- Montealegre-Z F, Morris GK, Mason AC (2006) Generation of extreme ultrasonics in rainforest katydids. *J Exp Biol* 209:4923–4937
- Montealegre-Z F, Jonsson T, Robert D (2011) Sound radiation and wing mechanics in stridulating field crickets (Orthoptera: Gryllidae). *J Exp Biol* 214:2105–2117
- Montealegre-Z F, Jonsson T, Robson-Brown T, Postles KA, Robert DM (2012) Convergent evolution between insect and mammalian audition. *Science* 338:968–971
- Morris GK, Mason AC, Wall P (1994) High ultrasonic and tremulation signals in neotropical katydids (Orthoptera: Tettigoniidae). *J Zool* 233:129–163
- Nolen TG, Hoy RR (1984) Initiation of behavior by single neurons: the role of behavioral context. *Science* 226:992–994
- Oldfield BP (1982) Tonotopic organisation of auditory receptors in tettigoniidae (Orthoptera: Ensifera). *J Comp Physiol* 147:461–469
- Palghat Udayashankar A, Kössl M, Nowotny M (2012) Tonotopically arranged traveling waves in the miniature hearing organ of bushcrickets. *PLoS One* 7(2), e31008. doi:[10.1371/journal.pone.0031008](https://doi.org/10.1371/journal.pone.0031008)
- Pollack GS (1988) Selective attention in an insect auditory neuron. *J Neurosci* 8:2635–2639
- Pollack GS (2014) Neurobiology of acoustically mediated predator detection. In: Römer H, Ronacher B (eds) *Insect hearing: from physics to ecology*. *J Comp Physiol A*. doi [10.1007/s00359-014-0948-5](https://doi.org/10.1007/s00359-014-0948-5)
- Pollack GS, Hoy RR (1989) Evasive acoustic behavior and its neurobiological basis. In: Huber F, Moore TE, Loher W (eds) *Cricket behavior and neurobiology*. Cornell University Press, Ithaca, pp 340–363
- Pollack GS, Imaizumi K (1999) Neural analysis of sound frequency in insects. *Bioessays* 21:295–303
- Popov AV (1981) Sound production and hearing in the cicada, *Cicadetta sinuatipennis* Osh. (Homoptera, Cicadidae). *J Comp Physiol* 142:271–280
- Portfors CV, Roberts PD (2014) Mismatch of structural and functional tonotopy for natural sounds in the auditory midbrain. *Neuroscience* 258:192–203
- Riabina O, Dai M, Duke T, Albert JT (2011) Active process mediates species-specific tuning of *Drosophila* ears. *Curr Biol* 21:658–664
- Robert D (2005) Directional hearing in insects. In: Fay RR, Popper AN (eds) *Sound source localization*. Springer, New York, pp 6–35

- Robert D, Göpfert M (2002) Novel schemes for hearing and orientation in insects. *Curr Opin Neurobiol* 12:715–720
- Robert D, Amoroso J, Hoy RR (1992) The evolutionary convergence of hearing in a parasitoid fly and its cricket host. *Science* 258:1135–1137
- Robinson DJ, Rheinlaender J, Hartley JC (1986) Temporal parameters of male-female sound communication in *Leptophyes punctatissima*. *Physiol Entomol* 11:317–323
- Roeder KD, Treat AE (1957) Ultrasonic reception by the tympanic organ of noctuid moths. *J Exp Zool* 134:127–157
- Römer H (1976) Die Informationsverarbeitung tympanaler Rezeptorelemente von *Locusta migratoria*. *J Comp Physiol A* 109:101–122
- Römer H (1983) Tonotopic organization of the auditory neuropile in the bushcricket *Tettigonia viridissima*. *Nature* 306:60–62
- Römer H (1985) Anatomical representation of frequency and intensity in the auditory system of Orthoptera. In: Elsner N, Kalmring K (eds) Acoustic and vibrational communication in insects. Paul Parey, Hamburg, pp 25–32
- Römer H (1987) Representation of auditory distance within a central neuropil of the bushcricket *Mygalopsis marki*. *J Comp Physiol A* 161:33–42
- Römer H (1998) The sensory ecology of acoustic communication in insects. In: Hoy RR, Popper AN, Fay RR (eds) Comparative hearing: insects. Springer, New York, pp 63–96
- Römer H (2014) Masking by noise in acoustic insects: Problems and solutions. In: Brumm H (ed) Animal communication and noise; animal signals and communication 2, doi:10.1007/978-3-642-41494-7_3
- Römer H, Bailey WJ (1986) Insect hearing in the field. II. Male spacing behavior and correlated acoustic cues in the bushcricket *Mygalopsis marki*. *J Comp Physiol A* 159:627–638
- Römer H, Bailey W (1998) Strategies for hearing in noise: peripheral control over auditory sensitivity in the bushcricket *Sciarasaga quadrata* (Austrosaginae:Tettigoniidae). *J Exp Biol* 201:1023–1033
- Römer H, Krusch M (2000) A gain-control mechanism for processing of chorus sounds in the afferent auditory pathway of the bushcricket *Tettigonia viridissima* (Orthoptera; Tettigoniidae). *J Comp Physiol A* 186:181–191
- Römer H, Lewald J (1992) High-frequency sound transmission in natural habitats: implications for the evolution of insect acoustic communication. *Behav Ecol Sociobiol* 29:437–444
- Römer H, Marquart V, Hardt M (1988) Organization of a sensory neuropile in the auditory pathway of two groups of Orthoptera. *J Comp Neurol* 275:201–215
- Römer H, Spickermann M, Bailey W (1998) Sensory basis for sound intensity discrimination in the bushcricket *Requena verticalis* (Tettigoniidae, Orthoptera). *J Comp Physiol A* 182:595–607
- Ronacher B (2014) Processing of species-specific signals in the auditory pathway of grasshoppers. In: Hedwig B (ed) Insect hearing and acoustic communication, vol 1, Animal signals and communication. Springer, Berlin, pp 185–204
- Ronacher B, Hennig RM, Clemens J (2014) Computational principles underlying recognition of acoustic signals in grasshoppers and crickets. *J Comp Physiol A*. doi:10.1007/s00359-014-0946-7
- Ryan MJ, Keddy-Hector A (1992) Directional patterns of female mate choice and the role of sensory biases. *Am Nat* 139:S4–S35
- Schildberger K (1984) Temporal selectivity of identified auditory neurons in the cricket brain. *J Comp Physiol A* 155:171–185
- Schildberger K, Hörner M (1988) The function of auditory neurons in cricket phonotaxis: I. Influence of hyperpolarization of identified neurons on sound localization. *J Comp Physiol A* 163:621–631
- Schildberger K, Huber F, Wohlers DW (1989) Central auditory pathway: neuronal correlates of phonotactic behavior. In: Huber F, Moore TE, Loher W (eds) Cricket behavior and neurobiology. Cornell University Press Ithaca, New York, pp 423–458

- Schmidt AKD, Römer H (2011) Solutions to the cocktail party problem in insects: selective filters, spatial release from masking and gain control in tropical crickets. *PLoS One* 6(12):e28593. doi:[10.1371/journal.pone.0028593](https://doi.org/10.1371/journal.pone.0028593)
- Schmidt AKD, Römer H (2013) Diversity of acoustic tracheal system and its role for directional hearing in crickets. *Front Zool* 10:61. doi:[10.1186/1742-9994-10-61](https://doi.org/10.1186/1742-9994-10-61)
- Schmidt AKD, Riede K, Römer H (2011) High background noise shapes selective auditory filters in a tropical cricket. *J Exp Biol* 214:1754–1762
- Schul J, Matt F, von Helversen O (2000) Listening for bats: the hearing range of the bushcricket *Phaneroptera falcata* for bat echolocation calls measured in the field. *Proc R Soc Lond* 267:1711–1715
- Schul J, Mayo AM, Triplehorn JD (2012) Auditory change detection by a single neuron in an insect. *J Comp Physiol* 198:695–704
- Shorey HH (1962) Nature of the sound produced by *Drosophila melanogaster* during courtship. *Science* 137:677–678
- Siegert ME, Römer H, Hartbauer M (2013) Maintaining acoustic communication at a cocktail party: heterospecific masking noise improves signal detection through frequency separation. *J Exp Biol* 216:4655–4665
- Stöltzing H, Stumpner A (1998) Tonotopic organization of auditory receptor cells in the bushcricket *Pholidoptera griseoptera* (De Geer 1771) (Tettigoniidae, Decticini). *Cell Tissue Res* 294:377–386
- Strauß J, Lehmann GUC, Lehmann AW, Lakes-Harlan R (2012) Spatial organization of Tettigoniid auditory receptors: insights from neuronal tracing. *J Morphol* 273:1280–1290
- Stumpner A (1996) Tonotopic organization of the hearing organ in a bushcricket. *Physiological characterization and complete staining of auditory receptor cells. Naturwissenschaften* 83:81–84
- Stumpner A (1998) Picrotoxin eliminates frequency selectivity of an auditory interneuron in a bushcricket. *J Neurophysiol* 79:2408–2415
- Stumpner A, Novotny M (2014) Neural processing in the bushcricket auditory pathway. In: Hedwig B (ed) *Insect hearing and acoustic communication*. Springer, Berlin. doi:[10.1007/978-3-642-40462-7_9](https://doi.org/10.1007/978-3-642-40462-7_9)
- Stumpner A, Allen GR, Lakes-Harlan R (2007) Hearing and frequency dependence of auditory interneurons in the parasitoid fly *Homotrixia alleni* (Tachinidae: Ormiini). *J Comp Physiol A* 193:1113–1125
- Surlykke A, Filskov M (1999) Auditory relationship to size in noctuid moths: bigger is better. *Naturwissenschaften* 86:238–241
- ter Hofstede HM, Goerlitz HR, Ratcliffe JM, Holderied MW, Surlykke A (2013) The simple ears of noctuid moths are tuned to the calls of their sympatric bat community. *J Exp Biol* 216:3954–3962
- Thiele D, Bailey WJ (1980) The function of sound in male spacing behavior in bush-cricket (Tettigoniidae, Orthoptera). *Aust J Ecol* 5:275–286
- van Staaen MJ, Römer H (1998) Evolutionary transition from stretch to hearing organs in ancient grasshoppers. *Nature* 394:773–776
- van Staaen MJ, Rieser M, Ott SR, Papst MA, Römer H (2003) Serial hearing organs in the atympanate grasshopper *Bullacris membracioides* (Orthoptera, Pneumoridae). *J Comp Neurol* 465:579–592
- Vaughan AG, Chuan Z, Manoli DS, Baker BS (2014) Neural pathways for the detection and discrimination of conspecific song in *D. melanogaster*. *Curr Biol* 24:1039–1049. doi:[10.1016/j.cub.2014.03.048](https://doi.org/10.1016/j.cub.2014.03.048)
- von Helversen D (1972) Gesang des Männchens und Lautschema des Weibchens bei der Feldheuschrecke *Chorthippus biguttulus* (Orthoptera, Acrididae). *J Comp Physiol A* 81:381–422
- Walker T (1957) Specificity in the response of female tree crickets (Orthoptera, Gryllidae, Oecanthinae) to calling songs of the males. *Ann Entomol Soc Am* 50:626–636

- Wehner R (1987) "Matched filters"—neural models of the external world. *J Comp Physiol A* 161:511–531
- Wendler G, Löhe G (1993) The role of the medial septum in the acoustic trachea of the cricket *Gryllus bimaculatus*. *J Comp Physiol A* 173:557–564
- Windmill J, Jackson J, Tuck E, Robert D (2006) Keeping up with bats: dynamic auditory tuning in a moth. *Curr Biol* 16:2418–2423
- Wytenbach RA, Farris HE (2004) Psychophysics in insect hearing. *Microsc Res Tech* 63:375–387
- Wytenbach RA, May ML, Hoy RR (1996) Categorical perception of sound frequency by crickets. *Science* 273:1542–1544
- Yack JE (2004) The structure and function of auditory chordotonal organs in insects. *Microsc Res Tech* 63:315–337
- Yack JE, Fullard JH (1993) What is an insect ear? *Ann Entomol Soc Am* 86:677–682
- Yack JE, Fullard JH (2000) Ultrasonic hearing in nocturnal butterflies. *Nature* 403:265–266
- Yager DD (1999) Structure, development and evolution of insect auditory systems. *Microsc Res Tech* 47:380–400
- Yager DD, Hoy RR (1989) Audition in the praying mantis, *Mantis religiosa* L.: identification of an interneuron mediating ultrasonic hearing. *J Comp Physiol A* 165:471–493
- Yager DD, Cook AP, Pearson DL, Spangler HG (2000) A comparative study of ultrasound-triggered behaviour in tiger beetles (Cicindelidae). *J Zool Lond* 251:355–368
- Zimmermann U, Rheinlaender J, Robinson DJ (1989) Cues for male phonotaxis in the duetting bushcricket *Leptophyes punctatissima*. *J Comp Physiol A* 164:621–628

Principles of Matched Filtering with Auditory Examples from Selected Vertebrates

5

Peter M. Narins and Grace A. Clark

Contents

5.1	Part I Principles of Matched Filtering	112
5.1.1	The Correlation Detector	114
5.1.2	Section Organization	114
5.2	An Example Detection Problem	114
5.2.1	Define the Signal-to-Noise Ratio (SNR)	115
5.3	The Matched Filter Detector	116
5.3.1	Convolution and Filtering	117
5.3.2	Correlation vs. Convolution	117
5.3.3	The Matched Filter	118
5.3.4	Example: Applying the Matched Filter to Our Example Signals	118
5.4	Bayesian Binary Hypothesis Testing and Performance Measurement	119
5.4.1	The Confusion Matrix (or Contingency Table)	120
5.4.2	Bayesian Hypothesis Testing for Multidimensional (Vector) Data	122
5.4.3	Training and Testing Phases of the Detection Process	123
5.4.4	The Receiver Operating Characteristic (ROC) Curve	124
5.4.5	Statistical Confidence Interval About the Probability of Correct Classification	125
5.5	Processing for the Example Problem	126
5.5.1	Experiment Design for the Example Problem	126
5.5.2	Processing Results for the Example Problem	127
5.5.3	Conclusions	130

P.M. Narins (✉)

Department of Integrative Biology and Physiology, University of California, Los Angeles, 621
Charles E. Young Drive South, Los Angeles, CA 90095, USA

Department of Ecology and Evolutionary Biology, University of California, Los Angeles, 621
Charles E. Young Drive South, Los Angeles, CA 90095, USA

e-mail: pnarins@ucla.edu

G.A. Clark, Ph.D., IEEE Fellow

Grace Clark Signal Sciences, 532 Alden Lane, Livermore, CA 94550, USA

e-mail: GCSS_Grace@comcast.net

5.6	Part II Auditory Matched Filtering: Biological Examples from Selected Vertebrates .	131
5.6.1	Weakly Electric Fish	132
5.6.2	Anuran Amphibians	132
5.6.3	Birds	137
5.6.4	Conclusions	138
	References	139

Abstract

This chapter consists of two parts. In the first part, a compact tutorial exposition of the principles of matched filtering for the biological scientist is introduced. The concept of matched filtering for detecting desired signals buried in noisy measurement signals is presented. It is shown that the matched filter is another name for the correlation detector or replica-correlation detector, which exploits prior knowledge in the form of an exemplar (or replica) of the desired signal. An example detection problem is used to demonstrate the matched filtering approach. The detection methodology comes from hypothesis testing algorithms in Bayesian detection theory. This Bayesian approach provides very powerful methods for evaluating detection performance in the form of the Receiver Operating Characteristic (ROC) curve and the statistical confidence interval about the probability of correct classification. It is shown that the matched filter can be an effective detection tool when exemplars of the desired signal are available a priori. In the second part, several key examples of matched filters in the auditory systems of several selected vertebrates are provided.

5.1 Part I Principles of Matched Filtering

This section presents a compact tutorial exposition of the principles of matched filtering for the biological scientist. The matched filter is a concept from communications and radar theory (Van Trees 1968; Whalen 1971; Kay 1998; Papoulis 1965) that has been applied widely to various other applications in science and engineering (Carpranica and Moffat 1983; Wehner 1987; Clark et al. 1999, 2000, 2009; Waltz and Llinas 1990; Clark 1999; Jazwinski 1970; Candy 2006). It is a statistical signal processing algorithm designed for detecting the existence of a desired signal that is buried in a noisy measurement signal. In general and for our purposes, a “signal” can be interpreted to be a scalar or multidimensional construct; e.g., a time series, an image, a three-dimensional volume, a video sequence, etc. The fundamental mathematical approaches are common to all of these modalities. For tutorial purposes, we focus here on the fundamental matched filtering approach for a time series. The literature in matched filtering is vast, and a full understanding of the concept requires a great deal of study. This section endeavors to encapsulate the most important principles of matched filtering so as to aid the biologist in processing experimental data. The concepts are introduced with the idea that the reader can consult the referenced literature for in-depth treatments.

Imagine that we are conducting a scientific experiment involving a physical process that generates a noisy discrete-time temporal signal (time series). Our goal is to make a judgment or decision about whether or not the noisy measured signal contains a particular desired signal component of interest to us. We can say that we wish to *detect* the desired signal component. More specifically, imagine that we have a real noisy measured discrete-time signal

$$x(n) = a(n - n_0) + v(n) \quad (\text{Noisy Measurement Signal}) \quad (5.1)$$

where $a(n - n_0)$ is a time delayed version of the desired signal $a(n)$ that we wish to detect, $v(n)$ is noise (undesired component of the signal), n denotes the discrete time index, $n = 0, 1, 2, \dots, N - 1$, n_0 is the time delay, and the sampling interval T is normalized to one (i.e., $T = 1$ s, so $nT = n$). We assume that the arrival time n_0 of the desired signal $a(n - n_0)$ is unknown to the user.

Perhaps the simplest way to *detect* the signal $a(n)$ in the noisy measurement $x(n)$ is to choose various values of a threshold γ and compare the amplitude values of $x(n)$ to that threshold at each value of time n . This is often called a “threshold detector” that uses the raw signal $x(n)$ as the *decision statistic* (the quantity we compare to the threshold). At each time instant n , if $x(n)$ is less than the threshold γ , then we declare that $a(n)$ is not present in the measurement at time n . If $x(n)$ is greater than or equal to the threshold γ , then we declare that $a(n)$ is present in the measurement at time n . Of course, our declarations will vary as we vary the threshold value. This section discusses methods for dealing with the various declarations and measuring the performance of the detection algorithm.

Note that the terms “detection” and “classification” are often used interchangeably, for good reason. Detection theory is often regarded as a subset of classification theory. Classification generally describes methods for multidimensional hypothesis testing, but detection theory was originally developed for scalar (one dimensional) hypothesis testing. The distinction is not nearly as important as understanding their common underlying concepts.

Imagine now a scenario in which we have prior information about the desired signal $a(n)$. In the signal processing world, we always welcome prior knowledge because we are often able to incorporate it into our processing algorithms to give us an advantage. In many applications (especially in communication and radar systems), we have available exemplars of the signal $a(n)$ we wish to detect. In radar, for example, we have a pulse generator and antenna system that create waves in the form of a transient pulse which are propagated through a channel, reflect from a physical target, propagate back through the channel, and are measured by the antenna and radar system. In this scenario, we have prior knowledge of the transmitted transient pulse used to interrogate the target, because we generated it ourselves. We can, of course, generate additional exemplars of the transmitted pulse. The issue now is whether or not we can use this prior knowledge to help us detect such a transient pulse in a measured waveform. The idea behind the *correlation detector* is that we can.

5.1.1 The Correlation Detector

The term “correlation detector” refers to a signal detection algorithm that cross-correlates the measured data with a replica or exemplar of the desired signal. It is also sometimes called a “correlator” or a “replica correlator.” The basic idea behind the correlation detector is to use the mathematical operation called *cross-correlation* to scan the measured signal $x(n)$ with an exemplar of $a(n)$. The cross-correlation result is $R_{ax}(k)$, a time waveform that is a function of the time delay k between $a(n)$ and $x(n)$ during the correlation process. The premise of the correlation detector is that the cross-correlation waveform will be large when the measurement $x(n)$ contains nonzero $a(n)$ and small when it does not. The correlation detector uses the cross-correlation waveform $R_{ax}(k)$ (or a function of $R_{ax}(k)$) as the *decision statistic* in a threshold detection algorithm. The hope is that using $R_{ax}(k)$ as the decision statistic will give better detection performance than that which would be obtained by using the raw signal $x(n)$ as the decision statistic. This hoped-for result is generally realized in practice. Prior knowledge is very helpful.

5.1.2 Section Organization

In the remainder of this section, we introduce the matched filter by examining an example detection problem and showing the steps in the detection process. We show that the *matched filter* is really another name for the correlation detector and why. We then step through the process of detecting a signal buried in a noisy measurement and develop the appropriate measures for evaluating detector performance. We show that the matched filter can be an effective detection tool when exemplars of the desired signal are available a priori.

5.2 An Example Detection Problem

The data for an example event signal detection problem are depicted in Fig. 5.1. The *top signal* is a transient “event waveform” $a(n)$ representing a physical event that we wish to detect. In this particular case, this event is a dissolver acid time series from a chemical processing plant. The *middle signal* is a delayed version of the transient waveform with delay equal to n_0 . The *bottom signal* denotes the noisy measurement signal $x(n) = a(n - n_0) + v(n)$. The noise $v(n)$ is statistically white, zero mean and Gaussian distributed with noise variance $\sigma_v^2 = .599$. We denote this as $v(n) \sim N(0, \sigma_v^2)$. Clearly, the noise power is fairly large, so the desired event signal $a(n)$ is significantly obscured in the measurement. This leads us to define the concept of *signal-to-noise ratio*.

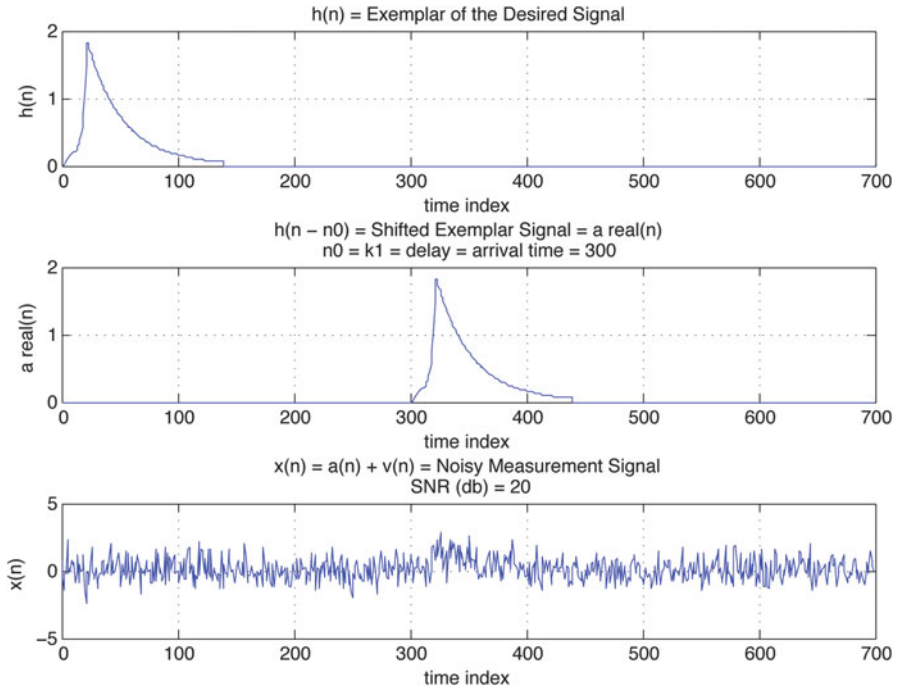


Fig. 5.1 Simulated measurement signal $x(n)$ created for our matched filtering example: (Top) Exemplar of the transient event waveform $a(n)$ we wish to detect in the noise measurement. (Middle) Time delayed version $a(n - n_0)$ of the transient waveform. (Bottom) Measured event plus noise signal $x(n) = a(n - n_0) + v(n)$. The signal-to-noise ratio is $\text{SNR} = 20$ dB. The magnitude units are arbitrary and the temporal sampling period $T = 1$

5.2.1 Define the Signal-to-Noise Ratio (SNR)

Consider a noisy measured signal as described in Eq. 5.1. In a nice theoretical simulation experiment, we can easily know the desired signal $a(n)$ and the noise $v(n)$ separately, because we create them ourselves. However, in many real-world experiments, we can measure only the sum in Eq. 5.1. In some experiments, the measured signal consists of pre-event noise (before a signal event occurs) followed in time by the sum of the event signal $a(n)$ and the noise $v(n)$. This occurs in, for example, seismic event signals. In this case, we can cut out a section of pre-event noise and compute its noise variance. In some rare applications, we have available a noiseless signal $a(n)$ before the physical system corrupts it (e.g., in communications and radar).

Let us assume for now that we have prior knowledge that allows us to separate the desired signal from the noise. In general, we define the signal-to-noise ratio (SNR) as follows (Kay 1998; Candy 2006):

$$\text{SNR} \triangleq \frac{\text{Signal energy}}{\text{Noise variance}} \quad (\text{Signal-to-noise ratio}) \quad (5.2)$$

$$\triangleq \frac{E_a}{\sigma_v^2} \quad (5.3)$$

where the energy in signal $a(n)$ is given by

$$E_a \triangleq \sum_{n=n_0}^{n_1} a^2(n) \quad (5.4)$$

and we calculate the energy in signal $a(n)$ over the time interval between appropriate time indices n_0 and n_1 . We denote the noise variance by σ_v^2 . We can express the SNR in the commonly used units of decibels (dB) by applying the following definition:

$$\text{SNR(dB)} \triangleq 10 \log_{10} \left[\frac{E_a}{\sigma_v^2} \right] \quad (5.5)$$

$$= 10 \log_{10}[R], \quad \text{where } R \triangleq E_a / \sigma_v^2 \quad (5.6)$$

Note that in a simulation experiment, once we have computed E_a for our particular signal and we know our desired SNR(dB), we can solve for the noise variance required to achieve that SNR(dB). If we define Q as follows, then we have:

$$Q \triangleq \text{SNR(dB)} / 10 \quad (5.7)$$

$$R = 10^Q \quad (5.8)$$

$$\sigma_v^2 = E_a / R \quad (5.9)$$

Consider a numerical example: Let $E_a = 4.2632$ and the desired SNR(dB) = 40. Then, we see that $Q = 4$, $R = 10^4$, and $\sigma_v^2 = 4.2532e - 4$. Note that in applications such as the seismic event signal described earlier, we can define an approximate SNR, call it *SNRE*, that consists of the ratio of the energy in the measured signal $x(n)$ and the noise variance (Clark and Rodgers 1981). This is one way in which we can cope with the lack of prior knowledge.

5.3 The Matched Filter Detector

The term *matched filter* is another name for the correlation detector. The fundamental principle of matched filtering is to exploit the prior knowledge we have about the desired signal of interest $a(n)$ to build a correlation detector. One might ask the question, "Then why do we call the correlation detector a matched filter?" The answer lies in the meaning of the mathematical operation of correlation, as we show next.

5.3.1 Convolution and Filtering

Given two discrete-time signals $a(n)$ of length M samples and $x(n)$ of length N samples, we can define the convolution $y(n)$ of the two signals as follows:

$$\begin{aligned} y(n) &= a(n) * x(n) = \sum_{k=-\infty}^{\infty} a(k)x(n-k) \\ &= x(n) * a(n) = \sum_{k=-\infty}^{\infty} x(k)a(n-k) \quad (\text{Convolution}) \quad (5.10) \end{aligned}$$

We see that convolution is commutative. The convolution operation can be interpreted as “flipping” (reversing) one of the two signals in time, then sliding it in time across the other signal and multiplying each of the values of the two signals together at each time sample and summing the products (Oppenheim and Schaffer 1975). The time-reversal operation is described mathematically by $x(-n)$ and $a(-n)$. The key concept is that a linear filtering operation in the time domain can be written as a convolution summation (Oppenheim and Schaffer 1975). Thus, if we filter a signal $x(n)$ with a linear filter impulse response $a(n)$, then that filtering operation is written as a convolution of the form in Eq. 5.11. Note that the convolution of a signal of length N with a signal of length M has length $N_c = N + M - 1$.

5.3.2 Correlation vs. Convolution

The correlation of two real discrete-time signals $a(n)$ of length M samples and $x(n)$ of length N samples is written as follows:

$$\begin{aligned} R_{ax}(n) &= a(n) * x(-n) = \sum_{k=-\infty}^{\infty} a(k)x(n+k) \\ &= x(n) * a(-n) = \sum_{k=-\infty}^{\infty} x(k)a(n+k) = R_{xa}(n) \quad (\text{Correlation}) \quad (5.11) \end{aligned}$$

We see from this equation that correlation is commutative, and the correlation operation can be written in terms of the convolution operation. If we do the convolution operation *without* reversing one of the two signals in time, then we get the correlation operation. We recall that the convolution operation reverses one of the signals in time before sliding it across the other signal. If we reverse one of the signals *before* doing the convolution, then the convolution reverses it again, so the result is an operation with a signal that has been reversed twice. This is equivalent to the *correlation* operation.

5.3.3 The Matched Filter

We are ready now to see why we call the correlation detector a *matched filter*. If we interpret the exemplar signal $a(n)$ to be the impulse response of a linear filter, then if we convolve $a(n)$ with $x(n)$, we are *filtering* the measurement $x(n)$ with a *filter matched to the signal of interest $a(n)$* . We have chosen a filter impulse response that is matched to the desired signal of interest $a(n)$. Because correlation is equivalent to convolution (with one of the signals flipped in time), we can think of the correlation operation as a filtering operation. Because the chosen filter impulse response is a signal matched to the desired signal, we call this filtering operation *matched filtering*. Of course, the term “matched filter” does not explicitly mention the fact that the filter output is used as the test statistic in a threshold detector, so the reader must infer that information without help from the name.

Figure 5.2 depicts the general block diagram for a matched filter detector, showing the filter, the test statistic, and the threshold test. In order to maximize detector performance and enable the proper measurement of performance, it can be shown (Kay 1998) that the threshold test must be conducted at the time sample corresponding to the largest value (peak) of the test statistic $r[y(n)]$. Letting n^* denote the time index corresponding to the peak of the test statistic, we conduct the threshold test at $r[y(n^*)]$.

5.3.4 Example: Applying the Matched Filter to Our Example Signals

Figure 5.3 depicts an example of a correlation detector scheme. We see that the scheme consists of a cross-correlation operation, a test statistic and a thresholding operation. Note the plots depicting the various signals at each step of the scheme. Note the very low noise level in the plot of the absolute value of the cross-correlation. This demonstrates a key property of the matched filter, that the matched filter maximizes the SNR at the output of the filter/correlator. We discuss the processing scheme in detail in the following sections.

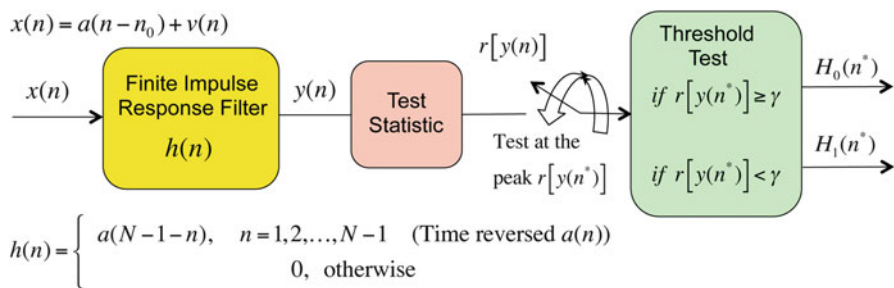


Fig. 5.2 General matched filter block diagram. Letting the time sample at which the test statistic is maximum be denoted by n^* , note that the threshold test is conducted at the peak $r[y(n^*)]$ of the test statistic r . Ideally, $n^* = n_0$. The decision threshold is denoted by γ

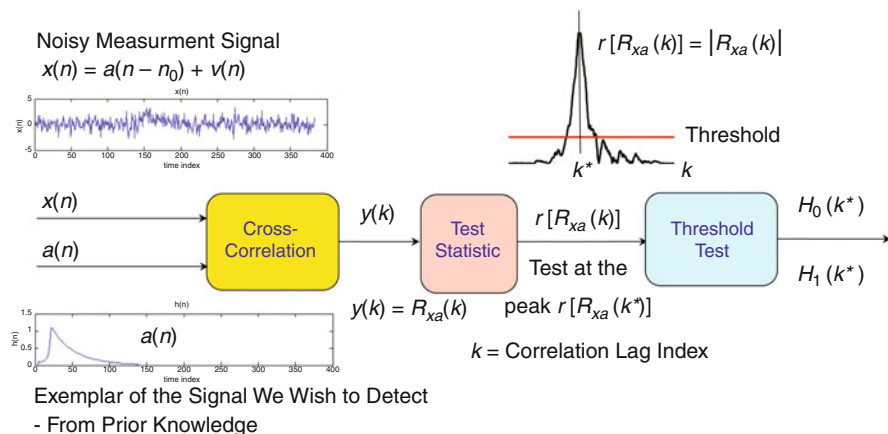


Fig. 5.3 Block diagram for the example problem. Letting the correlation lag index at which the test statistic is maximum be denoted by k^* , note that the threshold test is conducted at the peak of the test statistic, $r[R_{xa}(k^*)] = |R_{xa}(k^*)|$

5.4 Bayesian Binary Hypothesis Testing and Performance Measurement

Bayesian detection theory provides a rigorous foundation for evaluating detector performance (Whalen 1971; Van Trees 1968). Assume that we have a noisy one-dimensional (scalar) measured discrete-time signal (time series) as in Eq. 5.1. In general, the desired signal $a(n)$ can be deterministic or stochastic, and the noise $v(n)$ is modeled as stochastic and uncorrelated (statistically white) or correlated (statistically colored). In this tutorial, we model the desired signal $a(n)$ as deterministic (Papoulis 1965). We treat the noise as either uncorrelated or correlated. Most textbooks focus on the special case when the noise is Gaussian distributed (Whalen 1971; Kay 1998; Van Trees 1968), and for that case, the reader is directed to the references. For generality, this tutorial makes no assumptions about the form of the noise distribution.

We can use *binary hypothesis testing* to make decisions or *declarations* about whether or not the desired signal $a(n)$ is present in the measurement. The hypothesis that $a(n)$ is not present in measurement $x(n)$ is denoted H_0 , and the hypothesis that $a(n)$ is present in $x(n)$ is denoted H_1 .

$$\begin{aligned} H_0 : x(n) &= v(n) && \text{(Null Hypothesis: Desired Signal Not Present)} \\ H_1 : x(n) &= a(n - n_0) + v(n) && \text{(Alternative Hypothesis: Desired Signal Present)} \end{aligned} \quad (5.12)$$

Notice that this problem definition assumes that we do not know in advance the arrival time n_0 of the signal of interest $a(n - n_0)$. We must estimate the arrival time as part of the detection/classification process. As depicted in Figs. 5.2 and 5.3, the

general matched filter includes computing a test statistic $r[y(n)]$. This test statistic can take many forms; however, probably the most commonly used is the absolute value of the correlation result $y(n)$, as shown in the figure. Recall from before that this threshold test is conducted at the time sample at which the test statistic is maximum (Kay 1998). For our case, the test statistic is the absolute value of the cross-correlation. Because the correlation lag index is different from the signal time index n , we denote the lag index by k , and we denote the lag index at which the test statistic is maximum by k^* . This index k^* corresponds to the arrival time n_0 of the desired signal $a(n-n_0)$. Expressed mathematically, we define k^* as the correlation lag index that satisfies:

$$\max_{k \in [0, N-M]} |R_{xa}(k)| \quad (5.13)$$

Recall that N is the number of time samples in $x(n)$ and M is the length of $a(n)$. The set of k values over which to search is $[0, N - M]$ because that is the range over which the cross-correlation is affected by the signal $a(n)$ (Kay 1998). The decision is made when the test statistic evaluated at k^* is compared with the threshold γ :

$$r[R_{xa}(k^*)] \underset{H_0}{\overset{H_1}{\gtrless}} \gamma \quad (\text{Decision Rule}) \quad (5.14)$$

5.4.1 The Confusion Matrix (or Contingency Table)

Each time the hypothesis test is conducted, one of four events can occur: (1) H_0 is true and we declare H_0 , (2) H_0 is true and we declare H_1 , (3) H_1 is true and we declare H_1 , and (4) H_1 is true and we declare H_0 . The first and third alternatives correspond to correct choices. The second and fourth alternatives correspond to errors. The confusion matrix (or contingency table) depicted in Fig. 5.4 summarizes these four events, their associated probabilities, and the method for computing the four probabilities. The Bayes test assumes that there exist prior probabilities (priors) for the hypotheses and costs associated with the four courses of action. The priors $P(H_0)$ and $P(H_1)$ represent information available about the source prior to conducting the experiments. The costs for the four possible courses of action are given by C_{00} , C_{10} , C_{11} , and C_{01} , where C_{ij} is the cost of deciding H_i given that H_j is true. Once the costs have been assigned, the decision rule is based on minimizing the expected cost, which is known as the Bayes risk \mathfrak{R} (Van Trees 1968; Whalen 1971; Kay 1998):

$$\mathfrak{R} = \sum_{i=0}^1 \sum_{j=0}^1 C_{ij} P(H_i | H_j) P(H_j) \quad (\text{Bayes Risk}) \quad (5.15)$$

We assume throughout this discussion that the cost of an incorrect decision is higher than the cost of a correct decision. In other words, $C_{10} > C_{00}$ and $C_{01} > C_{11}$.

"Confusion Matrix" or Contingency Table for Binary Hypothesis Testing		
Truth Declaration	True Hypothesis H_0 (Null)	True Hypothesis H_1
Declared Hypothesis H_0 (Null)	$P(H_0 H_0) = P_{Spec} = \text{Specificity}$ $= \frac{\# H_0 \text{ Samples Declared } H_0}{\# H_0 \text{ Samples}}$	$P(H_0 H_1) = P_{Miss} = P(\text{Miss})$ $= \frac{\# H_1 \text{ Samples Declared } H_0}{\# H_1 \text{ Samples}}$
Declared Hypothesis H_1	$P(H_1 H_0) = P_{FA} = P(\text{False Alarm})$ $= \frac{\# H_0 \text{ Samples Declared } H_1}{\# H_0 \text{ Samples}}$	$P(H_1 H_1) = P_D = P(\text{Detection})$ $= \frac{\# H_1 \text{ Samples Declared } H_1}{\# H_1 \text{ Samples}}$
	$P(H_0 H_0) + P(H_1 H_0) = 1$	$P(H_0 H_1) + P(H_1 H_1) = 1$

$$P_{cc} = P(\text{Correct Classification}) = P(H_0 | H_0)P(H_0) + P(H_1 | H_1)P(H_1)$$

$$P_e = P(\text{Error}) = 1 - P_{cc} = P(H_0 | H_1)P(H_1) + P(H_1 | H_0)P(H_0)$$

Assume: Correct classification is given zero cost $\Rightarrow C_{00} = C_{11} = 0$

Incorrect classification is given full cost $\Rightarrow C_{01} = C_{10} = 1$

Fig. 5.4 Confusion matrix (contingency table): the two hypotheses are denoted H_0 , the null hypothesis, and H_1 , the alternative hypothesis. Note that for the special case in which the prior probabilities are equal ($P(H_0) = P(H_1) = \frac{1}{2}$), the probability of correct classification becomes $P_{CC} = \frac{1}{2}[P_D + (1 - P_{FA})]$. Note that we construct one confusion matrix for each value of the decision threshold γ

Note that in the confusion matrix, the probabilities in the two columns of the matrix each sum to one. An important special case of the Bayes criterion is that in which a correct classification is assigned zero cost and an incorrect classification is assigned full cost. In this case, we assign $C_{00} = C_{11} = 0$ and $C_{01} = C_{10} = 1$. Inserting these values in the Bayes Risk of Eq. 5.15 and using the fact that $P(\text{error}) + P(\text{correct classification}) = 1$, we obtain the probability of correct classification. Note that P_{cc} is the weighted sum along the main diagonal of the confusion matrix, weighted by the priors:

$$P(\text{Correct Classification}) = P_{CC} = P(H_1, H_1) + P(H_0, H_0) \tag{5.16}$$

$$= P(H_1 | H_1)P(H_1) + P(H_0 | H_0)P(H_0) \tag{5.17}$$

Often in practice, there exists insufficient information about an experiment to allow the user to assign the values of the prior probabilities P_0 and P_1 . In this case, it is common to assume that the priors are equal (no information), so $P(H_0) = P(H_1) = \frac{1}{2}$. Under this condition, the probability of correct classification becomes

$$P_{CC} = \frac{1}{2}[P(H_1|H_1) + P(H_0|H_0)] \quad (5.18)$$

This can now be written in terms of the probability of detection and probability of false alarm as follows:

$$P_{CC} = \frac{1}{2}[P_D + (1 - P_{FA})] \quad (\text{Probability of Correct Classification}) \quad (5.19)$$

5.4.2 Bayesian Hypothesis Testing for Multidimensional (Vector) Data

Let us now generalize our discussion. Our example problem specifies a scalar measurement signal $x(n)$. However, in general, we can have a vector of J observations denoted as follows.

$$\underline{X} = [x_1, x_2, \dots, x_J]^T \quad (\text{Observation Vector}) \quad (5.20)$$

The observations $x_j, j = 1, 2, \dots, J$ are called features of the physical process being observed, and T denotes the vector transpose. In our example problem, the vector has one element $x(n)$, the measurement signal. We assume throughout this discussion that the cost of an incorrect decision is higher than the cost of a correct decision. In other words, $C_{10} > C_{00}$ and $C_{01} > C_{11}$. Under this assumption, the detector that minimizes the Bayes risk is given by the following (Van Trees 1968):

$$\frac{f(\underline{X}|H_1)}{f(\underline{X}|H_0)} \underset{H_0}{\overset{H_1}{\gtrless}} \frac{P(H_0)(C_{10} - C_{00})}{P(H_1)(C_{01} - C_{11})} \quad (\text{Bayes Decision Criterion}) \quad (5.21)$$

where $f(\underline{X}|H_1)$ denotes the conditional probability density function (pdf) of the observation vector \underline{X} given that hypothesis H_1 is true, and $f(\underline{X}|H_0)$ denotes the conditional pdf of \underline{X} given that hypothesis H_0 is true (Kay 1998). The ratio of the conditional densities is called the likelihood ratio and is denoted by $\Lambda(\underline{X})$:

$$\Lambda(\underline{X}) = \frac{f(\underline{X}|H_1)}{f(\underline{X}|H_0)} \quad (\text{Likelihood Ratio}) \quad (5.22)$$

Because this is a ratio of two functions of a random variable, the likelihood ratio is a random variable. A very important result is that regardless of the dimensionality of the observations \underline{X} , the likelihood ratio $\Lambda(\underline{X})$ is a one-dimensional variable. This idea is of fundamental importance in hypothesis testing. Regardless of the dimension of the observation space, the decision space is one dimensional. The quantity on the right-hand side of the relation (5.21) is the threshold of the test and is denoted by γ :

$$\gamma \triangleq \frac{P(H_0)(C_{10} - C_{00})}{P(H_1)(C_{01} - C_{11})} \quad (\text{Decision Threshold}) \quad (5.23)$$

Thus, the Bayes criterion leads to a likelihood ratio test:

$$\Lambda(\underline{X}) \underset{H_0}{\overset{H_1}{\gtrless}} \gamma \quad (\text{Likelihood Ratio Test}) \quad (5.24)$$

We see that the test threshold allows for weighting according to the priors and the costs. This allows the user flexibility in choosing a threshold that is best for the problem at hand. Note that if we have available the conditional pdfs or estimates of them, we can construct the confusion matrices (one for each value of the threshold) by integrating under the pdfs as depicted in Fig. 5.6. In most practical problems, we do not have the pdfs, so we construct the confusion matrices using the threshold method shown in Fig. 5.2.

5.4.3 Training and Testing Phases of the Detection Process

In order to measure detection performance, we must be able to conduct controlled experiments in which we know the correct experimental outcomes (“ground truth”) a priori (Duda and Hart 1973; Duda et al. 2001). This is a very important point that is often overlooked. Our use of the threshold detector occurs in phases. (1) First, in the *Training Phase*, we conduct controlled experiments in which the ground truth is known in order to construct a Receiver Operating Characteristic (ROC) curve from which we determine the appropriate operating threshold for the detector. We use a set of known “training data” during this phase. (2) Second, in the *Testing Phase*, we use the selected operating threshold on a set of “testing data,” from which we produce operational detection results. The remainder of this section concentrates on the training phase. Note that the training and testing process involves a considerable “leap of faith” in which we assume that the training data are representative of the test data. Therefore, extreme care must be taken to ensure that this assumption is valid. Otherwise, interpretations of the processing results may be meaningless.

The user should carefully design the experiments so the statistical sample size (number of data samples we can use for performance evaluation) is large enough to enable the computation of meaningful confidence intervals (see the following two subsections). Figure 5.5 summarizes some rules of thumb for picking the training and testing data sets. Using ground truth, we create a labeled data set in which each data sample is labeled H_0 or H_1 . *Rule of Thumb 1*: We generally want to have a large sample size (approximately 100 or 1,000 or more). However, the real world often does not allow us this luxury. *Rule of Thumb 2*: If the data are Gaussian distributed, we need a minimum of about 30 or more samples to obtain reasonable confidence

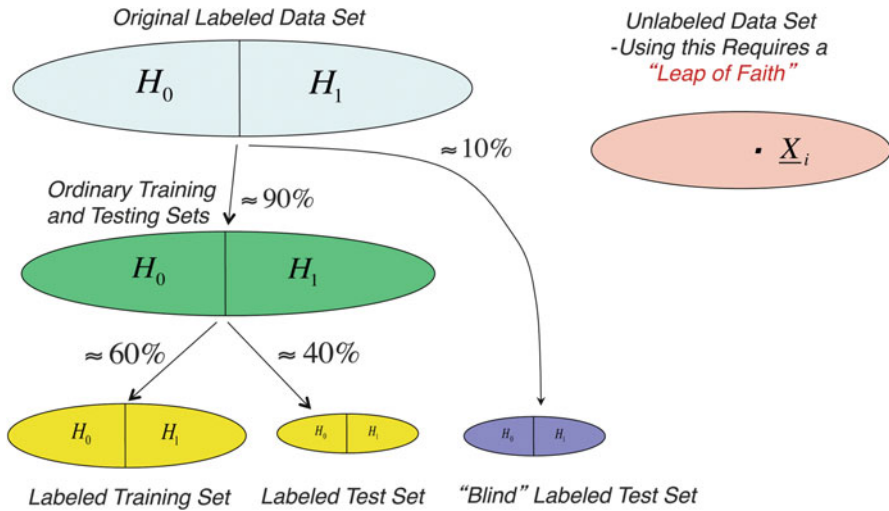


Fig. 5.5 (Left) Training data sets for controlled experiments are depicted on the left side. These include the standard labeled training and testing sets, as well as a possible blind test set that can be used if enough data are available. When using this, we can ask some unbiased users to conduct the experiment. (Right) The unlabeled test set is used after training and testing in the controlled experiments. To minimize the “leap of faith,” these data should be representative of the data in the training and testing sets

interval estimates (Hogg and Craig 1978). If our sample size is small, we turn to “hold one out” and bootstrap algorithms for estimating confidence intervals (Zoubir and Iskander 2004). Even with these methods, we cannot take too seriously any results with very small sample sizes. *Rule of Thumb 3*: Generally, we should set aside about 60 % of our labeled samples for the training phase and the other 40 % for the testing phase (Hand 1981; Devijver and Kittler 1987). *Hard Rule*: Never test on the training set. That is cheating and leads to improper inferences. Despite warnings, many people continue to do this. Please do not become one of them.

5.4.4 The Receiver Operating Characteristic (ROC) Curve

A Receiver Operating Characteristic (ROC) curve is constructed to quantify the tradeoff between the probability of detection P_D and the probability of false alarm P_{FA} versus the detection threshold γ , as depicted in Fig. 5.6 (Whalen 1971; Duda et al. 2001; Duda and Hart 1973; Van Trees 1968; Kay 1998). Note that this requires the construction of one confusion matrix for each value of the threshold. We vary the value of the decision threshold γ over the full range of values of the decision statistic $r[y(n)]$. For each measurement signal in the ensemble, at the time sample n^* , we compare the decision statistic to the decision threshold as in Fig. 5.2. If $r[y(n^*)] < \gamma$, we declare that H_0 is true. If $r[y(n^*)] \geq \gamma$, we declare that H_1 is true.

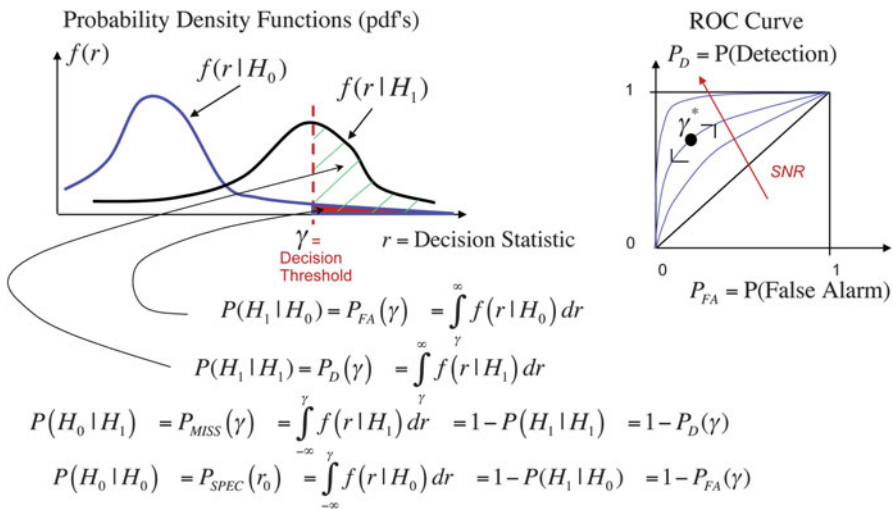


Fig. 5.6 The Receiver Operating Characteristic (ROC) curve can be constructed by integrating the conditional probability density functions depicted on the left. This, of course, assumes that the pdfs or estimates of them are available. If not, then we generally use the confusion matrix method

Once we have the ROC curve, we choose the “operating threshold” γ^* to be the one that maximizes $P_D(\gamma)$ and minimizes $P_{FA}(\gamma)$. This threshold value is found at the “knee” of the ROC curve at the appropriate SNR for the experiment. *Note that this knee occurs for the threshold value at which the probability of correct classification P_{CC} is maximum.* We denote this by $P_{cc}(\gamma^*)$.

5.4.5 Statistical Confidence Interval About the Probability of Correct Classification

The author believes that “the ROC curve is not finished until we have computed the confidence interval on the probability of correct classification.” Unfortunately, this last step is almost always overlooked by most practitioners. P_{cc} is not a deterministic quantity. It can be viewed as a random variable with an associated distribution.

The classifier/detector performs a random experiment, the outcome of which can be classified in one of two mutually exclusive and exhaustive ways: success or failure. Success means that the classification is correct. Failure means that the classification is incorrect. Let N equal the number of independent trials. Let $p = P_{cc}$ = the probability of correct classification. Assume that the true value p is the same on each repetition. Let $q = 1 - p$ = probability of error. For the classification problem in which we conduct an experiment, we can calculate the estimated quantities in the confusion matrix. The maximum likelihood estimate of p is given by \hat{p} and is the estimated \hat{P}_{CC} computed in the confusion matrix. We can

write the confidence interval about the true value of p as follows, where α , a probability, is the significance of the test.

$$P\{L < p < U\} = 1 - \alpha \quad (\text{Confidence Interval about } p) \quad (5.25)$$

where L and U are the lower and upper bounds, respectively, of the confidence interval. The most common interpretation is to read the confidence interval relation above as follows: “With confidence $1 - \alpha$, the true p lies between L and U .” However, this interpretation is not generally supported by statistical rigor. The preferred interpretation is: “Prior to the repeated independent performances of the random experiment, the probability is $1 - \alpha$ that the random interval (L , U) includes the unknown fixed point (parameter) p (Hogg and Craig 1978).” For our example problem, we arbitrarily choose $\alpha = 0.05$ so we have a “95 percent confidence interval.”

There exists a significantly large literature on how to compute the lower and upper bounds L and U . In most practical cases, the author prefers to use bounds that do not assume a particular distribution and which can be used for both small and large sample sizes N . To this end, a reasonable set of bounds is the following (Hogg and Craig 1978):

$$L = N\hat{p} + 2 - 2\sqrt{\frac{N\hat{p}(1-\hat{p})+1}{N+4}} \quad (\text{Lower Bound on } p) \quad (5.26)$$

$$U = N\hat{p} + 2 + 2\sqrt{\frac{N\hat{p}(1-\hat{p})+1}{N+4}} \quad (\text{Upper Bound on } p) \quad (5.27)$$

We can evaluate L and U and plot them versus the true p and the estimated \hat{p} , for various values of the sample size N , as in Figs. 5.8 and 5.10. These plots are very instructive in showing how confidence intervals tighten as the sample size increases. Bootstrap techniques for estimating confidence intervals from the data for small sample sizes are discussed in Zoubir and Iskander (2004).

5.5 Processing for the Example Problem

5.5.1 Experiment Design for the Example Problem

The *training data* were created so as to allow the computation of the confusion matrices necessary for computing the ROC curve and the confidence interval on P_{cc} . Please refer to Fig. 5.5. For the null hypothesis H_0 , we simulated an ensemble of $P = 300$ *labeled* realizations (each realization is labeled H_0) of the simulated measurement waveform $x(n)$ specified in Eq. 5.15 in which the desired signal $a(n) = 0$. Each realization of $x(n)$ is different because each has a different realization of the stochastic process $v(n)$. For hypothesis H_1 , we created an ensemble of $P = 300$ *labeled* realizations of the simulated measurement waveform $x(n)$ in which the desired signal $a(n)$ is nonzero. Again, each realization of $a(n)$ is different

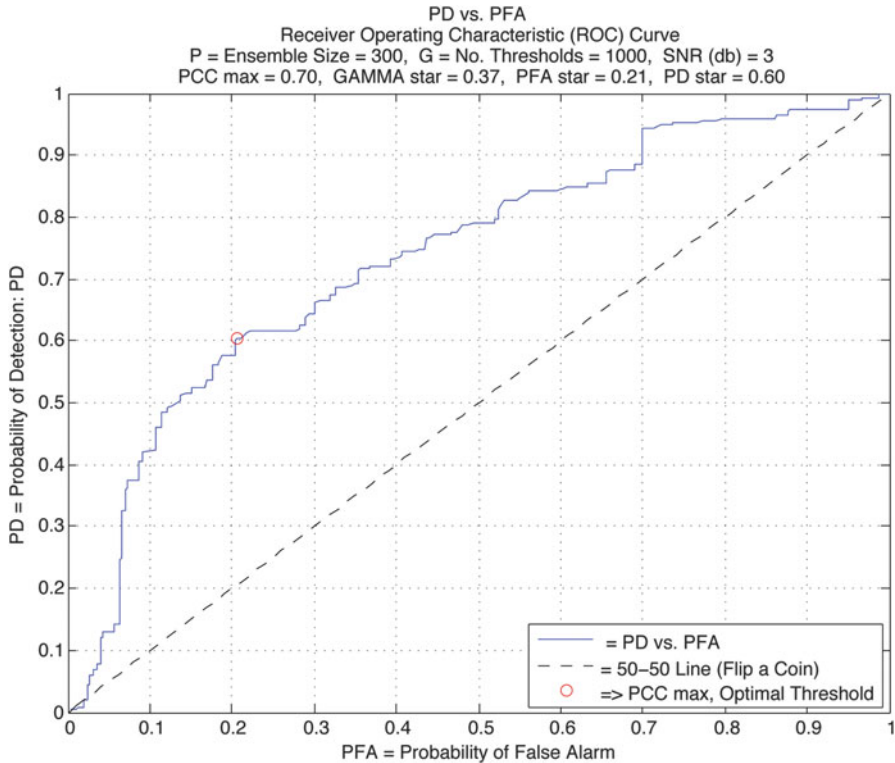


Fig. 5.7 Example problem for SNR = 3 dB: the ROC curve is plotted given the sample size $P = 300$ samples per class (300 for H_0 and 300 for H_1). The abscissa is probability of false alarm P_{FA} , and the ordinate is probability of detection P_D computed using confusion matrices. The knee of the curve (marked by a circle) occurs at $P_{CC}(\gamma^*) = .698$, $P_{FA}(\gamma^*) = .21$ and $P_D(\gamma^*) = .60$. The corresponding operating detection threshold is $\gamma^* = 0.37$

because each has a different realization of the stochastic process $v(n)$. These ensembles are sufficient to compute the performance indices. For *controlled testing* purposes, we can similarly simulate two more labeled ensembles of realizations of the stochastic process $x(n)$. For *blind controlled testing*, we can similarly simulate two additional *labeled* ensembles. For *uncontrolled testing*, we can similarly simulate two more *unlabeled* ensembles.

5.5.2 Processing Results for the Example Problem

For our example, we have no prior knowledge from which to derive prior probabilities $P(H_0)$ and $P(H_1)$ so we assume that the two hypotheses are equally likely, and $P(H_1) = P(H_0) = \frac{1}{2}$. Under this condition, the expression for P_{cc} is simplified, as shown in Eq. 5.19.

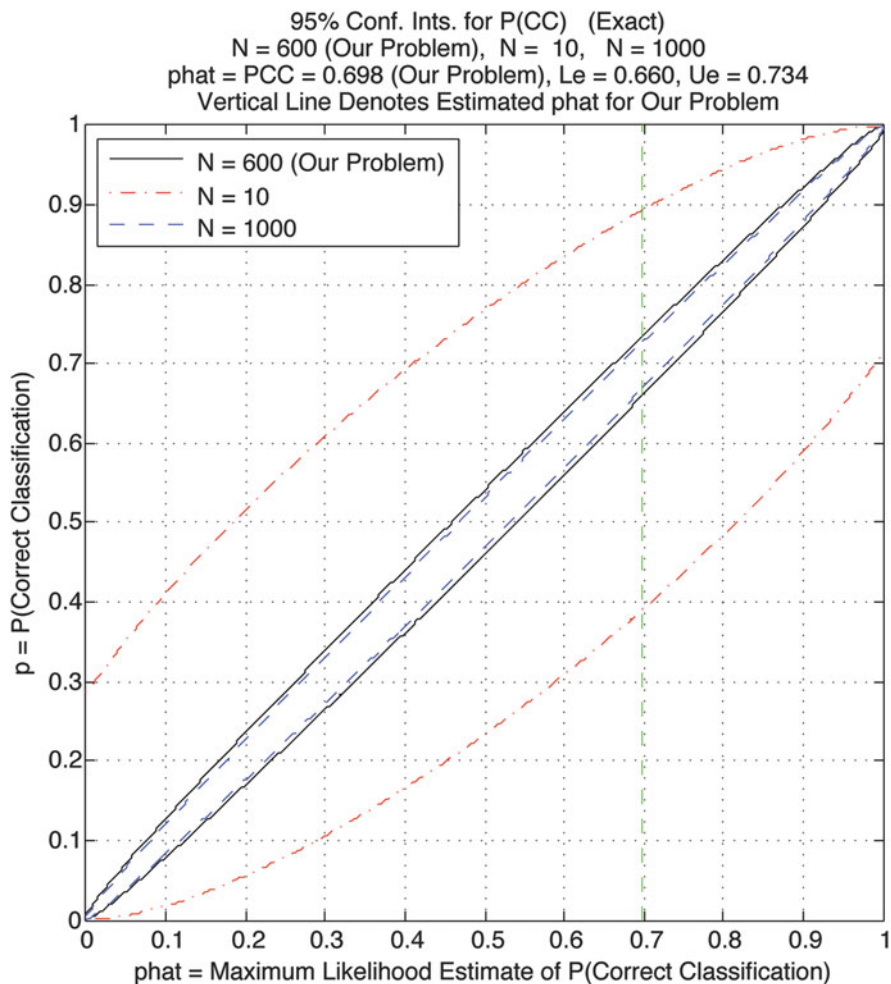


Fig. 5.8 Example problem for SNR=3 dB: the abscissa is \hat{p} = the maximum likelihood estimate of the probability of correct classification. The ordinate is p = the true value of the probability of correct classification. The 95 % ($1 - \alpha = .95$) confidence interval bounds (L, U) = (.66, .734) for the probability of correct classification are plotted, given the sample size $N = 600$ and $\hat{p}^* = P_{CC}(\gamma^*) = .698$ (the green vertical line). Note that the confidence interval tightens as the sample size N increases

Figure 5.7 depicts a ROC curve constructed for our threshold detector example in which the SNR is 3 dB. We see that with this low SNR, the curve is far away from the desired upper left-hand corner of the diagram, and the knee of the curve (marked by a circle) occurs at $P_{CC}(\gamma^*) = .667$, $P_{FA}(\gamma^*) = .36$ and $P_D(\gamma^*) = .76$. Figure 5.8 presents the confidence interval about the P_{CC} for this example in which the SNR is 3 dB. For our problem, the number of samples (signals) in the training data for both

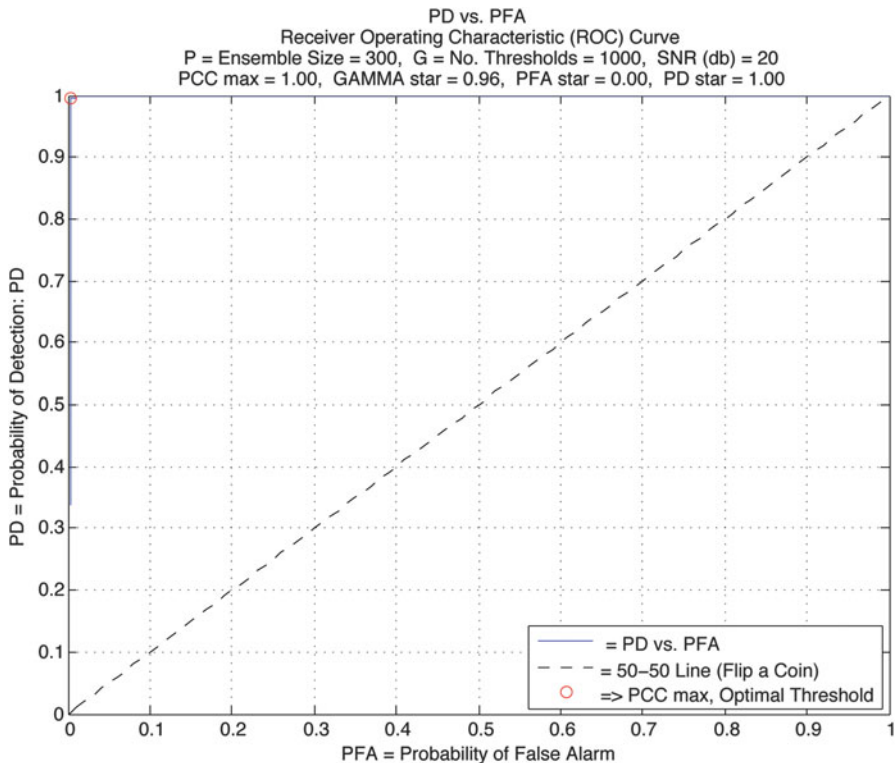


Fig. 5.9 Example problem for SNR = 20 dB: the ROC curve is plotted given the sample size $P = 300$ samples per class (300 for H_0 and 300 for H_1). The abscissa is probability of false alarm P_{FA} , and the ordinate is probability of detection P_D computed using confusion matrices. The knee of the curve (marked by a circle) occurs at $P_{CC}(\gamma^*) = .997$, $P_{FA}(\gamma^*) = .01$ and $P_D(\gamma^*) = 0.99$. The corresponding operating detection threshold is $\gamma^* = 0.96$

H_0 and H_1 is $N = 600$ and the estimate of $P_{CC}(\gamma^*) = \hat{p} = .667$. The green vertical line depicts \hat{p} , and the curves it crosses depict the lower and upper bounds on p . We see that the confidence interval is given by $P(.627 < p < .704) = .95$. The corresponding operating detection threshold is $\gamma^* = 0.36$. For tutorial purposes, the figure also shows what the bounds would be if $N = 10$ and $N = 1000$. We see that for small N , the bounds are very wide and for large N , the bounds are much narrower, as expected.

In Fig. 5.9, the SNR is 20 dB and the ROC curve lies in the desired upper left-hand corner. Here, the knee of the curve occurs at $P_{CC}(\gamma^*) = .997$, $P_{FA}(\gamma^*) = .01$ and $P_D(\gamma^*) = .99$. The corresponding operating detection threshold is $\gamma^* = 0.91$. Figure 5.10 shows the confidence interval for $N = 600$ and $\hat{p} = .993$. The estimated 95 % confidence interval is given by $P(.988 < p < .997) = .95$. We see the clear performance improvement that occurs with increased SNR.

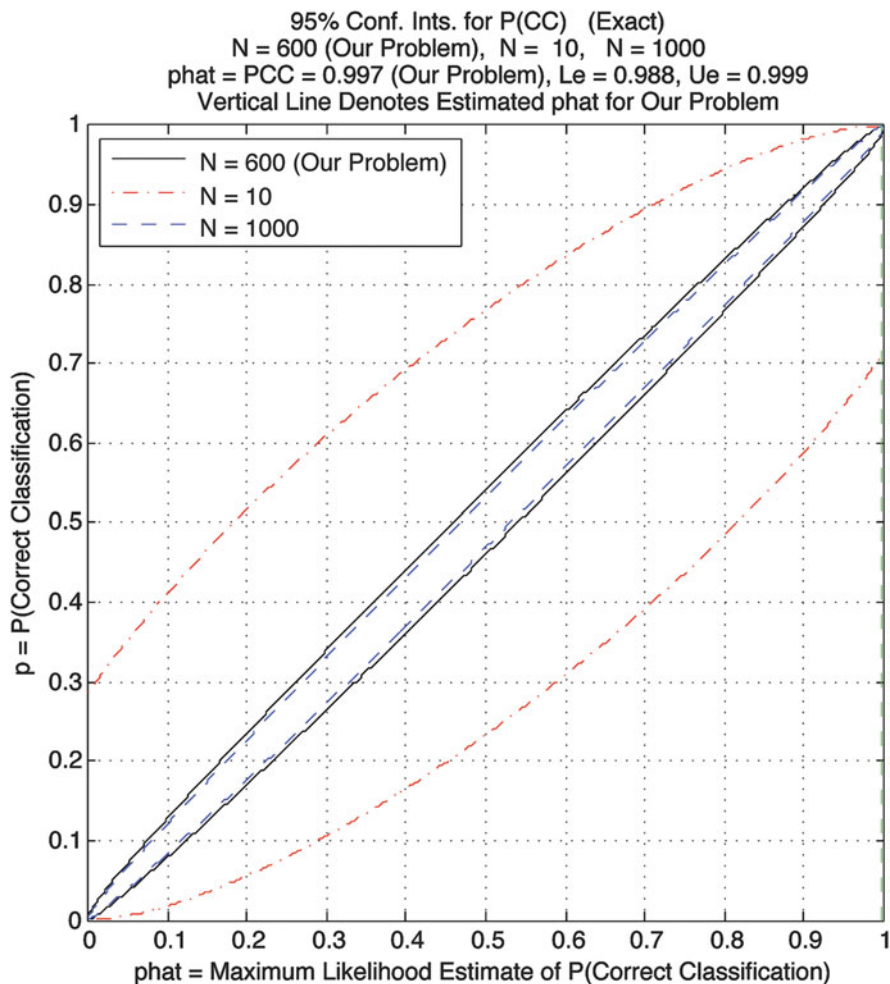


Fig. 5.10 Example problem for SNR=20 dB: The abscissa is \hat{p} = the maximum likelihood estimate of the probability of correct classification. The ordinate is p = the true value of the probability of correct classification. The 95 % ($1 - \alpha = 0.95$) confidence interval bounds $(L, U) = (.988, .999)$ for the probability of correct classification are plotted, given the sample size $N = 600$ and $\hat{p}^* = P_{CC}(\gamma^*) = .997$ (the *green vertical line*). Note that the confidence interval tightens as the sample size N increases

5.5.3 Conclusions

In this chapter, we introduce the concept of matched filtering for detecting desired signals buried in noisy measurement signals. We show that the *matched filter* is another name for the *correlation detector*, which exploits prior knowledge in the form of an exemplar of the desired signal. We use an example detection problem to

demonstrate the matched filtering approach. We see that the detection methodology comes from hypothesis testing algorithms in Bayesian detection theory. This Bayes approach gives us very powerful methods to choose the detection threshold and evaluate detection performance in the form of the Receiver Operating Characteristic (ROC) curve and the statistical confidence interval about the probability of correct classification. We show that the matched filter can be an effective detection tool when exemplars of the desired signal are available a priori.

5.6 Part II Auditory Matched Filtering: Biological Examples from Selected Vertebrates

According to the auditory matched filter hypothesis (Capranica and Moffat 1983), auditory information processing in sub-mammalian vertebrates (e.g., fishes, amphibians, reptiles, and to some extent birds) relies on extensive peripheral prefiltering. In other words, the auditory sensory filter (ear) is often tuned to signals of biological importance to the species so that less post-processing is required by the reduced central nervous systems in these species. In contrast, mammals can afford to “take in” all sensory input and rely on their superior brain power to sort out the meaning behind the message. The optimum receiver strategy, according to one formulation of the matched filter hypothesis, is to “design” a bias into the frequency response of the auditory system (Capranica and Moffat 1983; Wehner 1987). Rather than a high-fidelity flat frequency response (no bias), the receiver’s auditory system should have a frequency response which closely matches the envelope of the energy spectrum of the emitter’s call. This ensures that the receiver maximizes the signal-to-noise ratio in the frequency domain for that particular call. Figure 5.11 illustrates the decision criterion of such a matched filter detector. The received

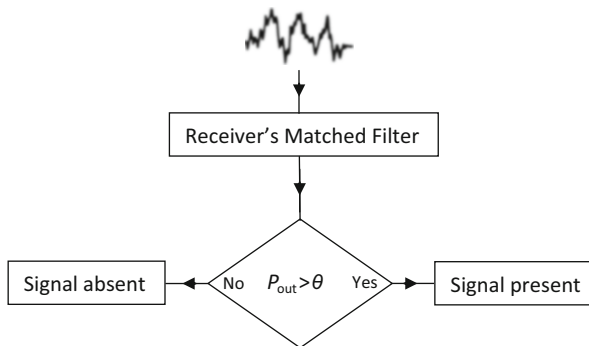


Fig. 5.11 Schematic diagram for the decision criterion of a matched filter detector. Signal propagation through the environment results in a noisy signal at the input to the receiver’s matched filter. If the power output (P_{out}) of the filter exceeds a certain threshold (θ), the receiver decides that the emitter’s signal is present. If P_{out} remains below this θ , the receiver decides that no signal is present. By adjusting the internal threshold, the reliability of the receiver’s decision can be modulated (Modified from Capranica and Rose (1983))

signal has been contaminated by unwanted noise. After passing through the filter, the receiver must make a decision if the signal is present or not. One decision criterion is to simply ask if the power (energy per unit time) output of the matched filter at any time exceeds some internal threshold (θ); if it has, the signal is present; if not, the signal is not present. But this statistical decision-making process depends critically on the setting of θ . If θ is set too low, the false alarm rate will be high; if θ is set too high, the receiver runs the risk of missing some of the signals (Capranica and Moffat 1983). In the following section, we have chosen several examples from the literature of sub-mammalian vertebrates which appear to exhibit a conspicuous match between the properties of their acoustic signals and the tuning of their auditory systems and thus provide evidence biological matched filters (Wehner 1987).

5.6.1 Weakly Electric Fish

5.6.1.1 Correspondence of Electric Organ Discharge and Electroreceptor Tuning

The wavelike electric organ discharge (EOD) in some gymnotoid species of South American weakly electric fish is one of the most regular of all known biological phenomena (Heiligenberg 1991). The internal fluctuation in the EOD rate is ca. 0.01 %. In these fish, the electric field is generated by the electric organ located in the tail, and the field is sensed by electroreceptors in the head region. In a landmark study of gymnotoids, the EOD frequencies of three species were recorded and compared to the best frequencies (BFs) of a population of tuning curves obtained electrophysiologically from individual fibers innervating electroreceptors (Hopkins 1976). Figure 5.12 is a plot of the electroreceptor BFs versus the EOD frequencies from the same fish, for three different species. Clearly, there is a high degree of matching between the electroreceptor tuning and the EOD rate.

5.6.1.2 Effect of Androgens on the Matched Filter

Meyer and Zakon (1982) confirmed the strong matching between the EOD discharge rate and electroreceptor tuning in another species of South American weakly electric fish—*Sternopygus*. Moreover, they demonstrated that systematic treatment of these fish with androgens—in this case 5 α -dihydrotestosterone (DHT)—lowered their EOD rate. Concomitantly, DHT caused decreases in electroreceptor best frequencies over a 2-week period, maintaining the close match between discharge frequency and receptor tuning. Thus, electroreceptor tuning is dynamic and it parallels natural shifts in the EOD frequency.

5.6.2 Anuran Amphibians

To help ensure that an appropriate behavioral response is evoked during acoustic communication, the anuran auditory system is often tuned to salient spectral and/or

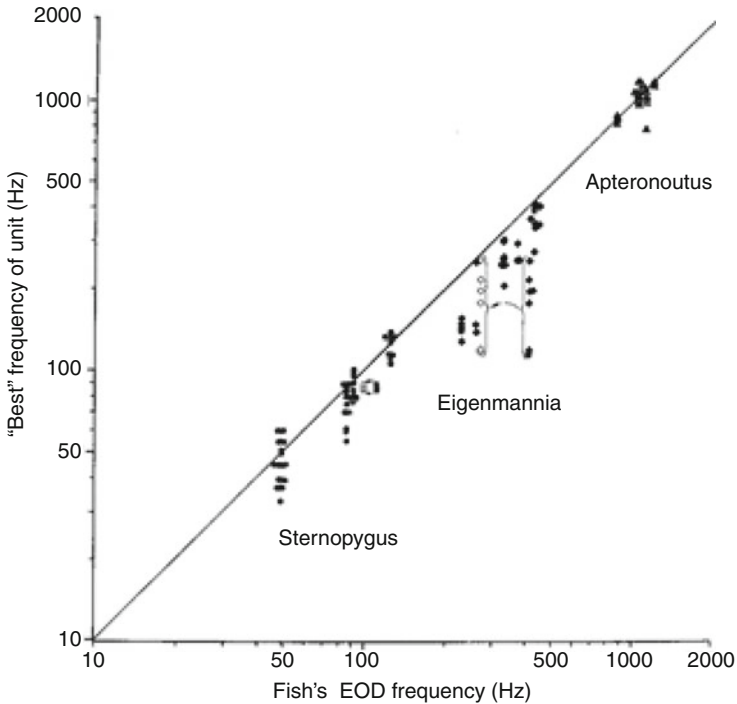


Fig. 5.12 Plot of the electroreceptor BFs versus the EOD frequencies from the same fish, for three different species of South American weakly electric fish (*Sternopygus macrurus*, *Eigenmannia virescens*, and *Aptereronotus albifrons*). Clearly, there is a high degree of matching between the electroreceptor tuning and the EOD rate. The *diagonal line* shows perfect correspondence between EOD frequency and BF (From Hopkins (1976))

temporal features of the conspecific call (Frishkopf et al. 1968; Capranica and Moffat 1975; Capranica and Rose 1983). The elegant coevolution of this relatively straightforward acoustic system has made anurans an extremely valuable neuroethological model for the study of acoustic communication.

5.6.2.1 The Puerto Rican Coqui (*Eleutherodactylus coqui*)

The Puerto Rican Coqui frog, *Eleutherodactylus coqui* (*Anura: Leptodactylidae*), is abundant in Puerto Rico where it can be found at altitudes from sea level to over 1,000 m above sea level (a.s.l.). Males of this arboreal amphibian are territorial, spaced several meters from each other, and call from tree branches or vegetation from sunset to shortly after midnight throughout 11 months of the year. They produce a characteristic two-note call (“Co-Qui”) in which each note has a different significance for each sex: males use the “Co”-note for territorial defense, while females are attracted to the “Qui”-note (Narins and Capranica 1976, 1978). In this species, the advertisement calls and snout-vent length (SVL) both exhibit an altitudinal gradient such that at 30 m.a.s.l., small males produce short, rapidly

repeating, high-pitched calls, whereas at 1,000 m.a.s.l., males are larger and the calls are longer, lower pitched, and repeated more slowly (Narins and Smith 1986). For example, the “Co”-note frequency produced by males at 30 m.a.s.l. is about a third of an octave higher in frequency than that produced by males at 1,000 m.a.s.l. More recently, it was found that the spectral contents of the males’ “Co”-note calls and the frequency to which the inner ear is most sensitive are tightly correlated and change concomitantly along this same altitudinal gradient (Meenderink et al. 2010). In that study, advertisement calls of males of *E. coqui* were recorded in situ along an altitudinal gradient ranging from 30 to 1,005 m.a.s.l. Following the recordings, males were captured and transported to a nearby lab in Puerto Rico where, the following day, distortion product otoacoustic emissions (DPOAEs) were measured from the anesthetized males. This was done by sweeping two primary tones (f_1 and f_2) from low frequencies to high frequencies and plotting the amplitude of the resulting third-order distortion product emission ($2f_1-f_2$) versus the lower primary frequency, f_1 , resulting in a DPOAE audiogram. From this audiogram, the frequency that results in maximum DPOAE amplitude (F_{maxDP}) can be identified and interpreted as the frequency to which the ear is most sensitive, or the frequency to which the ear is “tuned” (Meenderink et al. 2010). This frequency was then plotted against the frequency of the animal’s “Co”-note in its advertisement call. The resulting strong correlation (Fig. 5.13) is good evidence for a close match between the call note frequency (signal) and the peripheral auditory tuning (receiver characteristic) along the entire altitudinal gradient inhabited by these vocal animals. It was suggested that the animal’s body size, conditioned by the calling site temperature, determines the frequencies of the emitted calls and the best sensitivity of the inner ear (Meenderink et al. 2010).

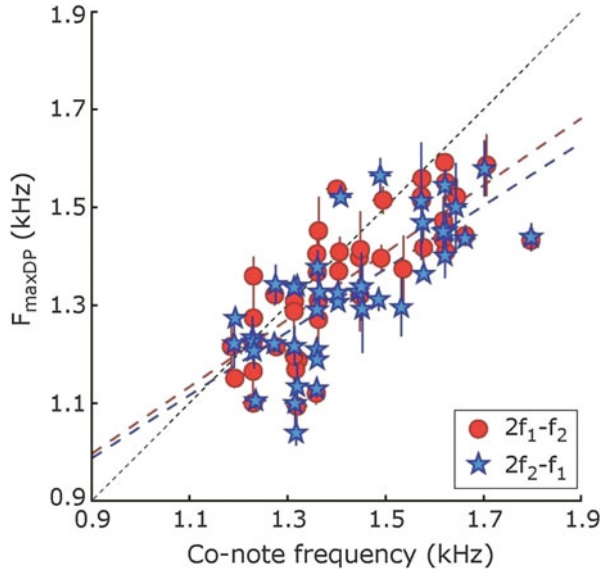
5.6.2.2 Ultrasonic Frogs

The Concave-Eared Torrent Frog (*Odorrana tormota*)

Odorrana tormota (previously *Amolops tormotus*) is known only from two provinces in central China (Zhou and Adler 1993). This species has unusually high-pitched calls containing substantial energy in the ultrasonic frequency range (above 20 kHz), and its hearing extends from less than or equal to 1 kHz to approximately 35 kHz (Narins et al. 2004; Feng et al. 2006), dramatically exceeding previously reported upper limits of anuran frequency sensitivity¹ (e.g., 8 kHz, Loftus-Hills and Johnstone 1970; 5 kHz, Fay 1988). Playback experiments in the animal’s natural habitat demonstrated that the ultrasonic elements are behaviorally relevant, and thus this extraordinary upward extension into the ultrasonic range of both the harmonic content of the advertisement calls and the frog’s hearing sensitivity is likely to have coevolved in response to the intense, predominantly

¹ Another sympatric species, *Odorrana graminea* (formerly *O. livida*), also has an extended high-frequency range (to 22–24 kHz) despite lacking the sunken tympana of *O. tormota* (Feng et al. 2006; Liu et al. 2014).

Fig. 5.13 Scatter plot showing the relationship between the frequency at maximum DPOAE amplitude ($F_{\max DP}$) and the dominant Co-note frequency in the call of the Puerto Rican Coqui frog, *Eleutherodactylus coqui*. Data points indicate median values \pm interquartile ranges. Gray circles, $2f_1-f_2$; black stars, $2f_2-f_1$. The diagonal (dashed) line represents equality between Co-note frequency and $F_{\max DP}$ (From Meenderink et al. (2010))



low-frequency ambient noise from local streams (Narins et al. 2004; Feng et al. 2006; Feng and Narins 2008). Because amphibians are a distinct evolutionary lineage from microchiropterans and cetaceans [which have evolved ultrasonic hearing to minimize spectral overlap in the frequency bands used for sound communication (Sales and Pye 1974) and to increase hunting efficacy in darkness (Bradbury and Vehrencamp 2011)], ultrasonic perception in amphibians represents a new example of independent evolution. Moreover, this example illustrates how a matched filter, when subject to selection pressure in the form of ambient noise, can respond appropriately to maintain the signal-to-noise ratio necessary for communication of biologically significant signals.

The Hole-in-the-Head Frog (*Huia cavitympanum*)

In addition to *Odorrana tormota*, only one other anuran species, *Huia cavitympanum*, is currently known to have recessed tympanic membranes (Inger 1966). *Odorrana tormota* and *H. cavitympanum* are both southeast Asian species in the family Ranidae, yet they do not overlap in geographical distribution and are unrelated at the generic level (Cai et al. 2007; Stuart 2008). The habitats in which the frogs are found, however, are remarkably similar; males of both species call in close proximity to rushing streams that produce substantial broadband background noise. Given the similarity of the species' acoustic environment and peripheral auditory morphology, Arch et al. (2008) predicted that they may have converged on the use of ultrasound for intraspecific communication. Recordings of the calls of *H. cavitympanum* in their natural habitat in Borneo obtained with ultrasonic detection and recording equipment demonstrated that males of this species are able to produce calls that are comprised entirely of ultrasound (Arch et al. 2008). To test

the hypothesis that these frogs use purely ultrasonic vocalizations for intraspecific communication, a series of acoustic playback experiments with male frogs in their natural calling sites was performed (Arch et al. 2009). These workers found that the frogs responded with increased calling to broadcasts of conspecific calls containing only ultrasound. The field study was complemented by electrophysiological recordings from the auditory midbrain and by laser Doppler vibrometer measurements of the tympanic membrane's response to acoustic stimulation. These measurements revealed that the frog's auditory system is broadly tuned over high frequencies, with peak sensitivity occurring within the ultrasonic frequency range (>20 kHz). Thus, *H. cavitympanum* is the first non-mammalian vertebrate reported to communicate with purely ultrasonic acoustic signals.

Structural Basis of the Matched Filter

In a detailed study of the inner ears of the three species of frog known to detect ultrasounds (*Odorrana tormota*, *Odorrana graminea*, and *Huia cavitympanum*), Arch et al. (2012) attempted to identify morphological correlates of high-frequency sound detection. These workers found that the three ultrasound-detecting species have converged on a series of small-scale functional modifications of the basilar papilla (BP), the high-frequency hearing organ in the frog inner ear. These modifications include (1) reduced BP chamber volume, (2) reduced tectorial membrane mass, (3) reduced hair bundle length, and (4) reduced hair cell soma length. While none of these factors on its own could completely account for the ultrasonic sensitivity of the inner ears of these species, the combination of these factors appears to extend their hearing bandwidth and thus facilitate high frequency/ultrasound detection. Similar morphological modifications are seen in the inner ears of *O. chloronota*—a poorly known species from the mountains of Laos. In fact, the striking similarity of the BP features of *O. chloronota* to those of the three amphibian species known to detect ultrasound suggests that this species is a potential candidate for high-frequency hearing sensitivity. These data form the foundation for future functional work probing the physiological bases of ultrasound detection by a non-mammalian ear (Fig. 5.14).

5.6.2.3 *Eupsophus roseus*: A Leptodactylid Frog from the South American Temperate Forest

In a recent test of the matched filter hypothesis, Moreno-Gomez et al. (2013) sought to test the concordance between the acoustic sensitivity of female frogs of *E. roseus* and (a) the spectral characteristics of the advertisement calls of conspecific males and (b) the spectral characteristics of the ambient noise in which these frogs breed. Audiograms measured from the torus semicircularis in the midbrain of anesthetized females exhibited two sensitivity peaks: one in the low-frequency range (LFR <700 Hz) and the second in the high-frequency range (HFR >700 Hz). Advertisement calls of conspecific males were characterized by three dominant harmonics of which the second and third fell within the bandwidth of the lowest thresholds in the female's HFR. In fact, the mean cross-correlation coefficient between the audiograms and the conspecific vocalization spectra was 0.4 (95 % CI: 0.3–0.5).

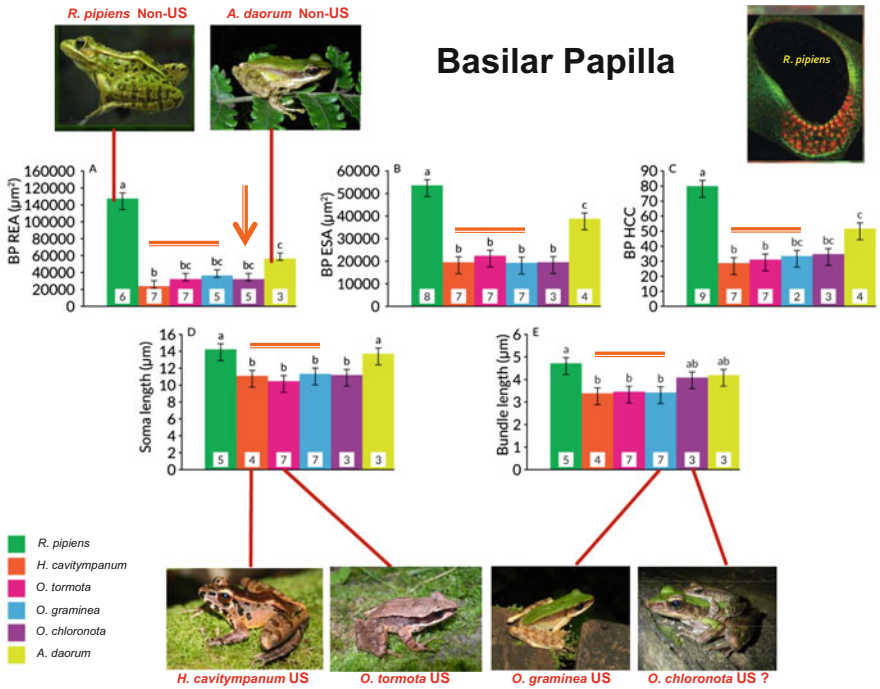


Fig. 5.14 Comparison of morphometric data from the basilar papillae of six amphibians. (a) Recess entrance area (REA); (b) Epithelium surface area (ESA); (c) Hair cell count (HCC); (d) Hair cell soma length; (e) Hair cell bundle length. Numbers indicate sample sizes. Letters denote statistically significant differences in pairwise comparisons using Tukey’s post hoc analysis with $\alpha = 0.05$. If a pair of species shares a common letter, they are not significantly different in that trait. Horizontal bars indicate the three amphibian species known to detect ultrasound (US). Vertical arrow indicates putative ultrasound detector—*O. chloronota*. Inset (upper right) shows the BP from *Rana pipiens*, a North American species known not to detect ultrasound (Non-US) (Modified from Arch et al. (2012))

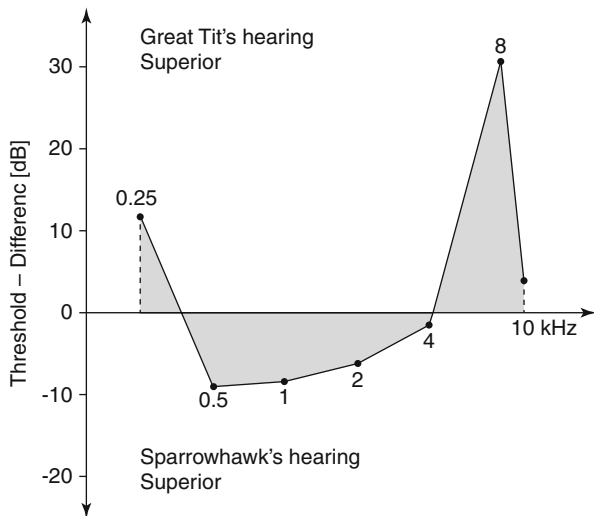
This coefficient was significantly higher than that between the audiograms and the background noise spectra over the 4 months for which data were available (Moreno-Gomez et al. 2013). Both this measured concordance and the mismatch between the auditory sensitivity of *E. roseus* females with both the local abiotic and biotic background noise are interpreted as adaptations to increase the signal-to-noise ratio in this communication system.

5.6.3 Birds

5.6.3.1 Unmatched Filters Between Predators and Prey

By exploiting call frequencies heard well by conspecifics but poorly by a prey species, animals may use a species-specific “private channel” to their advantage.

Fig. 5.15 The difference in the absolute thresholds between the great tit and the European sparrowhawk (thresholds in both species calculated using a $d' = 1.5$) (From Klump et al. (1986))



Using the method of constant stimuli in an operant positive reinforcement conditioning procedure, behavioral audiograms of the great tit (*Parus major*) and its principal avian predator, the European sparrowhawk (*Accipiter nisus*), were determined (Klump et al. 1986). The hawk was 6.5 dB more sensitive than the tit at 2 kHz—the best frequency of both species. Although the high-frequency cutoff was very similar in both species, at 8 kHz, the great tit was about 30 dB more sensitive than the sparrowhawk. Figure 5.15 shows the differences in the unmasked thresholds between the sparrowhawk and the great tit at various frequencies. When confronted by a European sparrowhawk, the great tit uses three different vocalizations: (a) the mobbing call (dominant frequency: 4.5 kHz), (b) the scolding call (dominant frequency: 4 kHz), and (c) the “seeet” call (dominant frequency: 8 kHz). The latter call is mainly used by the great tit when it detects a sparrowhawk flying at some distance (Klump et al. 1986) and is the aerial predator call described by Marler (1955). At the dominant frequency of the “seeet” call, the hearing of the great tit is 30 dB more sensitive than that of the European sparrowhawk. This example illustrates that prey species may warn other potential prey of an impending predator by exploiting the mismatch between predator and prey auditory sensitivities.

5.6.4 Conclusions

In this chapter, the concept of matched filtering for detecting desired signals buried in noisy measurement signals is presented. It is shown that the matched filter is another name for the correlation detector or replica-correlation detector, which exploits prior knowledge in the form of an exemplar (or replica) of the desired signal. An example detection problem is used to demonstrate the matched filtering

approach. The matched filter can be an effective detection tool when exemplars of the desired signal are available a priori. In the second part, several key examples of matched filters in the auditory systems of several selected sub-mammalian vertebrates are provided. These auditory systems implement matched filters by sculpting the receiver characteristics to the spectral and temporal features of the species-specific signals of biological importance. With the examples provided, it is hoped that the reader will more fully appreciate the adaptive value of the matched filter concept for reducing the effective noise and thus maximizing the signal-to-noise ratio.

References

- Arch VS, Grafe TU, Narins PM (2008) Ultrasonic signaling by a Bornean frog. *Biol Lett* 4:19–22
- Arch VS, Grafe TU, Gridi-Papp M, Narins PM (2009) Pure ultrasonic communication in an endemic Bornean frog. *PLoS One* 4:e5413. doi:10.1371/journal.pone.0005413
- Arch VS, Simmons DD, Quiñones PM, Feng AS, Jiang J, Stuart B, Shen J-X, Blair C, Narins PM (2012) Inner ear morphological correlates of ultrasonic hearing in frogs. *Hear Res* 283:70–79
- Bradbury JW, Vehrencamp SL (2011) Principles of animal communication, 2nd edn. Sinauer Associates, Sunderland
- Cai H-X, Che J, Pang J-F, Zhou E-M, Zhang Y-P (2007) Paraphyly of Chinese *Amolops* (Anura, Ranidae) and phylogenetic position of the rare Chinese frog, *Amolops tormotus*. *Zootaxa* 1531:49–55
- Candy JV (2006) Model-based signal processing. IEEE Press/Wiley-Interscience, Hoboken, New Jersey, USA
- Capranica RR, Moffat AJM (1975) Selectivity of the peripheral auditory system of spadefoot toads (*Scaphiopus couchii*) for sounds of biological significance. *J Comp Physiol* 100:231–249
- Capranica RR, Moffat AJM (1983) Neurobehavioral correlates of sound communication in amphibians. In: Ewert JP, Capranica RR, Ingle DJ (eds) *Advances in vertebrate neuroethology*. Plenum Press, New York, pp 701–730
- Capranica RR, Rose G (1983) Frequency and temporal processing in the auditory system of anurans. In: Huber F, Markl H (eds) *Neuroethology and behavioral physiology*. Springer, Berlin, pp 136–152
- Clark GA (1999) The revelations of acoustic waves. Science and technology review. Lawrence Livermore National Laboratory, UCRL-52000-99-5, U.S. Government Printing Office 1999/783-046-80013
- Clark GA, Rodgers PW (1981) Adaptive prediction applied to seismic event detection. *Proc IEEE* 69(9):1166–1168
- Clark GA, Axelrod MC, Scott DD (1999) Classification of heart valve sounds from experiments in an anechoic water tank. Lawrence Livermore National Laboratory report UCRL-JC-134634
- Clark GA, Sengupta SK, Aimonetti WD, Roeske JG, Donetti JG (2000) Multispectral image feature selection for land mine detection. *IEEE Trans Geosci Remote Sens* 38(1):304–311
- Clark GA, Robbins CL, Wade KA, Sousa PR (2009) Cable damage detection system and algorithms using time domain reflectometry. Lawrence Livermore National Laboratory report LLNL-TR-576314
- Devijver PA, Kittler J (1987) Pattern recognition theory and applications. In: Jain AK (ed) *Advances in statistical pattern recognition*. Springer, Berlin
- Duda RO, Hart PE (1973) *Pattern classification and scene analysis*. Wiley, New York
- Duda RO, Hart PE, Stork DG (2001) *Pattern classification*, 2nd edn. Wiley, New York
- Fay RR (1988) *Hearing in vertebrates: a psychophysics databook*. Hill-Fay Associates, Winnetka

- Feng AS, Narins PM (2008) Ultrasonic communication in concave-eared torrent frogs (*Amolops tormotus*). *J Comp Physiol* 194:159–167
- Feng AS, Narins PM, Xu C-H, Lin W-Y, Yu Z-L, Qiu Q, Xu Z-M, Shen J-X (2006) Ultrasonic communication in frogs. *Nature* 440:333–336
- Frishkopf LS, Capranica RR, Goldstein MH (1968) Neural coding in the bullfrog's auditory system – a teleological approach. *Proc IEEE* 56:969–980
- Hand DJ (1981) Discrimination and classification. Wiley, New York, p 218
- Heiligenberg W (1991) Neural nets in electric fish. MIT Press, Cambridge
- Hogg RV, Craig AT (1978) Introduction to mathematical statistics. Macmillan, New York
- Hopkins CD (1976) Stimulus filtering and electroreception: tuberous electroreceptors in three species of gymnotoid fish. *J Comp Physiol* 111:171–207
- Inger RF (1966) The systematics and zoogeography of the Amphibia of Borneo, vol 52, Fieldiana: Zoology. Field Museum of Natural History, Chicago
- Jazwinski A (1970) Stochastic processes and filtering theory. Academic, New York
- Kay SM (1998) Fundamentals of statistical signal processing, vol II, Detection theory. Prentice Hall, Upper Saddle River
- Klump GM, Kretzschmar E, Curio E (1986) The hearing of an avian predator and its avian prey. *Behav Ecol Sociobiol* 18:317–323
- Liu W-R, Shen J-X, Zhang Y-J, Xu Z-M, Qi Z, Xue M-Q (2014) Auditory sexual difference in the large odorous frog *Odorrana graminea*. *J Comp Physiol* 200:311–316
- Loftus-Hills JJ, Johnstone BM (1970) Auditory function, communication, and the brain-evoked response in anuran amphibians. *J Acoust Soc Am* 47:1131–1138
- Marler P (1955) Characteristics of some animal calls. *Nature* 176:6–8
- Meenderink SWF, Kits M, Narins PM (2010) Frequency matching of vocalizations to inner-ear sensitivity along an altitudinal gradient in the coqui frog. *Biol Lett* 6:278–281
- Meyer JH, Zakon HH (1982) Androgens alter the tuning of electroreceptors. *Science* 217:635–637
- Moreno-Gómez FN, Sueur J, Soto-Gamboa M, Penna M (2013) Female frog auditory sensitivity, male calls, and background noise: potential influences on the evolution of a peculiar matched filter. *Biol J Linn Soc* 110:814–827
- Narins PM, Capranica RR (1976) Sexual differences in the auditory system of the tree frog, *Eleutherodactylus coqui*. *Science* 192:378–380
- Narins PM, Capranica RR (1978) Communicative significance of the two – note call of the treefrog *Eleutherodactylus coqui*. *J Comp Physiol* 127:1–9
- Narins PM, Smith SL (1986) Clinal variation in anuran advertisement calls: basis for acoustic isolation? *Behav Ecol Sociobiol* 19:135–141
- Narins PM, Feng AS, Schnitzler H-U, Denzinger A, Suthers RA, Lin W, Xu C-H (2004) Old World frog and bird vocalizations contain prominent ultrasonic harmonics. *J Acoust Soc Am* 115:910–913
- Oppenheim AV, Schaffer RW (1975) Digital signal processing. Prentice-Hall, Englewood Cliff
- Papoulis A (1965) Probability, random variables, and stochastic processes. McGraw-Hill, New York
- Sales G, Pye D (1974) Ultrasonic communication by animals. Chapman and Hall, London
- Stuart BL (2008) The phylogenetic problem of *Huia* (Amphibia: Ranidae). *Mol Phylogenet Evol* 46:49–60
- Van Trees HL (1968) Detection, estimation and modulation theory, part I. Detection, estimation and linear modulation theory. Wiley, New York
- Waltz E, Llinas J (1990) Multisensor data fusion. Artech House, Norwood
- Wehner R (1987) 'Matched filters' – neural models of the external world. *J Comp Physiol* 161:511–531
- Whalen A (1971) Detection of signals in noise. Academic, New York
- Zhou EM, Adler K (1993) Herpetology of China. Society for the Study of Amphibians and Reptiles, Oxford
- Zoubir AM, Iskander DR (2004) Bootstrap techniques for signal processing. Cambridge University Press, Cambridge

Part III

Vision

Matched Filtering and the Ecology of Vision in Insects

6

Eric J. Warrant

Contents

6.1	Energy, Performance and Matched Filtering	144
6.2	Compound Eyes	147
6.3	Visual Matched Filtering in Insects	150
6.3.1	Peripheral Visual Matched Filtering in Insects	150
6.3.2	Central Visual Matched Filtering in Insects	156
6.4	Conclusions	164
	References	164

Abstract

In the words of Wehner (J Comp Physiol A 161:511–531, 1987) who first coined the term “matched filter” in the context of sensory systems, matched filters “severely limit the amount of information the brain can pick up from the outside world, but they free the brain from the need to perform more intricate computations to extract the information finally needed for fulfilling a particular task”. In other words, by matching the properties of neurons, circuits and sensory structures to the characteristics of the most crucial sensory stimuli that need to be detected, these stimuli can be rapidly and reliably extracted for further processing, thus drastically improving the efficiency of sensing. And by “severely limiting information picked up by the brain”, the energetic costs that would have been associated with coding superfluous information are effectively eliminated. Thus, “freeing the brain” not only frees it from the need to perform intricate computations, it also frees it from significant (and unnecessary) energetic costs. Not surprisingly, with their small eyes and brains and severely limited energy budgets, visual matched filtering is particularly well developed

E.J. Warrant (✉)

Lund Vision Group, Department of Biology, University of Lund, Sölvegatan 35, Lund 22362, Sweden

e-mail: Eric.Warrant@biol.lu.se

in small animals like insects. It is most obvious at the visual periphery, in the morphology and physiology of the compound eyes, but remarkable matched filters also occur at higher levels of visual processing. Using a number of case studies, I will show how visual matched filters have evolved for all aspects of insect life, including the detection and pursuit of mates and prey and for locomotion and navigation in the natural habitat.

6.1 Energy, Performance and Matched Filtering

The arthropods, arguably one of the most successful groups of animals on our planet, owe much of their success to the seemingly endless range of adaptations permitted by their hard cuticular exoskeletons. Due to its variable thickness and hardness, from heavy and armour-like to thin and rubber-like, and due to its variable opaqueness, where even transparent windows and lenses are possible, the arthropod cuticle has evolved far beyond being a simple skeletal element. All manner of cuticular appendages have evolved for locomotion, prey capture, defence and courtship, and the cuticle has been fashioned over millions of years into exquisitely sensitive sensory organs for vision, hearing, olfaction and mechanoreception. But despite its obvious evolutionary success, the arthropod exoskeleton is also a constraint – due partly to the finite mechanical strength of cuticular structures, arthropods tend to be limited in size, with the force of gravity in terrestrial environments favouring internal skeletons in larger animals such as vertebrates (although the buoyancy provided by water has in part allowed marine arthropods to grow larger than their terrestrial relatives). However, this typically small body size has by no means constrained the sophistication of arthropods (Eberhard 2007) – some species of bees and wasps are less than half a millimetre in length and yet still retain most of the locomotive and sensory capacities of their much larger relatives, a testament to the remarkable performance of their miniaturised musculature and nervous systems (Niven and Farris 2012).

To provide this sophistication in such a diminutive package (Chittka and Niven 2009), the comparatively small brains and nervous systems of arthropods have been honed by the forces of natural selection to provide neural circuits with functional repertoires that closely match a limited range of ecologically relevant behavioural tasks. Which circuits evolve – and which behavioural tasks take precedence – is determined not only by external ecological factors, such as the physical nature of the habitat or the presence of predators or prey, but also by various internal factors. One of the most important of these is undoubtedly the animal's finite metabolic energy budget (Niven and Laughlin 2008), the size of which tends to decrease as animals become smaller. As with all finite budgets, resources need to be allocated wisely – overinvestment in one area may be detrimental to others and thus negative for the system as a whole (and in the case of an animal, possibly fatally so). Thus, in response to the external forces of natural selection, an animal's finite energy budget

– determined largely by the availability of food and the ease with which it is attained – is carefully allocated for the development and maintenance of the animal's various organ systems. How much energy is allocated to a given organ system reflects the importance of that system for the animal's chances of survival and reproduction, with the benefits of the system weighed against its energetic cost. The ultimate currency of this evolutionary cost-benefit analysis is defined in terms of the number of ATP molecules that is required to perform specific tasks (Laughlin et al. 1998; Niven et al. 2007) and involves an evolutionary process whereby the benefit of an improved performance is weighed against the energetic cost of achieving it (Niven and Laughlin 2008). It turns out that this process invariably involves a law of diminishing returns – each unit increment in performance tends to cost disproportionately more than the previous increment (i.e. performance is not a linear function of cost). This means that the evolution of a high performance organ comes only at a significant energetic cost, a cost that is likely to be a substantial fraction of the animal's total energy budget (Niven et al. 2007; Niven and Laughlin 2008).

Nowhere is this truer than in the evolution of nervous systems, whose building blocks – neurons – are among the most energetically expensive cells in an animal's body. The main reason for this expense is the cost of maintaining the neuron's resting potential in readiness for electrical signalling. The resting potential, which is usually many tens of millivolts negative relative to the external cellular medium, is maintained (and restored following signalling) by active ion pumps that use energy from ATP molecules to pump sodium and potassium ions across the neuronal membrane against their passive electrical and concentration gradients. This energetic cost is substantial and is incurred even in the absence of signalling. The extra cost of signalling is simply added to this (Niven et al. 2007).

Due to their typical possession of a dense matrix of receptor neurons, sensory organs tend to be particularly expensive, but as with any organ, their cost can be weighed against the performance benefits they provide. One measure of this performance can be defined by the amount of information (in bits) gained by executing a particular sensory task, such as the transduction of photons of light by a photoreceptor, or of odour molecules by an olfactory receptor. This performance can be measured against its energetic cost, that is, the number of ATP molecules that are consumed to generate one bit of sensory information (Laughlin et al. 1998). For a light-adapted photoreceptor in a fly, this energetic cost is significant – depending on the species, between one million and ten million ATP molecules are consumed to generate a single bit of information, and a large fraction of this cost (around 20 %) is simply used to maintain the resting potential in the absence of signalling, that is, to maintain it in darkness (Laughlin et al. 1998; Niven et al. 2007). In fact, the “dark cost” of the entire retina is about 2 % of the fly's total resting metabolic rate! A significant dark cost has likewise been estimated for the vertebrate retina (Okawa et al. 2008). The photoreceptors of flies also demonstrate the law of diminishing returns mentioned above – even though the larger photoreceptors of larger fly species provide their owners with a greater maximum number of bits of information per second, they do so only at a disproportionately high cost

(Niven et al. 2007). In fact, across the flies, the total energy cost (in ATP molecules consumed per photoreceptor per second) rises almost with the square of the maximum information rate (in bits per second) coded by the photoreceptor (the actual exponent is 1.7).

The conclusion from the energetic arguments presented above is that larger eyes, with a greater number of larger photoreceptors, are likely to cost a disproportionate fraction of an animal's energy budget compared to smaller eyes with fewer and/or smaller photoreceptors. For this reason alone, larger eyes – especially those larger than expected from the size of the animal – would normally be selected against during evolution. When they do appear in the animal kingdom, they are invariably critically important for their owner's chances of survival, with the sizable energy commitment required being crucially necessary (as in the disproportionately large eyes of the giant deep-sea squid: Nilsson et al. 2012).

Not surprisingly, a number of strategies have evolved to make vision more efficient (Niven and Laughlin 2008), many of which are most obvious in small animals like arthropods with their small and limited energy budgets. Of these, matched sensory filtering is one of the most effective. By matching the properties of neurons, circuits and sensory structures to the characteristics of the most crucial visual stimuli that need to be detected, these stimuli can be directly and reliably extracted for further processing. All other visual stimuli – having little consequence for the animal's chances of reproduction and survival – are simply suppressed or filtered out altogether. To see “the world through such a matched filter”, to quote Rüdiger Wehner, who first coined the term in 1987, “severely limits the amount of information the brain can pick up from the outside world, but it frees the brain from the need to perform more intricate computations to extract the information finally needed for fulfilling a particular task” (Wehner 1987). By “severely limiting information picked up by the brain”, the energetic costs that would have been associated with coding superfluous information are effectively eliminated. And “freeing the brain” not only frees it from the need to perform intricate computations it also frees it from the significant energetic costs that would have arisen by possessing the neural circuits necessary to make these computations. Simply put, matched filtering saves energy by stripping away unnecessary energetic investments and efficiently redirecting the remaining energy to where it is needed most. With their miniature brains and nervous systems orchestrating complex behaviours on a small and limited energy budget, it should come as no surprise that the arthropods are richly endowed with visual matched filters.

The best understood matched filters are undoubtedly those found among the insects, and these have evolved in response to almost every aspect of their ecology, from locomotion and navigation to predator avoidance, food acquisition and courtship. These matched filters provide some of the most beautiful and remarkable products of natural selection that can be found in the natural world. Indeed, a few seem so “ingenious” to human observers that engineers have directly used them to create “smart solutions” for some of our latest electronic devices. In the pages that follow, I will showcase a selection of visual matched filters in insects, described

within the ecological contexts that they evolved. But before I do, it is first necessary to briefly describe the principle eye type possessed by insects – compound eyes.

6.2 Compound Eyes

Compound eyes are found in insects, crustaceans and some chelicerates (e.g. the horseshoe crab *Limulus*) and are composed of identical units called “ommatidia” (Fig. 6.1a). Each ommatidium consists of a lens element – the “corneal lens” and “crystalline cone” – that focuses light incident from a narrow region of space onto the “rhabdom”, a photoreceptive structure built from the contributions of at least eight photoreceptor (retinula) cells, each of which apportions a region of membranous microvilli that house the rhodopsin molecules. A compound eye may contain as many as 30,000 ommatidia, as in large dragonflies, or as few as 6, as in some ants. Each ommatidium is responsible for reading the average intensity, colour and (in some cases) plane of polarisation within the small region of space that they each view. Two neighbouring ommatidia view two neighbouring regions of space. Thus, each ommatidium supplies a “pixel” of information to a larger image of pixels that the entire compound eye constructs. Larger compound eyes with more ommatidia thus have the potential for greater spatial resolution.

Compound eyes come in two main forms: “apposition eyes” and “superposition eyes”. Each of these forms comes in various subforms, but these I will avoid describing here for the sake of brevity (for further details see Land 1981; Nilsson 1989; Land and Nilsson 2012).

Apposition eyes (Fig. 6.1b) are typical of (but not restricted to) animals living in bright habitats. Insects with apposition eyes include day-active butterflies, flies, bees, wasps, ants, dragonflies and grasshoppers. Many shrimps and shallow-living and terrestrial crabs also have apposition eyes. Each ommatidium in an apposition eye is isolated from its neighbours by a sleeve of light-absorbing screening pigment, thus preventing light reaching the photoreceptors from all but its own small corneal lens. This tiny lens – typically a few tens of microns across – represents the pupil of the apposition eye. Such a tiny pupil only allows very little light to be captured.

Superposition eyes (Fig. 6.1c) are typical for (but not restricted to) animals living in dimmer habitats. These include nocturnal moths and beetles and deeper living marine crustaceans, such as lobsters and krill. In superposition eyes, the pigment sleeve is withdrawn, and a wide optically transparent area, the clear zone, is interposed between the lenses and the retina. This clear zone (*cz* in Fig. 6.1c) – and specially modified crystalline cones – allows light from a narrow region of space to be collected by a large number of ommatidia (comprising the superposition aperture) and focussed onto a single photoreceptor. Unlike the crystalline cones of apposition eyes, those of superposition eyes have evolved refractive index gradients or reflecting surfaces, which allow as many as around 2,000 lenses to collect the light for a single photoreceptor (as in some large nocturnal moths). This represents a massive improvement in sensitivity while still producing a reasonably sharp image.

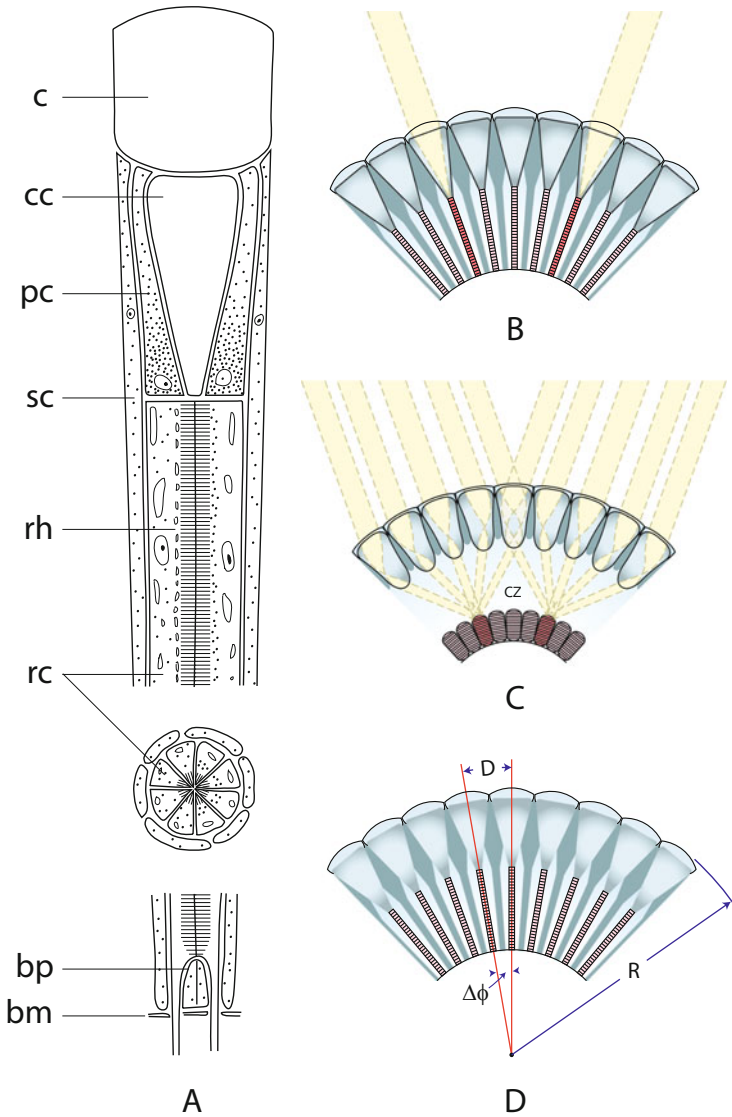


Fig. 6.1 Arthropod eye designs. (a) A schematic longitudinal section (and an *inset* of a transverse section) through a generalised Hymenopteran ommatidium, showing the corneal lens (*c*), the crystalline cone (*cc*), the primary pigment cells (*pc*), the secondary pigment cells (*sc*), the rhabdom (*rh*), the reticular cells (*rc*), the basal pigment cells (*bp*) and the basement membrane (*bm*). The *left half* of the ommatidium shows screening pigment granules in the dark-adapted state, while the *right half* shows them in the light-adapted state (Redrawn from Stavenga and Kuiper (1977)). (b) Apposition compound eye (in this case a focal apposition eye). (c) Superposition compound eye (in this case a refracting superposition eye). *cz* clear zone. (d) The definition of the interommatidial angle $\Delta\phi$. D distance between the centres of two adjacent corneal facet lenses (equal to the facet diameter) and R local radius of the eye surface (From Cronin et al. 2014. Images in B-D courtesy of Dan-Eric Nilsson)

As mentioned above, the spatial resolution of a compound eye is (in part) set by the density of its ommatidia. This is nicely illustrated by considering two extreme examples: large aeshnid dragonflies that may possess as many as 30,000 ommatidia in each of its apposition eyes and some groups of primitive ants that may possess fewer than ten. If the eyes of both insects view the same solid angular region of visual space, then the dragonfly will sample that region with vastly greater spatial resolution, simply because of its much higher density of sampling stations (i.e. ommatidia). This density is directly related to the local “interommatidial angle” $\Delta\phi$, the angular separation of two neighbouring ommatidia (Fig. 6.1d): smaller values of $\Delta\phi$ indicate a greater sampling density and a higher spatial resolution. The interommatidial angle depends primarily on two anatomical parameters, the facet diameter D and the eye radius R :

$$\Delta\phi = D/R \text{ (radians)}. \quad (6.1)$$

A larger local eye radius (i.e. a flatter eye surface), or a smaller facet, produces a smaller interommatidial angle. However, there is a limit to how much $\Delta\phi$ can be narrowed by decreasing the size of the facet – smaller facets sacrifice sensitivity to light (and degrade image quality due to diffraction). Nevertheless, it is possible to have a region of the eye that has such a large radius of curvature that an extremely small $\Delta\phi$ is still possible without having to sacrifice facet size. In fact, in many apposition eyes, the facets in these regions can actually be much *larger* than in other regions of the eye having double the $\Delta\phi$ (which is better for sensitivity)! Thus, particularly in apposition eyes, facet diameter and eye radius can both vary dramatically within a single eye, which means that the local interommatidial angle can also vary considerably – some directions of visual space can thereby be sampled much more densely than others. Such high-resolution “acute zones” (Horridge 1978) are common among insects and crustaceans and their size, shape and placement in an eye tend to reflect the habitat and ecological needs of the eye’s owner. As we will see below, these acute zones are the basis for many different types of visual matched filters.

In the absence of all other effects (such as the quality of the optical image focused on the retina), $\Delta\phi$ would set the finest spatial detail that could be seen. In reality, however, the finest spatial detail is determined by the size of the photoreceptor’s “receptive field”, that is, the size of the region of visual space from which the photoreceptor is capable of receiving photons. The diameter of this roughly circular receptive field is sometimes called the photoreceptor’s “acceptance angle” $\Delta\rho$, and smaller values indicate sharper spatial resolution. In most compound eyes, $\Delta\rho$ is typically larger than $\Delta\phi$ since eyes often possess one or more optical limitations (e.g. aberrations) that blur the image formed in the retina. This blurring broadens $\Delta\rho$ and this in turn coarsens spatial resolution to a value below that predicted by the photoreceptor matrix.

6.3 Visual Matched Filtering in Insects

Variation in the size, location and organisation of acute zones provides one of the most important routes via which visual matched filters have been created in insect compound eyes. There are acute zones matched to the physical features of the terrain, to the locations and visual characteristics of mates and prey and to the way the visual world appears during locomotion. However, they are by no means the only types of matched filters. Some matched filters can also be found at the level of single cells in the sensory periphery (particularly for the pursuit of mates and prey), while others are manifested in the properties of entire circuits of cells in central areas of visual processing (some of which have important roles in flight control and navigation). However, no matter what their use or origin, all these matched filters fulfil their primary evolutionary role, as so elegantly shown by Rüdiger Wehner more than a quarter of a century ago – to free the brain from the need (and substantial energy cost) of performing intricate computations to extract the information needed for fulfilling a particular task.

We will begin our discussion of matched filters by considering those that are most obvious at the visual periphery, namely, those manifested in the optical design and physiological properties of the compound eye itself. Back in 1987, when Wehner first coined the term “matched filter”, these were by and large the only types of visual matched filters known. But since then we have come to realise that matched filtering also occurs at more central levels of visual processing, notably by visual interneurons in the lobula of the optic lobe and in the central brain. By having very large visual fields receiving inputs from enormous numbers of ommatidia, and by spatially integrating signals generated locally from each, higher-order visual cells can function as highly efficient matched filters for specific features of the visual world (Krapp 2014). It turns out, as we will see below, that these matched filters are of crucial importance for locomotion and navigation.

6.3.1 Peripheral Visual Matched Filtering in Insects

Peripheral visual matched filtering has manifested itself in three very important aspects of insect ecology: in the detection, attraction and pursuit of mates, in the detection and pursuit of prey and in the insect’s relationship to its physical environment. Of these, possibly the most spectacular matched filters are those concerned with sex.

6.3.1.1 Matched Filters for Sex

The urgency to reproduce has led to some of the most extraordinary visual adaptations found in nature, particularly among insects, where males can sometimes possess entirely separate eyes exclusively devoted to sex. In march flies and mayflies, for instance, the male eye has become bi-lobed, with the upper lobe heavily flattened to drastically increase the retinal sampling density within a narrow upward field of view (Zeil 1983a), within which, silhouetted against the brighter

sky, females and rivals will appear as small dark moving spots (Zeil 1983b). The optical structure of their eyes and the physiology of the underlying neural circuitry that processes the visual image of a passing female together form a really impressive matched filter for detecting, pursuing and intercepting mates.

Sexual dimorphism in eye design need not necessarily result in the evolution of entirely separate eyes in males. In many species of brachyceran flies, for instance, the males instead have extended areas of compound eye that are missing in females. Whereas in females, the eyes remain widely separated, in males the eyes nearly (or completely) touch along the midline of the head (Fig. 6.2a, b). This extra piece of eye – the so-called love spot – is used by males exclusively for the detection and high-speed pursuit of females (Land and Collett 1974; Land and Eckert 1985). Love spot ommatidia are distinguished by their extra large facet lenses, and in the blowfly *Calliphora erythrocephala* (Fig. 6.2a, b) and the hoverfly *Volucella pellucens* (Fig. 6.2c), these collectively constitute an acute zone. This acute zone is clearly seen in male *Volucella* – each eye has a large love spot located frontally, 20° above the equator, within which the interommatidial angle $\Delta\phi$ falls to just 0.7° (Fig. 6.2c). The size of the acute zone (the eye region where, say, $\Delta\phi < 1.1^\circ$) occupies $2,230 \text{ deg}^2$ of the visual field (shaded area in Fig. 6.2c). In females, there is also an acute zone, but instead directed frontally (Fig. 6.2d). $\Delta\phi$ only falls to 0.9° , and the area of the acute zone ($\Delta\phi < 1.1^\circ$) is a mere 23 % as large as that of males (510 deg^2 : shaded area in Fig. 6.2d).

Interestingly, the male's matched filter is not restricted to the optics of the compound eyes. The photoreceptors of love spot ommatidia in the male housefly *Musca domestica* are 60 % faster than those of females and, due to the presence of the acute zone, spatially almost twice as acute (with acceptance angles $\Delta\rho$ around half those found in females: Hornstein et al. 2000). These properties make love spot photoreceptors especially well suited for detecting and pursuing small high-speed targets like females. The improved response speed is achieved by a faster transduction mechanism and a tuned voltage-activated conductance that enhances the membrane's frequency response – in the blowfly *Calliphora vicina*, this translates into an information rate (in bits/s) in male photoreceptors that is up to 40 % higher than that in females (Burton et al. 2001). Not surprisingly all these improvements only come at a cost – the extra-tuned conductance (which involves the passage of ions through dedicated channels in the photoreceptor membrane) is energetically expensive.

The visual matched filtering seen in the male's eye is preserved in the visual processing circuits of the optic lobe, particularly in the lobula. Here, large male-specific visual cells – which are entirely lacking or highly modified in females – respond maximally to small dark objects moving across the frontal-dorsal visual field corresponding to the love spots (Strausfeld 1991; Gilbert and Strausfeld 1991; Gronenberg and Strausfeld 1991). When stimulated with larger objects, the responses of these cells rapidly decline, a clear demonstration of matched filtering for small targets (Nordström and O'Carroll 2009).

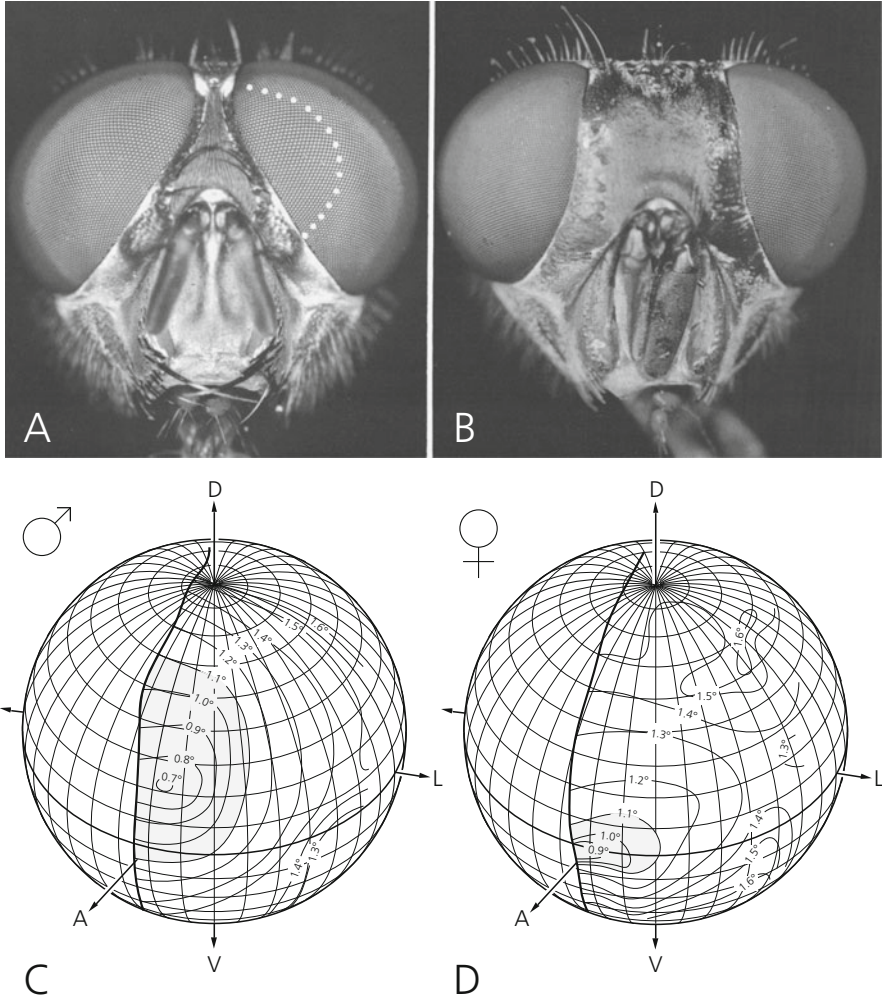


Fig. 6.2 Optical sexual dimorphism in the apposition eyes of flies. (a, b) Male (a) and female (b) blowfly heads (*Calliphora erythrocephala*). Note how the eyes of males almost touch, whereas those of females are quite separated. The extra eye surface – or “love spot” – of males (dotted white line) provides the input to a sophisticated neural pathway for detecting and chasing females (Images from Strausfeld 1991, with kind permission from Springer Science + Business Media). (c, d) In the hoverfly *Volucella pellucens* the male love spot is a large dorso-frontal acute zone, where interommatidial angles are small (c) and facet diameters are large. The visual fields of the left eyes of the two sexes, and interommatidial angles shown by isolines, are projected onto spheres. The females have a much smaller frontal acute zone (compare the shaded regions, where $\Delta\phi < 1.1^\circ$). D dorsal, V ventral, A anterior, L lateral (From Warrant 2001. Entire figure from Cronin et al. 2014)

6.3.1.2 Matched Filters for Prey Detection and Pursuit

In insects, the known visual matched filters for detecting and pursuing prey turn out to be very similar to those for detecting and pursuing mates. The reason for this is quite straightforward – the visual stimulus is nearly identical. Like the typical mates of flies, the prey items of many insects turn out to be small dark silhouettes moving rapidly across the bright background of the sky.

Dragonflies, for instance, have a highly developed dorsal acute zone, with huge facets and narrow interommatidial angles (Fig. 6.3a, b) – in the dragonfly *Anax junius*, $\Delta\phi$ falls to a phenomenally low 0.24° (Sherk 1978)! This acute zone scans the sky above and in front of the dragonfly, on the lookout for flying insect prey. And just as in the love spot photoreceptors of flies, the signals generated in the acute zone photoreceptors of dragonflies eventually feed into specialised neurons at higher levels of visual processing which collectively create a visual matched filter for detecting prey (Olberg 1981, 1986). One such neuron is the CSTMD4 cell, a large-field small-target-detecting cell from the lobula of the large Australian dragonfly *Hemicordulia tau* (O’Carroll 1993). This neuron has a response that is tuned to very small moving targets (Fig. 6.3c), around 1 square degree in size. When the target sizes increase, the response of CSTMD4 drops dramatically.

6.3.1.3 Matched Filters for the Physical Terrain

The physical environments where animals live have profoundly influenced the evolution of their senses, not the least vision. Despite what appear to be enormous differences in the appearance of different habitats – especially with regard to their topology and structural complexity – there are also some notable constants that are common to almost all natural scenes and to which most visual systems have adapted. For instance, the probability distribution of visual contrasts in the terrestrial world is remarkably similar from habitat to habitat (Laughlin 1981), as are the probability distributions of spatial and temporal frequencies (Atick and Redlich 1992; Dong and Atick 1995; Field 1999). Not surprisingly, this predictability in the structure of natural scenes has strongly steered the evolution of early visual processing (Srinivasan et al. 1982; Atick 1992) – because features in the environment that are predictable are also redundant, maximum coding efficiency arises by ignoring or eliminating this redundancy and concentrating on unpredictable (and thus visually interesting) features. By using a variety of neural mechanisms to remove redundancy, notably lateral inhibition or spatiotemporal summation, early visual processing (van Hateren 1992, 1993) – whether in a fly (Laughlin 1981) or a mammal (Field 1987; Atick and Redlich 1992) – is thereby matched to the predictable nature of visual scenes.

Nonetheless, despite these structural similarities, natural scenes also manifest distinct differences. Some environments, like an intertidal beach or the immense open grass plains of the African veldt, are wide and flat and dominated by a single visual feature – the sharp border between the ground and the sky provided by the horizon. It is here that almost everything of importance to an animal occurs – the courtship displays of mates, the sudden appearance and flight of prey or the unforeseen attacks of predators. Other environments are much more complex,

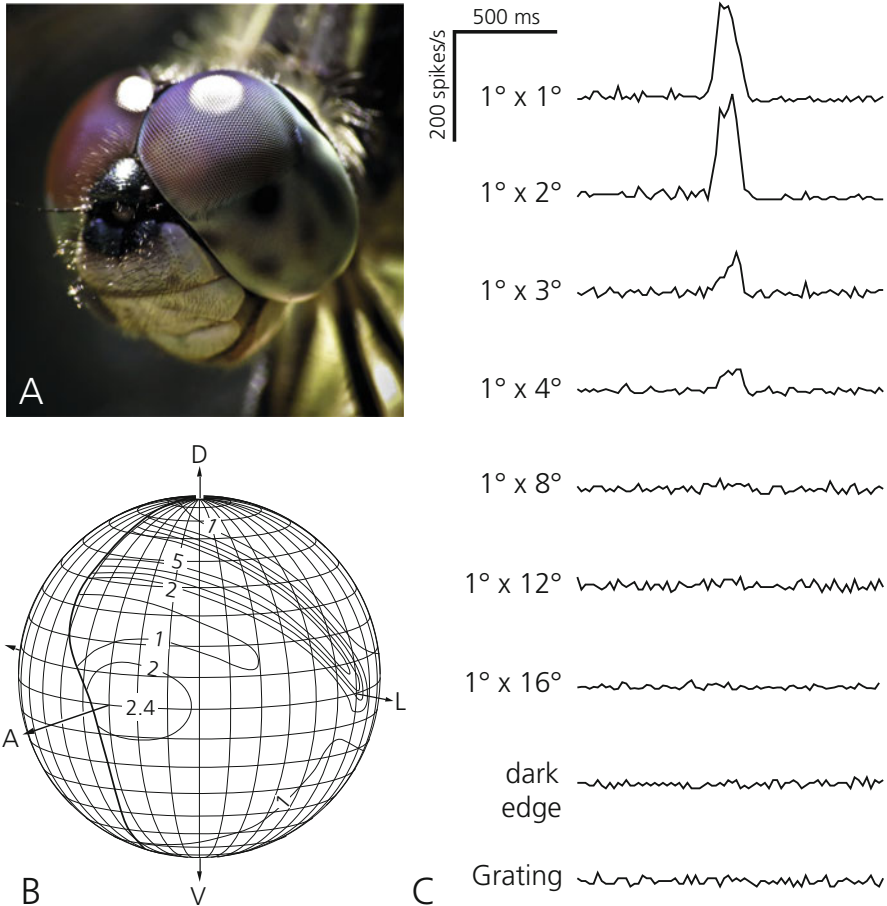


Fig. 6.3 The dorsal acute zone of dragonflies. (a) An unknown species of dragonfly with eyes possessing distinct dorsal acute zones with larger facet lenses (Photo credit: Tanya Consaul (123RF.com photo agency)). (b) A map of spatial resolution in the eye of the dragonfly *Anax junius* (expressed as the number of ommatidial axes per square degree). The density of ommatidia (and thus spatial resolution) increases rapidly in the dorsal (*D*) visual field. *V* ventral, *L* lateral, *A* anterior (Redrawn from Land and Nilsson 2012, with data from Sherk 1978). (c) The responses (peristimulus time histograms) of CSTMD4, a large-field small-target-detecting cell from the lobula of the dragonfly *Hemicordulia tau*. In the part of the cell's receptive field corresponding to its dorsal acute zone, the cell is most sensitive to small, dark, and reasonably slow-moving targets (as a fly might appear during a highly fixated pursuit). It is insensitive to large bars, edges and gratings (From O'Carroll 1993, reprinted with permission from Macmillan Publishers Ltd. Entire figure from Cronin et al. 2014)

like the tangled understorey of a tropical rainforest, a maze of tree trunks, bushes and vines that spread in every direction. At the other extreme is the vast and featureless dim blue world of the mesopelagic deep sea. All of these environments are visually very different, and not surprisingly eyes and neural processing have

evolved to match these habitats as closely as possible. For instance, desert ants (Wehner 1987), dance flies (Zeil et al. 1988) and fiddler crabs (Zeil et al. 1986; Zeil and Hemmi 2006; Smolka and Hemmi 2009) that inhabit flat and relatively featureless terrains or patrol water surfaces have evolved compound eyes whose sampling stations are densest – and resolution highest – in a narrow strip around the equator of the eye, thus creating a matched filter for sampling objects along the horizon, where the greatest density of visual information occurs. These so-called visual streaks of high resolution are a common evolutionary response to the demands of vision in a flat world (Hughes 1977).

Visual streaks are also found in the eyes of two water-dwelling bugs, both of which take advantage of the surface tension of water to position themselves at the water surface, one of them above it (the water strider *Gerris lacustris*, Fig. 6.4a) and the other below (the backswimmer *Notonecta glauca*, Fig. 6.4b). To detect their prey, both bugs are highly dependent on their eyes and on their ability to detect water ripples produced by small animals trapped at the water surface. With its long slender legs, the water strider is able to skate across the water film and to hold station on a slowly moving water surface by leaping upstream to counteract its displacement away from familiar shoreline landmarks (Junger and Varju 1990). To view this flat water surface, and the visual landmarks at its edge, the water strider has an extremely sharp visual streak aligned with this horizon, with vertical interommatidial angles falling at its centre to values close to the smallest recorded in insect eyes – 0.55° (Fig. 6.4a, Dahmen 1991).

The optical world experienced by a backswimmer that hangs suspended from the underside of the water surface is quite different to that experienced by a water strider. The fact that water has a higher refractive index than air means that the entire 180° dome of the sky is compressed to a 97° cone of light underwater. Within this cone of light – called “Snell’s window” – all the features of the terrestrial world above can be found, including the flat water surface, which is located at the edge of the cone (Walls 1942, p. 378). By looking upwards along the edge of the cone, a suspended backswimmer is able to have a periscopic view of the outside water surface and see anything, including prey, which might be trapped on it. The water surface is an important horizon for the backswimmer, and the ventral part of the eye possesses a well-developed visual streak (Fig. 6.4b) that watches the surface along the edge of Snell’s window (Schwind 1980). This matched filtering doesn’t stop at the optics of the eye: in the optic lobe, there are cells which have their visual fields coincident with the visual streak, and which respond maximally to prey-sized objects on the water surface (Schwind 1978). But the water surface is not the backswimmer’s only horizon. Frontwards, the backswimmer can also see the environment of the pond and any item of interest that might be located there. There is a second visual streak that views this direction as well (Schwind 1980).

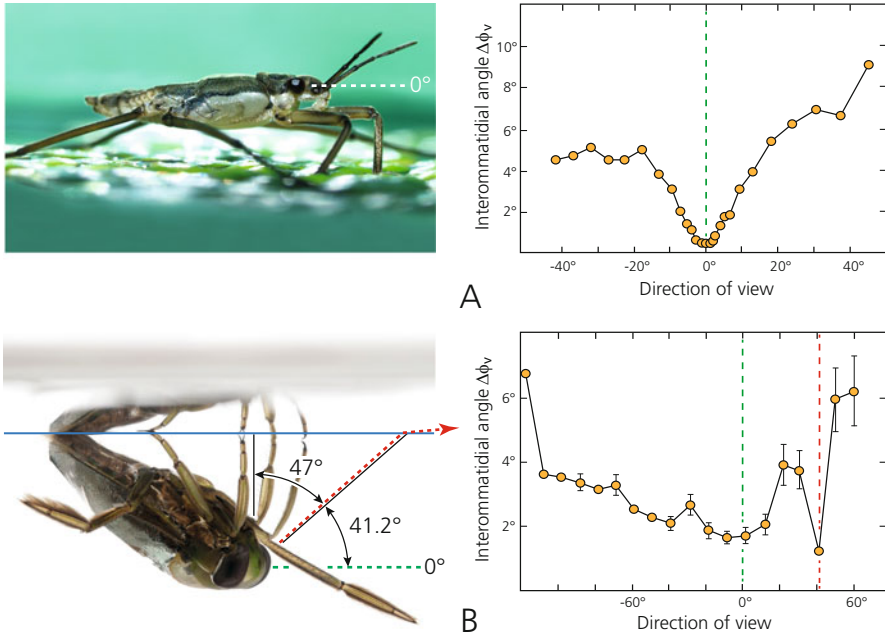


Fig. 6.4 Adaptations for vision at a flat water surface. **(a)** The sharp horizontal visual streak of the surface-dwelling water strider *Gerris lacustris*, where a vertical transect through the frontal eye, reveals a dramatic decrease in vertical interommatidial angle $\Delta\phi_v$ towards the equator of the eye (the eye region viewing the horizon). Here $\Delta\phi_v$ falls to a minimum value of 0.55° (Adapted from data taken from Dahmen 1991. Photo credit for the unknown species of *Gerris*: Ernie Cooper, www.macrocritters.wordpress.com). **(b)** Vision through Snell's window in the backswimmer *Notonecta glauca*, where the 180° view of the world above the water surface, is compressed due to refraction into a 97.6° wide cone below the water surface. The backswimmer hangs upside at the water surface, with the ommatidia in the ventral regions of its apposition eyes looking upwards (positive directions of view in the left panel). At precisely the boundary of Snell's window (red dashed lines), there is a sudden decrease in $\Delta\phi_v$ indicating enhanced spatial resolution for objects (prey) on the horizontal water surface above. In the horizontal direction below the water surface (0° : green dashed lines) $\Delta\phi_v$ is also minimal, indicating the presence of a second horizontal acute zone. In both panels, negative directions of view indicate ventral regions of the visual world, whereas positive directions indicate dorsal regions (note however that since the backswimmer hangs upside down, dorsal directions are viewed by the ventral eye and vice versa) (Adapted from Wehner 1987 (with kind permission from Springer Science + Business Media), with data and images from Schwind 1980. Photo credit: Eric Isselee (123RF.com photo agency). Panel B from Cronin et al. 2014)

6.3.2 Central Visual Matched Filtering in Insects

6.3.2.1 Matched Filters for Locomotion

Insects display all the forms of locomotion that have evolved in the animal kingdom, from walking and swimming, to flying and gliding. Some, like water striders, are even able to walk on water. But irrespective of its form, a characteristic of all modes of locomotion is its speed, and the speed of locomotion – or more

particularly, the speed with which the visual contrasts of the world traverse the receptive fields of visual cells – has led to the evolution of fundamental matched filters in the photoreceptors, the cells responsible for recording the very first impressions of the moving visual world.

Sixty-five years ago, the great German sensory physiologist Hansjochem Autrum measured extracellular responses to light flashes in the eyes of insects (so-called electroretinograms or ERGs) to discover that the eyes of insects are either “fast” or “slow”, with fast eyes being correlated with rapidly moving (and often) diurnal insects and slow eyes with slowly moving (and often) nocturnal insects (Autrum 1950). Later intracellular recordings from the photoreceptors of a range of different insects confirmed this notion (Howard et al. 1984; de Souza and Ventura 1989): the voltage responses of photoreceptors to brief dim flashes of light (known as “impulse responses”) had slower time courses in slowly moving species and faster time courses in rapidly moving species (Fig. 6.5), indicating fundamental

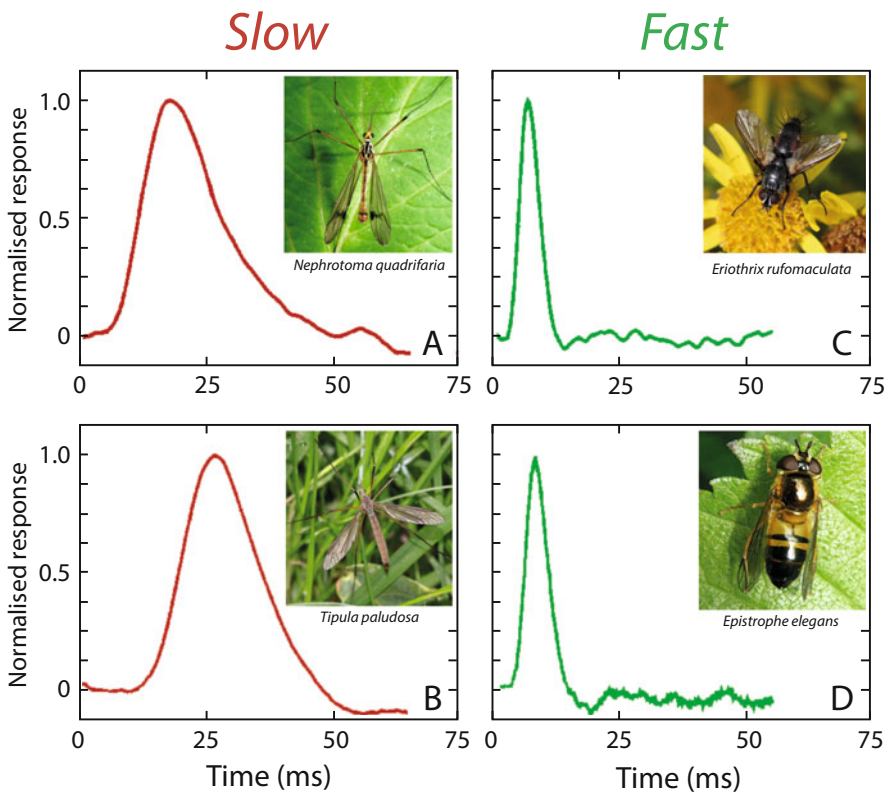


Fig. 6.5 Fast and slow photoreceptors in flies, as revealed by the light-adapted impulse response (the response to a very dim and brief flash of light delivered at time = 0). (a, b) Impulse responses in two species of crane flies (*Nephrotoma quadrifaria* a; *Tipula paludosa* b), slowly flying crepuscular insects that possess typical “slow” photoreceptors. (c, d) Impulse responses in the tachinid *Eriothrix rufomaculata* (c) and the hoverfly *Epistrophe elegans* (d), fast aerobic diurnal insects that possess typical “fast” photoreceptors (Adapted from Laughlin and Weckström 1993. Photo credits (www.naturespot.org.uk): a, d Graham Calow; b, c David Nicholls)

differences in the membrane properties of the two speed classes of photoreceptors. These differences, it turns out, are largely due to differences in the numbers and types of potassium (K^+) channels found in the photoreceptor membranes of fast and slow eyes (Laughlin and Weckström 1993; Weckström and Laughlin 1995; Salmela et al. 2012), the exact complement of channels creating a sensory filter matched to the speed of locomotion (Laughlin 1996). Among the flies, species that fly rapidly (such as the hoverfly *Epistrophe eligans*) have photoreceptors possessing delayed-rectified K^+ channels that allow a rapid response by reducing the membrane time constant. In contrast, the photoreceptors of slowly moving flies (like the crane fly *Tipula paludosa*) lack delayed rectifier channels, but instead express an inactivating K^+ current (Laughlin and Weckström 1993). Due to their large currents and conductances, the fast delayed rectifiers of rapidly flying flies are energetically more expensive than the K^+ currents of slowly moving flies which inactivate quickly (Laughlin and Weckström 1993), indicating that fast vision comes at a cost.

Interestingly, the “speed” of an eye can vary within the same animal, for example, during the transition from day to night. At night, the demands of seeing well in dim light tend to result in slower vision (van Hateren 1993; Warrant 1999; Frederiksen et al. 2008), and in the locust *Schistocerca gregaria* – an insect known to fly both day and night – the membrane filters are modulated accordingly. During the day, locust eyes are “fast”, with membrane filters functioning as delayed rectifiers, while at night their eyes are “slow”, with filters exhibiting inactivating K^+ currents (Cuttle et al. 1995). This daily transformation from fast to slow eyes (with a corresponding change in energy costs) appears to be under the control of the neuromodulator serotonin (Cuttle et al. 1995). Interestingly, the same transition from day to night also causes changes in the morphology of the photoreceptors that broadens their spatial receptive fields (Williams 1983) and thus decreases spatial resolution. Thus, in locust photoreceptors, the visual matched filters are plastic, changing from faster and more acute vision that is well matched to life in bright light during the day, to slower and coarser vision that is well matched to dim conditions at night.

Matched filters for locomotion are not only restricted to the photoreceptors. Flying insects – such as butterflies, flies, bees, grasshoppers and dragonflies – have equatorial gradients of spatial resolution that are adaptations for forward flight through a textured environment (Land 1989). When an insect (or any animal) moves forward through its surroundings, its eyes experience an optic flow of moving features (Gibson 1950; Wehner 1981). Features directly ahead appear to be almost stationary, while closer features to the side of this forward “pole” appear to move with a velocity which becomes maximal when they are located at the side of the eye, 90° from the pole. If we assume for simplicity that all photoreceptors within the eye sample photons during a fixed integration time Δt (which may not be the case, as in some flies: Burton et al. 2001), the motion of flow-field images from front to back across the eye will cause blurring. An object moving past the side of the eye (with velocity v deg/s) will appear as a horizontal spatial smear whose angular size will be approximately $v\Delta t$ degrees. This effectively widens the local optical acceptance angle $\Delta\rho$ to a new value of $\{\Delta\rho^2 + (v\Delta t)^2\}^{1/2}$ (Srinivasan and Bernard 1975). The extent of this widening is worse at the side of eye (higher v)

than at the front (lower v). In order to maintain an optimum sampling ratio of $\Delta\rho/\Delta\phi$ (Snyder 1977), the equatorial increase in $\Delta\rho$ posteriorly should be matched by an increase in $\Delta\phi$. This indeed seems to be the case in many flying insects, such as the Empress Leilia butterfly *Asterocampa leilia* (Rutowski and Warrant 2002). In *Asterocampa* $\Delta\phi$ increases smoothly along the equator from the front of the eye to the side, from 0.9 to 2.0° in males and from 1.3 to 2.2° in females.

Remarkably, the significant extent of matched filtering occurring in the optics and photoreceptors of the compound eye are even more evident at higher levels of processing in the optic lobe, notably in the wide-field motion detecting neurons of the lobula and lobula plate. The lobula plate of the blowfly *Calliphora erythrocephala* (Fig. 6.6a) has long been known to contain cells – known as “horizontal” (H) and “vertical” (V) cells – which respond to wide-field motion (Hausen 1982a, b). Some cells apparently prefer upward or downward motion, others leftward or rightward. By examining very small regions of the visual fields of these cells, Holger Krapp and colleagues (Krapp and Hengstenberg 1996; Krapp et al. 1998) discovered that the local direction preference was usually very different to the global

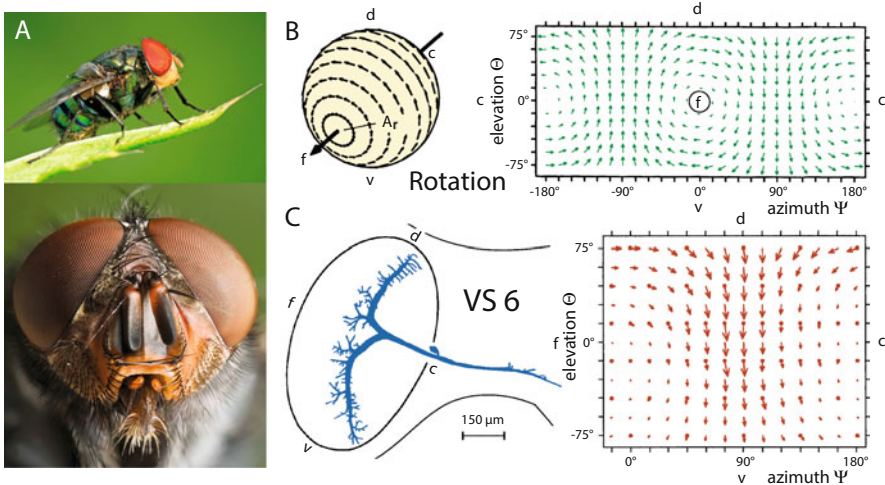


Fig. 6.6 Wide-field motion-sensitive cells in the lobula plate of the blowfly *Calliphora erythrocephala* (a) act as matched filters for optic flow during flight. (b) Local motion flow-field vectors at various azimuths Θ and elevations Ψ experienced during rotation about an axis of rotation A_r , in this case the body axis. At a lateral position with $\Psi = 90^\circ$, the local vectors are ventrally (v) oriented. At the opposite position ($\Psi = -90^\circ$), the local vectors are dorsally (d) oriented. Frontally at the “pole” ($\Psi = 0^\circ$, $\Theta = 0^\circ$: circled “f”), the local vector is zero. Between these extremes, the local vectors swirl in a clockwise direction around the frontal pole, and anti-clockwise around the caudal (c) pole. (c) The local directional preferences of optomotor cell VS6 for small moving black spots at different azimuths Θ and elevations Ψ . Spots were presented to the cell at various Θ and Ψ , and the preferred direction of movement measured electrophysiologically. The local directional preferences show a striking similarity to the motion vectors experienced by the fly during rotation (b), and this cell would respond maximally to such a flow field. In a similar manner, other optomotor cells respond maximally to translation and pitch (a Photo credit: Zhang Yuan Geng (123rf.com); b, c Modified from Krapp and Hengstenberg (1996))

preference. In fact, they found that the local preferred direction changed in a predictable manner from one region to the next, building up an orderly map of directions across the entire visual field of the cell (Fig. 6.6c). The most remarkable feature of these maps is that they are astonishingly good matches to the maps of motion vectors that describe flow fields (Fig. 6.6b). Cell VS6 (Fig. 6.6c) has a map of preferred motion directions that is extremely similar to the map of motion vectors that describes “roll”, the field of rotating features that results from a turn around the body axis (rotation: Fig. 6.6b). This means that if a fly makes a roll turn, VS6 will be maximally stimulated. Signals from these cells can then be used to activate muscles in the fly’s neck, compensating for the roll by returning the head to a horizontal position and maintaining the fly’s course. Similar matching can be found in other cells, including VS1 which matches “pitch”, the field of upwardly moving features resulting from a nose dive. The cell VS8 matches a field consisting of both pitch and roll. In other words, taken as a group, these cells respond vigorously whenever the fly experiences rotational optic flow and behave as impressive matched filters for a predictable and invariant feature of the visual world.

6.3.2.2 Matched Filters for Navigation

Despite their small brains, many insects are remarkable navigators. Some, like bees, wasps and ants, are able to learn visual landmarks around their nest and along a foraging route and then use them to successfully navigate to and from the nest in search of food (Zeil 2012). Others – like the North African desert ant *Cataglyphis bicolor* – are in addition able to continuously update a homebound vector of correct length and direction (via a process known as path integration) while foraging far from the nest in near featureless terrain, thus ensuring their safe return upon finding food (Müller and Wehner 1988). Several species of butterflies and moths (such as the Monarch butterfly *Danaus plexippus*) are even capable of migrating over thousands of kilometres to specific destinations – sites typically favoured by endless generations of their ancestors – only to return months later to where they began (Williams 1965). All of these insects rely on a suite of visual (and other sensory) cues to ensure successful navigation, and many depend on reliable visual compass cues present in the sky (Wehner 1984) – the disc of the sun or moon (Perez et al. 1997; Byrne et al. 2003; Ugolini et al. 2003; Heinze and Reppert 2011), the distributions of stars (Dacke et al. 2013) or the celestial pattern of polarised light (Wehner and Labhart 2006). Of these, the last is particularly widely used by insect navigators, much due to the fact that the celestial polarisation pattern – which is distributed across the entire dome of the sky – is often still visible when other celestial cues have become hidden by cloud or vegetation. Even though we ourselves are unable to see this pattern, most invertebrates (and probably even some vertebrates) see it clearly and can potentially use it as a celestial compass during navigation. It turns out that a remarkable neural matched filter for the celestial polarisation pattern exists in the insect’s central brain. However, before describing this filter, it is first necessary to describe the pattern of celestial polarised light and how polarised light is detected in the retina.

The polarisation properties of light arise from its electromagnetic nature: the plane of polarisation of a light wave is defined as the plane in which its electric field

wave (or E-vector) oscillates. Because of Rayleigh scattering of unpolarised sunlight in the atmosphere, each point in the sky emits light rays with a certain plane (direction) of polarisation. For scattered sunlight or moonlight, the exact direction of each light ray's electric field vector, and its degree of polarisation, varies systematically across the dome of the sky. Scattering thus creates a distinct pattern of skylight polarisation, within which the E-vectors are approximately arranged in concentric circles around the sun or moon (Fig. 6.7a). The pattern has a symmetry

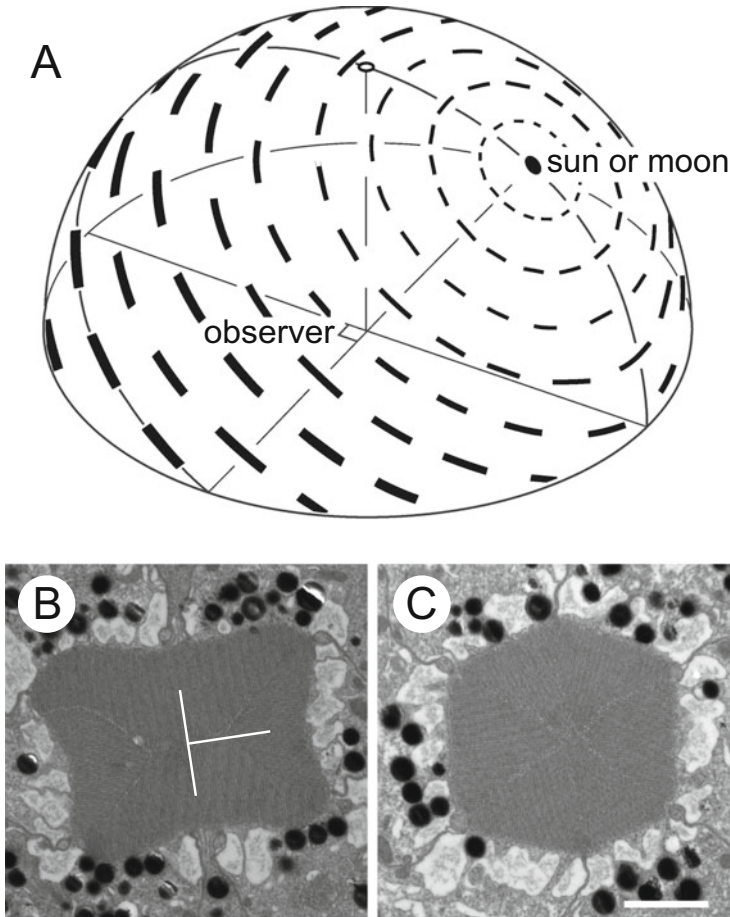


Fig. 6.7 Polarised light detection in insects. (a) The celestial polarisation pattern. The E-vectors of scattered plane-polarised light (*bars*) have directions that are arranged tangentially on concentric circular loci centred on the sun or moon. The degree of polarisation (*bar thickness*) is maximal at 90° from the sun. (b–c) Transverse sections of rhabdoms in the dorsal rim (b), and remainder of the eye (c), in the ant *Polyrhachis sokolova*. In the dorsal rim, the rhabdoms are dumbbell shaped and the rhabdomeres each have one of two possible perpendicular microvillar directions (*white “T”*). In the remainder of the eye, the rhabdoms are round and the rhabdomeres have microvilli oriented in one of several possible directions. Scale bar for both parts: $2\ \mu\text{m}$ (Sections taken from Narendra et al. (2013))

plane defined by the celestial meridian, the semicircular line that traverses the entire dome of the sky (from horizon to horizon) and contains both the sky's zenith (the point directly above the observer) and the sun or moon. This symmetry is the reason why many nocturnal and diurnal insects are able to use the polarisation pattern as a visual celestial compass during navigation.

The reason why insects can see plane-polarised light is due to the structure of their rhabdoms, which are formed from tube-like membranous microvilli. These microvilli – which are all highly aligned – each anchor and constrain the orientation of their resident rhodopsin molecules, so that they are aligned along the microvillar axis. Since each rhodopsin molecule is a linear absorption dipole, and the dipole orientation is constrained by the microvillus (and is identical to that for every other rhodopsin molecule), the rhabdom as a whole becomes highly polarisation sensitive in a direction parallel to the microvilli (Snyder and Laughlin 1975). The photoreceptors responsible for the detection and analysis of polarised skylight are housed within the “dorsal rim area” (or DRA), a narrow strip of ommatidia along the dorsal-most margin of the compound eye (reviewed by Wehner and Labhart 2006; Homberg and el Jundi 2014). The analysis of plane-polarised light requires each rhabdom of the DRA to house two “polarisation classes” of these photoreceptors – each with microvilli oriented in only one of two possible perpendicular directions (Fig. 6.7b, c) – thus forming two orthogonal analysis components for any direction of plane-polarised light. The neural signals generated in each class are then compared, via a neural opponency mechanism, at a subsequent (higher) level of the visual system.

How these signals are actually used as a celestial compass has, until very recently, remained unknown. It now turns out, however, that the insect central complex (CX), a sophisticated structure in the central brain that functions as a control centre for motor coordination and spatial orientation, seems to play a central role. Many neurons of the central complex are highly sensitive to polarised light – the protocerebral bridge, the uppermost region of the CX, even has a columnar architecture reminiscent of the mammalian cortex, in which each column houses interneurons tuned to a specific direction of polarised light (Heinze and Homberg 2007). Recent recordings from TL neurons in the lower division of the central body region of the CX (Fig. 6.8: Bech et al. 2014) not only indicate a sensitivity to polarised light but also reveal that the directional preference for the plane of polarised light, as well as the response strength, both change in a systematic fashion across the cell's enormous receptive field (which covers the entire dome of the sky). In one such cell, the directional preference and response strength (Fig. 6.8a) vary in such a way as to mimic the systematic variation in the direction and degree of polarisation across the dome of the sky when the sun is at an elevation of 10° (Fig. 6.8b), leading to a remarkably good match between the receptive field properties of the cell and the polarised light properties of the sky (Fig. 6.8c). At this sun elevation, and indeed for most elevations up to around 50° , as the locust rotates around its body axis under the sky, the receptive field of this cell would provide such a good match to the celestial polarisation pattern that its response would be strongest only for a single azimuthal direction (as determined by

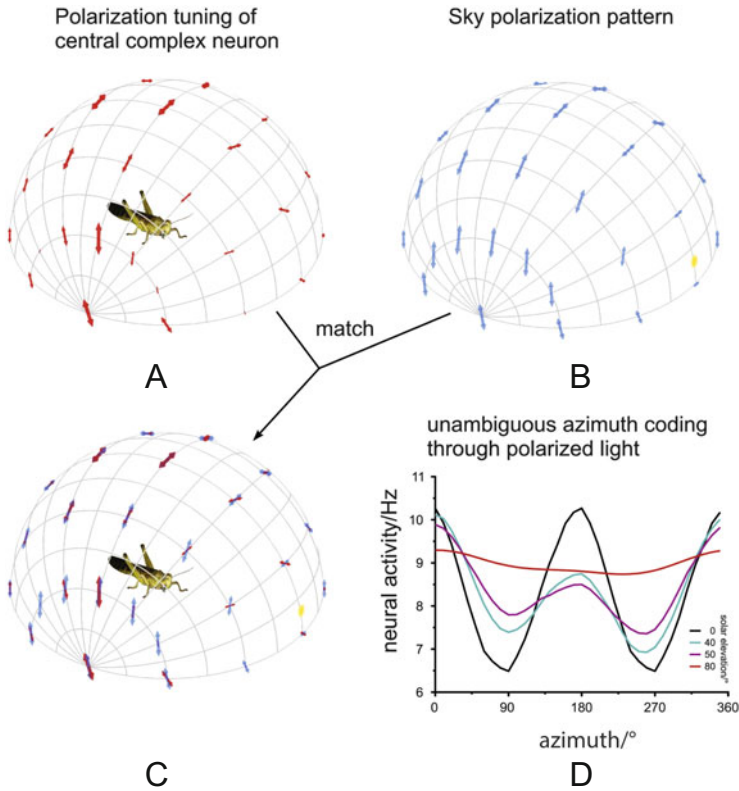


Fig. 6.8 Visual matched filtering to the celestial polarisation pattern. (a) The tuning of a TL neuron in the locust central complex in different parts of its receptive field (which occupies the entire celestial hemisphere), shown relative to the locust's body axis. The orientation of each *red arrow* shows the direction of polarised light that the TL neuron responded to best at that location in its visual field, while the length and thickness of each *arrow* represent the strength of the response. (b, c) The celestial polarisation pattern (b) that closely matched (c) the receptive field properties of the TL neuron shown in (a) has a sun elevation and azimuth of 10° and 0° (directly anterior of the locust), respectively (where *blue arrows* represent the angle and degree of polarisation of light at each point in the celestial hemisphere and the *yellow spot* represents the sun – see Fig. 6.7a). (d) Modelled neural responses of this TL neuron in response to the entire celestial polarisation pattern as a function of its position in the sky (as determined by the azimuth and elevation of the sun relative to the locust). For most sun elevations up to about 50° , there is a unique azimuth that leads to a maximal response in the TL neuron (and thus gives an unambiguous compass bearing). For elevations near 0° (sunrise/sunset), the neuron has greater difficulty to signal a unique azimuth (and compass bearing), although spectral gradients in the sky are likely used to overcome this ambiguity (Pfeiffer and Homberg 2007). For sun elevations above around 60° (approaching midday), the neuron also has difficulty to signal a unique azimuth, but other TL cells have receptive fields better matched to these elevations (From Bech et al. 2014)

modelling: Fig. 6.8d). Recordings from other TL cells show best matches to the celestial polarisation pattern for other elevations of the sun and strongest responses at other azimuths. Together the responses of all of these cells – each of them an impressive matched filter to a specific celestial polarisation pattern – are likely to be integrated in the brain to provide a robust compass system that allows the locust to unambiguously signal a chosen compass bearing.

6.4 Conclusions

From the optical structure of the compound eyes and the physiological properties of the photoreceptors, to the neural circuits that process visual information in the brain, visual matched filtering has constituted a major evolutionary strategy in insects. One reason for this is the necessity for a small visual system, like that of an insect, to be matched to the most pressing visual challenges that the species faces, at the expense of less pressing challenges. A second but no less important reason is that matched filtering undoubtedly saves energy, particularly in the brain, and in small animals like insects, with complex lifestyles but strictly limited energy budgets, this could be of critical benefit for freeing up energy that can be used for other vital functions. Both of these factors – pressing visual challenges and overriding energy constraints – have led to the enormous variety and sophistication of visual matched filters that we see among the insects today.

Acknowledgements This review was written during 2015 while I was a Visiting Fellow at the Research School of Biology at the Australian National University in Canberra, Australia. I am deeply indebted to Prof. Jochen Zeil who generously hosted me in his research group and provided critical comments on the manuscript.

References

- Atick JJ (1992) Could information theory provide an ecological theory of sensory processing? *Network* 3:213–251
- Atick JJ, Redlich AN (1992) What does the retina know about natural scenes? *Neural Comput* 4: 196–210
- Autrum H (1950) Die Belichtungspotentiale und das Sehen der Insekten (Untersuchungen an *Calliphora* und *Dixippus*). *Z Vergl Physiol* 32:176–227
- Bech M, Homberg U, Pfeiffer K (2014) Receptive fields of locust brain neurons are matched to polarization patterns of the sky. *Curr Biol* 24:2124–2129
- Burton BG, Tatler BW, Laughlin SB (2001) Variations in photoreceptor response dynamics across the fly retina. *J Neurophysiol* 86:950–960
- Byrne M, Dacke M, Nordström P, Scholtz C, Warrant EJ (2003) Visual cues used by ball-rolling dung beetles for orientation. *J Comp Physiol A* 189:411–418
- Chittka L, Niven JE (2009) Are bigger brains better? *Curr Biol* 19:R995–R1008
- Cronin TW, Johnsen S, Marshall NJ, Warrant EJ (2014) *Visual ecology*. Princeton University Press, Princeton
- Cuttle MF, Hevers W, Laughlin SB, Hardie RC (1995) Diurnal modulation of photoreceptor potassium conductance in the locust. *J Comp Physiol A* 176:307–316

- Dacke M, Baird E, Byrne M, Scholtz C, Warrant EJ (2013) Dung beetles use the milky way for orientation. *Curr Biol* 23:298–300
- Dahmen H (1991) Eye specialisations in waterstriders: an adaptation to life in a flat world. *J Comp Physiol A* 169:623–632
- de Souza JM, Ventura DF (1989) Comparative of temporal summation and response form in hymenopteran photoreceptors. *J Comp Physiol A* 165:237–245
- Dong DW, Atick JJ (1995) Statistics of natural time-varying images. *Netw Comput Neur Syst* 6: 345–358
- Eberhard WG (2007) Miniaturized orb-weaving spiders: behavioural precision is not limited by small size. *Proc Roy Soc B* 274:2203–2209
- Field DJ (1987) Relations between the statistics of natural images and the response properties of cortical cells. *J Opt Soc Am A* 4:2379–2394
- Field DJ (1999) Wavelets, vision and the statistics of natural scenes. *Phil Trans R Soc A* 357: 2527–2542
- Frederiksen R, Weislo WT, Warrant EJ (2008) Visual reliability and information rate in the retina of a nocturnal bee. *Curr Biol* 18:349–353
- Gibson JJ (1950) *The perception of the visual world*. Houghton Mifflin, Boston
- Gilbert C, Strausfeld NJ (1991) The functional organization of male-specific visual neurons in flies. *J Comp Physiol A* 169:395–411
- Gronenberg W, Strausfeld NJ (1991) Descending pathways connecting the male-specific visual system of flies to the neck and flight motor. *J Comp Physiol A* 169:413–426
- Hausen K (1982a) Motion sensitive interneurons in the optomotor system of the fly. 1. The horizontal cells – structure and signals. *Biol Cybern* 45:143–156
- Hausen K (1982b) Motion sensitive interneurons in the optomotor system of the fly. 2. The horizontal cells – receptive-field organization and response characteristics. *Biol Cybern* 46:67–79
- Heinze S, Homberg U (2007) Maplike representation of celestial E-vector orientations in the brain of an insect. *Science* 315:995–997
- Heinze S, Reppert SM (2011) Sun compass integration of skylight cues in migratory monarch butterflies. *Neuron* 69:345–358
- Homberg U, el Jundi B (2014) Polarization vision in arthropods. In: Werner JS, Chalupa LM (eds) *The new visual neurosciences*. MIT Press, Cambridge, MA, pp 1207–1218
- Hornstein EP, O'Carroll DC, Anderson JC, Laughlin SB (2000) Sexual dimorphism matches photoreceptor performance to behavioural requirements. *Proc R Soc Lond B* 267:2111–2117
- HorrIDGE GA (1978) The separation of visual axes in apposition compound eyes. *Phil Trans Roy Soc Lond B* 285:1–59
- Howard J, Blakeslee B, Laughlin SB (1984) The dynamics of phototransduction in insects: a comparative study. *J Comp Physiol A* 154:707–718
- Hughes A (1977) The topography of vision in mammals of contrasting life style: comparative optics and retinal organisation. In: Crescitelli F (ed) *Handbook of sensory physiology*, vol VII/5. Springer, Berlin, pp 613–756
- Junger W, Varju D (1990) Drift compensation and its sensory basis in waterstriders (*Gerris paludum* F.). *J Comp Physiol A* 167:441–446
- Krapp HG (2014) Sensory integration: neuronal filters for polarized light patterns. *Curr Biol* 24: R840–R841
- Krapp HG, Hengstenberg R (1996) Estimation of self-motion by optic flow processing in single visual neurons. *Nature* 384:463–466
- Krapp HG, Hengstenberg B, Hengstenberg R (1998) Dendritic structure and receptive field organization of optic flow processing interneurons in the fly. *J Neurophysiol* 79:1902–1917
- Land MF (1981) Optics and vision in invertebrates. In: Autrum H (ed) *Handbook of sensory physiology*, vol VII/6B. Springer, Berlin, pp 471–592
- Land MF (1989) Variations in the structure and design of compound eyes. In: Stavenga DG, Hardie RC (eds) *Facets of vision*. Springer, Berlin, pp 90–111

- Land MF, Collett TS (1974) Chasing behaviour of houseflies (*Fannia canicularis*): a description and analysis. *J Comp Physiol* 89:331–357
- Land MF, Eckert H (1985) Maps of the acute zones of fly eyes. *J Comp Physiol A* 156:525–538
- Land MF, Nilsson DE (2012) *Animal eyes*. Oxford University Press, Oxford
- Laughlin S (1981) A simple coding procedure enhances a neuron's information capacity. *Z Naturforsch* 36C:910–912
- Laughlin SB (1996) Matched filtering by a photoreceptor membrane. *Vision Res* 36:1529–1541
- Laughlin SB, Weckström M (1993) Fast and slow photoreceptors – a comparative study of the functional diversity of coding and conductances in the Diptera. *J Comp Physiol A* 172:593–609
- Laughlin SB, de Ruyter van Steveninck RR, Anderson JC (1998) The metabolic cost of neural information. *Nat Neurosci* 1:36–41
- Müller M, Wehner R (1988) Path integration in desert ants, *Cataglyphis fortis*. *Proc Natl Acad Sci U S A* 85:5287–5290
- Narendra A, Alkaladi A, Raderschall CA, Robson SKA, Ribi WA (2013) Compound eye adaptations for diurnal and nocturnal lifestyle in the intertidal ant, *Polyrhachis sokolova*. *PLoS One* 8(10):e76015
- Nilsson DE (1989) Optics and evolution of the compound eye. In: Stavenga DG, Hardie RC (eds) *Facets of vision*. Springer, Berlin, pp 30–73
- Nilsson DE, Warrant EJ, Johnsen S, Hanlon R, Shashar N (2012) A unique advantage for giant eyes in giant squid. *Curr Biol* 22:683–688
- Niven JE, Farris SM (2012) Miniaturization of nervous systems and neurons. *Curr Biol* 22:R323–R329
- Niven JE, Laughlin SB (2008) Energy limitations as a selective pressure on the evolution of sensory systems. *J Exp Biol* 211:1792–1804
- Niven JE, Anderson JC, Laughlin SB (2007) Fly photoreceptors demonstrate energy-information trade-offs in neural coding. *PLoS Biol* 5(4):e91
- Nordström K, O'Carroll DC (2009) Feature detection and the hypercomplex property in insects. *TINS* 32:383–391
- O'Carroll DC (1993) Feature-detecting neurons in dragonflies. *Nature* 362:541–543
- Okawa H, Sampath AP, Laughlin SB, Fain GL (2008) ATP consumption by mammalian rod photoreceptors in darkness and in light. *Curr Biol* 18:1917–1921
- Olberg RM (1981) Object- and self-movement detectors in the ventral cord of the dragonfly. *J Comp Physiol A* 141:327–334
- Olberg RM (1986) Identified target-selective visual interneurons descending from the dragonfly brain. *J Comp Physiol A* 159:827–840
- Perez SM, Taylor OR, Jander R (1997) A sun compass in monarch butterflies. *Nature* 387:29
- Pfeiffer K, Homberg U (2007) Coding of azimuthal directions via time-compensated combination of celestial compass cues. *Curr Biol* 17:960–965
- Rutowski RL, Warrant EJ (2002) Visual field structure in a butterfly *Asterocampa leilia* (Lepidoptera, Nymphalidae): dimensions and regional variation in acuity. *J Comp Physiol A* 188:1–12
- Salmela I, Immonen EV, Frolov R, Krause S, Krause Y, Vähäsöyrinki M, Weckström M (2012) Cellular elements for seeing in the dark: voltage-dependent conductances in cockroach photoreceptors. *BMC Neurosci* 13:93
- Schwind R (1978) Visual system of *Notonecta glauca*: a neuron sensitive to movement in the binocular visual field. *J Comp Physiol* 123:315–328
- Schwind R (1980) Geometrical optics of the *Notonecta* eye: adaptations to optical environment and way of life. *J Comp Physiol* 140:59–68
- Sherk TE (1978) Development of the compound eyes of dragonflies (Odonata). III Adult compound eyes. *J Exp Zool* 203:61–80
- Smolka J, Hemmi JM (2009) Topography of vision and behavior. *J Exp Biol* 212:3522–3532
- Snyder AW (1977) Acuity of compound eyes: physical limitations and design. *J Comp Physiol* 116:161–182

- Snyder AW, Laughlin SB (1975) Dichroism and absorption by photoreceptors. *J Comp Physiol* 100:101–116
- Srinivasan MV, Bernard GD (1975) The effect of motion on visual acuity of the compound eye: a theoretical analysis. *Vision Res* 15:515–525
- Srinivasan MV, Laughlin SB, Dubs A (1982) Predictive coding: a fresh view of inhibition in the retina. *Proc R Soc Lond B* 216:427–459
- Stavenga DG, Kuiper JW (1977) Insect pupil mechanisms. I. On the pigment migration in the retinula cells of Hymenoptera (suborder Apocrita). *J Comp Physiol* 113:55–72
- Strausfeld NJ (1991) Structural organization of male-specific visual neurons in calliphorid optic lobe. *J Comp Physiol A* 169:379–393
- Ugolini A, Fantini T, Innocenti R (2003) Orientation at night: an innate moon compass in sandhoppers (Amphipoda: Talitridae). *Proc Roy Soc Lond B* 270:279–281
- van Hateren JH (1992) Real and optimal neural images in early vision. *Nature* 360:68–70
- van Hateren JH (1993) Spatiotemporal contrast sensitivity of early vision. *Vision Res* 33:257–267
- Walls GL (1942) The vertebrate eye and its adaptive radiation. The Cranbrook Press, Bloomfield Hills
- Warrant EJ (1999) Seeing better at night: life style, eye design and the optimum strategy of spatial and temporal summation. *Vision Res* 39:1611–1630
- Warrant EJ (2001) The design of compound eyes and the illumination of natural habitats. In: Barth FG, Schmid A (eds) *Ecology of sensing*. Springer, Berlin, pp 187–213
- Weckström M, Laughlin SB (1995) Visual ecology and voltage-gated ion channels in insect photoreceptors. *Trends Neurosci* 18:17–21
- Wehner R (1981) Spatial vision in arthropods. In: Autrum H (ed) *Handbook of sensory physiology*, vol VII/6C. Springer, Berlin, pp 287–616
- Wehner R (1984) Astronavigation in insects. *Annu Rev Entom* 29:277–298
- Wehner R (1987) “Matched filters” – neural models of the external world. *J Comp Physiol A* 161: 511–531
- Wehner R, Labhart T (2006) Polarisation vision. In: Warrant EJ, Nilsson DE (eds) *Invertebrate vision*. Cambridge University Press, Cambridge, pp 291–348
- Williams CB (1965) *Insect migration*. Collins, London
- Williams DS (1983) Changes of photoreceptor performance associated with the daily turnover of photoreceptor membrane in locusts. *J Comp Physiol* 150:509–519
- Zeil J (1983a) Sexual dimorphism in the visual system of flies: the compound eyes and neural superposition in Bibionidae (Diptera). *J Comp Physiol* 150:379–393
- Zeil J (1983b) Sexual dimorphism in the visual system of flies: the free flight behaviour of male Bibionidae (Diptera). *J Comp Physiol* 150:395–412
- Zeil J (2012) Visual homing: an insect perspective. *Curr Opin Neurobiol* 22:285–293
- Zeil J, Hemmi JM (2006) The visual ecology of fiddler crabs. *J Comp Physiol A* 192:1–25
- Zeil J, Nalbach G, Nalbach H-O (1986) Eyes, eye stalks and the visual world of semi-terrestrial crabs. *J Comp Physiol* 159:801–811
- Zeil J, Nalbach G, Nalbach H-O (1988) Spatial vision in a flat world: optical and neural adaptations in arthropods. In: Singh RH, Strausfeld N (eds) *Neurobiology of sensory systems*. Plenum Press, New York, pp 123–137

R.H. Douglas and T.W. Cronin

Contents

7.1	Introduction	170
7.2	A Primer of Vertebrate Vision	171
7.2.1	What Wavelengths Are Potentially Available for Vision?	172
7.2.2	The Different Functions of Rods and Cones	173
7.3	Filters That Alter the Amount of Shortwave Radiation Incident on Photoreceptors ...	175
7.3.1	Distribution	175
7.3.2	Function of Removing Short Wavelengths in Most Species	176
7.3.3	Short-Wave-Absorbing Pigments in the Lenses of Deep-Sea Fish	178
7.4	Post-retinal Filters	179
7.4.1	Melanin	179
7.4.2	Tapeta	179
7.5	Spectral Tuning Within Photoreceptors	180
7.5.1	Visual Pigments	181
7.5.2	A Unique Retinal Photosensitiser	183
7.5.3	Inner Segment Filters	183
7.6	Optical Filters	186
7.6.1	Optical Imperfections	186
7.6.2	Image Focus	187
7.6.3	The Pupil as a ‘Matched Filter’	189
7.6.4	The Lens as a ‘Matched Filter’	190
7.7	Filtering of Spatial Properties of Visual Fields	191
7.7.1	Retinal Spatial Filters	191
7.7.2	Optical Spatial Filters: Tubular Eyes	194

R.H. Douglas (✉)

Department of Optometry & Visual Science, City University London, Northampton Square,
London EC1V 0HB, UK

e-mail: r.h.douglas@city.ac.uk

T.W. Cronin

Department of Biological Sciences, University of Maryland, Baltimore County,
1000 Hilltop Circle, Baltimore, MD 21250, USA

e-mail: cronin@umbc.edu

7.8	Polarisation Filtering	195
7.8.1	Polarisation Sensing in Vertebrates	195
7.8.2	Mechanisms of Detecting Polarisation	197
7.8.3	Matched Filtering in a Bird Retina: Magnetic Compass Calibration	197
7.9	Summary and Conclusions	198
	References	198

Abstract

Despite their large brains, vertebrates extensively filter visual information with numerous adaptations within their eyes, simplifying the stream of neuronal traffic sent centrally and protecting retinal structures from photodamage. Each filtering mechanism can be considered ‘matched’ in the sense that it removes a particular component of incoming light. In this chapter, we consider these peripheral sensory filters of vertebrate eyes. While such eyes are built on a conserved design, they nevertheless incorporate a huge diversity of specialisations, including pigment filters, tuned visual pigments, optical adjustments and retinal sampling variations, all of which enhance the speed and utility of visual perception and simultaneously reduce the energetic cost of vision. Unlike invertebrates, many of whom figuratively re-engineer eye design from the ground up to favour particular visual tasks, vertebrates show enormous plasticity founded on a single fundamental design. This plasticity ranges among species, habitats and even seasons in some species, giving vertebrates as a group the ability to function in any location on earth that provides at least a few photons on which vision can be based.

7.1 Introduction

A visual stimulus can have many attributes: form, brightness, colour, polarisation as well as temporal and spatial variation in all of these. Not surprisingly therefore, approximately one third of the human cortex is involved in processing visual images, a greater neural commitment than to any other sense. Vision is a very costly process. Any adaptation that reduces this cost without significantly affecting the performance will be selected for during evolution. Here we will discuss various ways in which vertebrates have reduced the cost inherent in complex neural processing by filtering stimuli before they reach photoreceptors, in the photoreceptors themselves, and in the ways that photoreceptors link to retinal ganglion cells, the ultimate conduit to the brain.

Rüdiger Wehner’s (1987) original presentation of ‘matched filters’ emphasised the filtering of sensory information at a very early level, in the array of photoreceptor elements and their associated interactions. Vertebrates have matched filters of this class. But with their large brains, a more generalised receptor array can be analysed intensively for significant aspects of a stimulus. In an extreme case, single cells in the human medial temporal lobe can be activated by a picture of a particular

person, place, or thing – even when pictures have been taken from different aspects or locations (Quiroga et al. 2005). Such cells are ‘matched filters’, since they are devoted to just one stimulus source. However, vertebrate eyes also filter information at or near the periphery, reducing the costs of characterising all stimulus attributes and deleting the irrelevant ones. Early filtering can also remove potentially damaging stimuli, preventing the costs that would be incurred if the eye was either permanently damaged or needed to be repaired.

7.2 A Primer of Vertebrate Vision

All vertebrate eyes have the same basic structure (Fig. 7.1) in which light is focused onto a light-sensitive retina by a cornea and a lens. The space between these two structures is filled with a nutritive aqueous humour and is divided into anterior and posterior chambers by an iris, which forms the pupil whose diameter can be adjusted using muscles within the iris. Posterior to the lens, the eye is filled with the jelly-like, transparent vitreous humour.

The image formed by the anterior eye is focused on a layered retina composed of a variety of neural cell types and neuroglia. Here, light is converted into neurobiological activity by photoreceptors within the outer retina. The outer segments of these rods and cones contain visual pigments consisting of a chromophore bound to a protein, opsin. All such pigments have a similar bell-shaped absorption profile

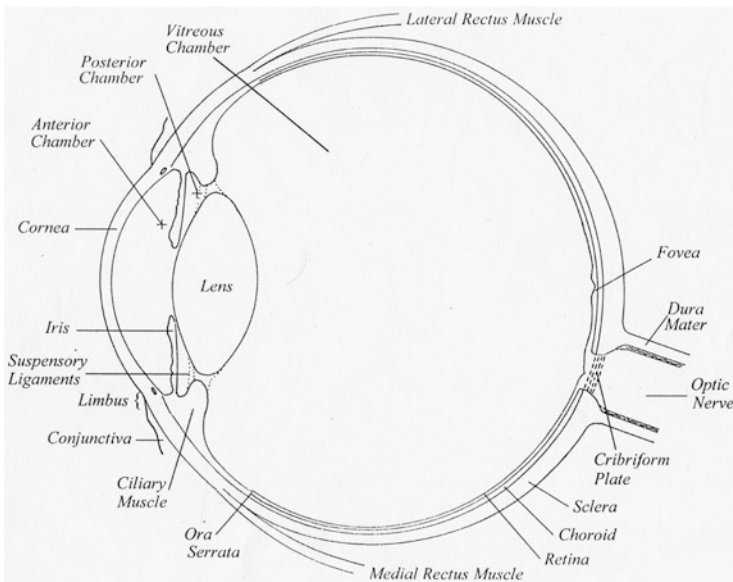


Fig. 7.1 Simplified transverse section of the human eye. Most vertebrate eyes have a similar structure although some things, such as eye and lens shape, may differ (Drawn by GL Ruskell)

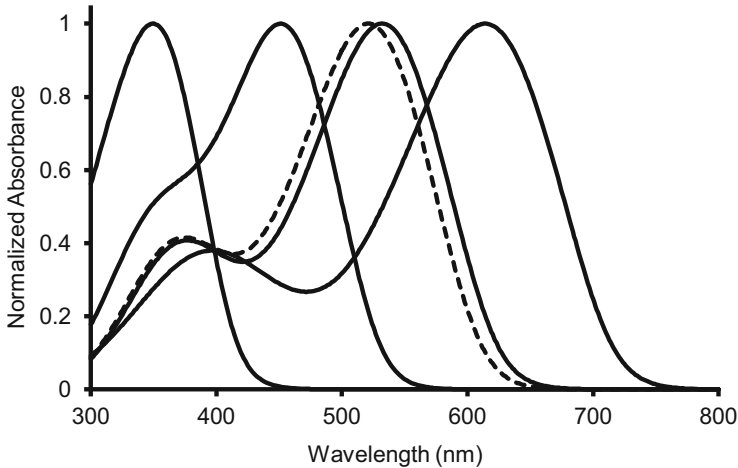


Fig. 7.2 Normalised absorbance spectra of goldfish visual pigments. The goldfish retina contains visual pigments representing all five opsin gene families, a rod pigment with λ_{\max} 521 nm (RH1) and four spectral classes of cone absorbing maximally at 355 nm (SWS2), 452 nm (SWS1), 532 nm (RH2) and 614 nm (LWS). These are porphyropsins and the figure shows templates fitted to data of Bowmaker et al. (1991a)

(Fig. 7.2). In vertebrates, five broad classes of visual pigment are coded for by different opsin gene families. All rods contain an RH1 pigment with maximal absorption (λ_{\max}) 460–530 nm, while there are four different types of cone pigment: LWS (λ_{\max} 490–570 nm), RH2 (λ_{\max} 480–535 nm), SWS1 and SWS2 (λ_{\max} 410–490 and 355–440 nm, respectively) (Collin et al. 2009). These absorption maxima assume that the opsin is bound to the vitamin A₁-derived chromophore retinal, as is the case in most vertebrates, forming ‘rhodopsin’ visual pigments. However, in some freshwater and deep-sea fish, amphibia and reptiles, these absorption maxima are shifted towards longer wavelengths by the use of a vitamin A₂-derived chromophore, 3,4-dehydroretinal, forming ‘porphyropsin’ pigments. Photoreceptors can contain either only rhodopsins or porphyropsins or a mixture of the two.

When a photon activates the visual pigment, the retinal isomerises from the 11-*cis* isomer to the all-*trans* form altering the conformation of the opsin. This initiates a G-protein-coupled enzyme cascade, ultimately resulting in the closure of cation channels and the hyperpolarisation of the photoreceptor. The resulting signal is processed by the other cells of the retina and transmitted to the brain via ganglion cell axons making up the optic nerve, eventually leading to visual perception.

7.2.1 What Wavelengths Are Potentially Available for Vision?

Visible radiation represents a tiny fraction of the electromagnetic spectrum, ranging across species from approximately 300 to 800 nm. Wavelengths below ~300 nm are

removed by the proteins and nucleic acids of the cornea, lens and humours (Douglas and Marshall 1999). These ocular media may contain filtering pigments that reduce the range of short wavelengths transmitted even further (see Sect. 7.3). Above about 500 nm, the ocular media of all species transmit light effectively far into the infrared, and the limit of long-wave sensitivity is set by the visual pigments. The most long-wave-sensitive visual pigments, found in many freshwater fish, for example (Fig. 7.2), absorb maximally around 630 nm and are sensitive up to about 800 nm.

7.2.2 The Different Functions of Rods and Cones

The rod system, which is used in low (scotopic) light levels, optimises absolute sensitivity, but almost never provides information about object colour. It has relatively poor temporal and spatial resolution. The cone system, on the other hand, which is active at higher (photopic) light levels, provides high spatial and temporal acuity. While cones mediate colour vision, they have poor absolute sensitivity.

The light levels at midday on sunny Caribbean beach compared to those in a forest on a rainy Scottish winter's night differ by ~ 12 log units. In the sea, light used in vision has an even greater range, spanning 16 log units (Clarke and Denton 1962). While some animals, such as deep-sea fish, are permanently exposed to low light levels and thus have pure rod retinæ, and others, such as chameleons, are only active during the day and have pure cone retinæ, most animals can see something throughout much of the range of available intensities, by switching between the two photoreceptor types whose sensitivity can be further adjusted by anatomical, biochemical and physiological means (Perlman and Normann 1998; Lamb and Pugh 2004). However, most animals are specialised for vision within a particular intensity range and are optimised for either spatial resolution or sensitivity (Land and Nilsson 2012; Cronin et al. 2014).

7.2.2.1 Requirements for High Absolute Sensitivity

In low light levels, sensitivity is increased primarily by maximising the number of photons captured by the photoreceptors. Consequently, animals active in dim light have many of the following characteristics:

- Large pupils and short focal length lenses so that each photoreceptor collects light effectively over a greater angle. This requires a large eye.
- Ocular media that transmit as many photons as possible.
- A reflective tapetum underlying the retina.
- A retina dominated by rods.

Rods are more sensitive than cones in part because they have relatively larger outer segments, boosting visual pigment content. This is taken to extremes in some deep-sea fish, which either have rods several times as long as those of shallow-

water species or several superimposed tiers of normally sized rods (Wagner et al. 1998). Another adaptation in the rods of some nocturnal mammals is an unusual remodelling of nuclear chromatin, converting the nucleus into a miniature light-gathering element (Solovei et al. 2009). Compared to cones, rods also tend to have a slower phototransduction cascade that has both lower dark noise levels and higher gain. The end product is a photoreceptor with excellent light-trapping capacity, robust responses at low levels of photon catch and outstanding signal-to-noise characteristics.

However, the main cause of higher rod sensitivity is the high convergence ratio of rods onto post-receptor neurons. Such spatial summation is required, as photoreceptors are inherently noisy and are occasionally activated even in the absence of light. To ensure that the visual pathway does not respond to such 'dark noise', retinal ganglion cell activation requires several independent signals indicating visual pigment isomerisation. The likelihood of this in low light levels is increased by hundreds of rods feeding into one ganglion cell. Such convergence ratios of photoreceptors onto ganglion cells vary not only between species, depending on their ecological requirements, but also regionally within a single retina (see Sect. 7.7.1).

7.2.2.2 Requirements for High Spatial Resolution

A convenient way to think of spatial resolution (acuity) is in terms of the capacity of the eye to resolve a black and white grating. The closer the individual elements of the grating before they appear as an indistinct grey mass, the higher the acuity. In general, to resolve the lines of the grating, two adjacent white bars must be imaged on two individual photoreceptors separated by a photoreceptor covered by the black bar in between.

For the highest possible spatial acuity, the output of the individual photoreceptors must be analysed individually. The rod system, with its high level of convergence, is thus unsuitable for the perception of fine detail. In contrast, there is often little convergence of cone photoreceptor outputs. The retinae of diurnal animals thus have both a greater proportion of cones than those of animals active in lower light levels and a greater number of post-receptor neurons to handle the density of sensory traffic.

High acuity demands a large eye and a lens with a long focal length, essentially spreading the image over a large surface area, coupled to a high density of cones with little convergence. However, spatial acuity is not determined solely by a number of photoreceptors sampling the image. Optical imperfections can degrade the image before it gets to the photoreceptors (see Sect. 7.6.1). Many of the filters described in this chapter serve to minimise such optical imperfections.

7.3 Filters That Alter the Amount of Shortwave Radiation Incident on Photoreceptors

7.3.1 Distribution

The corneas and humours of most animals serve purely protective, refractive or nutritive functions and are unpigmented, transmitting most radiation down to ~300 nm (Fig. 7.3a). With the notable exception of some deep-sea fish (see Sect. 7.3.3), animals active in low light levels also have unpigmented lenses that transmit as much shortwave radiation as possible (Fig. 7.3a). In contrast, many diurnal animals have ocular media that contain short-wave-absorbing compounds that remove variable amounts of light between 300 and 500 nm.

Only two species of marine teleosts are known to have vitreous humours that absorb significant amounts of shortwave radiation (Nelson et al. 2001; Losey et al. 2003). Pigmented corneas are somewhat more common, occurring in some diurnal fish whose corneas appear yellow due to carotenoids within them (Siebeck and Marshall 2001; Douglas and Marshall 1999).

The lenses of many (mostly diurnal) species contain pigments that effectively block variable amounts of short wavelengths (Fig. 7.3). While all vertebrate classes include species whose lenses contain a degree of UV-absorbing pigmentation (Douglas and Marshall 1999), the concentration is often insufficient to absorb visible radiation and the lenses appear colourless. High levels of pigmentation that additionally remove significant amounts of blue light, resulting in visibly yellow lenses, are more restricted. First described in snakes and squirrels (Walls 1931), yellow lenses have now been observed in other mammals (Douglas and Jeffery 2014) and are also common in fish (Thorpe et al. 1993; Siebeck and Marshall 2000) and occur in some reptiles (Walls 1931, Ellingson et al. 1995) (Fig. 7.3a). Some bird (Lind et al. 2014) and amphibian (Douglas and Marshall 1999) lenses are sufficiently pigmented to remove UV, but none appear yellow.

The macula region of primates, where the retina is specialised for high spatial acuity (see Sect. 7.7.1), also contains high levels of carotenoids absorbing heavily between 400 and 500 nm, making it appear yellow (Whitehead et al. 2006). The pigments occur primarily in the axons of the cones (Henle fibres), filtering light before it impinges on the photoreceptor outer segments.

Short-wave-absorbing filters are only adaptive when light levels are high (see Sect. 7.3.2). In lower light levels, they absorb photons that could be used to boost sensitivity. Thus, in the cornea pigmentation is often restricted to the dorsal region through which the brighter light from the water's surface enters, leaving the ventral cornea, which receives the dimmer upwelling illumination, unpigmented (Douglas 1989; Siebeck and Marshall 2001). A similar effect is produced in some species of fish by reflective iridescent structures within the cornea (Lythgoe 1971). Furthermore, the corneas of some fish are 'occlusable' (Siebeck et al. 2003; Kondrashev 2008). In bright light, pigments are dispersed within chromatophores covering the whole cornea, while in lower light levels they aggregate around the rim of the cornea, leaving the bulk of it unpigmented.

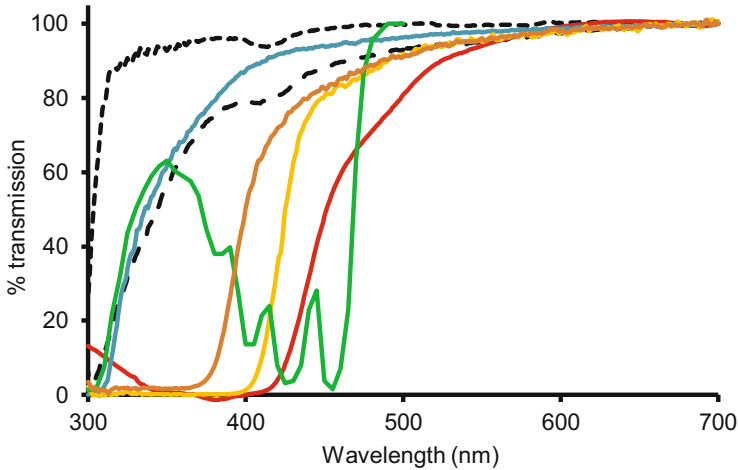


Fig. 7.3 Spectral transmission of vertebrate ocular media. (a) The *dotted* and *dashed* lines represent the transmission of the bovine vitreous humour and cornea, respectively. The *blue* curve shows the spectral transmission of an elephant fish (*Gnathonemus petersii*) lens. All these structures are unpigmented and shortwave absorption is due to the structural elements of the tissues. The *brown* curve shows the 'colourless' lens of an Arabian Oryx (*Oryx leucoryx*) which contains some UV-absorbing pigmentation. The *yellow* and *red* curves depict such curves for the pigmented yellow lenses of an Alaotran gentle lemur (*Haplemur alaotrensis*) and a colubrid snake (*Malpolon monspessulanus*), respectively. The *green* curve shows the spectral transmission of a yellow lens from the mesopelagic teleost *Argyropseleniscus sladeni* whose shape is indicative of a carotenoid. (b) The mesopelagic teleost *Scopelarchus analis* viewed from above, showing both a bright yellow lens and the upwardly directed tube eye (Photo NJ Marshall)

7.3.2 Function of Removing Short Wavelengths in Most Species

All filters discussed above, no matter where they are located, remove short wavelengths and are likely to have similar functions (Walls 1963). Because they decrease the sensitivity of an animal and prevent the perception of potentially

useful ultraviolet light, they must benefit the animal in some other way. Two such roles are immediately apparent: to protect the retina or to improve spatial resolution. These two functions are not mutually exclusive, and both would explain why short-wave-absorbing filters occur mainly in diurnal animals and why, when they are unevenly distributed, as in the corneas of some fish (see Sect. 7.3.1), it is the brighter downwelling light that is filtered.

7.3.2.1 Protection of the Retina from Light Damage

Light can damage the retina photochemically, and the risk is considerably increased at shorter wavelengths (van Norren and Gorgels 2011). Therefore, removing short wavelengths, especially in long-lived diurnal species exposed to large amounts of light in their lifetime, could serve to protect the retina.

Some pigments, such as carotenoids, protect ocular structures in another way, unrelated to their spectral filtering. Biological tissue is susceptible to photooxidative damage through the production of free radicals, including singlet oxygen. Carotenoids, such as the human macular pigment (see Sect. 7.3.1), are effective scavengers of such harmful molecules and could serve to protect the retina. Carotenoids in the cornea, lens and uveal tract (Bernstein et al. 2001) may serve a similar protective role.

Relatively short-lived nocturnal animals would benefit from both the increased photon capture afforded by UV-transparent ocular media and (as all visual pigments absorb light below 400 nm) any other advantages resulting from sensitivity in the UV (Douglas and Jeffery 2014). However, parrots (Carvalho et al. 2011) and arctic reindeer (Hogg et al. 2011) are neither predominantly nocturnal nor short lived, yet have ocular media that transmit near-UV radiation. In these species, the benefits of allowing UV to reach the retina must outweigh the dangers. In the Arctic, for example, UV sensitivity will increase the contrast of both the vegetation that reindeer eat and the white fur of predators such as polar bears (which both absorb UV) when seen against the UV-reflecting snow (Hogg et al. 2011; Tyler et al. 2014). Although the benefits of having UV-transmissive ocular media are clear, it is unclear why the retinæ of these animals apparently show no ill effects of significant shortwave exposure.

7.3.2.2 Improvement of Image Quality

As both Rayleigh scattering and chromatic aberration are increased at short wavelengths, filters that remove this part of the spectrum provide improved image quality. The UV-absorbing ocular media of diurnal raptors, such as kestrels, may be an adaptation to facilitate their extremely high visual acuity (Lind et al. 2014). Some data from mammals are consistent with this notion. Species with highly pigmented yellow lenses have retinæ either containing a large proportion of cones or areas of very high cone density (or both), features which would be expected in the eyes adapted for high spatial resolution (Douglas and Jeffery 2014).

Light scatter, and the subsequent degradation of the image, is a particular problem underwater as light can be scattered both by water molecules and by small particles, such as plankton, suspended within the water. This reduces the range at which objects can be seen (Muntz 1976a) and could explain why short-wave-absorbing filters are more common in fish than in other vertebrates, occurring not only in lenses but also the cornea and even the humours of some species (see Sect. 7.3.1).

7.3.3 Short-Wave-Absorbing Pigments in the Lenses of Deep-Sea Fish

Surprisingly, yellow lenses occur in several species of fish inhabiting the dimly lit mesopelagic zone of the ocean (Douglas and Thorpe 1992) (Fig. 7.3a, b), where light levels are so low that protecting the retina is unnecessary. The high degree of convergence of the output of deep-sea fish rods (Wagner et al. 1998) also makes improving image quality an unlikely function of such lenses. Since they decrease the overall intensity of light incident on the retina by as much as 80 %, in animals for whom maximising photon capture is at a premium, such lenses must fulfil some other important function. Furthermore, short wavelengths are removed by several, unrelated, compounds within the lenses of different species, suggesting this trait has independently evolved on a number of occasions (Douglas et al. 1998a).

There are two sources of light in the deep sea: downwelling sunlight in the upper 1,000 m (Denton 1990) and bioluminescence. Most mesopelagic animals bioluminesce to attract prey, startle or warn predators, enhance camouflage or provide intraspecific signalling (Widder 2010; Haddock et al. 2010). Bioluminescence is the only light available for vision at night and below 1,000 m, but is probably also the most significant visual stimulus even during the day at shallower depths for many animals (Turner et al. 2009). During the day background spacielight will decrease the contrast of bioluminescent signals, impairing their visibility. Yellow lenses may solve this problem.

As one descends the water column, light levels decrease and the spectral quality of the downwelling illumination changes, with long wavelengths being rapidly absorbed (Beebe 1935). Below a few hundred metres, most light is limited to a narrow waveband around 450–500 nm. Peak emission of most bioluminescence is in the same spectral region, although emission maxima at longer wavelengths do occur. Significantly, the bioluminescence emission spectrum is also often broader at longer wavelengths than the downwelling sunlight. Thus, short-wave-absorbing yellow lenses will remove more of the veiling background than the bioluminescence, enhancing the visibility of the light produced by the animals (Somiya 1976; Muntz 1976b; Douglas and Thorpe 1992).

7.4 Post-retinal Filters

7.4.1 Melanin

Open any optical device and you'll find it's coloured black on the inside to minimise reflection. Similarly, the inner surfaces of the posterior segment of the eye are usually coated by a continuous layer of melanin, found in the posterior epithelium of the iris, the outer epithelium of the ciliary body and the retinal pigment epithelium (RPE) and choroid underlying the retina. Any light that is not absorbed directly by the photoreceptors would be scattered by a reflective surface and reduce the quality of the image. Melanin prevents this.

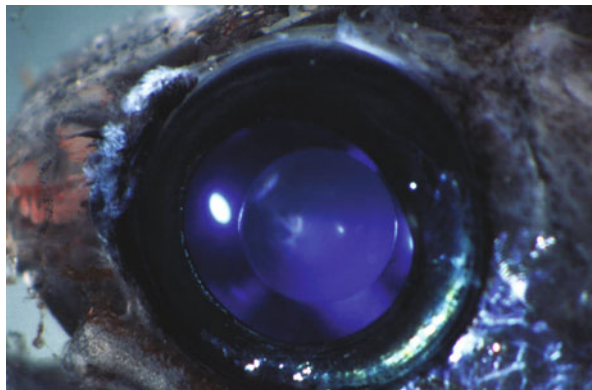
Ocular melanin is not at first sight an obvious filter, as no melanised structures interrupt the direct passage of light towards the photoreceptors, and it is a relatively non-selective spectral absorber. However, as it is a photostable pigment, it is 'cheap' to maintain and is therefore a cost-effective way of enhancing image quality, fulfilling the main criterion of a matched filter, reducing the energetic cost of visual processing.

7.4.2 Tapeta

Much light incident on the retina misses the photoreceptors, or the angle of incidence is so oblique that it is not absorbed. In diurnal animals the melanin within the RPE traps such light, which would otherwise degrade the image (see Sect. 7.4.1). Nocturnal animals, however, often sacrifice image quality to maximise photon capture. Consequently, many animals routinely active at low light levels have a reflective *tapetum lucidum* underlying the photoreceptors, giving photons that have passed through the retina a second chance of activating the rods. Such tapeta are widespread among vertebrates, but the location, structure and nature of the reflective material are varied (Walls 1963; Nicol 1981; Ollivier et al. 2004). Like teleost corneal pigmentation (see Sect. 7.3.1), tapetal reflection is often not uniform throughout the eye, being present to a greater degree in the dorsal retina. As the ventral retina receives the brighter light from above, there is less need to increase the sensitivity of this part of the retina. The dorsal part of the eye, on the other hand, receives dimmer illumination from below and would benefit from amplification of the signal.

Tapetal reflections, seen externally as 'eye shine', are sometimes broadband, appearing silver/white. If the wavelengths reflected are more restricted, tapeta are coloured. The wavelengths reflected sometimes relate to the spectrum of the environmental radiation, especially in fish, whose environment is spectrally diverse. For example, as both most bioluminescence and residual sunlight in the deep sea are restricted to blue part of the spectrum (Sect. 7.3.3), these are the only wavelengths reflected by the tapeta of most deep-sea fish (Fig. 7.4) (Douglas et al. 1998a). A striking exception is *Malacosteus niger*, whose long-wave-reflecting, astaxanthin-based tapetum (Somiya 1982; Bowmaker et al. 1988; Fig. 7.7a) matches the bathochromic shift of its visual pigments (Sect. 7.5.2). Unlike

Fig. 7.4 Tapetal reflection of a myctophid fish (Photo courtesy of N.J. Marshall)



seawater, much freshwater preferentially absorbs short wavelengths, so long wavelengths dominate. Thus, many freshwater fish also have tapeta that reflect this part of the spectrum (Wang and Nicol 1974). However, even among fish the correlation between spectral reflectance and environment is not always obvious (Douglas and Marshall 1999).

Tapeta of terrestrial animals also range widely in colour. However, since terrestrial environments tend to be spectrally similar, correlations between tapetal spectral reflectance and environmental illumination are rare. An exception may be the reindeer, whose tapetum is deep blue in winter, when the environment is dominated by short wavelengths due to atmospheric Rayleigh scattering and reflection from snow, and golden in the warmer light of summer (Stokkan et al. 2013).

Since a broadband-reflecting tapetum will always be more efficient for increasing photon capture than one reflecting only a limited wavelength range, why don't all tapeta reflect a wide span of wavelengths? Possibly, potential costs inherent in a broadband reflector are reduced in a spectrally more selective one. For tapeta consisting of multilayer stacks, the most efficient reflector is produced by a quarter-wave stack. This has reflectance values approaching 100 %, with relatively few layers, but has a narrow reflection bandwidth. Broadband, silver multilayer reflectors, in contrast, need more layers and have to be randomly organised to have high non-polarising reflectivity (Jordan et al. 2012).

7.5 Spectral Tuning Within Photoreceptors

Photoreceptors are composed of an outer segment containing the visual pigment connected to an inner segment by an eccentrically placed cilium. The inner segment is divided into the distal mitochondria-rich ellipsoid and a proximal myoid housing endoplasmic reticula. Internal to the inner segment, a cell body is connected to a process (axon) ending in a synaptic terminal. The following section considers filters within the outer and inner segments that could modify the spectral response of the photoreceptor.

7.5.1 Visual Pigments

One could argue that visual pigments are the original matched filters in eyes, as they respond more at some wavelengths than others (Fig. 7.2). As the likelihood of visual pigment isomerisation depends not only on the wavelength of the stimulating light but also on its brightness, the degree of hyperpolarisation of a single class of photoreceptor cannot be used as a basis for colour vision. For this an animal must have at least two types of spectrally distinct photoreceptors whose neurobiological output can be compared. Some vertebrates which live in relatively low-light environments, such as some bats, marine mammals, owl monkeys and fish, possess a single spectral class of rod and one type of cone, whose interaction may provide a rudimentary form of colour vision in mesopic conditions. The minimum requirement for true photopic colour vision is two distinct classes of cone. Such dichromacy occurs, for example, in most placental mammals and many coastal marine fish. Colour vision, based on three distinct cone pigments (trichromacy), occurs in some marsupials and primates and is common in fish and amphibia. However, many diurnal teleost fish, reptiles and birds express visual pigments based on at least four cone opsin genes and potentially have tetrachromatic colour vision (Fig. 7.2; Bowmaker 2008). On the other hand, the only photoreceptor of most deep-sea fish is a single spectral type of rod (Douglas et al. 1998a). Many whales also lack functional cone photoreceptors (Meredith et al. 2013). Such animals will not see colour.

Because visual pigments have absorption maxima that vary by nearly 300 nm in spectral placement (~360–630 nm), they seem ideal candidates for matched filtering. Changing the amino acid sequence of the opsin even slightly can produce major shifts in their spectral positioning, making them easy targets for evolutionary tuning. Much of the early research on characterising visual pigment spectra focused on the question of spectral matching (Lythgoe 1972, 1979; Cronin et al. 2014).

If visual pigments are matched filters for light stimuli, what should they be matched to? One possibility is coloured signals of other animals. Another is the spectral irradiance of the scene. However, the only natural spectra that present something obvious to ‘match’ are found at depth in water. Understanding visual pigment matches here is simple because most deep-sea fish have relatively simple retinas, and much early research considered spectral matching of visual pigments in fishes living at various depths (Douglas 2001). The general pattern is that spectral complexity of the retinas of fishes decreases as habitat depth increases. In the deep sea, only rods remain, and their maximal absorbance (Fig. 7.5) approximates the blue spacelight of mesopelagic waters and especially bioluminescent emission spectra (Turner et al. 2009).

Rod pigments in marine mammals also seem to match vision to the light at their depths of foraging. Thus, as species dive to increasing depths, the rods contain shorter-wavelength visual pigments (Fig. 7.6). Those marine mammals that have not abandoned cones completely (Meredith et al. 2013) have almost all discarded their blue-sensitive cones, leaving them only with green-sensitive ones. At present, there is no clear relationship between the cone sensitivity and environmental

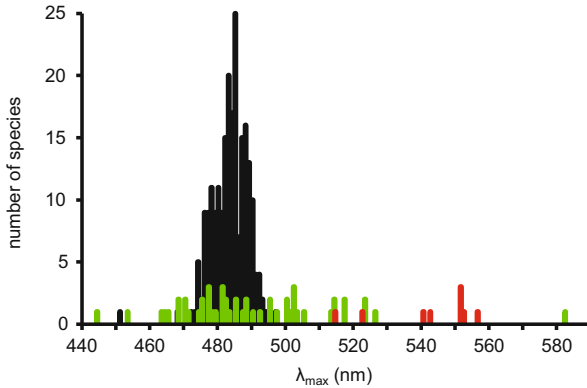


Fig. 7.5 Histogram to show peak absorbance wavelengths for the visual pigments in the rods of 248 species of deep-sea fish. Most species have only a single visual pigment in their retina, a rhodopsin peaking around 470–490 nm (shown in *black*). Twenty-nine have more than one visual pigment (rhodopsins are shown in *green* and porphyropsins in *red*)

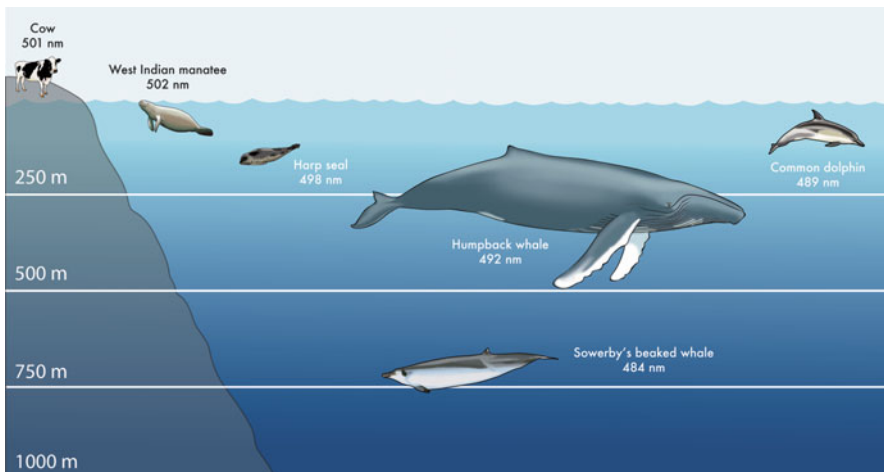


Fig. 7.6 Wavelength of maximum absorption of the visual pigments of various marine mammals foraging at different depths. The data are compared to the cow, a representative terrestrial vertebrate (Based on data from Fasick and Robinson 2000, drawn by E.L. Cronin)

shortwave radiation in these species. However, the coastal origins of their ancestors may help explain the apparent mismatch between cone visual pigments and the current light environment (Peichl et al. 2001).

When vertebrates left the water, they faced an entirely new world of light, one that is both very bright during the day and spectrally broad. There is no obvious way to ‘match’ such a spectrum. However, one class of stimuli might encourage matched filtering: the bright and often saturated colours of other animals or plants.

Even here, though, there is little sign of tuning of receptors to signals – with one major exception. These are bioluminescent signals, often the only light that is visible in nocturnal (or deep-sea) habitats. We saw above that deep-sea visual pigments are ideally matched to bioluminescent signals (Turner et al. 2009; see also Sect. 7.5.2). Fireflies also match vision to the expected spectra of the flashes of their conspecifics (Cronin et al. 2000). Unfortunately, no terrestrial vertebrate is bioluminescent.

7.5.2 A Unique Retinal Photosensitiser

Although most illumination in the deep sea, be it bioluminescence or dim downwelling sunlight, is short wavelength, there is one major exception: three genera of stomiid dragonfish produce far-red bioluminescence from photophores below their eyes in addition to conventional shortwave bioluminescence from post-orbital photophores (Fig. 7.7) (Denton et al. 1970, 1985; Widder et al. 1984). Although most deep-sea fish, with a single visual pigment absorbing maximally around 470–490 nm, will be sensitive to the shortwave bioluminescence (Fig. 7.7b), they will not see the red light. Dragonfish retinas, in contrast, contain several visual pigments that are long wave shifted compared to those of other deep-sea fish (Fig. 7.7b; Douglas et al. 1998a).

Although dragonfish visual pigments provide some of the best examples of pigments matched to a specific photic requirement, the coincidence of their absorption spectra and the far-red bioluminescence produced by these animals is far from perfect, especially in *Malacosteus*, whose visual pigments are less long wave shifted than those of the other two red light-producing dragonfish (Douglas et al. 1998a) (Fig. 7.7b). However, besides their visual pigments, *Malacosteus* rods contain photostable pigments absorbing strongly close to the red bioluminescent emission maximum (Bowmaker et al. 1988) (Fig. 7.7b). These are a mixture of derivatives of bacteriochlorophylls *c* and *d* and act as photosensitisers, absorbing the bioluminescence and indirectly activating the visual pigments (Douglas et al. 1998b, 1999).

The far-red light produced by the dragonfish suborbital photophores gives these stomiids a private part of the spectrum they can use for covert illumination of prey or secret intraspecific communication immune from detection by potential prey and predators alike. Interestingly, it appears that some myctophids, which form an important part of the dragonfish diet, may also have evolved both long-wave-shifted visual pigments and red-absorbing photosensitisers (Hasegawa et al. 2008; Douglas et al. 2002a, 2003; Turner et al. 2009).

7.5.3 Inner Segment Filters

The inner segments of many bird cones contain coloured oil droplets (Fig. 7.8a) composed of a variety of dietary-derived carotenoids (Hart 2001). Since these

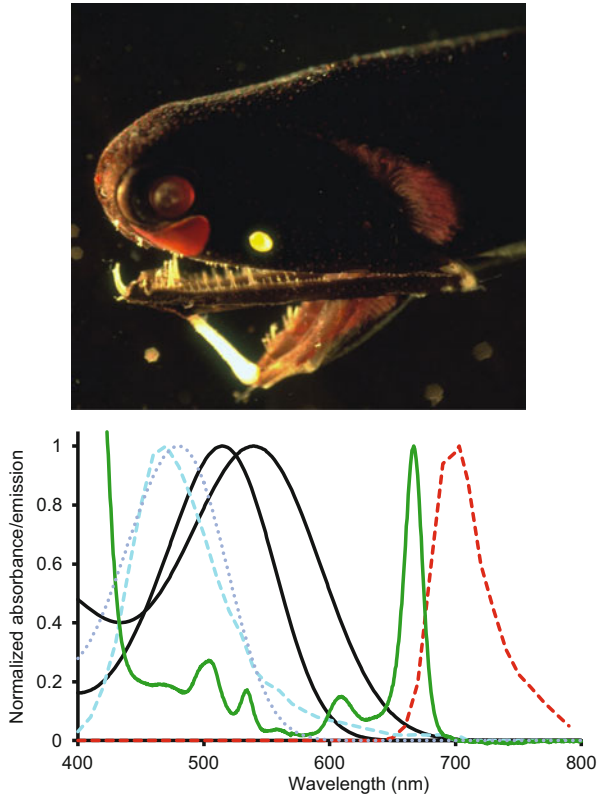
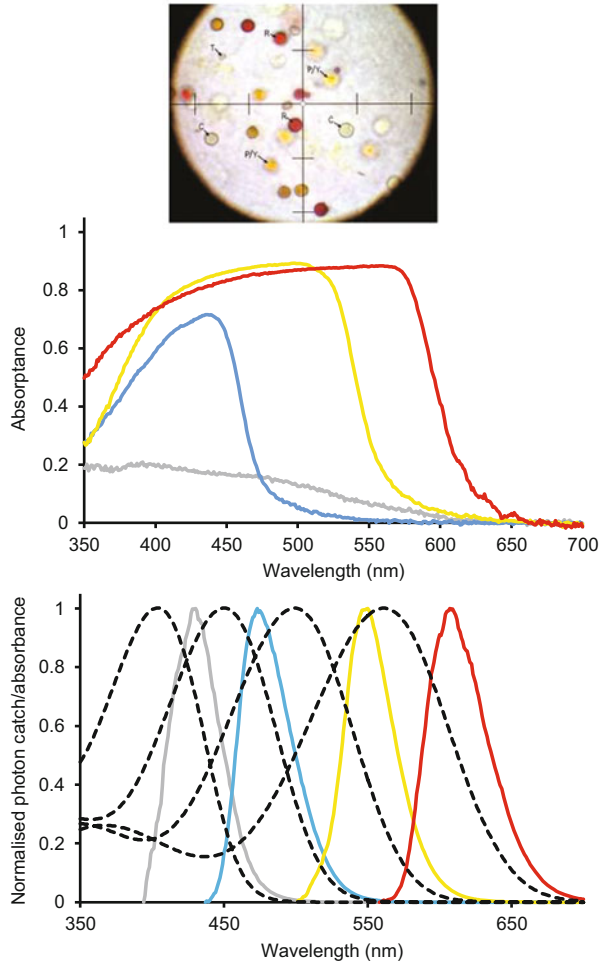


Fig. 7.7 Dragonfish retinal pigments. **(a)** *Malacosteus niger* showing the teardrop-shaped suborbital photophore that produces long-wave bioluminescence and the post-orbital photophore (yellow) that emits conventional short-wave bioluminescence (Photo courtesy of T. Frank). **(b)** The dashed lines represent the emission spectra of the blue- and red-emitting photophores. The dotted line shows the absorbance spectrum of a conventional deep-sea visual pigment maximally sensitive at 480 nm compared to which the *Malacosteus* visual pigments (black lines) are long wave shifted. A form of bacteriochlorophyll (green curve) acts as a 'photosensitiser' absorbing the red bioluminescence emitted by its suborbital photophore and activating the visual pigments (Data from Douglas et al. 1999)

pigments occur in high densities and are positioned between the incoming light and the photoreceptive outer segments, they filter out variable amounts of incoming light (Fig. 7.8b). Similar structures occur in some reptiles (Loew and Govardovskii 2001; Loew et al. 2002) and lungfish (Robinson 1994; Hart et al. 2008). Colourless droplets occur in a few other vertebrates. Coloured oil droplets are confined to diurnal species and are associated with retinæ containing several spectral cone types. Although structurally, biochemically and ontogenetically distinct from oil droplets, the inner segments of several vertebrate classes contain structures such as modified mitochondria and endoplasmic reticula that might also act as similar

Fig. 7.8 Whooping crane oil droplets and visual pigments. (a) Oil droplets seen through a microscope lens. (b) Baseline-corrected absorbance of the oil droplets found in single cones. From right to left these are red (R-type), yellow (Y-type), clear (C-type) and translucent (T-type). (c) The black dashed curves are templates of the normalised absorbance spectra of four cone visual pigments with peak absorption (λ_{\max}) values 404 nm, 450 nm, 499 nm and 561 nm. The coloured curves represent the calculated normalised spectral sensitivities of the four single cone types after filtering of light by the oil droplets within them. Such calculations assume the oil droplets act as cut-off filters for reasons described by Hart and Vorobyev (2005) (Original data from Porter et al. (2014))



selective filters (Bowmaker et al. 1991b; Collin et al. 2003; Lluch et al. 2003; Novalés-Flamarique and Hárosi 2000; Tarboush et al. 2014).

Many roles have been assigned to coloured oil droplets (Douglas and Marshall 1999). They may function, in part, in a manner analogous to other short-wave-absorbing filters to both protect the photoreceptors and enhance acuity (see Sect. 7.3.2). Unlike more distal, global filters, oil droplets filter light in individual photoreceptors. Since cones containing increasingly longer-wavelength-sensitive visual pigments usually have oil droplets removing more of the spectrum, each photoreceptor removes as much short-wavelength light as is practical. However, the most likely function of oil droplets is to enhance colour vision by modifying the spectral sensitivity of the photoreceptors.

Most birds have retinæ with four spectral classes of single cones (SWS1, SWS2, RH2 and LWS; see Sect. 7.5.1) (Hart 2001), thought to be involved in colour vision. These contain oil droplets that remove wavelengths below 350 nm (T-type), 399–449 nm (C-type), 505–516 nm (Y-type) and 552–586 nm (R-type), respectively (Hart and Vorobyev 2005). Oil droplets tune the sensitivity of the underlying visual pigments to longer wavelengths, narrowing the sensitivity function of the photoreceptor and reducing overlap with adjacent photoreceptor spectral types (Fig. 7.8c). This will significantly improve the discrimination of broadband reflectance spectra and may enhance colour constancy (Vorobyev 2003; Hart et al. 2008).

7.6 Optical Filters

As light emanating from an object can potentially travel in any direction, for it to be perceived as anything more than dim diffuse illumination, it must be focused back to a point on the light-sensitive retina. In terrestrial vertebrates, this is achieved by refraction of the light by the anterior curved surface of the cornea, whose refractive index is considerably higher than that of air. The lens, whose refractive index is similar to that of the surrounding humours, is usually relatively flattened and only responsible for adjusting the fine focus of the image. Underwater, however, the cornea is optically ineffective as its refractive index is very close to that of water, and virtually all refraction in aquatic species is achieved by a spherical, more powerful, lens.

7.6.1 Optical Imperfections

A perfect optical system would focus all light rays that emanate from a single object point back into a single point in the image. In reality, few optical systems are this good, and rays originating from a point will be focused as a larger blurred area (Land and Nilsson 2012).

Wave properties of light degrade image quality, causing scattering of light both within the atmosphere and in the eye itself. When light is refracted by the optical elements of the eye, the resulting image will also be subject to chromatic and spherical aberration. Longitudinal spherical aberration exists because light entering the eye near the margins of the lens is focused nearer the lens than light closer to the optic axis, creating a blur circle (Fig. 7.9a). Longitudinal chromatic aberration occurs because the refractive index of a substance varies with wavelength. Short wavelengths are refracted more strongly than longer ones and are focused closer to a lens, once more causing image blur if a range of wavelengths form the image (Fig. 7.9b right). Any adaptation that reduces these imperfections potentially saves costly neural processing.

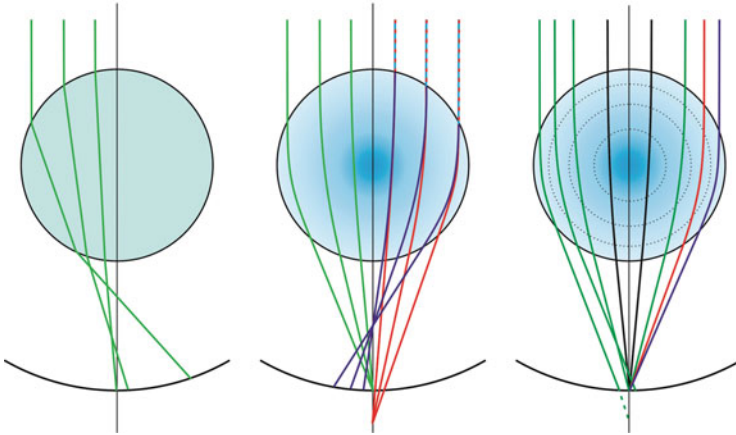


Fig. 7.9 Illustration of the optical function of different types of spherical lens. (a) A homogeneous lens suffers from longitudinal spherical aberration (LSA) as light passing through the periphery of the lens is focused closer to the lens than light close to the optical axis. (b) A gradient-index lens free of LSA focuses all light of the same wavelength (*green* in this example) on the retina. Because of longitudinal chromatic aberration (LCA), other wavelengths of light are focused at other distances from the lens. (c) A gradient-index multifocal fish lens has concentric zones of different focal lengths for monochromatic light (*green* is shown). A well-focused colour image is created on the retina despite the defocusing effect of LCA. Depth of focus is long for the central part of the lens, such that all wavelengths are in focus on the retina (*black lines*) (From Kröger 2013)

7.6.2 Image Focus

For a well-focused image, the dioptric power of the optical components of the eye must match the position of the light-sensitive retina. In an emmetropic eye, parallel light rays, like those coming from a distant object, are focused to a point on the retina. As an object approaches such an eye, its image will be focused progressively further behind the retina. However, the retina has a certain tolerance to blur, and the defocus will not be detected until the object is quite close. Thus, in an emmetropic eye, everything beyond a few metres is perceived as sharply focused. In a myopic (short-sighted) eye, parallel light rays entering the eye are focused in front of the retina, while in a long-sighted (hyperopic) eye, they are imaged behind the retina. Myopic eyes are thus focused for close objects, while in a hyperopic eye little is in focus. Once the hyperopic artefact of small eyes is accounted for (Glickstein and Millodot 1970), the majority of animals are, as logic would suggest, close to emmetropic, although some animals, such as fish living in turbid water and interested primarily in close objects, are probably myopic.

The above discussion assumes the optics of the eye are fixed. Thus, an object close to an emmetropic eye would appear blurred. To avoid this, the dioptric power of the eye of most vertebrates can be changed by the process of accommodation. Mammals focus closer objects by increasing the curvature of their lens indirectly,

birds and reptiles directly deform the lens (and some also change the curvature of the cornea), while fish and amphibia, respectively, move their more spherical lens backwards and forwards (Sivak 1980; Ott 2006).

Accommodative amplitude varies widely between species, depending on an animal's requirements for close vision. A rhinoceros, for example, is close to emmetropic and with limited accommodation can focus objects to only around 25–33 cm which, given the length of its nose, is sufficient (Howland et al. 1993). A chameleon, on the other hand, which catches nearby prey by shooting out its sticky tongue, can accommodate very quickly and accurately to focus on objects as close as 2 cm (Ott et al. 1998).

An asymmetric eye also has the potential to give an animal variable focus with the added advantage that it does not require active accommodation. For example, in some ground-foraging birds, the lower visual field is myopic, allowing them to keep their prey in focus, while an emmetropic upper visual field keeps a look out for distant predators (Hodos and Erichsen 1990). Similar 'lower-field myopia' has been observed in some amphibia (Schaeffel et al. 1994), flat fish (Sivak 1980) and reptiles (Henze et al. 2004). This is most easily achieved by a 'ramp retina' where the dorsal retina is further from the lens (making it myopic), while ventrally the retina is closer to the lens.

7.6.2.1 The Problem of Amphibious Vision

When we open our eyes underwater, the world appears blurred, as the refractive power of the cornea is lost and objects are focused behind the retina. Aquatic animals avoid such extreme hyperopia by having a more powerful, spherical, lens. Such animals would of course be very myopic in air. This presents an obvious problem for amphibious animals. Some are visually adapted for only one medium. Crocodiles, for example, are emmetropic in air but, like us, become very hyperopic underwater (Fleishman et al. 1988). However, many amphibious species do have a well-focused image in both air and water.

The simplest tactic for providing comparable underwater and aerial acuity is to have a powerful lens suitable for underwater vision while minimising the refractive capability of the cornea in air by either reducing its overall curvature or incorporating flattened facets (Dawson et al. 1987; Sivak et al. 1987, 1989; Hanke et al. 2006). An alternative strategy adopted by some aquatic mammals is to have a spherical lens whose refractive effects in air are minimised by the large depth of field afforded by a constricted pupil (Sivak 1980). Interestingly, humans may be able to do something analogous. The Moken are a nomadic tribe of sea gypsies whose children forage underwater, often without face masks. Their acuity underwater is about twice as good as that of untrained Europeans, a feat they achieve by maximal accommodation and constricting their pupils (Gislen et al. 2003, 2006).

Some amphibious animals manage the transition from air to water by having extreme accommodation in which a flattened soft lens adapted for aerial vision is forced through a toughened constricted pupil underwater, forming a highly refractive 'nipple' on its anterior surface. In this way, otters, sea lions, aquatic snakes,

turtles, and diving birds see well in both air and water (Sivak 1980; Sivak et al. 1985; Murphy et al. 1990; Katzir and Howland 2003).

A particularly severe optical challenge is faced by the ‘four-eyed’ fish, *Anableps anableps*, which spends most of its time at the water surface feeding off insects with half of each eye above the water and half beneath. It is able to see simultaneously in both media as its lens is ovoid and positioned such that light entering the eye from the air, and hence going through the refractive cornea, passes through the short axis of the lens and therefore is refracted less by the lens. Light from below the animal, passing through the optically ineffective cornea, goes through the lens’s more powerful long axis (Sivak 1980).

7.6.3 The Pupil as a ‘Matched Filter’

The pupil in most vertebrates constricts at higher light levels. In some species it also does so when viewing near objects and can be influenced by higher brain function. In teleost fish, contractile pupils are restricted to a few bottom-dwelling species (Douglas et al. 1998c, 2002b).

Varying the diameter of the pupil is most obviously a means of adjusting the degree of retinal illumination. However, the human pupil, for example, maximally changes area by a factor of 16, which alters retinal illumination by only 1.2 log units, much less than the total range of illumination used for vision (see Sect. 7.2.2). While a dilated pupil in low light levels obviously increases the degree of retinal illumination, a large pupillary aperture also results in significant amounts of spherical aberration (see Sect. 7.6.1) as most of the lens and cornea are used in image formation. In such scotopic conditions, spatial acuity is rarely an issue, as the rod system is being employed (see Sect. 7.2.2.1). However, in brighter light the cone system mediates higher spatial resolution (see Sect. 7.2.2.2) which will be aided by the smaller amounts of spherical aberration afforded by a constricted pupil. On the other hand, diffraction increases as the pupil constricts as does the depth of field, making the relationship between pupil size and acuity complex.

In most species the dilated pupil is more or less round, but often the light-adapted pupil consists of either a vertical or horizontal slit. The area of a round pupil is decreased by a sphincter muscle within the iris running around the pupillary margin. Due to spatial constraints, there is a limit to how small such a muscle can make the pupillary aperture. The muscles controlling a slit pupil can form a much smaller opening (Walls 1963). This is beneficial, as most animals with slit pupils are nocturnal and thus have a rod-dominated retina that needs greater protection from high light levels than that of a diurnal animal.

Crescent-shaped pupils occur in many, mainly bottom-dwelling, fish and are due to a dorsal operculum that covers the centre of the lens (Fig. 7.10b). Such an arrangement utilises only the outer portion of the lens, which should decrease longitudinal spherical aberration. By using the lens periphery, the visual field is enhanced compared to a central circular pupil of the same area (Murphy and Howland 1991). In fact, most fish lenses suffer little from longitudinal spherical

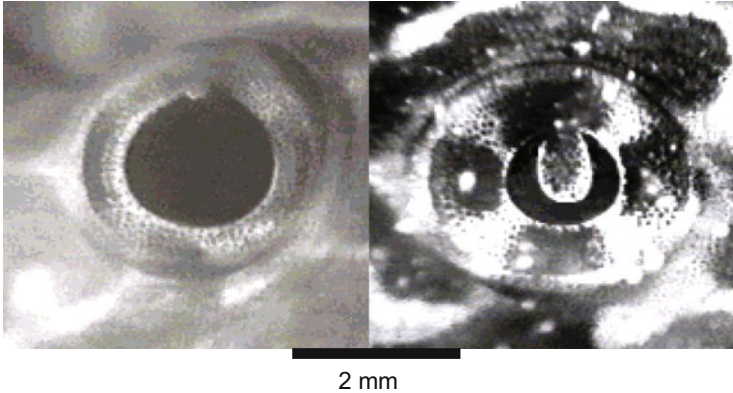


Fig. 7.10 Crescent-shaped pupils of an armoured catfish. Infrared video images of the eye (a) in the absence of any visible light and (b) after 60 min exposure to $5.6 \times 10^3 \mu\text{W}/\text{cm}^2$ white light (From Douglas et al. 2002b)

aberration (see Sect. 7.6.4), and the amount of such aberration in species with a crescent-shaped pupil is similar to that of species with immobile pupils (Sivak 1991; Douglas et al. 2002b). Therefore, pupillary constriction in bottom-dwelling fish probably serves a function unrelated to reducing aberration, such as disguising the pupil.

Finally, some constricted pupils, most notably those of geckos, take the form of two or more pinholes (Walls 1963; Murphy and Howland 1991). Although a single small pupil increases the depth of field, multiple pupillary apertures decrease the depth of field significantly, which is of value to animals with laterally placed eyes that use their accommodative system to judge object distance (Murphy and Howland 1991).

7.6.4 The Lens as a 'Matched Filter'

As we have seen above (Sect. 7.6.3), one way of reducing spherical aberration is to only use part of the lens by constricting the pupil. However, another approach is to 'design' a lens that minimises this optical defect. A lens with a homogenous refractive index will have significant longitudinal spherical aberration (see Sect. 7.6.1; Fig. 7.9a). As the lens in a fish's eye is its only refractive component and as the pupils of most species cannot constrict (see Sect. 7.6.3), the fish lens instead has a graded refractive index. Light passing through the low refractive index periphery is refracted less than light passing through the higher refractive index of the central lens, counteracting the spherical aberration induced by differences in surface curvature (Fig. 7.9b left) (Land and Nilsson 2012; Kröger 2013). Similar refractive index gradients occur in most vertebrate lenses.

Longitudinal spherical aberration can result at any refractive surface, not just the lens. Thus, the cornea is potentially also a source of such imperfections in terrestrial animals. The human cornea, for example, gets over this problem as the peripheral cornea is less steeply curved than more central regions.

The other major optical defect suffered by lenses is longitudinal chromatic aberration, where short wavelengths are focused closer to the lens than longer ones (Fig. 7.9b right) (see Sect. 7.6.1). This can potentially also be ‘filtered’ by the eye. As we have seen previously (see Sect. 7.3), short wavelengths can be absorbed by pigments in various ocular structures, removing the spectral region most prone to chromatic aberration. Some animals are also able to minimise the chromatic blur circle using multifocal lenses (Kröger et al. 1999), which are present in all vertebrate groups. Such lenses consist of concentric shells of differing refractive index. The outer low refractive index shell focuses short wavelengths on the retina, and inner shells focus progressively longer wavelengths (Fig. 7.9c right). The wavelengths brought to focus on the retina coincide very closely to the maximum sensitivity of the various cone types. The drawback of this arrangement is that there is a background of out-of-focus light that will reduce the overall contrast of the image (Fig. 7.9c left) (Kröger 2013).

7.7 Filtering of Spatial Properties of Visual Fields

Visual environments and the objects within them have characteristic spatial structures. Here, we consider adaptations to filter the spatial structure of the visual field, either fitting the visual world to overall geometrical properties of the environment or maximising visual effectiveness in particular directions of view.

7.7.1 Retinal Spatial Filters

Since vertebrate eyes operate like cameras with well-designed optics, the only way to improve the image is to work with the ‘film’, which in an eye is the retina. But no retina is like the uniform array of chemicals on a sheet of film or pixels in a digital sensor. Instead, variable numbers of sensing elements are devoted to regions of the image falling on different parts of the retina. As processing of visual information is probably a power function of the number of sensing units, it is biologically (and evolutionarily) impossible to manage a nervous system that can fully analyse all the available detail in a retinal image.

One way to improve spatial vision is to pack receptors more tightly on the retinal surface (see Sect. 7.2.2.2). Normally, rods and cones fully tile this surface, so the only way to increase receptor density is to make the outer segments thinner. Receptor densities increase in regions where high spatial acuity is required. Cones that occupy foveae of vertebrates are tiny, near the optical limit to how small a light-trapping device can become (Land and Nilsson 2012), while cones in other retinal regions tend to be thicker and interspersed with rods.

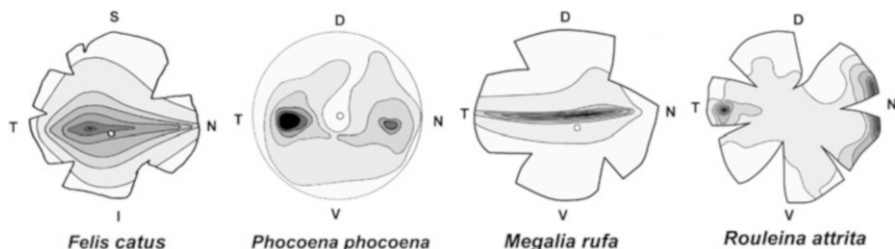


Fig. 7.11 Densities of ganglion cells on the surfaces of flattened retinas of several vertebrate species from different habitats. *S* superior, *I* inferior, *T* temporal, *N* nasal, *D* dorsal and *V* ventral. The empty circles are the location of the optic disk. Darker areas indicate regions of higher cell density, which implies more acute sampling of visual space (Images based on Land and Nilsson (2012), Mass et al. (1986), Collin (1999), and Wagner et al. (1998))

Most of the variation in spatial sampling in the retina, however, is due to the amount of convergence between photoreceptors and retinal ganglion cells. When vision must be acute, each receptor is linked ultimately to a single ganglion cell (Sect. 7.2.2.2) so that receptor size limits spatial acuity. But in locations where spatial acuity can be sacrificed with little fitness loss, convergence increases. This improves sensitivity (Sect. 7.2.2.1) while reducing neural traffic to the brain and the requirement for massive analytical power (and brain size).

Another way to increase receptor density is to increase retinal area locally by indenting the retinal surface, providing more surface on which to crowd receptors. This is usually accompanied by lateral shifts in the neural layers that overlie the receptors, decreasing light scattering within these layers, giving optical as well as geometrical benefits. The human fovea consists of only a shallow depression of the retinal surface. In many birds and reptiles, the ‘convexiculate’ foveal pit is much deeper, almost V-shaped, greatly expanding local retinal surface area. Counter-intuitively, the deep V does not preclude a sharp image at the receptor layer, because the pit acts like a local negative lens that spreads out the image and displaces it slightly. By such means, birds of prey can increase spatial resolution by factors of two or three over human limits.

Beyond the varying mosaic of receptor outer segments, the distributions of retinal ganglion cells determine retinal acuity – ganglion cells will be massed where convergence is low and will become spread out as increasing numbers of receptors feed into each ganglion cell. Contour maps of ganglion cell densities exist for many vertebrates (Collin 1999; Collin and Shand 2003), and these maps indicate how animals filter spatial information in the retinal image (Fig. 7.11).

Ganglion cell distributions fall into various patterns, often with strong local concentrations. Sometimes, high densities form tight patches called ‘areas’ which in contour plots look like bull’s-eyes, with increasing cell concentrations towards the centre. These are called *areae temporales*, *areae nasales* or *areae centrales* depending on where they lie on the retina. Retinas can have more than one such

area. The other extreme is for the regions of high concentration to be spread out linearly across the retina in a 'visual streak'.

The simplest pattern is a single area, located at the fovea and corresponding to the point of visual fixation. Animals with these must move their eyes or heads to inspect an object of visual significance. Such foveae occur in predators or in animals that must closely examine the terrain (generally the substrate) for food. They're also common in animals that move along a particular axis, such as flying birds or swimming fishes. These animals often have two foveae, one in the temporal retina receiving the image from directly ahead and a second nasally looking to the side. Visual streaks, on the other hand, occur in animals that survey a visual world with an extended horizon, such as mammals that graze on grasslands or fishes that swim near the substrate. They are particularly common in prey animals who must maintain vigilance for predators that approach in the plane of the horizon.

Examples of these types of retinal filters are illustrated in Fig. 7.11, where the various layouts give insight into the concerns of animals with each type of retina. The cat (*Felis catus*) has a slightly spread out visual streak with a tight fovea in its centre, appropriate for an animal that stalks along the ground with its head low, fixating on prey at eye level. Porpoises (*Phocoena phocoena*) have two areas, one temporally located to fixate prey and other objects ahead of them and a smaller and less dense one positioned laterally, perhaps to watch its fellows swimming alongside (Mass et al. 1986). Red kangaroos, *Megaleia rufa*, hop along the Australian plains and have the classic visual streak for visualising other animals and plants distributed throughout the horizontal plane (Collin 1999). The deep-sea fish, *Rouleina attrita*, is particularly interesting because it lives below depths to which sunlight can penetrate. One might expect it to have at best a retina diffusely populated with ganglion cells. Instead, it has a very tight convexiclvate temporal fovea densely packed with ganglion cells (Wagner et al. 1998). This is perfect for fixating the only visual stimulus available, compact bioluminescent points of light (see Sect. 7.3.3), facilitating the fish's forward-directed predatory lunges.

Animals that feed at (or even above) the water's surface must cope with the sudden change in refractive index when looking into air from water (see Sect. 7.6.2.1). The Asian killifish *Aplocheilus lineatus* specialises on food located in the surface layer. Its eyes (Fig. 7.12a) have two parallel visual streaks (Munk 1970). One inspects the visual field directly lateral to the fish. The other is displaced ventrally, intercepting light rays arriving from the edge of Snell's window (the cone of light 97.6° across that contains the refracted image of the aerial world above the water). The fish can thus see objects either above or below the water's surface in detail. It can even visualise any item that breaks the water's surface, seeing its lower parts with the central visual streak and its upper bits with the ventrally displaced one. Another surface feeder, the archerfish *Toxotes chatareus*, blasts insect prey off leaves above the water using an accurately aimed watery jet. To localise prey, it has to deal with the altered axis of light rays as they are refracted at the air-water boundary. Thus, its fovea examines the displaced images of aerial targets located at the preferred spitting angle (Temple et al. 2010). Their dense temporal fovea,

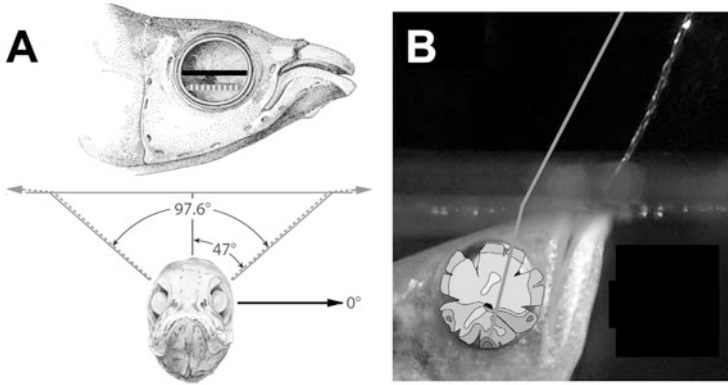


Fig. 7.12 Eyes of fishes living near the air-water interface. (a) *Aplocheilichthys lineatus*, a freshwater fish with two visual streaks, indicated by the horizontal solid and dashed lines in the drawing on the left (After Munk 1970; Wehner 1987). (b) A diagrammatic image of the retina of the archerfish (*Toxotes chatareus*) superimposed on a view of the fish itself engaged in spitting at insect prey. Darker regions of the retinal diagram indicate areas of higher densities of ganglion cells (After Temple et al. 2010)

placed slightly below the anterior-posterior axis of the eye, receives the refracted image of intended prey (Fig. 7.12b).

7.7.2 Optical Spatial Filters: Tubular Eyes

Tubular eyes of mesopelagic fishes are optically adapted to the light field. Their world is lit by a dim, symmetrical overhead patch of downwelling light against which predators, prey and conspecifics may be seen in silhouette. Eyes are energetically expensive, and big eyes – necessary for the sensitivity required to see dim light – are especially costly. The combination of a limited light field, the need for high sensitivity and the cost of a large eye has fostered the evolution of tubular eyes (Munk 1966; Lockett 1977; Collin et al. 1997; Figs. 7.3b and 7.13). These long, bullet-shaped eyes have lenses that are large for the eye's volume, and the visual fields of their main retinas are essentially matched to the downwelling light field.

Tubular eyes usually provide extended and relatively insensitive vision laterally, often with poor resolution. Most have an 'accessory retina' extending up the medial wall of the tube for lateral vision (Fig. 7.13a; Warrant et al. 2003), and additional modifications can extend vision further downward. The lateral 'lens pad' of scopolarchids, for example, guides light from up to 70° ventrally to the accessory retina (Fig. 7.13b, Warrant et al. 2003; Lockett 2000). The 'optical folds' of evermannellids serve a similar function. A few species extend their visual fields even further by having outpockets (diverticula) of their eyes' lateral walls that are lined with retina and have ventrolateral transparent 'windows' (Partridge et al. 2014). The ultimate structures found so far are mirror imaging systems in the diverticula of the

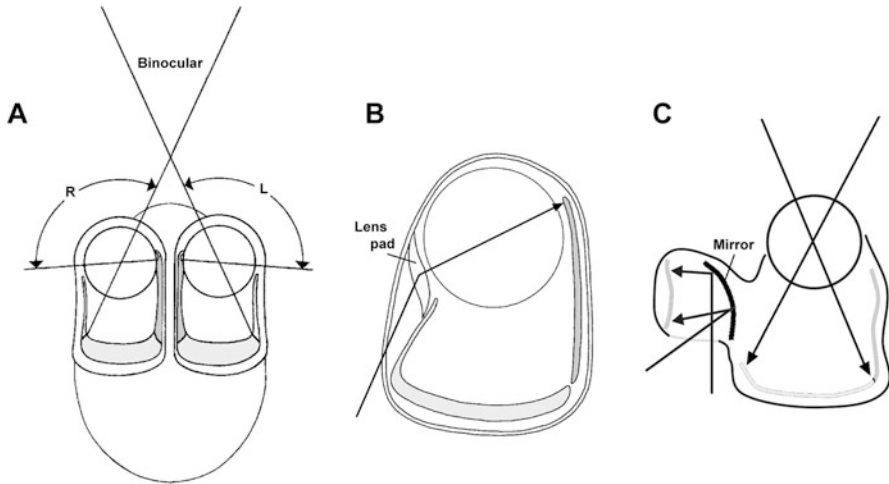


Fig. 7.13 Tubular eyes of mesopelagic (deep-sea) fishes. (a) Shows a typical tubular eye, with most of the well-focused visual field restricted to the region of the relatively brighter light directly above the fish, but with an unfocused region of medial retina (darker grey) looking to the side (After Warrant et al. 2003). (b) A lens pad, a wave-guiding structure that redirects ventral light to the medial retina (After Locket 2000). (c) Some spookfish use a reflective mirror situated in an outpocketing of the retina located lateral to the rest of the tubular eye (After Land 2009)

spookfish *Dolichopteryx longipes* (Wagner et al. 2009) and *Rhynchohyalus natalensis* (Partridge et al. 2014). The mirror forms a very well-resolved image, allowing not only the detection of ventral bioluminescence but also a fairly precise knowledge of its location (Fig. 7.13c).

7.8 Polarisation Filtering

7.8.1 Polarisation Sensing in Vertebrates

Invertebrate eyes often include polarisation-sensitive arrays matched to natural light polarisation patterns. In contrast, no vertebrate is known to have a matched polarisation filter. Nevertheless, many vertebrates are capable of detecting the polarisation properties of light and may filter natural polarisation fields.

Neither the sun nor the moon emits detectable polarised light, yet it is abundant in nature. This is because reflection or scattering often polarises light, which some vertebrates can detect. This is possible because all visual pigments are naturally dichroic, preferentially absorbing light that has its electric vector (e-vector) parallel to the axis of the conjugated tails of the chromophores of visual pigments. All that is necessary to make a photoreceptive cell polarisation sensitive is to align

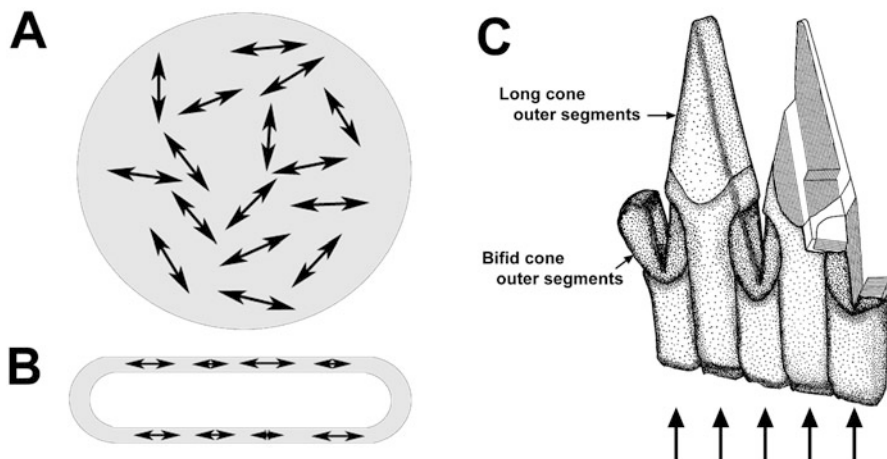


Fig. 7.14 Polarisation absorption in membranes of vertebrate photoreceptors. Schematic of absorption dipoles of chromophores of visual pigments in rod outer segment disk membranes. Cone outer segment lamellae would be similar, but the membranes would be a series of infoldings with the flat layers perpendicular to incoming light. (a) Surface view (seen from the direction that light reaches the membrane disk). The absorption dipoles are oriented randomly, with equal total absorption being independent of the e-vector orientation of incoming polarised light. (b) Lateral view. From this viewpoint, the absorption dipoles are all parallel to the plane of the membrane. If light were to enter laterally, the outer segment would be most sensitive to horizontally polarised light. (c) Diagrammatic view of cones in anchovy retinas. The *left* pair of cones is drawn to show the entire cone, while on the *right* the orientation of the cone outer segment lamellae are shown. The *large arrows* at the bottom suggest the direction of incoming light (Modified from Fineran and Nicol 1978)

chromophores of different visual pigment molecules so that they are parallel – a feat that both invertebrates and vertebrates achieve. In fact, rods and cones come by their polarisation sensitivity as an epiphenomenon of their membrane layout (Roberts et al. 2011).

Few vertebrates, however, physiologically respond to light's polarisation. Rods and cones are sensitive to polarisation only for laterally directed light, parallel to the membranes of the outer segments, but light almost always enters them axially, making its polarisation undetectable (Fig. 7.14a, b). Even when a physiological response seems to be present, polarisation artefacts are extremely easy to generate and extremely difficult to detect. Experimental outcomes – especially those that suggest behavioural responses to polarised light stimuli – are suspect and must be documented with a variety of experimental approaches. Despite all these caveats, behavioural responses to polarised light have been credibly reported in some vertebrates (Horváth and Varjú 2004).

7.8.2 Mechanisms of Detecting Polarisation

In anchovy retinas, the outer segment membranes of some cones are not arrayed perpendicular to incoming light, but instead tilted nearly vertically (Fineran and Nicol 1978). These cones best absorb light that is polarised with an e-vector parallel to the vertically extended sheets of the membrane. The anchovy retina has two types of cone whose outer segment membranes are perpendicular to each other (Fig. 7.14c). By comparing signals from the different cone types, anchovies can – in principle at least – partially analyse the polarisation of light.

Other than anchovies, no mechanism of polarisation detection has been demonstrated in vertebrate photoreceptors. Suggested mechanisms include lateral scattering of light into outer segments, internal reflections from inner segment membranes, effects of oil droplets, slightly tilted outer segment membranes, and other subtle optical phenomena (Roberts et al. 2011). Whether any of these operate in real eyes is unknown, as is whether any of these systems, including the orthogonal cones of anchovies, are organised on large scales to produce matched visual filters for polarisation.

7.8.3 Matched Filtering in a Bird Retina: Magnetic Compass Calibration

There is one possible (but unlikely) case of matched polarisation filtering in vertebrates. Birds are well known for their long-distance migrations, and many species use internal magnetic compasses to direct them. A magnetic compass by itself is unreliable, especially for long-range flights: local magnetic fields can vary unpredictably, and magnetic declination near the magnetic poles rapidly changes the apparent direction of true north or south. Also, the strength and polarity of the magnetic field change radically over evolutionary time, so a fixed compass eventually takes a species to extinction. Some, and perhaps most, birds evade all these problems by recalibrating their magnetic compasses daily against a reliable astronomical compass (Cochran et al. 2004). Songbirds apparently use polarisation patterns at sunset to recalibrate their magnetic compasses for the following day (Muheim 2011; Muheim et al. 2006; Phillips and Waldvogel 1988). In fact, their magnetic and polarisational compasses might be connected. The magnetic compass apparently involves photoreceptors that have both well-tuned spectral and magnetic sensitivities (Phillips et al. 2001, 2010). In birds, the sensing molecules could be cryptochromes in either retinal ganglion cells or other spatially distributed cell types in the retina. A system like this could represent the first proper matched filter for polarisation (and magnetic) sensing in any vertebrate.

7.9 Summary and Conclusions

Unlike invertebrates, which employ a seemingly limitless diversity of eye designs, and specialised remodelling within them, vertebrates all see using one fundamental anatomical and optical plan. With their large, competent brains, one might expect that vertebrates manage their visual filtering centrally. Yet there are numerous modifications to the basic vertebrate eye design that simplify visual information at the most peripheral levels and often serve to protect visual structures from light-induced damage. Such modifications reduce the costs of processing visual information and of maintaining a fully competent visual system. They include coloured pigments in otherwise transparent ocular structures, melanin, tapeta, features that combat optical aberrations in lens and cornea, variations in visual pigment spectral absorbance, regional specialisations in photoreceptor convergence onto ganglion cells and possibly adaptations to visualise polarised light. Vertebrate matched filters ultimately are a reflection of the flexibility afforded by a big brain and a sound basic optical plan. This flexibility exists between vertebrate classes, among species, and even over varying timescales within a single individual, giving vertebrates as a whole the ability to inhabit and see in any earthly habitat lit by at least a few photons.

References

- Beebe W (1935) *Half mile down*. The Bodley Head, London
- Bernstein PS, Khachik F, Carvalho LS, Muir GJ, Zhao D-Y, Katz NB (2001) Identification and quantitation of carotenoids and their metabolites in the tissues of the human eye. *Exp Eye Res* 72:215–223
- Bowmaker JK (2008) Evolution of vertebrate visual pigments. *Vis Res* 48:2022–2041
- Bowmaker JK, Dartnall HJA, Herring PJ (1988) Longwave-sensitive visual pigments in some deep sea fishes: segregation of ‘paired’ rhodopsins and porphyropsins. *J Comp Phys A* 163: 685–698
- Bowmaker JK, Thorpe A, Douglas RH (1991a) Ultraviolet-sensitive cones in the goldfish. *Vis Res* 31:349–352
- Bowmaker JK, Astell S, Hunt D, Mollon J (1991b) Photosensitive and photostable pigments in the retinæ of old world monkeys. *J Exp Biol* 156:1–19
- Carvalho LS, Knott B, Berg ML, Bennett ATD, Hunt DM (2011) Ultraviolet-sensitive vision in long-lived birds. *Proc R Soc Lond B* 278:107–114
- Clarke GL, Denton EJ (1962) Light and animal life. In: Hill MN (ed) *The sea*. Wiley, New York, pp 456–468
- Cochran WW, Mouritsen H, Wikelski M (2004) Migrating songbirds recalibrate their magnetic compasses daily from twilight cues. *Science* 304:405–408
- Collin SP (1999) Behavioural ecology and retinal cell topography. In: Archer SN, Djamgoz MBA, Loew ER, Partridge JC, Vallerga S (eds) *Adaptive mechanisms in the ecology of vision*. Kluwer Academic Publishers, Dordrecht, pp 509–535
- Collin SP, Shand J (2003) Retinal sampling and the visual field in fishes. In: Collin SP, Marshall NJ (eds) *Sensory processing in aquatic environments*. Springer, Berlin, pp p139–p169
- Collin SP, Hoskins RV, Partridge JC (1997) Tubular eyes of deep-sea fishes: a comparative study of retinal topography. *Brain Behav Evol* 50:335–357

- Collin SP, Hart NS, Shand J, Potter IC (2003) Morphology and spectral absorption characteristics of retinal photoreceptors in the southern hemisphere lamprey (*Geotria australis*). *Vis Neurosci* 20:119–130
- Collin SP, Davies WL, Hart NS, Hunt DM (2009) The evolution of early vertebrate photoreceptors. *Phil Trans R Soc Lond B* 364:2925–2940
- Cronin TW, Järvilehto M, Weckström M, Lall AB (2000) Tuning of photoreceptor spectral sensitivity in fireflies (Coleoptera: Lampyridae). *J Comp Phys A* 186:1–12
- Cronin TW, Johnsen S, Marshall NJ, Warrant EJ (2014) *Visual ecology*. Princeton University Press, Princeton
- Dawson WW, Schroeder JP, Sharpe SN (1987) Corneal surface properties of two marine mammal species. *Mar Mamm Sci* 3:186–197
- Denton EJ (1990) Light and vision at depths greater than 200m. In: Herring PJ, Campbell AK, Whitfield M, Maddock L (eds) *Light and life in the sea*. Cambridge University Press, Cambridge, pp 127–148
- Denton EJ, Gilpin-Brown JB, Wright PG (1970) On the ‘filters’ in the photophores of mesopelagic fish and on a fish emitting red light and especially sensitive to red light. *J Physiol Lond* 208: 72–73P
- Denton EJ, Herring PJ, Widder EA, Latz MF, Case JF (1985) The roles of filters in the photophores of oceanic animals and their relation to vision in the oceanic environment. *Proc R Soc Lond B* 225:63–97
- Douglas RH (1989) The spectral transmission of the lens and cornea of the brown trout (*Salmo trutta*) and goldfish (*Carassius auratus*) – effect of age and implications for ultraviolet vision. *Vision Res* 29(7):861–869
- Douglas RH (2001) The ecology of teleost fish visual pigments: a good example of sensory adaptation to the environment? In: Barth FG, Schmidt A (eds) *Ecology of sensing*. Springer, Berlin, pp 215–235
- Douglas RH, Jeffery G (2014) The spectral transmission of ocular media suggest ultraviolet sensitivity is widespread among mammals. *Proc R Soc Lond B* 281:20132995
- Douglas RH, Marshall NJ (1999) A review of vertebrate and invertebrate ocular filters. In: Archer SN, Djamgoz MBA, Loew ER, Partridge JC, Vallerga S (eds) *Adaptive mechanisms in the ecology of vision*. Kluwer Academic Publishers, Dordrecht, pp 95–162
- Douglas RH, Thorpe A (1992) Short wave absorbing pigments in the ocular lenses of deep-sea teleosts. *J Mar Biol Assoc UK* 72:93–112
- Douglas RH, Partridge JC, Marshall NJ (1998a) The eyes of deep-sea fish I: lens pigmentation, tapeta and visual pigments. *Prog Retin Eye Res* 17:597–636
- Douglas RH, Partridge JC, Dulai K, Hunt D, Mullineaux CW, Tauber A, Hynninen PH (1998b) Dragon fish see using chlorophyll. *Nature* 393:423–424
- Douglas RH, Harper RD, Case JF (1998c) The pupil response of a teleost fish, *Porichthys notatus*: description and comparison to other species. *Vis Res* 38:2697–2710
- Douglas RH, Partridge JC, Dulai KS, Hunt DM, Mullineaux CW, Hynninen PH (1999) Enhanced retinal longwave sensitivity using a chlorophyll-derived photosensitiser in *Malacosteus niger*, a deep-sea dragon fish with far red bioluminescence. *Vis Res* 39:2817–2832
- Douglas RH, Bowmaker JK, Mullineaux CW (2002a) A possible retinal longwave detecting system in a myctophid fish without far-red bioluminescence; evidence for a sensory arms race in the deep-sea. In: Stanley PE, Kricka LJ (eds) *Bioluminescence and chemiluminescence; progress and current applications*. World Scientific, River Edge, pp 391–394
- Douglas RH, Collin SP, Corrigan J (2002b) The eyes of suckermouth armoured catfish (Loricariidae, subfamily Hypostomus): pupil response, lenticular longitudinal spherical aberration and retinal topography. *J Exp Biol* 205:3425–3433
- Douglas RH, Hunt DM, Bowmaker JK (2003) Spectral sensitivity tuning in the deep-sea. In: Collin SP, Marshall NJ (eds) *Sensory processing in aquatic environments*. Springer, New York, pp 323–342
- Ellingson JM, Fleishman LJ, Loew ER (1995) Visual pigments and spectral sensitivity of the diurnal gecko *Gonotodes albogularis*. *J Comp Phys A* 177:559–567

- Fasick JL, Robison PR (2000) Spectral-tuning mechanisms of marine mammal rhodopsins and correlations with foraging depth. *Vis Neurosci* 17:781–788
- Fineran BA, Nichol JAC (1978) Studies on the photoreceptors of *Anchoa mitchilli* and *A. hepsetus* (Engraulidae) with particular reference to the cones. *Phil Trans R Soc Lond B* 283:25–60
- Fleishman LJ, Howland HC, Howland MJ, Rand AS, Davenport ML (1988) Crocodiles don't focus underwater. *J Comp Phys A* 163:441–443
- Gislen A, Dacke M, Kröger RHH, Abrahamsson M, Nilsson DE, Warrant EJ (2003) Superior underwater vision in a human population of sea gypsies. *Curr Biol* 13:33–836
- Gislen A, Warrant EJ, Dacke M, Kröger RHH (2006) Visual training improves underwater vision in children. *Vis Res* 48:3443–3450
- Glickstein M, Millodot M (1970) Retinoscopy and eye size. *Science* 168:605–606
- Haddock SHD, Moline MA, Case JF (2010) Bioluminescence in the sea. *Ann Rev Mar Sci* 2: 443–493
- Hanke FD, Dehnhardt G, Schaeffel F, Hanke W (2006) Corneal topography, refractive state, and accommodation in harbour seals (*Phoca vitulina*). *Vis Res* 46:837–847
- Hart NS (2001) The visual ecology of avian photoreceptors. *Prog Retin Eye Res* 20:675–703
- Hart NS, Vorobyev M (2005) Modelling oil droplet absorption spectra and spectral sensitivities of bird cone photoreceptors. *J Comp Phys A* 191:381–392
- Hart NS, Bailes HJ, Vorobyev M, Marshall NJ, Collin SP (2008) Visual ecology of the Australian lungfish (*Neoceratodus forsteri*). *BMC Ecol* 8:21. doi:10.1186/1472-6785-8-21
- Hasegawa E, Sawada K, Abe K, Watanabe K, Uchikawa K, Okazaki Y, Toyama M, Douglas RH (2008) The visual pigments of a deep-sea myctophid fish *Myctophum nitidulum* (Garman); an HPLC and spectroscopic description of a non-paired rhodopsin–porphyropsin system. *J Fish Biol* 72:937–945
- Henze MJ, Shaeffel F, Ott M (2004) Variations in the off-axis refractive state in the eye of the Vietnamese leaf turtle (*Geoemyda spengleri*). *J Comp Phys A* 190:131–137
- Hodos W, Erichsen JT (1990) Lower-field myopia in birds: an adaptation that keeps the ground in focus. *Vis Res* 30:653–657
- Hogg C, Neveu M, Stokkan K-A, Folkow L, Cottril P, Douglas RH, Hunt DM, Jeffery G (2011) Arctic reindeer extend their visual range into the ultraviolet. *J Exp Biol* 214:2014–2019
- Horváth G, Varjú D (2004) Polarized light in animal vision. Springer, Berlin
- Howland HC, Howland M, Murphy CJ (1993) Refractive state of the rhinoceros. *Vis Res* 33: 2649–2651
- Jordan TM, Roberts NW, Partridge JC (2012) An omnidirectional broadband mirror design inspired by biological multilayer reflectors. *Proc SPIE* 8339:83390G
- Katzir G, Howland HC (2003) Corneal power and underwater accommodation in great cormorants (*Phalacrocorax carbo sinensis*). *J Exp Biol* 206:833–841
- Kondrashev SL (2008) Long-wave sensitivity in the masked greenling (*Hexagrammos octogrammus*), a shallow-water marine fish. *Vis Res* 48:2269–2274
- Kröger RHH (2013) Optical plasticity in fish lenses. *Prog Retin Eye Res* 34:78–88
- Kröger RHH, Campbell MCW, Fernald RD, Wagner HJ (1999) Multifocal lenses compensate for chromatic defocus in vertebrate eyes. *J Comp Phys A* 184:36–369
- Lamb TD, Pugh EN (2004) Dark adaptation and the retinoid cycle of vision. *Prog Retin Eye Res* 23:307–380
- Land MF (2009) Biological optics: deep reflections. *Curr Biol* 19:R78–R80
- Land MF, Nilsson D-E (2012) Animal eyes, 2nd edn. Oxford University Press, Oxford
- Lind O, Mitkus M, Olsson P, Kelber A (2014) Ultraviolet vision in birds: the importance of transparent eye media. *Proc R Soc Lond B* 281:20132209
- Lluch S, Lopez-Fuster MJ, Ventura J (2003) Giant mitochondria in the retina cone inner segments of shrews of genus *Sorex* (Insectivora, Soricidae). *Anat Rec Part A* 272A:484–490
- Locket NA (1977) Adaptations to the deep-sea environment. In: Crescitelli F (ed) Handbook of sensory physiology VII/5; the visual system of vertebrates. Springer, New York, pp 67–192

- Locket NA (2000) On the lens pad of *Benthalbella infans*, a scopolarchid deep-sea teleost. *Phil Trans R Soc Lond B* 355:1167–1169
- Loew ER, Govardovskii VI (2001) Photoreceptors and visual pigments in the red-eared turtle, *Trachemys scripta elegans*. *Vis Neurosci* 18:753–757
- Loew ER, Fleishman LJ, Foster RG, Provencio I (2002) Visual pigments and oil droplets in diurnal lizards: a comparative study of Caribbean anoles. *J Exp Biol* 205:927–938
- Losey GS, McFarland WN, Loew ER, Zamzow JP, Nelson PA, Marshall NJ (2003) Visual biology of Hawaiian coral reef fishes. 1. Ocular transmission and visual pigments. *Copeia* 2003: 433–454
- Lythgoe JN (1971) Iridescent corneas in fish. *Nature* 233:205–207
- Lythgoe JN (1972) The adaptation of visual pigments to the photic environment. In: Dartnall HJA (ed) *Handbook of sensory physiology VII/1; photochemistry of vision*. Springer, Berlin, pp 566–624
- Lythgoe JN (1979) *The ecology of vision*. Clarendon Press, Oxford
- Mass AM, Supin AY, Severtov AN (1986) Topographic representation of sizes and density of ganglion cells in the retina of a Porpoise, *Phocoena phocoena*. *Aquat Mamm* 12:95–102
- Meredith RW, Gatesy J, Emerling CA, York VM, Springer MS (2013) Rod monochromacy and the evolution of cetacean retinal opsins. *PLoS Genet* 9:e1003432
- Muheim R (2011) Behavioural and physiological mechanisms of polarized light sensitivity in birds. *Phil Trans R Soc Lond B* 366:763–771
- Muheim R, Phillips JB, Akesson S (2006) Polarized light cues underlie compass calibration in migratory songbirds. *Science* 313:837–839
- Munk O (1966) Ocular anatomy of some deep-sea teleosts. *Dana Rep* 70:1–71
- Munk O (1970) On the occurrence and significance of horizontal band-shaped retinal areas in teleosts. *Vidensk Medd Dan Naturhist Foren* 133:85–120
- Muntz WRA (1976a) The visual consequences of yellow filtering pigments. In: Evans GC, Bainbridge R, Rackham O (eds) *Light as an ecological factor: II*. Blackwell Scientific Publications, Oxford, pp 271–287
- Muntz WRA (1976b) On yellow lenses in mesopelagic animals. *J Mar Biol Assoc UK* 56:963–976
- Murphy CJ, Howland HC (1991) The functional significance of crescent-shaped pupils and multiple pupillary apertures. *J Exp Zool Suppl* 5:22–28
- Murphy CJ, Bellhorn RW, Williams T, Burns MS, Schaeffel F, Howland HC (1990) Refractive state, ocular anatomy, and accommodative range of the sea otter (*Enhydra lutris*). *Vis Res* 30: 23–32
- Nelson PA, Zamzow JP, Losey GS (2001) Ultraviolet blocking in the ocular humors of the teleost fish *Acanthocybium solandri* (Scombridae). *Can J Zool* 79:1714–1718
- Nicol JAC (1981) Tapeta lucida of vertebrates. In: Enoch JM, Tobey FL (eds) *Vertebrate photo-receptor optics*. Springer, Berlin, pp 401–431
- Novales-Flamarique I, Hárosi F (2000) Photoreceptors, visual pigments, and ellipsosomes in the killifish, *Fundulus heteroclitus*: a microspectrophotometric and histological study. *Vis Neurosci* 17:403–420
- Ollivier FJ, Samuelson DA, Brooks DE, Lewis PA, Kallberg ME, Komáromy AM (2004) Comparative morphology of the tapetum lucidum (among selected species). *Vet Ophthalmol* 7:11–22
- Ott M (2006) Visual accommodation in vertebrates: mechanisms, physiological response and stimuli. *J Comp Phys A* 192:97–111
- Ott M, Schaeffel F, Krimse W (1998) Binocular vision and accommodation in prey-catching chameleons. *J Comp Phys A* 182:319–330
- Partridge JC, Douglas RH, Marshall NJ, Chung W-S, Jordan TM, Wagner HJ (2014) Reflecting optics in the diverticular eye of a deep-sea barreleye fish (*Rhynchohyalus natalensis*). *Proc R Soc Lond B* 281:20133223
- Peichl L, Behrmann G, Kröger RHH (2001) For whales and seals the ocean is not blue: a visual pigment loss in marine mammals. *Eur J Neurosci* 13:1520–1528

- Perlman I, Normann A (1998) Light adaptation and sensitivity controlling mechanisms in vertebrate photoreceptors. *Prog Retin Eye Res* 17:523–563
- Phillips JB, Waldvogel JA (1988) Celestial polarized patterns as a calibration reference for sun compass of homing pigeons. *J Theor Biol* 131:55–67
- Phillips JB, Deutschlander ME, Freaque MJ, Borland SC (2001) The role of extraocular photoreceptors in newt magnetic compass orientation: parallels between light-dependent magnetoreception and polarized light detection. *J Exp Biol* 204:2543–2552
- Phillips JB, Muheim R, Jorge PE (2010) A behavioral perspective on the biophysics of the light-dependent magnetic compass: a link between directional and spatial perception? *J Exp Biol* 213:3247–3255
- Porter ML, McCready R, Kingston A, Cameron E, Hofmann C, Suarez L, Olsen GH, Cronin TW, Robinson PR (2014) Visual pigments, oil droplets, lens, and cornea characterization in the whooping crane (*Grus americana*). *J Exp Biol* 217:3883–3890
- Quiroga RQ, Reddy L, Kreiman G, Koch C, Fried I (2005) Invariant visual representation by single neurons in the human brain. *Nature* 435:1102–1107
- Roberts NW, Porter ML, Cronin TW (2011) The molecular basis of mechanisms underlying polarization vision. *Phil Trans R Soc Lond B* 366:627–637
- Robinson SR (1994) Early vertebrate colour vision. *Nature* 367:121
- Schaeffel F, Hagel G, Eikermann J, Collett T (1994) Lower-field myopia and astigmatism in amphibians and chickens. *J Opt Soc Am A* 11:487–497
- Siebeck UE, Marshall NJ (2000) Transmission of ocular media in labrid fishes. *Phil Trans R Soc Lond B* 355:1257–1261
- Siebeck UE, Marshall NJ (2001) Ocular media transmission of coral reef fish – can coral reef fish see ultraviolet light? *Vis Res* 41:133–149
- Siebeck UE, Collin SP, Ghodduzi M, Marshall NJ (2003) Occlusable corneas in toadfishes: light transmission, movement and ultrastructure of pigment during light- and dark-adaptation. *J Exp Biol* 206:2177–2190
- Sivak JG (1980) Accommodation in vertebrates. In: Zadunaisky JA, Davson H (eds) *Current topics in eye research*. Academic, New York, pp p281–p330
- Sivak JG (1991) Elasmobranch visual optics. *J Exp Zool Suppl* 5:13–21
- Sivak JG, Hildebrand T, Lebert C (1985) Magnitude and rate of accommodation in diving and nondiving birds. *Vis Res* 25:925–933
- Sivak J, Howland HC, McGill-Harelstad P (1987) Vision in the Humboldt penguin (*Spheniscus humboldti*) in air and water. *Proc R Soc Lond B* 229:467–472
- Sivak JG, Howland HC, West J, Weerheim J (1989) The eye of the hooded seal, *Cystophora cristata*, in air and water. *J Comp Phys A* 165:771–777
- Solovei I, Kreysing M, Lancot C, Kosem S, Peichl L, Cremer T, Guck J, Joffe B (2009) Nuclear architecture of rod photoreceptor cells adapts to vision in mammalian evolution. *Cell* 137:356–368
- Somiya H (1976) Functional significance of the yellow lens in the eyes of *Argyropelecus affinis*. *Mar Biol* 34:93–99
- Somiya H (1982) “Yellow lens” eyes of a stomiatoid deep-sea fish *Malacosteus niger*. *Proc R Soc Lond B* 215:481–489
- Stokkan K-A, Folkow L, Dukes J, Neveu M, Hogg C, Siefken S, Dakin SC, Jeffery G (2013) Shifting mirrors: adaptive changes in retinal reflections to winter darkness in Arctic reindeer. *Proc Roy Soc Lond B* 280:20132451
- Tarboush R, Novales-Flamarique I, Chapman GB, Connaughton VP (2014) Variability in mitochondria of zebrafish photoreceptor ellipsoids. *Vis Neurosci* 31:11–23
- Temple S, Hart NS, Marshall NJ, Collin SP (2010) A spitting image: specializations in archerfish eyes for vision at the interface between air and water. *Proc R Soc Lond B* 277:2607–2615
- Thorpe A, Douglas RH, Truscott RJW (1993) Spectral transmission and short-wave absorbing pigments in the fish lens. I Phylogenetic distribution and identity. *Vis Res* 33:289–300

- Turner JR, White EM, Collins MA, Partridge JC, Douglas RH (2009) Vision in lanternfish (Myctophidae): adaptations for viewing bioluminescence in the deep-sea. *Deep-Sea Res Pt I* 56:1003–1017
- Tyler NJC, Jeffery G, Hogg CR, Stokkan K-A (2014) Ultraviolet vision may enhance the ability of reindeer to discriminate plants in snow. *Arctic* 67:159–166
- van Norren D, Gorgels TGMF (2011) The action spectrum of photochemical damage to the retina: a review of monochromatic threshold data. *Photochem Photobiol* 87:747–753
- Vorobyev M (2003) Coloured oil droplets enhance colour discrimination. *Proc R Soc Lond B* 270:1255–1261
- Wagner HJ, Fröhlich E, Negishi K, Collin SP (1998) The eyes of deep-sea fishes II functional morphology of the retina. *Prog Retin Eye Res* 17:637–685
- Wagner HJ, Douglas RH, Frank TM, Roberts NW, Partridge JC (2009) A novel vertebrate eye using both reflective and refractive optics. *Curr Biol* 19:108–114
- Walls GL (1931) The occurrence of coloured lenses in the eyes of snakes and squirrels, and their probable significance. *Copeia* 1931:125–127
- Walls GL (1963) *The vertebrate eye and its adaptive radiation*. Hafner Publishing Co, New York
- Wang RT, Nicol JAC (1974) The tapetum lucidum of gars (Lepisosteidae) and its role as a reflector. *Can J Zool* 52:1523–1530
- Warrant EJ, Collin SP, Lockett NA (2003) Eye design and vision in deep-sea fishes. In: Collin SP, Marshall NJ (eds) *Sensory processing in aquatic environments*. Springer, New York, pp 303–322
- Wehner R (1987) ‘Matched filters’ – neural models of the external world. *J Comp Physiol A* 161:511–531
- Whitehead AJ, Mares JA, Danis RP (2006) Macular pigment: a review of current knowledge. *Arch Ophthalmol* 124:1038–1045
- Widder EA (2010) Bioluminescence in the ocean: origins of biological, chemical and ecological diversity. *Science* 328:704–708
- Widder EA, Latz MI, Herring PJ, Case JF (1984) Far red bioluminescence from two deep-sea fishes. *Science* 225:512–514

Part IV

Infrared-Perception

Matched Filter Properties of Infrared Receptors Used for Fire and Heat Detection in Insects

Helmut Schmitz, Anke Schmitz, and Erik S. Schneider

Contents

8.1	Nature and Perception of Infrared Radiation	208
8.2	IR Receptors in the Animal Kingdom	211
8.3	Advantages of Detecting Forest Fires by IR Radiation	212
8.4	Diversity of IR Receptors in Pyrophilous Insects: An Overview	214
8.4.1	The “Little Ash Beetle” <i>Acanthocnemus nigricans</i>	215
8.4.2	IR Receptors in <i>Merimna atrata</i>	218
8.4.3	IR Receptors in Pyrophilous <i>Melanophila</i> Beetles	221
8.4.4	IR Receptors in Pyrophilous <i>Aradus</i> Bugs	224
8.5	The Development of IR Receptors in Pyrophilous Insects	228
8.6	Matched Filters Permit the Best Possible Function of IR Receptors in Pyrophilous Insects	229
	References	230

Abstract

About 25 insect species are attracted by forest fires and thus can be found on freshly burnt areas after fires. In three genera of pyrophilous beetles and one genus of pyrophilous bugs, infrared (IR) receptors have been discovered. From a technical point of view, insect IR receptors can be classified into two classes: bolometer-like sensors innervated by thermoreceptors and so-called photomechanic sensors which are innervated by mechanoreceptors. Despite of their different functional principles, insect IR receptors all show the same built-in filter properties. Remarkably, these filters were already preset by the absorption spectra of the gases in the atmosphere and the chemical composition of the insect cuticle. The atmospheric windows can be regarded as valuable filters (Filter 1) because emission maxima of relevant IR sources like fires or warm-

H. Schmitz (✉) • A. Schmitz • E.S. Schneider
Institute for Zoology, Rheinische Friedrich-Wilhelms-University Bonn, Bonn, Germany
e-mail: h.schmitz@uni-bonn.de

blooded creatures are located within the MW(mid-wavelength)IR and LW(long wavelength)IR windows. Filter 2 is given by cuticular absorption. Insect cuticle can be regarded as a composite material consisting of biopolymers that show strong IR absorption bands in the MWIR. Because both filters perfectly match, an IR-sensitive pyrophilous insect is able to efficiently sense MWIR radiation emitted by a forest fire. Thus, filters could be used without further modifications enabling the underlying sensory cells to perceive a maximum of temperature increase and/or thermal expansion.

8.1 Nature and Perception of Infrared Radiation


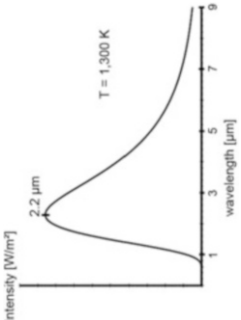


Independent from its condition of aggregation, every matter with a temperature above the absolute zero point emits electromagnetic radiation. This is caused by molecular movements starting above 0 K. In the context of this chapter, electromagnetic radiation significant for living organisms is considered. Here, the upper limit is represented by the surface temperature of sun at 5,800 K, the lower limit by objects at ambient temperature (cf. Table 8.1). Thus, under normal conditions, organisms are primarily subjected to a radiation spectrum ranging from high-level *ultraviolet* (UV) down to low-energy *infrared* (IR) radiation (Fig. 8.1). The spectral distribution of the radiation emitted, e.g., by a high-intensity forest fire with a temperature of 1,300 K, can be calculated according to Planck's radiation law (on the right in Table 8.1). At a given temperature, the wavelength at which most of the radiant energy is emitted (λ_{\max}) can be easily calculated by the law of Wien:

$$\lambda_{\max} = \frac{2,897.8 [\mu\text{m}\cdot\text{K}]}{T[\text{K}]}$$

where T is the absolute temperature given in Kelvin [K]. Temperatures and values for λ_{\max} are given in Table 8.1 for the sun, fires at high and low intensities, and a mouse.

For the perception of radiation in the mentioned wavelength range, the photon energy is of special importance. When trying to detect an object by electromagnetic radiation (either emitted or reflected by the object), an appropriate sensor should have its highest sensitivity at λ_{\max} of the radiation source. This is realized in, e.g., human photoreceptors, where the rhodopsin of the light-sensitive rods enabling scotopic vision exhibits its λ_{\max} at about 0.5 μm (Schoenlein et al. 1991; Bowmaker and Hunt 2006), perfectly matching the emission maximum of the sun (cf. Table 8.1). In general, the spectral sensitivity of photopigments is determined by the interaction of retinal with specific amino acids lining the ligand-binding pocket within the opsin (Bowmaker and Hunt 2006). Thus, the ability to see in the IR requires pigments showing sufficient absorption (i) in the *near infrared* (NIR, 0.75–1.4 μm (D'Amico et al. 2008)), (ii) in the *mid-wavelength infrared* (MWIR, 3–8 μm), or (iii) even in the *long wavelength infrared* (LWIR, 8–15 μm ; Fig. 8.1).

Table 8.1 Characteristics of different thermal sources in view of emission of electromagnetic radiation

Source	T [K]	λ_{max} [μm]	Total energy emitted per m^2 (assuming an emissivity of 0.98)	Photon energy (1 photon)	Spectral distribution of radiation intensity emitted from a high intensity forest fire according to Planck's radiation law
 Sun	5,800	0.5	62.89 MW	398 zJ 2.5 eV	
 Fire	High int. 1,300 800 low int.	2.2 3.6	159 KW 22.8 KW	90 zJ (0.6 eV) 55 zJ (0.3 eV)	
 Mouse	310	9.3	450 W	21 zJ (0.1 eV)	

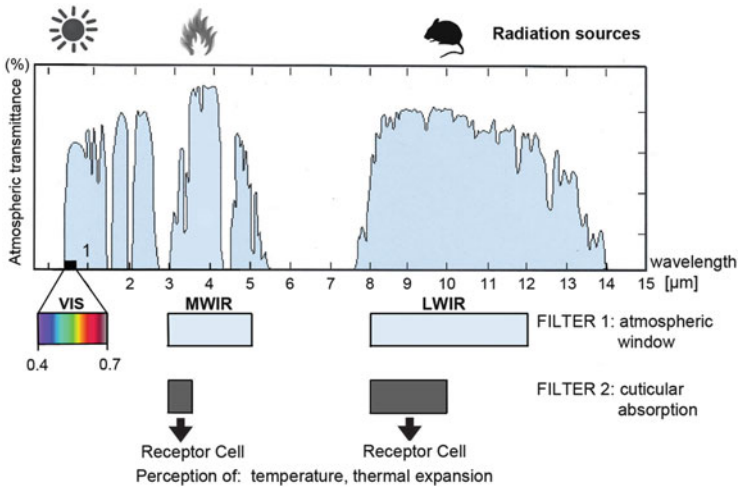


Fig. 8.1 Atmospheric transmittance of electromagnetic radiation emitted from objects with biological relevance. Atmospheric windows exist for visible light (VIS) radiated from the sun, MWIR radiated from high temperature sources like forest fires, and LWIR radiated from low temperature sources like warm-blooded creatures. Maxima of cuticular absorption (After Vondran et al. 1995) are also indicated below. Transmission spectrum adopted from the Naval Air Warfare Center

Although some animals, e.g., some fish living in turbid waters, are obviously able to see in the NIR (Meuthen et al. 2012; Shcherbakov et al. 2013), “long wavelength” (LW) photoreceptors with absorption maxima beyond 670 nm (Douglas et al. 1998) are unknown. The first essential step in vision always is the cis-trans torsional isomerization of the rhodopsin chromophore (Schoenlein et al. 1991). This conformational switch at least requires a photon energy of more than 1.24 eV (the energy content of a 1 μm photon). As can be derived from Table 8.1, IR photons emitted by a fire or a warm-blooded creature do not carry enough energy to initiate the isomerization of a visual pigment.

Nevertheless, the IR photons must be absorbed efficiently to cause distinct effects in the receptor. Absorption will be maximal if the frequency of vibration of a chemical bond between two atoms and the frequency of an incoming photon match (so-called resonance condition). Most organic molecules show vibrational absorption bands in the MWIR region (Barth 2007). The insect cuticle consists of protein and chitin (N-acetylglucosamines) showing many C–H, N–H, and O–H groups (Chapman 1998; Neville 1975). Molecules with these groups oscillate with frequencies of about 100 THz and, therefore, show stretch or vibrational resonances around 3 μm (Herzberg and Huber 1950). In general, most organic molecules strongly absorb in the MWIR and LWIR region of the electromagnetic spectrum (Hesse et al. 1995). In case of absorption of an IR photon, the vibrational energy is converted within fractions of a millisecond into translational energy, i.e., heat, by non-radiative de-excitation processes. Any heating inevitably also causes thermal

deformation. The absorber of a thermal IR detector, therefore, has to be monitored by a temperature and/or a mechanical displacement sensor.

8.2 IR Receptors in the Animal Kingdom

True IR receptors are relatively rare in animals. In vertebrates, receptors especially evolved for the detection of LWIR (8–15 μm (D'Amico et al. 2008)) can be found in vampire bats of the species *Desmodus rotundus* (Kürten and Schmidt 1982) and in three families of snakes: in the Boidae, the Pythonidae, and – within the family of Viperidae – in the subfamily Crotalinae, commonly known as pit vipers (Molenaar 1992; Bullock and Barrett 1968). Although the vertebrate IR organs have a very diverse appearance, receptors are all located on the head close to the mouth and are innervated by highly thermosensitive fibers of the trigeminal nervous system. When crawling on a warm-blooded host (e.g., a cow), the nocturnal blood-feeding vampire bats use their IR receptors for the localization of a rewarding biting site well supplied with blood (Kürten and Schmidt 1982). Large numbers of thermoreceptors were found in the central nose leaf yielding strong evidence that this facial area is responsible for the IR-receptive capabilities of the vampire bats (Kürten et al. 1984b). Receptors are sensitive to weak IR radiation down to an intensity of 50 $\mu\text{W}/\text{cm}^2$ enabling the bat to detect thermal radiation emitted from human skin up to a distance of 13 cm (Kürten and Schmidt 1982; Kürten et al. 1984b). Terminal sensory units for the perception of temperature differences are free nerve endings of warm and cold fibers ramifying directly under the epidermis (Kürten et al. 1984a). The molecular bases for IR reception in vampire bats most probably are specialized TRPV1 channels (transient receptor potential cation channel V1) (Gracheva et al. 2011).

The IR-sensitive snakes preferentially also hunt at night and use their IR receptors to locate warm-blooded prey. From outside, IR receptors are hard to detect at the heads of most boid snakes. Receptors are much better to discover in most pythons as small labial pits in the supra- and infralabials bordering the jaw and easy to identify in pit vipers as a pair of prominent holes in the loreal region located between the eyes and the nostrils (Molenaar 1992). As in vampire bats, the outer IR-absorbing surfaces are innervated by thermosensitive trigeminal fibers. The terminal endings of these fibers, however, show a unique feature increasing the sensitivity of the snake IR systems: so-called *terminal nerve masses* (TNMs). In brief, a TNM can be regarded as inflated terminus of a fine free nerve ending that contains enormous masses of mitochondria. The overall diameter of a TNM is about 30–50 μm (Terashima et al. 1970; Bullock and Fox 1957; Amemiya et al. 1996). TNMs are supplied with blood by a rich capillary network that also can afford rapid cooling of irradiated spots within the receptor. Among IR-sensitive snakes, pit vipers possess the most sophisticated IR receptors showing the highest sensitivity. Because the TNMs are embedded in a very thin membrane of only about 15 μm thickness providing a strongly reduced heat capacity, the sensitivity threshold has been determined to be only 3.35 $\mu\text{W}/\text{cm}^2$ in the western diamondback

rattlesnake, *Crotalus atrox*. This remarkable sensitivity enables the rattlesnake to detect a mouse from a distance of 1 m in complete darkness (Ebert and Westhoff 2006). The ion channels most probably responsible for the high sensitivity are modified TRPA1 channels (Gracheva et al. 2010).

A look at the IR receptors in invertebrates reveals a higher diversity. Although IR receptors hitherto have been found only in very few insects, they are very different from each other and can be located at different parts of the body.




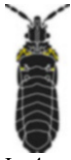
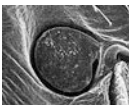
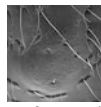


At first it is reasonable to suppose that – like in IR-sensitive snakes – also many nocturnal blood-feeding insects like mosquitoes could possess IR receptors for the detection of LWIR emitted by their warm-blooded prey. So far, however, IR sensory capabilities have only been demonstrated in certain blood-sucking triatomine bugs. These predatory insects search for a blood meal at night and for close range orientation in the centimeter range also use IR radiation given off by their warm-blooded hosts (Lazzari and Núñez 1989; Schmitz et al. 2000b; Guenstein and Lazzari 2009). According to the current knowledge, however, IR reception in triatomine bugs is accomplished by highly sensitive antennal thermoreceptors (Insausti et al. 1999; Bernard 1974; Lazzari and Wicklein 1994; Guenstein and Lazzari 2009). The response of thermoreceptors is ambiguous with regard to the temperature source, because convective as well as radiant heat results in a temperature increase of the cuticular portion of the receptors. Nevertheless, because thermoreceptive sensilla appear as conical, cylindrical, or hairlike structures, the transfer of radiant heat, which is limited to the surface area exposed to the radiation source, will be less important than convection (Gingl and Tichy 2001). On the other hand, flat extended areas on the body surface should be optimal for the transfer of radiant heat. Most probably, antennal thermoreceptors can be found on every insect antenna (Altner and Loftus 1985). Until now, additional extra-antennal IR receptors have not been described morphologically and/or physiologically for blood-sucking bugs or any other insect supposed to use IR radiation for the detection of low temperature IR sources.

In contrast, IR receptors developed in addition to the antennal thermoreceptive sensilla have only been found in very few insect species. These receptors are used for the detection of MWIR radiation (3–8 μm (D’Amico et al. 2008)) emitted from fires. Thus, insects equipped with extra-antennal IR receptors belong to a small group of specialists that are associated with forest fires. These “fire-loving” (pyrophilous) insects generally depend on forest fires for their reproduction and, therefore, approach ongoing fires and immediately invade freshly burnt areas to start reproduction.

8.3 Advantages of Detecting Forest Fires by IR Radiation

All pyrophilous insect species depicted in Table 8.2 and described below in more detail are attracted by forest fires. The main reason for this unusual behavior is that these insects as well as their offspring make use of the food resources made available by the fire. After a fire, the freshly burnt area becomes immediately

Table 8.2 Infrared receptors in pyrophilous insects

	“Little ash beetle”	“Australian fire beetle”	“Black fire beetle”	“Pyrophilous flat bugs”
	<i>Acanthocnemus nigricans</i>	<i>Merimna atrata</i>		<i>Aradus spec.</i>
	Only species in the genus	Only species in the genus	<i>Melanophila spec.</i> 11 species	4 IR-sensitive species in the genus <i>Aradus</i> (200 species)
Systematic position	Beetle (family: Acanthocnemidae)	Jewel beetles (family: Buprestidae)		Flat bugs (family: Aradidae)
Ventral habitus				
IR organs/receptors indicated in yellow	L: 4 mm	L: 20 mm	L: 10 mm	L: 4 mm
Legs omitted L: body length				
Position of IR receptor	Prothorax	Abdomen	Metathorax	Pro-/mesothorax
Picture of IR organ or single sensillum	 Left IR organ (sensory disk with numerous tiny sensilla)	 Left anterior IR organ (trough-shaped cuticular depression)	 Single IR sensillum (about 70 dome-shaped sensilla in a sensory pit)	 Single IR sensillum (dome-shaped sensilla interspersed between hair mechanoreceptors)
Mode of operation	Bolometer (in <i>Merimna</i> with additional photomechanic unit)		Photomechanic receptors	

populated by the insects because it initially serves as a safe meeting place for the sexes; potential predators are efficiently kept away by heat and smoke. Consequently, fire detection is an essential precondition for the survival of pyrophilous insects. The outbreak of a forest fire, however, is highly unpredictable. Therefore, pyrophilous insects should be able to detect fires from distances as large as possible. It is reasonable to suppose that the sensory organs, which are used for fire detection, have been subjected to a strong evolutionary pressure with regard to sensitivity. Additionally, when flying over a burnt area in search for a landing ground, the insect has to avoid to land on “hot spots” with dangerous surface temperatures of more than 60 °C. These two different requirements therefore request a rather large dynamic range of perception.

In a first approach to understand the phenomenon how a small insect could be able to approach a fire over distances of many kilometers, it is obvious to propose that olfaction plays a major role. However, there is no experimental evidence that flying pyrophilous insects could be lured to an odor source by the smell of smoke. A recent study has shown that pyrophilous *Melanophila* beetles can be attracted by certain volatiles emitted by burning or smoldering wood (Paczkowski et al. 2013). In the study, beetles were tested crawling around in a two-arm olfactometer at temperatures of 30 °C. No information about the sex and mating state of the beetles is provided. So these data are more likely suited to show that beetles (e.g., mated females?), once having landed on a burnt tree, can detect a suitable spot for oviposition by olfactory cues. Furthermore, evaluations of satellite images very often yielded the result that the large smoke plume from a forest fire initially is driven away from the fire by the wind in a narrow angle over distances of many kilometers, meanwhile slowly ascending to higher altitudes. Only beetles closer to the ground and inside the smoke plume would have a chance to become aware of the fire solely by olfactory cues. In contrast, beetles that are already close to the fire but outside the smoke plume most probably can see the plume but cannot smell the smoke. Also the light of the flames – generally only visible at night – may not play an important role, because *Melanophila* beetles, as nearly all jewel beetles, are active during the day (Evans et al. 2007).

According to the current conception of how pyrophilous insects may be able to become aware of a fire from large distances, these IR-sensitive insects most probably use a combination of visual cues (view of a big “cloud” against the horizon) and IR radiation (Schmitz and Bousack 2012). To make sure that a smoke plume and not a cloud bank is approached over many kilometers, a zone of IR emission has to exist at the base of the cloud just above treetop level. It is proposed that pyrophilous insects carefully screen the place of origin of the potential smoke plume for additional IR emission before they start to approach the fire. In contrast to an approach by olfactory cues which can be considerably impeded by the wind, especially over longer distances, an orientation by electromagnetic radiation in the visible and in the infrared spectrum allows a straight approach to the source. This is also promoted by an atmospheric window transparent for MWIR radiation between 3 and 5 μm (Fig. 8.1).

8.4 Diversity of IR Receptors in Pyrophilous Insects: An Overview

Currently, only 17 insect species out of four genera are known to possess IR sensory organs (Table 8.2). Compared to the amount of known insect species (roughly one million), this indeed is a negligible number. Nevertheless, a closer look at the IR receptors in the different genera reveals a surprising diversity. At least three fundamentally different types of receptors could be identified: a pair of prothoracic disks covered with numerous tiny sensilla in *Acanthocnemus nigricans*, one to three pairs of roundish abdominal IR organs in *Merimna atrata*, and the so-called

photomechanic IR sensilla in *Melanophila* beetles and in a few pyrophilous *Aradus* bugs. With regard to the functional principles, two categories exist: bolometer-like receptors in *Acanthocnemus* and *Merimna* and photomechanic sensilla in *Melanophila* and *Aradus* (cf. Table 8.2). The different shapes as well as the location at different spots on the thorax or the abdomen already provide evidence that IR receptors in the four genera have evolved independently from each other. Therefore, it can be stated that no “standard” IR receptor seems to exist in insects. This becomes especially evident when comparing the IR receptors in *Melanophila* beetles and in *Merimna atrata*. Although both beetles belong to the family of jewel beetles, make use of the same ecological niche after fires, and show the same biology and pyrophilous behavior, their IR receptors are totally different from each other as will be explained below in more detail. In contrast, a striking similarity exists between the photomechanic IR sensilla found in *Melanophila* beetles and *Aradus* bugs. Because the lineages of beetles and bugs most probably have already separated in the Permian about 270 mya, there is little doubt that IR sensilla in both genera have developed independently. In this particular case, the independent evolution has led to more or less the same type of mechanoreceptor-based IR sensillum.

The sensory ecology and the IR receptors of the mentioned pyrophilous insects will be described in more detail in the following.

8.4.1 The “Little Ash Beetle” *Acanthocnemus nigricans*

8.4.1.1 Biology and Behavior

A. nigricans is the only species within its family. Originally, the “little ash beetle” *A. nigricans* (family Acanthocnemidae, Table 8.2) was endemic to Australia (Champion 1922). In the last decades, however, this beetle has been exported out of Australia and nowadays can be found in several European countries like Spain, Italy, and Portugal (Alonso-Zarazaga et al. 2003; Mayor 2007; Liberti 2009; Valcárcel and Piloña 2009; Kovalenko 2011). In 2011 it was also found in Russia (Kovalenko 2011). The inconspicuous beetle is only 3–5 mm long and is attracted by forest fires (own observations in the last 10 years). Immediately after a fire, *A. nigricans* can be found on freshly burnt areas, preferably close to spots of hot ashes. However, its biology is nearly unknown. It has been speculated that the sexes meet around the hot spots in order to mate. Observations of the behavior are very difficult because after landing on the ash and a short period of hectically running around, the beetles dive into the ash and become invisible. So the substrate to which the eggs may be deposited is unknown. In summary, there is strong evidence that *Acanthocnemus* depends on fires for its reproduction. As special adaptation to its pyrophilous way of life, the beetle is equipped with a pair of complex IR receptors located behind the head on the first segment of the thorax (Kreiss et al. 2005).

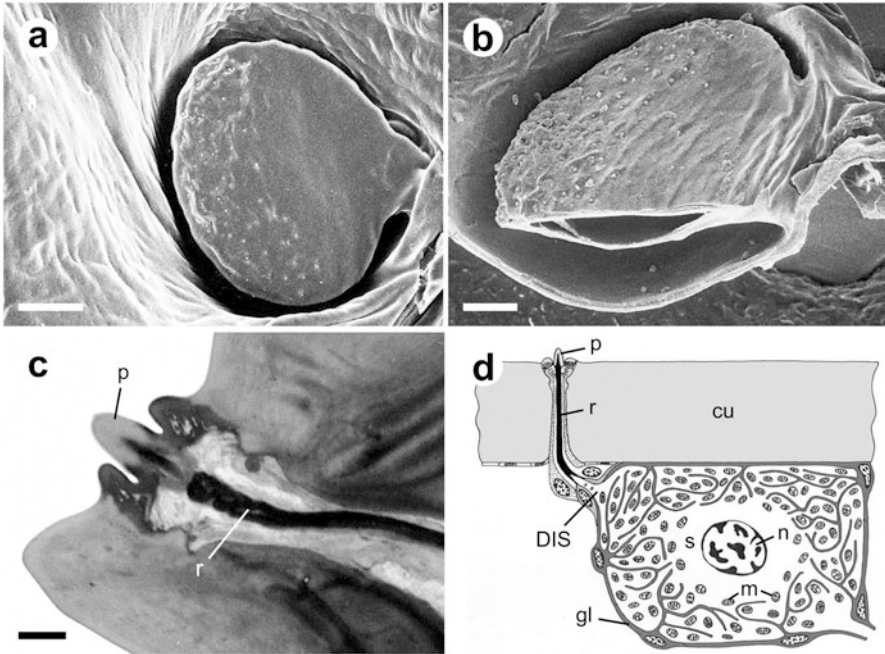


Fig. 8.2 (a) Left IR organ of *Acanthocnemus nigricans* (head is located on the left). A little cuticular disk (diameter 150 μm) is situated on the lateral prothorax directly in front of the coxa of the foreleg. About 90 tiny sensilla are located on the anterior half of the disk. Bar: 30 μm (b) Cut through the ventral part of the disk and the underlying cavity shows the composition of the organ. The disk is held above the cavity by a small posterior stalk. Bar: 20 μm . (c) Section through a single sensillum at the anterior rim of the disk. An electron dense rod (*r*) is connected to the outer peg (*p*) and continues through the dendritic canal down to the soma of a sensory cell located below the cuticle. Bar: 1 μm . (d) Schematic drawing of a disk sensillum. Note that numerous mitochondria (*m*) are housed inside the soma (*DIS* short dendritic inner segment, *gl* glial cells, *n* nucleus, *p* peg, *r* rod, *s* soma) (d modified after Kreiss et al. 2005)

8.4.1.2 Structure and Function of the Prothoracic IR Organs

The IR organs are unique in *A. nigricans*. As depicted in Table 8.2 and Fig. 8.2a, b, one pair of IR organs is located on the prothorax (Schmitz et al. 2002; Kreiss et al. 2005). The main component of each organ is a little cuticular disk which is situated over a cavity. The air within the cavity beneath the disk communicates with the ambient air by a small gap around the disk (Fig. 8.2a, b). By this construction, the thermal mass of the disk is considerably reduced and the underlying air layer thermally insulates the disk from the body. On the anterior surface of the disk, about 90 tiny cuticular sensilla are situated. This is the part of the disk with the lowest thermal mass. A single disk sensillum consists of a small cuticular peg (diameter about 1.5 μm , length about 2 μm) which is connected to an unusual electron dense rod (Fig. 8.2c, d). The rod most probably represents the extremely hypertrophied dendritic sheath normally ensheathing the outer dendritic segment (DOS) in other

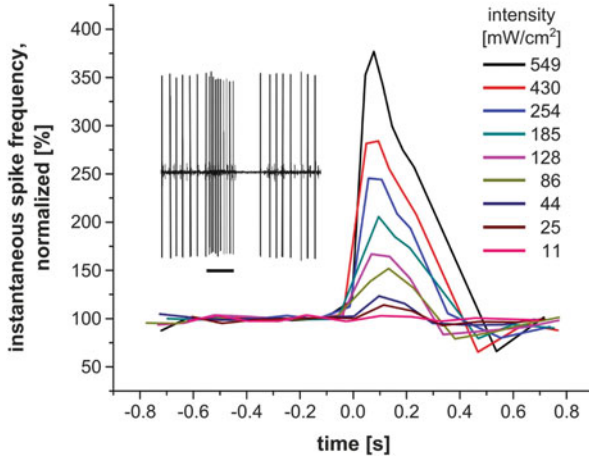


Fig. 8.3 Single unit recording from an IR sensillum on the sensory disk of *Acanthocnemus nigricans*. *Inset* shows the typical phasic-tonic response pattern to a stimulus applied by a red helium-neon laser (380 mW/cm²). Increase in spike frequency (normalized to the frequency without stimulus which was set to 100 %) depended on stimulus intensity (11–549 mW/cm² tested). *Black bar* indicates duration of stimulus (250 ms) (Adapted from Kreiss et al. 2007)

mechanosensory sensilla. In the *A. nigricans* IR sensillum, the outer peg effectively is connected to the inner dendritic segment (DIS) of the sensory cell, which is situated under the cuticle (Fig. 8.2d). However, the function of the rod remains enigmatic. The soma of the sensory cell as well as the DIS is characterized by many deep invaginations of the cell membrane. The narrow extracellular spaces enclosed by the invaginated membranes are filled by darker glial cells. Especially the peripheral intracellular compartments inside the soma are densely filled with mitochondria (Fig. 8.2d).

Electrophysiological recordings from single disk sensilla have shown that sensilla responded with a phasic-tonic increase of neuronal activity to increasing temperature (Fig. 8.3; Kreiss et al. 2007). In principle, this corresponds to the typical response pattern of a warm cell (Gingl and Tichy 2001). Threshold sensitivity has been determined to be between 11 and 25 mW/cm² tested with a red helium-neon laser (Kreiss et al. 2007).

Due to its morphology and response behavior, the IR organs of *Acanthocnemus* can be classified as microbolometer-like IR sensors (cf. Table 8.2). In a bolometer, absorbed IR radiation heats up a thin absorber that corresponds to the outer surface of the disk. The resulting increase in temperature is measured by the sensory cells inside the disk. Commonly, the absorbers of a technical microbolometer are coated with, e.g., vanadium oxide, whose electrical resistance strongly changes with temperature. This can be easily measured by an appropriate readout circuit (Rogalski 2002). Compared to microbolometer sensors used nowadays for thermal imaging, the sensitivity of the *Acanthocnemus* IR receptors is rather low. Current technical microbolometers have sensitivities of a few $\mu\text{W}/\text{cm}^2$ (Budzier and

Gerlach 2011), and, therefore, it is unlikely that *Acanthocnemus* uses its IR organs for fire detection from larger distances. Theoretical calculations suggest that *Acanthocnemus* might be able to detect a large fire of, e.g., 10 ha from distances of a few kilometers. However, this has to be shown experimentally. More likely, beetles use their thoracic IR organs for navigation on freshly burnt areas that still show many hot spots. *Acanthocnemus* is active during the day and most hot spots cannot be seen with eyes under bright daylight. Because it has been frequently observed by the authors that beetles seem to aggregate very close to smaller hot spots (e.g., patches of hot ashes around a burnt stump), it can be concluded that the beetles are able to detect those hot spots from distances of some meters by their IR receptors. Furthermore, IR receptors could serve as early warning systems to avoid a landing on a hot spot.

8.4.2 IR Receptors in *Merimna atrata*

8.4.2.1 Biology and Behavior

M. atrata is the only species within the genus *Merimna* and is distributed all over Australia (Hawkeswood 2007). Up to now, *Merimna* has not been found outside the Australian mainland. *Merimna* exclusively breeds in different species of fire-killed eucalyptus trees (Myrtaceae (Hawkeswood and Peterson 1982; Kitchin 2009)). Immediately after a fire, first *Merimna* beetles arrive at the border of the freshly burnt area where they can be observed resting or running around on the vegetation. However, to the earliest time when a human is able to enter the burnt area, the beetles also start to invade the scorched terrain (own observations). Beetles rapidly spread over the burnt area and can be observed flying around relatively low or running over the ground, trees, and shrubs (Schmitz and Schmitz 2002; Poulton 1915). Males primarily are in search for females. After copulation, the females start to deposit their eggs under the bark of fire-scorched eucalyptus trees by inserting their ovipositor in small crevices. After hatching, the larvae start to feed inside the wood of the fire-killed trees; the new generation of beetles will emerge 1 or 2 years later (Kitchin 2009).

Additionally, *Merimna* also extensively uses the opportunity to forage on the burnt area. All material potentially edible is investigated and, if consumable, eaten up. Also carcasses of small fire-killed vertebrates are devoured.

8.4.2.2 Structure and Function of the Abdominal IR Organs

In *M. atrata*, one pair of IR organs is located ventrolaterally on the second, third, and sometimes also on the fourth abdominal sternite each (Mainz et al. 2004). The IR organs consist of an external cuticular part – the radiation-absorbing area – and an internal sensory complex innervating this area (Fig. 8.4a–c, Schmitz et al. 2001).

The absorbing area is a roundish and shallow dint of the cuticle. Depending on the size of the beetle, the average diameter is about 500 μm and the depth is about 150 μm (Fig. 8.4a, e, Schneider and Schmitz 2013). It is characterized by the following special features: (i) a lack of dark pigments within the exocuticle

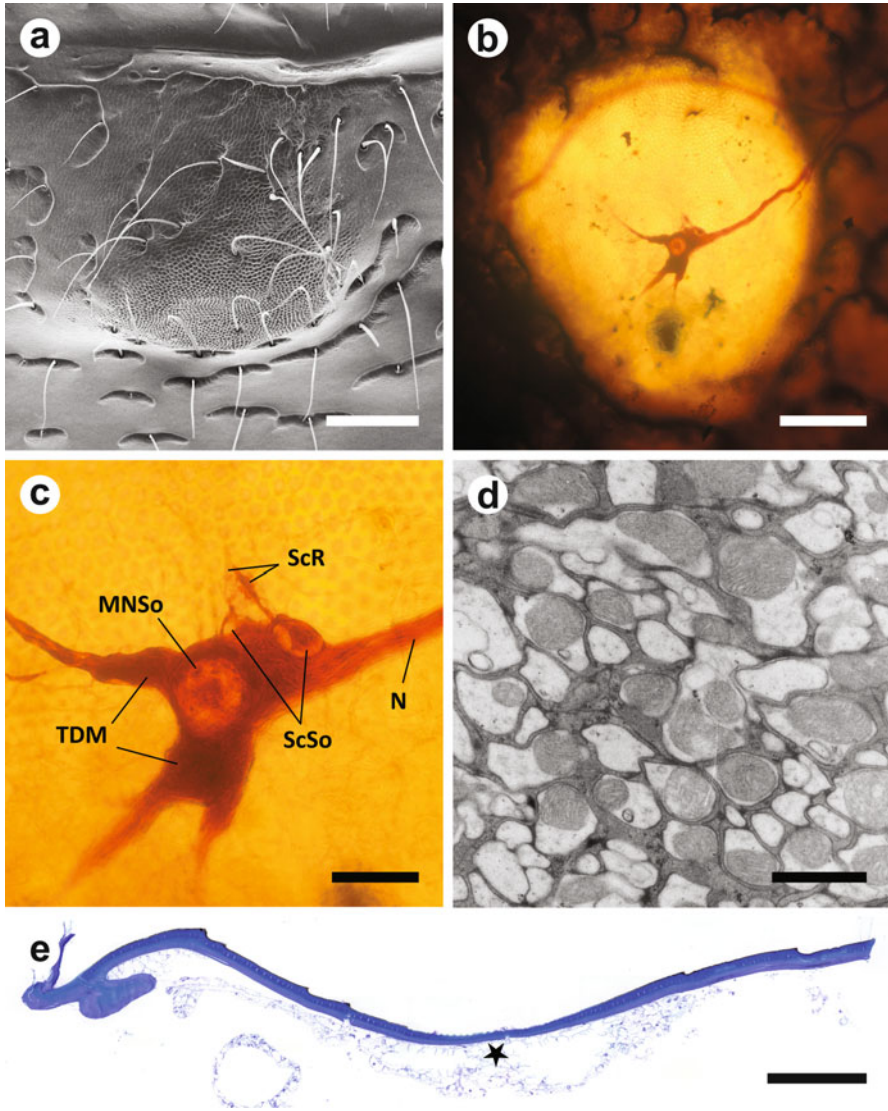


Fig. 8.4 IR organ of *Merimna atrata*. (a) SEM image of the absorbing area showing its three-dimensional shape and honeycomb-like surface structure. Bar: 200 μ m. (b) LM micrograph of the sensory complex stained with cobalt/nickel innervating the yellowish absorbing area. Bar: 200 μ m. (c) Sensory complex shown in (b) at higher magnification. MNSo soma with nucleus of multipolar neuron, N nerve, ScSo somata of the sensory cells of two scolopidia, ScR scolopale rods, TDM terminal dendritic mass of the multipolar neuron. Bar: 50 μ m. Orientation in (a–c): top = anterior, bottom = posterior, left = lateral, right = medial. (d) TEM micrograph of the TDM of the thermosensitive multipolar neuron. Bar: 1 μ m. (e) Longitudinal section through the center of the absorbing area stained with toluidine-blue/borax (LM-image). Asterisk indicates position of the sensory complex. Orientation: top = exterior, bottom = interior, left = anterior, right = posterior. Bar: 100 μ m (a and d modified after Kahl et al. (2014, b and c modified after Schneider and Schmitz 2013)

resulting in a yellowish color of the IR organ in contrast to the glossy dark brown color of “normal” cuticle surrounding the absorbing area (Fig. 8.4b, Schmitz et al. 2001), (ii) a honeycomb-like microstructure in the central region of the absorbing area (Fig. 8.4a, Schmitz et al. 2000a), and (iii) a reduced thickness of the cuticle in the center (Fig. 8.4e, Schneider and Schmitz 2013, 2014) under which the sensory complex is situated. It can be proposed that the lack of dark pigments in the cuticle of the absorbing area significantly reduces the absorption of visible light and subsequent heating, because dark pigments like melanins have their absorption maxima within the range of visible light (Stark et al. 2005).

The sensory complex comprises a large multipolar type 1 neuron with a specialized dendritic region called terminal dendritic mass (TDM, Fig. 8.4c) and in close proximity to that a chordotonal organ (CO), represented by two scolopidia (Fig. 8.4c, Schneider and Schmitz 2013). The thermoreceptive function of the multipolar neuron has been confirmed by electrophysiological recordings (Schmitz and Trenner 2003). Like the disk sensilla in *Acanthocnemus*, the neuron responds in a phasic-tonic way with an increase of its spike frequency to increasing temperature (Fig. 8.5). Thus, the thermoreceptive modality of the multipolar neuron also allows a classification of the *Merimna* IR organ as a bolometer. However, because of the

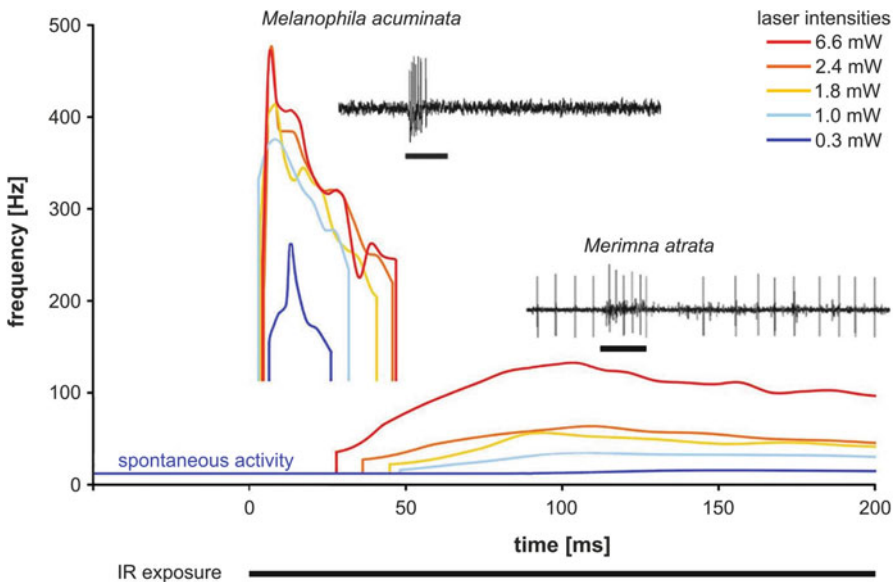


Fig. 8.5 Electrophysiological recordings from a single IR sensillum in the pit organ of *Melanophila acuminata* (left) and from the thermosensitive multipolar neuron in the *Merimna* IR organ (right). Receptors were stimulated with a red laser at different intensities from 0.3 to 6.6 mW. Stimulation always started at 0 ms and lasted 200 ms (black bar indicates IR exposure). Note the fast and strictly phasic response pattern of the *Melanophila* sensillum with very short latencies and the long-lasting phasic-tonic response of the *Merimna* receptor with considerable longer latencies. Insets are examples of single original recordings (Adapted from Schmitz and Trenner 2003)

rather low threshold sensitivity of 40 mW/cm^2 , determined in the electrophysiological experiments conducted so far (Schmitz and Trenner 2003), it has been concluded that the *Merimna* IR organ is not suitable for remote sensing of forest fires but rather for short-distance sensing, e.g., to prevent the beetle from landing on hot surfaces (Schmitz and Trenner 2003). More recent investigations have concentrated on the CO as a second, putative receptor system also involved in IR perception, which may enable the beetle to detect also remote forest fires (Schneider and Schmitz 2013). The CO represents a mechanosensory unit, consisting of two mononematic monodynamal scolopidia, located in direct proximity to the multipolar neuron in the center of the absorbing area (Fig. 8.4c, Schneider and Schmitz 2013). Just like other scolopidia of this type, they are supposed to respond to axial stress or bending (Field and Matheson 1998). In general, scolopidia function as proprioceptors or specialized mechanoreceptor organs, capable of detecting mechanical displacements over several orders of magnitude (Field and Matheson 1998) down to 0.6 nm (Michelsen and Larsen 1985). Therefore, it has been proposed that the absorption of IR radiation could also lead to minute deformations of the absorbing area with its highest extend in the central region, corresponding to the attachment site of the CO (see asterisk in Fig. 8.4e). The CO could perceive these mechanical events and thus probably extend the measuring range, thereby increasing the sensitivity of the IR organ (Mainz et al. 2004; Schneider and Schmitz 2013). Other probable benefits provided by the additional mechanoreceptive innervation of the IR organ by the CO could include, e.g., faster response times, a larger dynamic range, higher reliability or improved filter properties. In summary, this could increase the overall performance of the whole IR organ (Schneider and Schmitz 2014). However, unambiguous electrophysiological recordings from the CO are missing so far.

8.4.3 IR Receptors in Pyrophilous *Melanophila* Beetles

8.4.3.1 Biology and Behavior

Beetles of the genus *Melanophila* inhabit nearly all continents except Australia and Antarctica and use fire-killed trees as food for their larvae (Table 8.3, Bellamy 2008; Evans 1964, 1966b; Linsley 1933, 1943; Manee 1913; Ricksecker 1885; Sharp 1918; Sloop 1937; VanDyke 1926; Wikars 1997). As far as it is known, nearly all recent species show the same pyrophilous biology and behavior as reported above for *Merimna* in Australia. Of course both genera use different tree species. Whereas *Merimna* breeds in scorched eucalyptus trees, it has been reported that *Melanophila* species breed in a variety of burnt conifers as well as in several species of scorched deciduous trees (Apel 1991; Horion 1955). Thus, it can be stated that the two buprestid genera have occupied the same ecological niche and have developed a nearly identical pyrophilous way of life on different continents. Surprisingly, their IR receptors are totally different!

Table 8.3 Recent species of the genus *Melanophila* according to Bellamy (2008), distribution, and early records of pyrophilous behavior and/or IR organs

Recent <i>Melanophila</i> species	Distribution	Pyrophilous behavior described by	IR organs described by
<i>M. acuminata</i>	African; Nearctic; Neotropical; Oriental; Palearctic	Ricksecker (1885), Manee (1913), Sharp (1918), and Linsley (1933)	Sloop (1937) and Evans (1964)
<i>M. atra</i>	Neotropical	–	Evans (1966a)
<i>M. atropurpurea</i>	Nearctic	Linsley (1933)	Sloop (1937)
<i>M. caudata</i>	Nearctic	–	Sloop (1937)
<i>M. consputa</i>	Nearctic	Ricksecker (1885), VanDyke (1926), and Linsley (1933)	Sloop (1937)
<i>M. coriacea</i>	Oriental	Wikars (1997)	Evans (1966)
<i>M. cuspidata</i> (syn.: <i>M. nigrita</i>)	African; Palearctic	Wikars (1997)	Evans (1966)
<i>M. gestroi</i>	African; Palearctic	–	–
<i>M. ignicola</i>	Oriental; Palearctic	Champion (1918)	Sloop (1937)
<i>M. notata</i>	Nearctic; Neotropical; Palearctic; oriental	Manee (1913) and Linsley (1933)	Sloop (1937)
<i>M. obscurata</i>	Palearctic	–	–
<i>M. occidentalis</i>	Nearctic	Obenberger 1928 in Linsley (1943)	Sloop (1937)
<i>M. unicolor</i>	African	–	Evans (1966)

8.4.3.2 Structure, Function, and Possible Detection Range of the Metathoracic IR Organs

The IR receptors are situated in two pit organs which are located on the metathorax (cf. Table 8.2). Each IR organ houses about 70 IR sensilla which are closely packed together at the bottom of the pit (Fig. 8.6a, Evans 1966a; Vondran et al. 1995). From the outside, a single sensillum can be recognized by a hemispherical dome with a diameter of about 12–15 μm . The dome is built by a thin cuticle which represents the outer boundary of a spherical internal cavity. The cavity is almost completely filled out by a tiny cuticular sphere with a diameter of about 10 μm (Fig. 8.6b). Based on transmission electron microscopic (TEM) observations, Vondran et al. (1995) described that the sphere consists of three different zones: (i) an outer lamellated mantle, (ii) an intermediate layer of unstructured cuticle revealing many irregularly arranged microcavities (mc in Fig. 8.6b), and (iii) an innermost central zone where the cuticle appears uniform except for some spots of higher electron density. The sphere is connected to the vertex of the outer cuticular dome by a small cuticular stalk. The narrow gap surrounding the sphere is filled out by leaflike extensions of at least two enveloping cells (not visible in the dried cuticular specimen shown in Fig. 8.6b). From below, the sphere is innervated by a single sensory cell (Fig. 8.6c). As a prominent feature, it has been found that the outermost

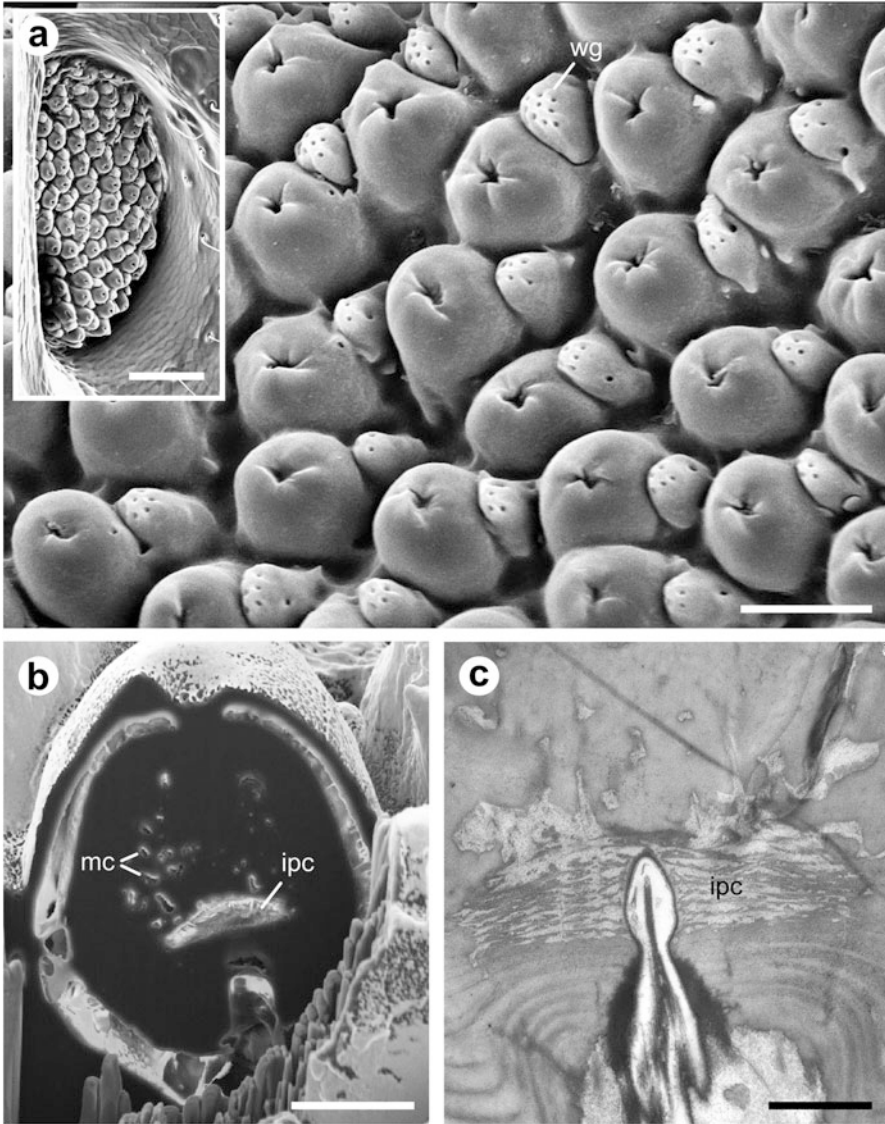


Fig. 8.6 Morphology of the IR organ of *Melanophila acuminata*. (a) Dome-shaped IR sensilla at the bottom of a pit organ (shown in the *inset*). Each sensillum is accompanied by a smaller wax gland (*wg*) characterized by tiny pores. SEM micrographs, *Bar*: 15 μm (*Inset* 100 μm) (b) Single IR sensillum centrally opened by focused ion beam (FIB) in a SEM. Specimen was air-dried; therefore, only the cuticle is preserved. Microcavities (*mc*) of the intermediate layer and the inner pressure chamber (*ipc*) can be discerned inside the sphere. *Bar*: 5 μm . (c) Outermost tip of the ciliary dendrite of the mechanosensitive cell inside the inner pressure chamber (*ipc*). The tip is suspended by fine filaments inside the fluid-filled chamber which communicates with the fluid in the microcavities. Any increase in fluid pressure is transferred onto the dendritic membrane. TEM micrograph, *Bar*: 1 μm (c adapted from Schmitz et al. 2007)

tip of the dendrite is located inside an inner pressure chamber in the sphere (IPC in Fig. 8.6c). All morphological as well as all physiological data available so far have demonstrated that this cell is a ciliary mechanoreceptor (Vondran et al. 1995; Schmitz and Bleckmann 1998; Schmitz et al. 1997).

According to the current conception of how IR radiation may be converted into a mechanical event perceivable by the mechanoreceptive cell, absorbed IR radiation heats the sphere and causes an increase in pressure in the fluid-filled system of communicating microcavities inside the sphere. Because the outer lamellated mantle consists of hard exocuticle reinforced by layers of chitin fibers (Schmitz et al. 2007), the only compliant structure in the sphere is the olive-shaped tip of the dendrite in the inner pressure chamber which becomes slightly squeezed by the increasing pressure. This lateral compression of the dendritic tip is the adequate stimulus for the mechanoreceptor (French 1992; Thurm et al. 1983).

Up to now the crucial question from which distances *Melanophila* beetles can detect a fire by IR reception cannot be answered satisfactorily. Extracellular electrophysiological recordings obtained by inserting a metal electrode between the IR sensilla have revealed a fast and strictly phasic response to heating (Fig. 8.5) (Schmitz et al. 1997), and a threshold sensitivity of $500 \mu\text{W}/\text{cm}^2$ has been estimated (Schmitz and Bleckmann 1998). It has been calculated that this sensitivity would enable a beetle to detect a larger forest fire of 10 ha with a temperature of 700°C from a distance of about 10 km (Schmitz and Bleckmann 1998). However, because the metal electrode may have sucked considerable amounts of heat energy away from the sensilla, this threshold most probably is underestimated. A recent in-depth modeling of a big historic oil-tank fire, which attracted untold numbers of *Melanophila consputa* in California 90 years ago (VanDyke 1926), suggested a much higher sensitivity of the IR receptors (Schmitz and Bousack 2012). The analysis of the geographical conditions around the tank fire yielded the result that most beetles must have become aware of this fire from a distance of 130 km. If IR radiation really was a crucial cue used by the beetles to detect the fire, this would result in a sensitivity of $40 \text{ nW}/\text{cm}^2$ (Schmitz and Bousack 2012). In principle this would mean that the IR receptors of *Melanophila* beetles can compete even with technical high sensitivity quantum IR sensors that have to be cooled, e.g., with liquid nitrogen, to suppress the thermal noise. However, additional mechanisms like active amplification, which, already has been described for auditory hearing organs in insects (Göpfert and Robert 2001, 2003; Mhatre and Robert 2013), and effective noise suppression have to be postulated to make this unbelievable sensitivity imaginable.

8.4.4 IR Receptors in Pyrophilous Aradus Bugs

The family of Aradidae (flat bugs) comprises about 200 species (Heiss and Pericart 2007). Within this large family, only eight species have been described to be associated with forest fires because these species were found on burnt areas relatively soon after a fire (Table 8.4; (Baena and Torres 2013; Johansson

Table 8.4 *Aradus* species found shortly after a fire on a burnt area and/or their IR receptors

<i>Aradus</i> species	Distribution	Pyrophilous behavior described by	IR receptors existing (+); missing (–); no data available (n.a.); according to Schmitz et al. (2010)
<i>A. albicornis</i>	Australian	Schmitz et al. (2008)	+
<i>A. anisotomus</i> = <i>anullicornis</i>	Eurasian	Wikars (1997) and Wyniger et al. (2002)	n.a.
<i>A. crenaticollis</i>	Eurasian	Wikars (1997) and Johansson et al. (2010)	–
<i>A. flavicornis</i>	Eurasian, African	Baena and Torres (2013)	+
<i>A. fuscicornis</i>	Australian	Schmitz et al. (2010)	+
<i>A. laeviusculus</i>	Eurasian	Lappalainen and Simola (1998)	–
<i>A. lugubris</i>	Eurasian, North- American	Wyniger et al. (2002) and Johansson et al. (2010)	+
<i>A. signaticornis</i>	Eurasian, North- American	Wikars (1997) and Wyniger et al. (2002)	n.a.

et al. 2010; Lappalainen and Simola 1998; Schmitz et al. 2008, 2010; Wikars 1997; Wyniger et al. 2002)). Also in *A. gracilicornis* and *A. gracilis*, a pyrophilous behavior has been described (Deyrup and Mosley 2004). However, both species were found more than 1 year after the fire. Thus, the time of arrival of the pioneer generation and, hence, a pronounced pyrophilous behavior is uncertain (see also next section). Within this small group of pyrophilous flat bugs, IR receptors so far were only found in four species: namely, in *A. albicornis*, *A. flavicornis*, *A. fuscicornis*, and *A. lugubris* (cf. Tables 8.2 and 8.4; Schmitz et al. 2010).

8.4.4.1 Biology and Behavior

There is strong evidence that pyrophilous *Aradus* bugs listed in Table 8.4 are lured to burnt trees by fire-specific cues like smoke, heat, and – after the fire has ceased – persisting smell of burning. Attracted by these cues, those fire-adapted species arrive early on a burnt area. The behavior of *Aradus* species in general is hard to observe because the tiny flat bugs conceal themselves under the bark of the burnt trees. According to the current knowledge, the adult bugs and their larvae feed on the mycelia of fast-growing post-fire fungi, which start to grow on burnt wood immediately after a fire (Froeschner 1988; Wikars 1992). Sporadic own observations on *A. albicornis* in Western Australia revealed that bugs arrive on freshly burnt areas a few hours after a fire has raged over a forest. Apparently, bugs prefer to colonize weak moisture-loving eucalyptus trees growing near creeks or

lakes like *Eucalyptus rudis*. After copulation, the females deposit their eggs at the base of the stem already hidden a few centimeters in the soil. In this so-called collar region, lignotuber bulges were frequently observed. These are specialized woody storage organs with an active cambium layer, therefore still having a high moisture content, that are capable of resprouting after a fire even if the above-ground part of the tree is totally burnt. This obviously is the zone where the fungi find good conditions and start to grow. If the collar region is carefully excavated about a week after the fire, groups of adults and first larvae can be found between the superficial roots sucking on the mycelia. There is evidence that the pyrophilous *Aradus* species continue to reproduce at these favorable spots as long as the fungi stay alive.

8.4.4.2 Structure and Function of the Prothoracic IR Organs

Photomechanic IR receptors are mainly located on both propleurae of the prothorax (Table 8.2). The propleurae extend behind the bulges of the prothoracic leg bases and are developed as thin winglike duplications of the body wall. Accordingly, the thermal mass is rather low. Very few IR sensilla were also found directly posterior to the bases of the mesothoracic legs (cf. Table 8.2, Schmitz et al. 2010). At a first glance, a single IR sensillum strongly resembles an IR sensillum located in the pit organs of *Melanophila* (cf. Table 8.2, Figs. 8.6a, 8.7a, and 8.8). However, numbers of sensilla are much lower in *Aradus* (one or two dozen on each propleura) and the sensilla are loosely interspersed between the bollard-like hair mechanoreceptors (Fig. 8.7a). TEM micrographs show that two further differences to the *Melanophila* sensilla exist: a distinct cleft around the sphere is missing in the *Aradus* sensillum (Figs. 8.7b and 8.8), and the outermost tip of the mechanosensitive dendrite anchored in the cuticle of the sphere remains only about 500 nm below the bottom of the indentation in the center of the sphere (Fig. 8.7b, c). On the other hand, the same basic components of a photomechanic IR sensillum described in *Melanophila* beetles are present: an outer lamellated shell enclosing a microfluidic core which is innervated by one ciliary mechanosensory cell. At its outermost tip, the dendrite of the mechanoreceptor is in direct contact to the fluid inside the sphere (Figs. 8.7b, c). Thus, the IR sensilla of pyrophilous *Aradus* bugs also can be classified as photomechanic IR receptors.

First electrophysiological recordings revealed that the sensillum responds to heating in a phasic-tonic way. At high stimulation intensities, first spike latencies were only 3–7 ms like in the *Melanophila* sensilla (Fig. 8.7d). However, the sensitivity seems to be considerably lower. So far a threshold sensitivity of 11 mW/cm² has been determined by extracellular recordings (Schmitz et al. 2008). As in the beetle *Acanthocnemus*, it cannot be completely ruled out that the bugs may use their IR receptors for the detection of fires from distances of some kilometers. Because the pyrophilous *Aradus* species are also very small and appear to be weak flyers, it seems unlikely that they use their IR receptor for fire detection from larger distances. Most probably, bugs also use the IR sensilla for the localization of hot spots prior to landing.

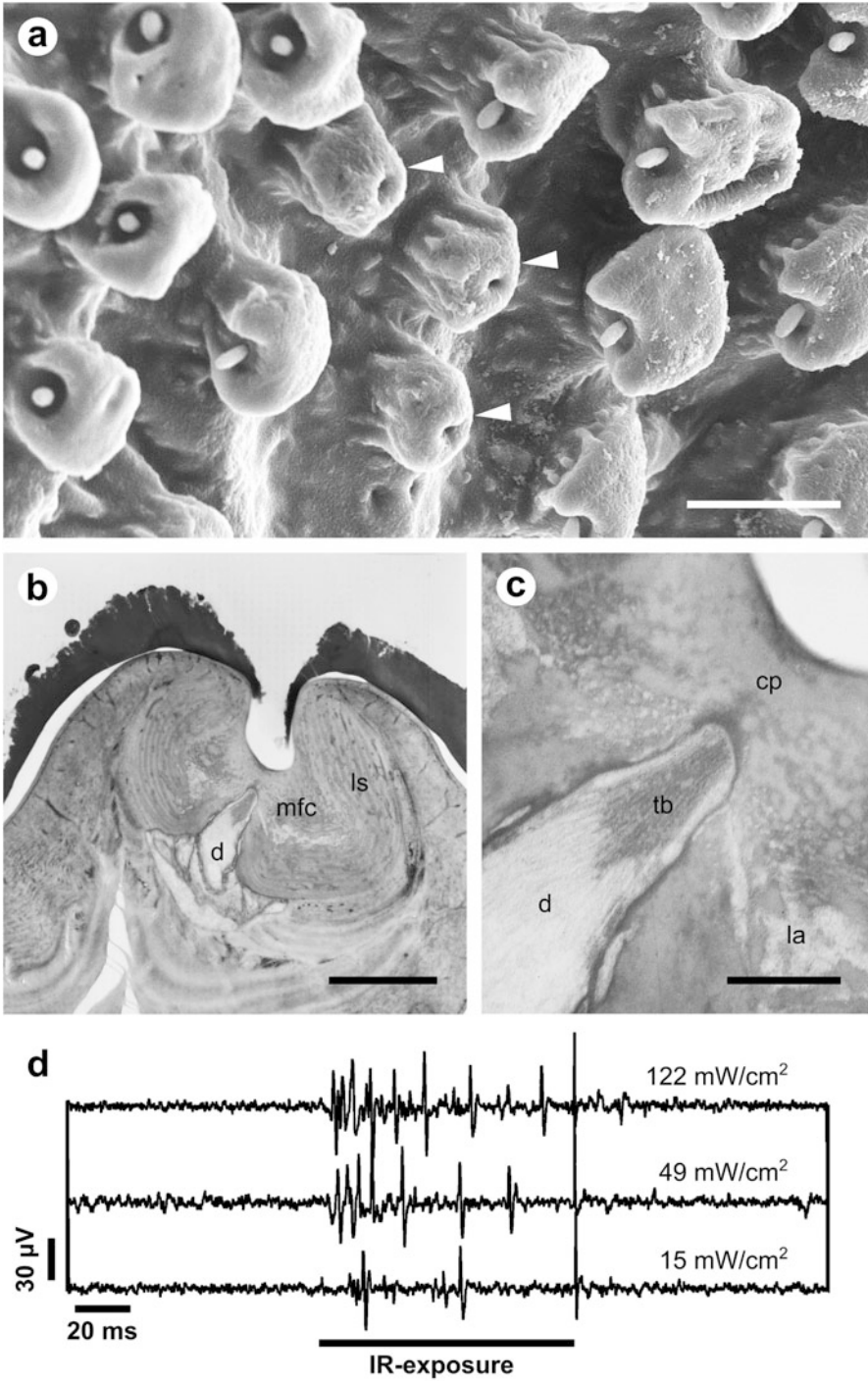


Fig. 8.7 (a) Detail from the right propleura of *Aradus albicornis*. Between several bollard-like hair mechanoreceptors with short bristles, three IR sensilla are interspersed (white arrowheads,

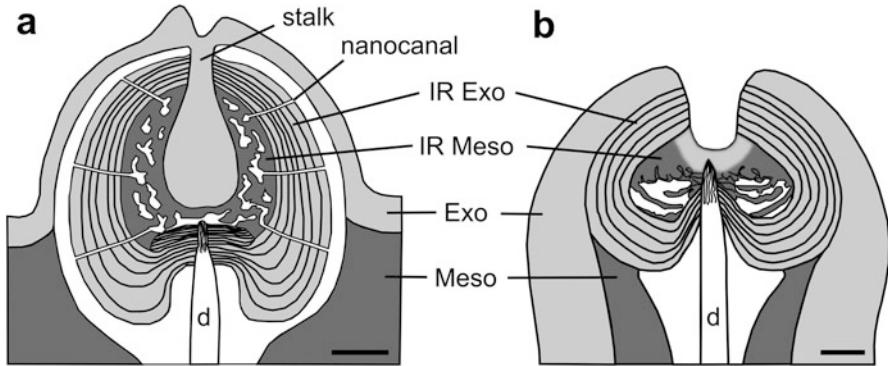


Fig. 8.8 Schematic drawings of photomechanic IR sensilla in (a) *Melanophila* beetles and (b) pyrophilous *Aradus* bugs. In both receptors, the expansion of the fluid encapsulated inside an inner microfluidic center is measured by a ciliary mechanosensitive cell (a adapted from Schmitz et al. 2007, b adapted from Schmitz et al. 2008)

8.5 The Development of IR Receptors in Pyrophilous Insects

For several reasons, pyrophilous insects appear to be predestined to develop IR receptors. First of all, the flames and hot surfaces of a fire emit additional quantities of MWIR radiation, which is well transmitted through the corresponding atmospheric window into the surroundings (Fig. 8.1). Thus, this invisible electromagnetic radiation can serve as a valuable source of information permitting the detection of a fire from larger distances as well as the early contactless detection of unfavorable hot spots. The existence of IR receptors, therefore, is a clear advantage for a pyrophilous insect.

A fire creates a very interesting ecological niche within a few minutes: the burnt area (Bond and Keeley 2005). On a burnt area, most biotic as well as many abiotic factors have changed dramatically. For insect species which feed on dead wood or fungi, this spot is a kind of paradise (Saint-Germain et al. 2008). However, the area has to be approached quickly before competitors, also appetent to colonize the dead

Fig. 8.7 (continued) Bar: 20 μm). IR sensilla are characterized by a central indentation. SEM micrograph. (b) Section through the center of an IR sensillum at the position of the indentation. The sensillum is covered by an electron dense superficial layer. The internal sphere with a diameter of 10 μm shows a lamellated shell (*ls*) and contains a microfluidic core (*mfc*). In the center of the core, the dendritic tip (*d*) of the mechanosensory neuron is situated. TEM micrograph, Bar: 3 μm . (c) Detail of the insertion site of the dendrite. The dendrite contains a well-developed tubular body (*tb*), which is characteristic for insect mechanoreceptors, and ends in a cuticular plug (*cp*) about 500 nm below the bottom of the central indentation of the sphere. *la* lacuna of the fluidic core. TEM micrograph, Bar: 0.5 μm . (d) Electrophysiological recordings from a single IR sensillum with different radiation intensities applied with a red helium-neon laser. At high irradiation intensities, first spike latencies were only 3–7 ms (d adapted from Schmitz et al. 2008)

wood, arrive. The group of pyrophilous insects consists of about 40 species from the orders of Coleoptera, Hemiptera, Diptera, and Lepidoptera (Wikars 1997). In general, it can be proposed that this specialized group of insects has developed sensory and behavioral adaptations to master this task. There is evidence that adaptations in the jewel beetles *Melanophila* and *Merimna* toward a pyrophilous biology have advanced to an extent that successful reproduction obviously is impossible without a fire. Thus, the development of IR sensory capabilities is plausible in both genera.

The driving forces fostering the development of IR receptors can be summarized as follows: in insects, which already had started to develop a pyrophilous way of life, heat from hot surfaces on a burnt area may have stimulated unspecifically some peripheral receptors. Primarily, this may have affected external mechanoreceptors exposed to incoming IR radiation that were stimulated by thermal expansion of nearby cuticle or water in the respective receptor lymph cavities. By this, an evolutionary pressure came into play and – as a first important step – the IR-absorbing outer cuticular apparatus of the evolving IR sensillum had to be optimized. This can be exemplified by looking at the photomechanic sensilla in *Melanophila* beetles and *Aradus* bugs (Fig. 8.8). As discussed by Schmitz et al. (2007, 2010), there is strong evidence that in both pyrophilous species, the IR sensilla have evolved directly from hair mechanoreceptors (sensilla trichodea). However, because photomechanic IR sensilla so far have only been found in recent species of the genus *Melanophila* within the beetles and in very few pyrophilous species of the genus *Aradus* within the bugs, sensilla must have developed independently in both genera. It is imaginable that, e.g., the dome-shaped surface provides a good surface-to-volume ratio allowing enhanced absorption of IR photons; the diameter of the sphere could reflect the penetration depth of IR photons into the cuticle of 3–4 μm (Schmitz et al. 2010).

Nevertheless, the routes of evolution toward an IR receptor in pyrophilous insects have found at least two other ways. IR receptors in *Merimna atrata* and *Acanthocnemus nigricans* are very different from each other and also from the photomechanic IR receptors. Currently, there is no concept available to trace back IR receptors in all genera of pyrophilous insects to a common ancestral form. Most probably, all receptors have evolved independently.

8.6 Matched Filters Permit the Best Possible Function of IR Receptors in Pyrophilous Insects

Despite of their independent evolution, insect IR receptors depicted in this chapter all show the same built-in filter properties! Remarkably, these filters were already preset by the absorption spectra of the gases in the atmosphere and the chemical composition of the insect cuticle. As depicted in Table 8.2, filters could be used (integrated into the sensor) without modifications enabling the underlying sensory cells to perceive a maximum of temperature increase and/or thermal expansion.

The atmospheric windows can be regarded as valuable filters (Filter 1) because emission maxima of relevant IR sources like fires or warm-blooded creatures are located within the MWIR and LWIR windows. These windows can be regarded as matched band-pass filters also accounted for in all technical IR sensors (Budzier and Gerlach 2011; Gaussorgues 1994).

Filter 2 is given by cuticular absorption. As pointed out in previous publications (Schmitz et al. 2007; Vondran et al. 1995; Schmitz and Bleckmann 1997), insect cuticle per se can be regarded as a composite material consisting of biopolymers that show strong IR absorption bands in the MWIR. This may have been a very important prerequisite for the evolution of all insect IR receptors. Because both filters perfectly match, an IR-sensitive pyrophilous insect is able to efficiently sense MWIR radiation by using its IR receptors that consist of optimized cuticular absorbers combined with appropriate sensory cells.

References

- Alonso-Zarazaga M, Sánchez-Ruiz M, Sánchez-Ruiz A (2003) Una nueva familia de Coleoptera para España: Acanthocnemidae. *Bol Soc Entomológica Aragonesa* 32:179–180
- Altner H, Loftus R (1985) Ultrastructure and function of insect thermo- and hygroreceptors. *Annu Rev Entomol* 30(1):273–295
- Amemiya F, Ushiki T, Goris RC, Atobe Y, Kusunoki T (1996) Ultrastructure of the crotaline snake infrared pit receptors: SEM confirmation of TEM findings. *Anat Rec* 246(1):135–146. doi:[10.1002/\(SICI\)1097-0185\(199609\)](https://doi.org/10.1002/(SICI)1097-0185(199609)246:1<135::AID-AR135>3.0.CO;2-1)
- Apel K-H (1991) Die Kiefernprachtkäfer. Merkblatt Nr. 50. Forschungsanstalt für Forst- und Holzwirtschaft, Eberswalde
- Baena M, Torres JL (2013) Notes on the biology and Iberian distribution of *Aradus flavicornis* (Dalman, 1823) (Hemiptera, Heteroptera, Aradidae). *Bol Asoc Esp Entomol* 37 (3–4):277–284
- Barth A (2007) Infrared spectroscopy of proteins. *Biochim Biophys Acta* 1767(9):1073–1101, doi:[http://dx.doi.org/10.1016/j.bbaprot.2007.06.004](https://doi.org/10.1016/j.bbaprot.2007.06.004)
- Bellamy CL (2008) A world catalogue and bibliography of the jewel beetles (Coleoptera: Buprestoidea), vol 3, Buprestinae: Pterobothrini through Agrilinae: Rhaeboscelina. Faunistica. Pensoft, Sofia
- Bernard J (1974) Etude électrophysiologique de récepteurs impliqués dans l'orientation vers l'hôte et dans l'acte hématophage chez une Hémiptère: *Triatoma infestans*. Dissertation, University of Rennes
- Bond WJ, Keeley JE (2005) Fire as a global 'herbivore': the ecology and evolution of flammable ecosystems. *Trends Ecol Evol* 20(7):387–394, doi:[http://dx.doi.org/10.1016/j.tree.2005.04.025](https://doi.org/10.1016/j.tree.2005.04.025)
- Bowmaker J, Hunt D (2006) Evolution of vertebrate visual pigments. *Curr Biol* 16(13):R484–R487. doi:[10.1016/j.cub.2006.06.016](https://doi.org/10.1016/j.cub.2006.06.016)
- Budzier H, Gerlach G (2011) Thermal infrared sensors. Wiley, Chichester
- Bullock TH, Barrett R (1968) Radiant heat reception in snakes. *Commun Behav Biol* 1:19–29
- Bullock TH, Fox W (1957) The anatomy of the infra-red sense organ in the facial pit of pit vipers. *Q J Microsc Sci* 3(42):219–234
- Champion GC (1918) A note on the habits of a *Melanophila* (Buprestidae) and other Indian Coleoptera. *Entomol Mon Mag* 54:199–200
- Champion GC (1922) The geographical distribution and synonymy of the dasytid-beetle *Acanthocnemus nigricans* Hope (= *ciliatus* Perris). *Entomol Mon Mag* 58:77–79

- Chapman RF (1998) The insects: structure and function, 4th edn. Cambridge University Press, Cambridge, UK
- D'Amico A, Di Natale C, Castro FL, Iarossi S, Catini A, Martinelli E (2008) Volatile compounds detection by IR acousto-optic detectors. In: Byrnes J (ed) Unexploded ordnance detection and mitigation. Springer, Ciocco, pp 21–59
- Deyrup M, Mosley JG (2004) Natural history of the flat bug *Aradus glaucicornis* in fire-killed pines (Heteroptera: Aradidae). Fla Entomol 87(1):79–81. doi:[10.1653/0015-4040\(2004\)087\[0079:NHOTFB\]2.0.CO;2](https://doi.org/10.1653/0015-4040(2004)087[0079:NHOTFB]2.0.CO;2)
- Douglas RH, Partridge JC, Dulai K, Hunt D, Mullineaux CW, Tauber AY, Hynninen PH (1998) Dragon fish see using chlorophyll. Nature 393(6684):423–424. doi:[10.1038/30871](https://doi.org/10.1038/30871)
- Ebert J, Westhoff G (2006) Behavioural examination of the infrared sensitivity of rattlesnakes (*Crotalus atrox*). J Comp Physiol A 192(9):941–947. doi:[10.1007/s00359-006-0131-8](https://doi.org/10.1007/s00359-006-0131-8)
- Evans WG (1964) Infra-red receptors in *Melanophila acuminata* DeGeer. Nature 202 (4928):211–211
- Evans WG (1966a) Morphology of the infrared sense organ of *Melanophila acuminata* (Buprestidae: Coleoptera). Ann Entomol Soc Am 59:873–877
- Evans WG (1966b) Perception of infrared radiation from forest fires by *Melanophila acuminata* de Geer (Buprestidae, Coleoptera). Ecology 47(6):1061–1065. doi:[10.2307/1935658](https://doi.org/10.2307/1935658)
- Evans HF, Moraal LG, Pajares JA (2007) Biology, ecology and economic importance of Buprestidae and Cerambycidae. In: Lieutier F, Day KR, Battisti A, Grégoire J-C, Evans HF (eds) Bark and wood boring insects in living trees in Europe, a synthesis. Springer, Dordrecht, pp 447–474
- Field LH, Matheson T (1998) Chordotonal organs of insects. In: Evans PD (ed) Advances in insect physiology, vol 27. Academic, San Diego, pp 1–228
- French AS (1992) Mechanotransduction. Annu Rev Physiol 54(1):135–152. doi:[10.1146/annurev.ph.54.030192.001031](https://doi.org/10.1146/annurev.ph.54.030192.001031)
- Froeschner RC (1988) Family Aradidae Spinola 1837 (=Dysodiidae Reuter, 1912; Meziridae Oshanin, 1908), the flat bugs. In: Henry TJ, Froeschner RC (eds) Catalog of the Heteroptera, or true bugs, of Canada and the United States. E. J. Brill Co., New York, pp 29–46
- Gaussorgues G (1994) Infrared thermography, vol 5, Microwave technology. Chapman & Hall, London
- Gingl E, Tichy H (2001) Infrared sensitivity of thermoreceptors. J Comp Physiol A Sens Neural Behav Physiol 187(6):467–475
- Göpfert MC, Robert D (2001) Active auditory mechanics in mosquitoes. Proc R Soc Lond Ser B Biol Sci 268(1465):333–339. doi:[10.1098/rspb.2000.1376](https://doi.org/10.1098/rspb.2000.1376)
- Göpfert MC, Robert D (2003) Motion generation by *Drosophila* mechanosensory neurons. Proc Natl Acad Sci 100(9):5514–5519. doi:[10.1073/pnas.0737564100](https://doi.org/10.1073/pnas.0737564100)
- Gracheva EO, Ingolia NT, Kelly YM, Cordero-Morales JF, Hollopeter G, Chesler AT, Sanchez EE, Perez JC, Weissman JS, Julius D (2010) Molecular basis of infrared detection by snakes. Nature 464(7291):1006–1011. doi:[10.1038/nature08943](https://doi.org/10.1038/nature08943)
- Gracheva EO, Cordero-Morales JF, Gonzalez-Carcacia JA, Ingolia NT, Manno C, Aranguren CI, Weissman JS, Julius D (2011) Ganglion-specific splicing of TRPV1 underlies infrared sensation in vampire bats. Nature 476(7358):88–91. doi:[10.1038/nature10245](https://doi.org/10.1038/nature10245)
- Guerestein PG, Lazzari CR (2009) Host-seeking: how triatomines acquire and make use of information to find blood. Acta Trop 110:148–158
- Hawkeswood TJ (2007) Review of the biology of the genus *Merimna* Saunders, 1868 (Coleoptera: Buprestidae). Calodema 9:12–13
- Hawkeswood TJ, Peterson M (1982) A review of the larval host records for Australian jewel beetles (Coleoptera: Buprestidae). Vic Nat (Blackburn) 99:240–251
- Heiss E, Pericart J, de France F (2007) Hemiptères Aradidae Piesmatidae et Dipsocoromorphes Euro-méditerranéens, vol 91, Faune de France. Fédération Française des Sociétés de Sciences Naturelles, Paris

- Herzberg H, Huber K-P (1950) Molecular spectra and molecular structure. I. Spectra of diatomic molecules. Van Nostrand Reinhold, New York
- Hesse M, Meier H, Zeeh B (1995) Spektroskopische Methoden in der organischen Chemie, 5th edn. Georg Thieme Verlag, Stuttgart
- Horion A (1955) Faunistik der mitteleuropäischen Käfer. 4. Sternoxia (Buprestidae), Fossipedes, Macroductylia, Brachymera. In: Entomologische Arbeiten aus dem Museum G. Frey, Sonderband. Selbstverlag, München
- Insausti TC, Lazzari CR, Campanucci VA (1999) Neurobiology of behaviour. A morphology of the nervous system and sense organs. In: Carcavallo RU, Giron IG, Jurberg J, Lent H (eds) Atlas of chagas disease vectors in America, vol 3. Editoria Fiocruz, Rio de Janeiro, pp 1017–1051
- Johansson T, Hjältén J, Stenbacka F, Dynesius M (2010) Responses of eight boreal flat bug (Heteroptera: Aradidae) species to clear-cutting and forest fire. *J Insect Conserv* 14(1):3–9. doi:[10.1007/s10841-009-9218-1](https://doi.org/10.1007/s10841-009-9218-1)
- Kahl T, Bousack H, Schneider ES, Schmitz H (2014) Infrared receptors of pyrophilous jewel beetles as model for new infrared sensor. *Sens Rev* 34(1):123–134
- Kitchin DR (2009) Notes on the biology of *Merimna atrata* (Gory & Laporte) (Coleoptera: Buprestidae). *Aust Entomol* 36(1):1–2
- Kovalenko YN (2011) Acanthocnemidae (Coleoptera), a family of beetles new to Russia. *Zoosystematica Rossica* 20(1):71–73
- Kreiss E-J, Schmitz A, Schmitz H (2005) Morphology of the prothoracic discs and associated sensilla of *Acanthocnemus nigricans* (Coleoptera, Acanthocnemidae). *Arthropod Struct Dev* 34(4):419–428. doi:[10.1016/j.asd.2005.06.001](https://doi.org/10.1016/j.asd.2005.06.001)
- Kreiss E-J, Schmitz H, Gebhardt M (2007) Electrophysiological characterisation of the infrared organ of the Australian “Little Ash Beetle” *Acanthocnemus nigricans* (Coleoptera, Acanthocnemidae). *J Comp Physiol A Sens Neural Behav Physiol* 193(7):729–739
- Kürten L, Schmidt U (1982) Thermoperception in the common vampire bat (*Desmodus rotundus*). *J Comp Physiol* 146(2):223–228. doi:[10.1007/bf00610241](https://doi.org/10.1007/bf00610241)
- Kürten L, Schäfer K, Schmidt U (1984a) Wärmewahrnehmung bei der Vampirfledermaus *Desmodus rotundus* – Verhaltens- und elektrophysiologische Untersuchungen. *Verh Dtsch Ges Pathol* 77:303
- Kürten L, Schmidt U, Schäfer K (1984b) Warm and cold receptors in the nose of the vampire bat *Desmodus rotundus*. *Naturwissenschaften* 71(6):327–328. doi:[10.1007/BF00396621](https://doi.org/10.1007/BF00396621)
- Lappalainen H, Simola H (1998) The fire-adapted flatbug *Aradus laevisculus* Reuter (Heteroptera, Aradidae) rediscovered in Finland (North Karelia, Koli National Park). *Entomol Fenn* 9(1):3–4
- Lazzari CR, Núñez J (1989) The response to radiant heat and the estimation of the temperature of distant sources in *Triatoma infestans*. *J Insect Physiol* 35(6):525–529, doi:[http://dx.doi.org/10.1016/0022-1910\(89\)90060-7](http://dx.doi.org/10.1016/0022-1910(89)90060-7)
- Lazzari C, Wicklein M (1994) The cave-like sense organ in the antennae of Triatominae bugs. *Mem Inst Oswaldo Cruz* 89(4):643–648
- Liberti G (2009) The Dasytidae (Coleoptera) of Sardinia. *Zootaxa* 2318:339–385
- Linsley EG (1933) Some observations on the swarming of *Melanophila*. *Pan Pac Entomol* 9:138
- Linsley EG (1943) Attraction of *Melanophila* beetles by fire and smoke. *J Econ Entomol* 36(2):341–342
- Mainz T, Schmitz A, Schmitz H (2004) Variation in number and differentiation of the abdominal infrared receptors in the Australian ‘fire-beetle’ *Merimna atrata* (Coleoptera, Buprestidae). *Arthropod Struct Dev* 33(4):419–430
- Manee AH (1913) Observations on Buprestidae at Southern Pines, North Carolina. *Entomol News* 24:167–171
- Mayor A (2007) Acanthocnemidae; Prionoceridae; Melyridae; Dasytidae. In: Löbl I, Smetana A (eds) Catalogue of Palaearctic Coleoptera, vol 4, Elateroidea – Derodontoidea – Bostrichoidea – Lymexyloidea – Cleroidea – Cucujoidea. Apollo Books, Stenstrup, pp 384–415

- Meuthen D, Rick IP, Thünken T, Baldauf SA (2012) Visual prey detection by near-infrared cues in a fish. *Naturwissenschaften* 99:1063–1066
- Mhatre N, Robert D (2013) A tympanal insect ear exploits a critical oscillator for active amplification and tuning. *Curr Biol* 23:1–6, doi:<http://dx.doi.org/10.1016/j.cub.2013.08.028>
- Michelsen A, Larsen ON (1985) Hearing and sound. In: Kerkut GA, Gilbert LI (eds) *Comprehensive insect physiology, biochemistry, and pharmacology*. Pergamon Press, New York, pp 495–556
- Molenaar GJ (1992) Anatomy and physiology of infrared sensitivity of snakes. In: Gans C, Ulinski PS (eds) *Biology of the reptilia*, vol 17, *Biology of the reptilia*. University of Chicago, Chicago, pp 367–453
- Neville AC (1975) *Biology of the arthropod cuticle*. Springer, Berlin
- Paczkowski S, Paczkowska M, Dippel S, Schulze N, Schütz S, Sauerwald T, Weiß A, Bauer M, Gottschald J, Kohl C-D (2013) The olfaction of a fire beetle leads to new concepts for early fire warning systems. *Sensors Actuators B* 183(0):273–282, doi:<http://dx.doi.org/10.1016/j.snb.2013.03.123>
- Poulton EB (1915) The habits of the Australian buprestid “fire-beetle” *Merimna atrata*, (Laporte and Gory). *Trans Entomol Soc Lond Part 1. (Proceedings):*iii–iv
- Ricksecker LE (1885) Habits of some California beetles. *Entomol Am* 1:96–98
- Rogalski A (2002) Infrared detectors: an overview. *Infrared Phys Technol* 43(3–5):187–210
- Saint-Germain M, Drapeau P, Buddle CM (2008) Persistence of pyrophilous insects in fire-driven boreal forests: population dynamics in burned and unburned habitats. *Divers Distrib* 14(4):713–720. doi:[10.1111/j.1472-4642.2007.00452.x](https://doi.org/10.1111/j.1472-4642.2007.00452.x)
- Schmitz H, Bleckmann H (1997) Fine structure and physiology of the infrared receptor of beetles of the genus *Melanophila* (Coleoptera: Buprestidae). *Int J Insect Morphol Embryol* 26(3–4):205–215
- Schmitz H, Bleckmann H (1998) The photomechanic infrared receptor for the detection of forest fires in the beetle *Melanophila acuminata* (Coleoptera: Buprestidae). *J Comp Physiol A* 182(5):647–657. doi:[10.1007/s003590050210](https://doi.org/10.1007/s003590050210)
- Schmitz H, Bousack H (2012) Modelling a historic oil-tank fire allows an estimation of the sensitivity of the infrared receptors in pyrophilous *Melanophila* beetles. *PLoS One* 7(5), e37627. doi:[10.1371/journal.pone.0037627](https://doi.org/10.1371/journal.pone.0037627)
- Schmitz H, Schmitz A (2002) Australian fire-beetles. *Landscape* 18(1):36–41
- Schmitz H, Trenner S (2003) Electrophysiological characterization of the multipolar thermoreceptors in the “ fire-beetle” *Merimna atrata* and comparison with the infrared sensilla of *Melanophila acuminata* (both Coleoptera, Buprestidae). *J Comp Physiol A Sens Neural Behav Physiol* 189(9):715–722
- Schmitz H, Bleckmann H, Murtz M (1997) Infrared detection in a beetle. *Nature* 386(6627):773–774
- Schmitz H, Schmitz A, Bleckmann H (2000a) A new type of infrared organ in the Australian “ fire-beetle” *Merimna atrata* (Coleoptera: Buprestidae). *Naturwissenschaften* 87(12):542–545
- Schmitz H, Trenner S, Hofmann MH, Bleckmann H (2000b) The ability of *Rhodnius prolixus* (Hemiptera; Reduviidae) to approach a thermal source solely by its infrared radiation. *J Insect Physiol* 46(5):745–751
- Schmitz H, Schmitz A, Bleckmann H (2001) Morphology of a thermosensitive multipolar neuron in the infrared organ of *Merimna atrata* (Coleoptera, Buprestidae). *Arthropod Struct Dev* 30(2):99–111
- Schmitz H, Schmitz A, Trenner S, Bleckmann H (2002) A new type of insect infrared organ of low thermal mass. *Naturwissenschaften* 89(5):226–229
- Schmitz A, Sehrbrock A, Schmitz H (2007) The analysis of the mechanosensory origin of the infrared sensilla in *Melanophila acuminata* (Coleoptera; Buprestidae) adduces new insight into the transduction mechanism. *Arthropod Struct Dev* 36(3):291–303
- Schmitz A, Gebhardt M, Schmitz H (2008) Microfluidic photomechanic infrared receptors in a pyrophilous flat bug. *Naturwissenschaften* 95(5):455–460. doi:[10.1007/s00114-008-0344-5](https://doi.org/10.1007/s00114-008-0344-5)

- Schmitz A, Schätzel H, Schmitz H (2010) Distribution and functional morphology of photomechanic infrared sensilla in flat bugs of the genus *Aradus* (Heteroptera, Aradidae). *Arthropod Struct Dev* 39(1):17–25. doi:[10.1016/j.asd.2009.10.007](https://doi.org/10.1016/j.asd.2009.10.007)
- Schneider ES, Schmitz H (2013) Bimodal innervation of the infrared organ of *Merimna atrata* (Coleoptera, Buprestidae) by thermo- and mechanosensory units. *Arthropod Struct Dev* 42(2):135–142. doi:<http://dx.doi.org/10.1016/j.asd.2012.11.001>
- Schneider ES, Schmitz H (2014) Thermomechanical properties of the stimulus transducing cuticle in the infrared organ of *Merimna atrata* (Coleoptera, Buprestidae). *J Morphol* 275(9):991–1003. doi:[10.1002/jmor.20276](https://doi.org/10.1002/jmor.20276)
- Schoenlein R, Peteanu L, Mathies R, Shank C (1991) The first step in vision: femtosecond isomerization of rhodopsin. *Science* 254(5030):412–415. doi:[10.1126/science.1925597](https://doi.org/10.1126/science.1925597)
- Sharp WE (1918) *Melanophila acuminata* in Berkshire. *Entomol Mon Mag* 54:244–245
- Shcherbakov D, Knörzer A, Espenhahn S, Hilbig R, Haas U, Blum M (2013) Sensitivity differences in fish offer near-infrared vision as an adaptable evolutionary trait. *PLoS One* 8(5), e64429. doi:[10.1371/journal.pone.0064429](https://doi.org/10.1371/journal.pone.0064429)
- Sloop KD (1937) A revision of the North American buprestid beetles belonging to the genus *Melanophila* (Coleoptera, Buprestidae), vol 7. University of California Publications in Entomology, Berkeley
- Stark KB, Gallas JM, Zajac GW, Golab JT, Gidanian S, McIntire T, Farmer PJ (2005) Effect of stacking and redox state on optical absorption spectra of melanins—Comparison of theoretical and experimental results. *J Phys Chem B* 109(5):1970–1977. doi:[10.1021/jp046710z](https://doi.org/10.1021/jp046710z)
- Terashima S-I, Goris RC, Katsuki Y (1970) Structure of warm fiber terminals in the pit membrane of vipers. *J Ultrastruct Res* 31(5–6):494–506
- Thurm U, Erler G, Gödde J, Kastrup H, Keil T, Völker W, Vohwinkel B (1983) Cilia specialized for mechanoreception. *J Submicrosc Cytol Pathol* 15(1):151–155
- Valcárcel JP, Piloña FP (2009) NOTA BREVE/SHORT NOTE Nota adicional sobre la presencia de *Acanthocnemus nigricans* (Hope, 1843) en la Península Ibérica. *Arq Entomoloxicos Galegos* 2:21
- VanDyke EC (1926) Buprestid swarming. *Pan Pac Entomol* 3:41
- Vondran T, Apel K-H, Schmitz H (1995) The infrared receptor of *Melanophila acuminata* De Geer (Coleoptera: Buprestidae): ultrastructural study of a unique insect thermoreceptor and its possible descent from a hair mechanoreceptor. *Tissue Cell* 27(6):645–658
- Wikars L-O (1992) Skogsbränder och insekter. *Entomol Tidskr* 113(4):1–12
- Wikars L-O (1997) Effects of forest fire and the ecology of fire-adapted insects. Uppsala University, Sweden
- Wyniger D, Moretti M, Duelli P (2002) *Aradus lugubris* Fallen, 1807 (Hemiptera, Heteroptera, Aradidae) in a chestnut forest of Southern Switzerland after a fire experiment. *Mitt Schweiz Entomol Ges* 75(1/2):61–64

Part V

Electroreception

Matched Filtering in African Weakly Electric Fish: Two Senses with Complementary Filters

Gerhard von der Emde and Tim Ruhl

Contents

9.1	Electroreception	238
9.2	Weakly Electric Fish	238
9.3	The Elephant Nose Fish <i>Gnathonemus petersii</i> as a Model System in Sensory Ecology	240
9.4	The Electric Sense in the Weakly Electric Fish <i>Gnathonemus petersii</i>	242
9.4.1	Prey Detection	242
9.4.2	The Electric Fovea Hypothesis	245
9.4.3	Production of Electric Signals and the Self-Produced Field of <i>G. petersii</i>	246
9.5	The Visual Sense in the Weakly Electric Fish <i>Gnathonemus petersii</i>	250
9.5.1	Anatomy, Morphology, and Cytoarchitecture of the <i>Gnathonemus</i> Retina	250
9.5.2	Anatomy of Visual Brain Areas	253
9.5.3	Functional Aspects of the Visual System	255
9.6	Partitioning of Environmental Sensing	258
	References	259

Abstract

African weakly electric fish live nocturnally in tropical freshwater streams. To sense their surroundings, they have developed a highly specialized system of two senses, which allows them to perceive nearby objects at high precision with an active electric sense and to detect large, fast-moving objects with their visual sense at greater distances. Both senses are highly specialized and are equipped with matched filters for efficient detection and analysis of relevant object features and for neglecting unimportant items. Active electrolocation in the near field involves the production of an electric signal, which serves as a carrier for sensory information. This signal and the resulting electric field around the fish are shaped by the fish's body and its internal structure. The electric skin

G. von der Emde (✉) • T. Ruhl
Institute for Zoology, University of Bonn, Endenicher Alle 11-13, 53115 Bonn, Germany
e-mail: vonderemde@uni-bonn.de

properties and the accessory structures of the electroreceptor organs further filter the signal and form two electroreceptive foveae. In contrast, the visual system is adapted for detecting large objects at longer distances. A grouped retina forms a visual matched filter, which filters out small, nearby objects but efficiently detects fast-moving distant objects even under noisy and dim light conditions.

9.1 Electroreception

Many aquatic animals are able to detect naturally occurring electric signals coming from the environment. Electroreception is an ancient sensory modality which was present already in early fishlike vertebrates (Bullock et al. 1983). The fact that electroreception is still present in most fish taxa, with the notable exception of many teleosts, shows that the perception of electric signals offers an advantage in the aquatic habitat. The majority of electroreceptive animals use *passive* electrolocation, during which they can detect and analyze electric signals from the environment (Bodznick and Montgomery 2005; Wilkens and Hofmann 2005). Besides fish, only a few vertebrates and maybe some invertebrates possess this sense, i.e., several aquatic urodele amphibians, the platypus (*Ornithorhynchus anatinus*), the short-beaked echidna (*Tachyglossus aculeatus*) (Pettigrew 1999; Proske et al. 1998; Scheich et al. 1986), and the Guiana dolphin (*Sotalia guianensis*) (Czech-Damal et al. 2012). All these animals probably detect environmental electric fields for orientation and for prey detection, i.e., to find and identify benthic prey animals by the electric fields they unintentionally emit. Passively electrolocating animals have developed matched filters for these types of signals, which, however, will not be reviewed in this chapter (for additional information, see, e.g., Hofmann et al. 2005).

9.2 Weakly Electric Fish

In addition to being able to passively perceive environmental electric signals, weakly electric fish can actively produce electric signals for the purpose of *active* electrolocation (Lissmann and Machin 1958) and for electrocommunication (Szabo and Moller 1984). African (Mormyriiformes) and South American (Gymnotiformes) weakly electric fish use specialized electric organs to produce their high frequency electric signals (i.e., with significant energy up to about 5 kHz or more), which are therefore called electric organ discharges (EOD). There are two main types of EODs: (1) brief, pulse-like signals and (2) continuous wave-type discharges. Pulse-type EODs have a duration that is much shorter than the inter-pulse intervals, which means they can be shorter than 200 μ s in some mormyrids, while other species generate EODs with durations of several milliseconds. In the case of mormyrids, inter-pulse intervals of single individuals are highly variable

and depend on the behavioral context. Most pulse-type EODs have extremely constant waveforms, which depends on the species, the sex, and the hormonal state of the sender animal. Since the animals cannot vary the EOD waveform on a short-term basis, they have to rely on other means such as modulating the inter-pulse intervals to change the information content during electrocommunication.

Since weakly electric fish produce their own signals for environmental sensing and for electrocommunication, they have to invest stimulus – energy. Even though there are no experimental studies on the costs of electric signaling in mormyrids, it has been found that in the gymnotiform pulse-fish *Brachyhypopomus gauderio* females allocate only a small fraction (3 %) of their daily energy budget to electrogenesis. In contrast, males of this species invest daily 11–22 %, on average 15 %, of their energy into the production of their sexually dimorphic signals (Salazar and Stoddard 2008; Stoddard and Salazar 2011). This discrepancy originates from males producing EODs of higher amplitude and longer duration than females in order to signal territory ownership and attract females. Their high energy allocation therefore serves communicative functions during female sexual selection, while EODs in females are used for navigational purposes only. Males may respond to these high energetic costs by showing a daily plasticity in EOD production with EOD duration and amplitude being reduced during daytime, when the fish are inactive and resting. In a recent article, the energetics of electric organ discharge generation in gymnotiform weakly electric fish was investigated in a theoretical analysis (Salazar et al. 2013). This study showed that performance-related costs of EOD generation in Gymnotiformes can be surprisingly high, up to 30 % of the routine energy consumption, but it depends very much on the species, the sex, and the behavioral situation of the animal. Similar studies on the mormyrid *G. petersii* are missing, but it can be assumed that for mormyrids, energy costs for EOD production may be similar to those measured for female Gymnotiformes, indicating that in general production of navigational signals in African electric fish may represent only a relatively small fraction of their total energy budget (Stoddard and Salazar 2011), similar to a bat's navigational sonar (Speakman and Ravey 1991). In contrast, the processing of electrosensory input in mormyrids may be much more costly. In one study, it was shown that the huge brain of *G. petersii* is responsible for 60 % of the resting energy consumption (Nilsson 1996).

Weakly electric fish are usually active at night, and in the absence of light, they use their EODs for active electrolocation and electrocommunication. An advantage of the use of electric signals for these tasks in contrast to acoustic or visual signals is that EOD waveform is only little distorted by the environment (Hopkins 2009). Whereas acoustic signals are often distorted by the medium and objects within it in various and often frequency-dependent ways (reflection, refraction, scattering, attenuation), electric signals are only attenuated (but not in a frequency-dependent way) and their waveforms pass almost unaffected through the medium, even if this is turbid and noisy. As a consequence, the shape of the received signals varies only slightly from the emitted signals. Weakly electric fish exploit this fact by using

temporal and waveform cues during both electrocommunication and active electrolocation (von der Emde 2011).

All electroreceptive animals possess specialized electroreceptor organs, which are located in their skins (Hopkins 2009). In weakly electric fish, three types of special receptor organs are used for passive electrolocation, for active electrolocation, and for electrocommunication. During active electrolocation, a weakly electric fish discharges its electric organ and thus builds up an electric field around its body that is perceived by an array of cutaneous electroreceptor organs that are distributed over almost the entire body surface of the fish (Hollmann et al. 2008). Objects differing in electric impedance from the surrounding water are detected because they interact with the electric field and modulate the EOD amplitude and waveform, which is detected by the animal's electroreceptor organs (von der Emde and Engelmann 2011).

9.3 The Elephant Nose Fish *Gnathonemus petersii* as a Model System in Sensory Ecology

In this chapter, we will concentrate on the weakly electric fish *Gnathonemus petersii*, the elephantnose fish, which is a well-studied example for sensory adaptations and matched filtering in several sensory modalities. *Gnathonemus* is well known for its movable chin appendix, the Schnauzenorgan, a characteristic fingerlike sense organ covered densely by electroreceptor organs (Amey-Özel et al. 2015). Since we know a lot not only about *G. petersii*'s electric sense but also about its visual sense, this species is a perfect example of how animal senses adapt to environmental conditions and how different sensing tasks are allocated to different sensory modalities.

G. petersii lives in small creeks and rivers of Central and West Africa, where – at least seasonally – floods might cause a high turbidity of the water (Moller 1995). The major freshwater environments inhabited by *G. petersii* are moist forest rivers, but they were also found in savanna/dry forest rivers as well as in floodplains, swamps and lakes, and large river deltas (Moritz 2010). Common features of all these habitats are relative low light levels because of shade provided by tree or bush cover, a reddish color of the water, and often rather fast-flowing currents (Fig. 9.1). The water is of low electric conductivity, usually below 100 $\mu\text{s/cm}$, and has temperatures above 25° C. *G. petersii* was regularly observed within fast-flowing parts of the river (e.g., under roots and driftwood), in holes in the embankment, or at sites of dense vegetation, always close to current (Moritz 2010). The turbidity of the water was found to be relatively high, with turbidity values between 45 and 1,670.5 FTU (Ogbeibu and Ezeunara 2005; Francke et al. 2014). In such an environment, active electrolocation offers clear advantages, because electric signals in contrast to visual or acoustic signals are better suited to pass unaffected through the turbid and noisy water environment (Hopkins 2009).

Like most mormyrids, *G. petersii* hides during the day, becomes active at dusk, and stays so throughout the night (Moller et al. 1979; Okedi 1965). It is a bottom



Fig. 9.1 Typical habitat of *Gnathonemus petersii*, the Iguidi river in Benin, a relatively fast-moving creek during daytime. *G. petersii* (inset) lives in red-colored forest streams shaded by vegetation (Photo by Vivica von Vietinghoff. Inset photo by Maik Dobiéy taken in the lab of the authors)

feeder, searching for small insect larvae, mainly chironomids (Diptera), which are buried in the soil. *G. petersii* digs them out, using its Schnauzenorgan. This is also indicated by the large amount of sand and organic matter found in their stomachs (Nwani et al. 2011). For detecting its prey on the ground, the active electric sense (active electrolocation) plays a dominant role, accompanied by the chemical senses (von der Emde and Bleckmann 1998). To do so, the fish have evolved a special matched filter for electric prey detection (see below). The presence of light does not improve prey detection, suggesting that vision is not used for prey identification. The prey items are rather small and thus probably not visually detectable by the fish, since *G. petersii* cannot see objects spanning less than about 3° of visual angle (see below, Schuster and Amtsfeld 2002; Landsberger et al. 2008; Kreysing et al. 2012).

Generally, the dominant sense for object detection and identification in *G. petersii* is the active electric sense. It is very difficult to train the fish to react to the presence of an object which they only can see but not electrolocate (Schuster and Amtsfeld 2002; Landsberger et al. 2008). In contrast, several studies have shown that *G. petersii* can quickly and easily learn to discriminate electrically between two objects differing in shape, size, material composition, or distance (von der Emde et al. 2010; von der Emde and Fetz 2007). These studies also showed that the fish usually do not use vision to discriminate between stationary objects (even large objects of several centimeter size).

Nevertheless, the eyes of *G. petersii* are large and well developed, and the fish obviously respond to visual signals, which can be noticed easily when keeping the fish in an aquarium. So, what is the function of the visual sense in these animals? Below, we will argue that these fish have a division of labor between the active electric and the visual senses: Since the electric sense takes over the tasks of prey detection and close-up object inspection, the visual sense has evolved a matched filter for the detection of large moving objects and the detection of self-movement in fast water currents. In addition, the fish have developed a unique anti-noise filter, which allows them to see through turbid (“noisy”) waters carrying lots of small particles.

9.4 The Electric Sense in the Weakly Electric Fish *Gnathonemus petersii*

9.4.1 Prey Detection

As mentioned above, *G. petersii* employs active electrolocation for navigating in its environment and for detecting prey (mosquito larvae) during its nocturnal activity period. Detecting a partially buried, tiny insect larva on the ground of a tropical river is not an easy task, considering the abundance of many similarly shaped nearby objects, which may have similar electric resistances as the prey. One might think that prey detection and especially prey identification is like finding a “needle in the haystack” and requires complex and thus “costly” neural machinery with a lot of signal processing power. However, as shown below, this is not the case. The solution to the problem is the exploitation of characteristic sensory features of living prey items and the use of matched filters for their detection.

Finding prey might be easier for an electric fish if the prey item has unique properties, which are absent in the multitude of other objects surrounding the prey. It was suggested that such a unique mark might be the *capacitive properties*, which only living objects (water plants, other fishes, and insect larvae) possess in addition to resistive components (Schwan 1963; Heiligenberg 1973). To test whether mormyrids can perceive capacitive object properties, behavioral experiments were conducted. It turned out that indeed *G. petersii* (von der Emde 1990) and other mormyrids (von der Emde and Ringer 1992) can unambiguously discriminate between resistive and capacitive objects. They can distinguish a capacitor from a resistor, and thus a living prey item from a dead object, by measuring the capacitive-induced *waveform distortions* of the locally perceived EOD (von der Emde and Bleckmann 1992a). Waveform distortions only occur in the presence of capacitive, i.e., living, objects. They depend on the capacitive value of the object (as well as on its size and shape) and are thus unique indicators of certain prey items. Using active electrolocation, mormyrids are able to measure quantitatively even very small EOD waveform distortions caused by a living object and thus identify their prey (von der Emde and Ronacher 1994). Because of this, it was suggested that capacitive properties of prey items are like colors of visually

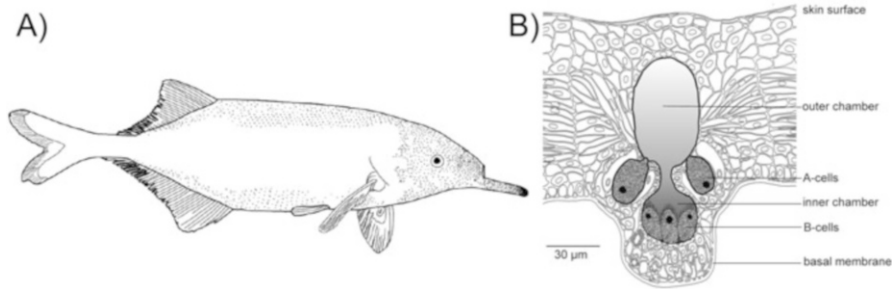


Fig. 9.2 (a) Density of mormyromast electroreceptors over the body surface of *G. petersii* (Modified after Hollmann et al. 2008), showing highest numbers of electroreceptor organs at the tip of the Schnauzenorgan. (b) Drawing of a section through the skin of *G. petersii* with a mormyromast organ (Modified after von der Emde et al. 2008)

perceived objects, and in analogy, capacitance detection was called “electric color perception” in weakly electric fish (von der Emde 1993; von der Emde and Schwarz 2002). A living insect larva on the ground of the river thus stands out of the surrounding inanimate objects by having an “electric color” and is thus quickly detected and identified by foraging *G. petersii*.

9.4.1.1 Matched Filters for Prey Identification

According to Wehner’s definition (1987), a matched filter is an arrangement of specialized sensory elements in such a way that it is matched to the sensory stimuli to be received. As a consequence, the sensors respond optimally only to those stimuli that the animal aims to detect, while other stimuli are discarded. Because the unwanted stimuli do not even reach the brain, the nervous system is freed of dealing with them and can concentrate on the relevant aspects of sensory input. The periphery takes over the task of filtering the sensory input, which results in a fast and effective recognition of relevant sensory information.

The relevant stimuli for prey identification are the waveform distortions of the local EOD, which are caused by the capacitive properties of the prey items. How are they detected? The local EOD has a duration of only about 500 μs , and to detect minute distortions of such a short signal might require an extremely fast receptor unit with a sampling rate in the nanosecond range, which a biological receptor cell cannot achieve. The solution to this problem is matched filtering realized by pre-receptor mechanisms of the electroreceptor organs.

The electroreceptor organs used for active electrolocation are the so-called mormyromasts (Szabo and Wersäll 1970). There are about 2,500 mormyromasts in the skin of a *G. petersii*, and they are distributed over large parts of the body surface except for an area at the flanks of the animal (Fig. 9.2a). Like all electroreceptor organs, mormyromasts are located in the epidermis and contain several electroreceptor cells and supporting structures. Each mormyromast houses two types of receptor cells that are tuned to different aspects of the signal carrier, i.e.,

one channel for amplitude and one for waveform coding. A-cells are found at the basal part of the outer chamber, while B-cells are located inside of an inner chamber (Fig. 9.2b). Both are innervated by separate nerve fibers, which project to the brain, where type A and B afferents terminate in separate areas (Bell 1990). The most important difference between A- and B-type afferent fibers is the sensitivity of only the B-cells to waveform distortions of the EOD, such as those which are caused by capacitive objects (von der Emde and Bleckmann 1992a). Type B cells are exquisitely sensitive to such distortions, whereas type A cells are not. Both are similarly sensitive to changes in EOD amplitude. It follows that in the presence of a capacitive object, B-cells but not A-cells will respond by firing more action potentials because of the waveform distortions caused by the object. These findings suggest that the fish sense the capacitive properties of objects independently of the resistive properties, by centrally comparing the responses of A- and B-cells.

How does the waveform sensitivity of the B-cells come about? A “normal” electroreceptor cell would not respond to waveform distortions at all, but would require other signal properties such as higher signal amplitudes to increase firing. The B-cells are located inside an inner chamber of the mormyromast, which is connected to an outer chamber through a small canal. The outer chamber houses the A-cells and is connected by another canal to the surface of the skin, where the mormyromast forms a small pore (Fig. 9.2b) (Amey-Özel et al. 2012). The chambers and the canals of the whole organ are loosely filled with epidermal cells, and the walls are made by supporting cells, which form a tight barrier between the surrounding tissue and the inside of the chambers. This arrangement of the mormyromast is crucial for the sensory properties of the electroreceptor organ and for the waveform sensitivity of the B-cells, in particular. The building blocks of the mormyromasts shape, or filter, the sensory signal (the locally occurring EOD) in such a way that even minor waveform distortions of the local EOD caused by living prey items will depolarize the membrane of B-cells and cause it to fire action potentials (von der Emde and Bleckmann 1992b). This filtering is exactly matched to those waveform distortions, which are caused by living objects. Other, unnatural types of waveform distortions are not affective and will either not work at all or even inhibit the receptor cell (von der Emde and Bleckmann 1997).

As mentioned above, A-cells do not respond to waveform distortions and therefore should not change their firing activity in the presence of a capacitive object that does not change signal amplitude. To our surprise, however, when recording from A-cell afferents, we found that A-cells responded negatively, i.e., with a reduced firing activity, when a capacitive object approached the receptor pore (von der Emde and Bleckmann 1992a). The reason for this is that A-cells are tuned to much lower frequencies than those at the peak of the spectrum of a single EOD. Capacitive objects not only distort the EOD waveform but in addition they shift the peak power spectral frequency to higher values, even further away from the optimal frequency of the A-cell's tuning curve. A frequency shift to higher values thus causes A-cells to fire less when a capacitive object is present. As a result, capacitive objects evoke an opposite response in A- and B-cells, which increases the contrast in firing behavior between the two cell types. All this is achieved by the

peripheral filtering apparatus of the receptor organ, only, and without any neural processing.

The described matched filter for capacitive object properties is located in the periphery of the electrosensory system and makes complex neural machinery for signal analysis unnecessary. Instead of involving a multitude of downstream neurons in the brain, the job is done in the periphery by the membrane properties of the receptor cells and by a certain arrangement of supporting non-sensory structures of simple and “cheap” epidermal cells.

9.4.2 The Electric Fovea Hypothesis

Mormyrid fish possess three types of epidermal electroreceptor organs, each containing at least one type of electroreceptor cell. In addition to the mormyromasts, which are exquisitely employed for active electrolocation, African electric pulse fish also have so-called ampullary receptor organs (used for passive electrolocation) and Knollenorgan receptor organs (used for electrocommunication). Electroreceptor organs form arrays on the skin of weakly electric fish and the spatial arrangement of the organs affects the functional properties of the whole array during environmental imaging. A certain arrangement can therefore be regarded as a kind of filter that can extract certain stimulus parameters and dismiss others. This principle can be shown for the array of mormyromast receptor organs, which are used for imaging of the environment during active electrolocation. In most mormyrids, mormyromasts are distributed unevenly over the body surface and generally occur at highest density at the head, especially at the Schnauzenorgan, while the tail and the lateral sides of the trunk are free of electroreceptor organs (Harder 1968). Hollmann et al. (2008) divided the fish’s electrosensitive skin into three regions: the Schnauzenorgan, where a continuous decrease from extremely high concentration of mormyromasts at the tip toward moderate density at the base was found; the nasal region above the mouth, where a moderate yet still about three-times higher density occurred compared with the third region, which is the rest of the body (Fig. 9.2a). A similar concentration of receptor organs employed for active electrolocation around the snout was observed in some South American electric fish leading to the idea that this arrangement bears some resemblance to the visual fovea in the retina of vertebrate eyes. Castello et al. (2000) suggested that Gymnotiformes have an electric fovea and a “parafovea” around their mouth and von der Emde and Schwarz (2001b, 2002) described two electric foveae in *G. petersii*, at the Schnauzenorgan and at the nasal region.

G. petersii has two areas of high receptor organ densities, one at the Schnauzenorgan and the second one at the nasal region. Both of these regions can be regarded as electric foveae, because besides a high receptor density, they have additional specializations that turn them into specialized matched filters (von der Emde et al. 2008). The receptor organs in the foveal regions are smaller and have fewer receptor cells than those outside the foveae (Amey-Özel et al. 2012). As in the visual fovea, both foveal regions of *G. petersii* are overrepresented in the brain,

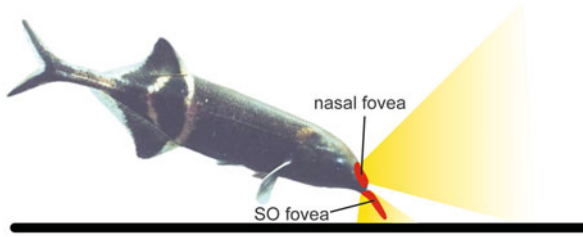


Fig. 9.3 Swimming posture of *G. petersii* when searching for prey on the ground. The two electric foveae at the nasal region and the Schnauzenorgan (SO) are highlighted in red, and their regions of sensory input are indicated by yellow areas

which means that more nerve cells process the information from a single receptor organ (Bacelo et al. 2008). Finally, there are behavioral adaptations for focusing an object of interest onto the fovea for detailed analysis. Because the nasal region has a circumferential view of the surroundings, by placing it at an angle of ca. 50° relative to the ground, it is brought into a position to optimally inspect the space in front of and at the side of the animal during foraging (Fig. 9.3). In contrast, the Schnauzenorgan performs rhythmic left-right movements. This ensures that during foraging it performs sweeping movements over the ground in order to detect possible prey items with its sensible tip (Fig. 9.3). When an object of interest is encountered, the Schnauzenorgan interrupts its left and right rhythm and moves over the object, following its outline in a certain “fixation pattern.”

The two foveae serve different functions: the nasal region is a long-range guidance system that is used to detect obstacles or other large objects during foraging. Because of the properties of the skin and the internal tissue of the fish (see below) and because of the arrangement of the mormyromast receptor organs, the nasal fovea responds best to larger objects in front of and at the side of the animal. The Schnauzenorgan, on the other hand, is short-range movable (prey) detection system that is used to find and identify prey on the ground or inspect details of objects. The anatomical structure of the Schnauzenorgan fovea and the special arrangement of mormyromasts turn this area into an effective prey detection device, i.e., a matched filter for living chironomid larvae in and on the ground (see above). Even without neural processing by specialized brain areas, the electroreceptors at the two electric foveae respond only to the relevant stimuli they are specialized for.

9.4.3 Production of Electric Signals and the Self-Produced Field of *G. petersii*

As shown above, weakly electric fish developed matched filters that delegate certain tasks of signal analysis into the periphery. Because *G. petersii* uses an active electrosensory system, matched filtering in these animals also involves the production of the appropriate EODs, which function as the carriers of

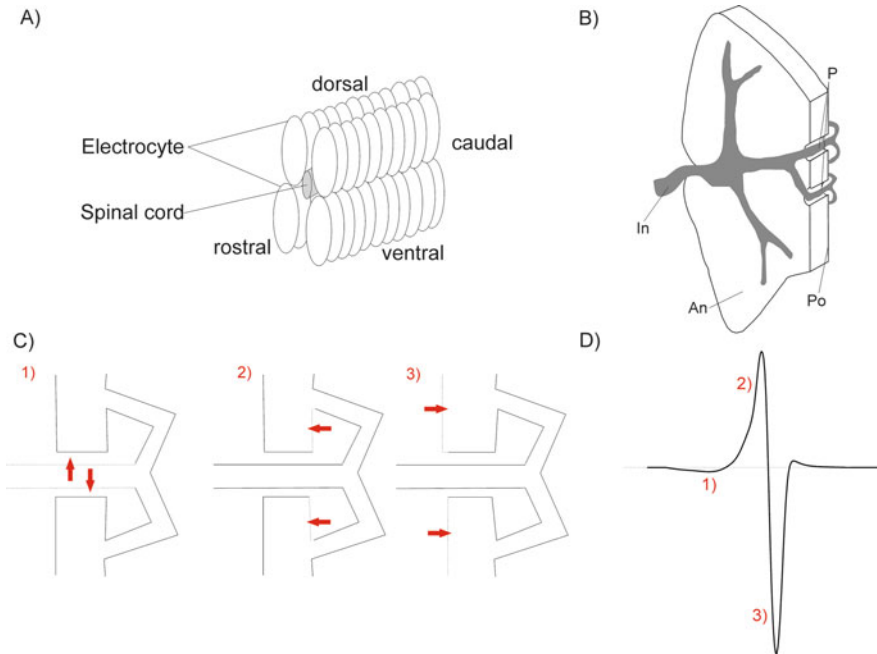


Fig. 9.4 (a) Simplified organization of *G. petersii*'s electric organ located in the caudal peduncle of the tail (Modified after Carlson and Gallant 2013). (b) PA-type electrocyte; Penetrating with anterior innervation of stalk (*In* innervation, *An* anterior, *Po* posterior, *P* penetration) (Modified after Cheng 2012) (c) Depolarizing current flow through electrocyte, which determines EOD polarity and number of phases (Modified after Carlson and Gallant 2013). (d) *Gnathonemus* EOD with references to phases of (c)

electrosensory information. Especially at the two foveal regions, the electric field is conditioned by pre-receptor mechanisms to provide a suitable carrier for the respective filtering task.

In mormyrids, the electric organ which emits the EOD is localized in the caudal peduncle of the fish (Fig. 9.4a, b). Electric organs of mormyrids evolved out of the skeletal musculature which used to move the tail of the animals. Tail movement now is achieved through tendons connecting the tail fin to muscles in the trunk anterior to the caudal peduncle. The electric organ consists of hundreds of electrocytes arranged in four columns, which all fire synchronously and thus emit an extremely constant and precise electric signal that builds up an electric field around the animal and ultimately stimulates the epidermal electroreceptor organs (Fig. 9.5a).

Mormyrids produce a short multiphasic electric signal, which has a species-specific (and sometimes sex specific) extremely constant waveform and frequency composition. This constancy is important for active electrolocation, because the electroreceptors respond to even minute changes in signal amplitude and waveform caused by nearby objects. The waveform of the EOD needs to be constant and

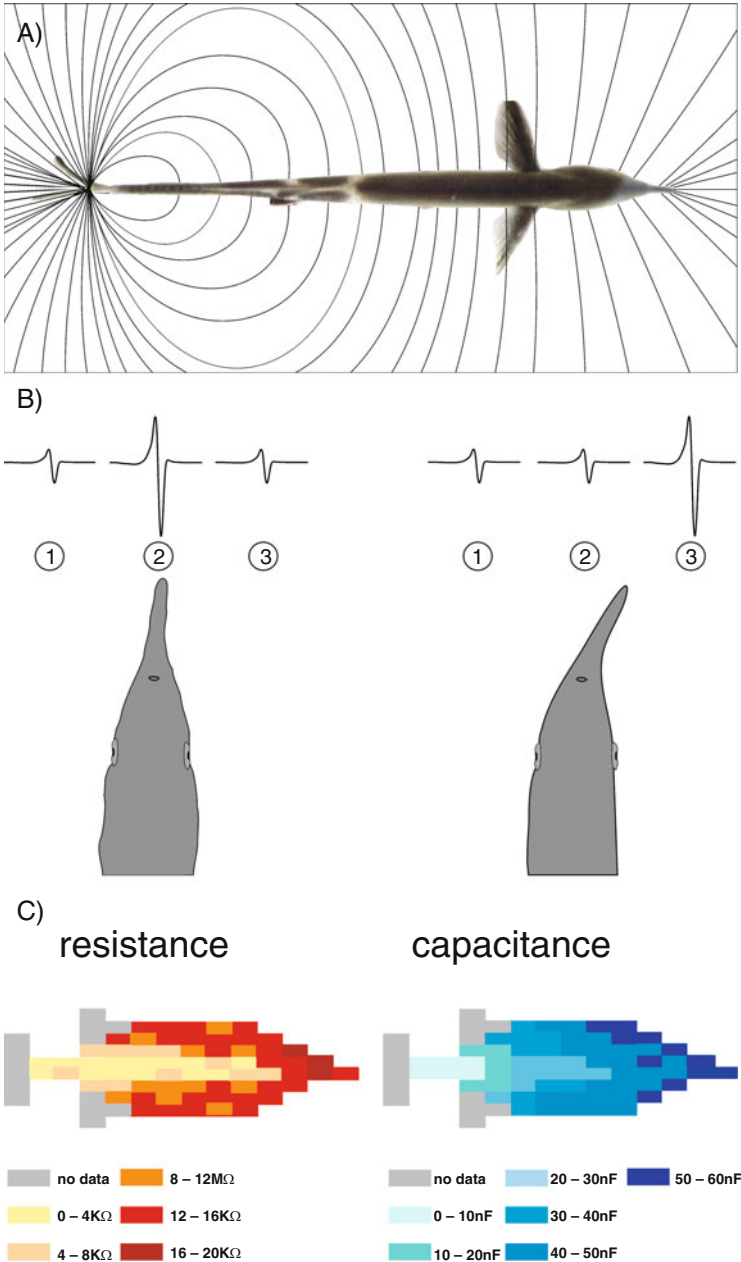


Fig. 9.5 (a) Electric field lines around *Gnathonemus*' body during an EOD. (b) Effect of movement of the Schnauzenorgan on the amplitude of the local EOD. The circles indicate the positions of the recording electrodes with the local EOD recorded at that position shown above. On the left, the electrode at circle 2 records the EOD directly at the tip of the Schnauzenorgan. The amplitudes measured at circles 1 and 3 are much lower. When the Schnauzenorgan is bent to the right by about 62°, the EOD amplitude remains high at the tip (electrode 3) and decreases at electrode 2 (After Pusch et al. 2008). (c) Resistive (left) and capacitive (right) skin properties of

reliable especially for capacitance detection, which is achieved by measuring waveform distortions of the local signal (see above).

The discharge of the electric organ builds up an electric field around the fish, which is shaped by the electric properties of the fish's skin and its internal tissue. For optimal filtering at the two foveal regions at the front of the fish, the field has to be strong enough also at the anterior body parts. This is achieved by an increase in skin resistance and capacitance along the fish's body (Fig. 9.5c) and a low electric resistance of the internal body tissue (von der Emde and Schwarz 2001a; Castello et al. 2000). This ensures that the electric current is funneled through the fish's body to the head region; a mechanism called "funneling effect." Currents are additionally channeled by the constantly open mouth, which leads to a homogenous voltage distribution at the nasal region. The vectorial components of the local EOD are out of phase at the trunk of the fish, resulting in a loss of signal intensity. In contrast, at the two foveal regions, these EOD components are highly in phase, which is called "collimation effect." As a result, the EOD amplitude is almost uniform at the nasal region and the direction toward the sensory surface is constant (Pusch et al. 2008; Castello et al. 2000). This makes the signal carrier equally sensitive to objects located in all three axial spatial dimensions in front of the fish. *G. petersii* can thus detect and analyze objects that are located in front and at the sides of the fish turning the nasal fovea into a specialized all-round detection device.

Funneling of currents together with the so-called tip effect ensures high-amplitude EODs also at the tip of the Schnauzenorgan, the region with the highest density of receptor organs. The angle of the electric field vector at the Schnauzenorgan is approximately 45° and thus different from that at other body regions, where it is about 90° . To affect the signal carrier at the Schnauzenorgan, an object has to be placed right in front of the animal. Interestingly, the high EOD amplitude at the tip of the Schnauzenorgan is not affected by movements of the chin appendix (Fig. 9.5b). During exploratory and foraging behaviors, *Gnathonemus* can move its Schnauzenorgan at high velocity of up to $800^\circ/\text{s}$. These regular scanning movements are often associated with EOD frequencies of 60–80 Hz. Thus, *Gnathonemus* scans the direct surrounding of the Schnauzenorgan at a rate of up to $10^\circ/\text{EOD}$ (von der Emde et al. 2008). Because of the funneling, collimation, and tip effects, the electric field at the Schnauzenorgan's tip is very stable and persistent. As a consequence, the receptors at the Schnauzenorgan perceive a constant electric field, which is not altered by self-generated motions.

Alterations of the electric field by body movements and thus a change in electroreceptor input can pose a problem for signal processing in weakly electric fish. In order to detect an object, the fish have to detect even minute object-caused amplitude changes, which are often much weaker than those caused by movements of the fish's body. In order to perceive object-induced amplitude changes, the brain

Fig. 9.5 (continued) *G. petersii*. Electric properties are color coded onto the contour of a fish (lateral view) with darker colors indicating higher values (Modified after von der Emde and Schwarz 2001b)

of the animal has to filter out the self-induced EOD alterations, which requires a complex neuronal machinery and a lot of brain power. The fact that in *G. petersii* EOD amplitude remains constant even during strong Schnauzenorgan movements thus relieves the nervous system of the task to calculate the exact amount of movement-induced amplitude change and makes the sensory system much more sensitive.

9.5 The Visual Sense in the Weakly Electric Fish *Gnathonemus petersii*

Because of their nocturnal activity and their turbid and noisy blackwater habitats, mormyrids were thought to have only a poor sense of vision (Moller et al. 1979). In addition, the structures of the mormyrid visual brain areas in the mes- and dien-cephalon appear to be highly reduced (Wullimann and Northcutt 1990; Lazar et al. 1984). However, many mormyrids have rather large eyes and also respond sensitively to visual stimuli when held in captivity. In early anatomical work on the eyes of mormyrid fish, which was done even before their active electrosensory system was discovered, it was found by Franz (1921) and then later described in detail by McEwan (1938) that the retina of mormyrids contains large bundles of photoreceptor cells which are collectively ensheathed by large retinal pigment epithelial cells forming cuplike structures. In this section, we argue that the function of the retina in *G. petersii* is not to transmit information about the point-to-point pattern of the distribution of light and dark in a visual image but to analyze visual stimuli for the detection of fast-moving, low-contrast objects under “noisy” conditions.

9.5.1 Anatomy, Morphology, and Cytoarchitecture of the *Gnathonemus* Retina

On the one hand, the retina of *G. petersii* shows the typical five-layered structure of a vertebrate retina (Kreysing et al. 2012; Landsberger et al. 2008), while on the other hand, it reveals some gross anatomical specializations, which make it very special when compared to other teleosts (Francke et al. 2014) (Fig. 9.6). As in most teleosts, the inner retina consists of the retinal ganglion cells (RGCs) separated by a peculiarly thin inner plexiform layer (IPL) from the inner nuclear layer (INL). The very thin outer plexiform layer (OPL) separates the inner retina from the outer retina. The latter is composed of the photoreceptor nuclei, representing the outer nuclear layer (ONL), and the photoreceptor inner and photosensitive outer segments. In *G. petersii*, the ONL is formed by two layers of outer segments (Fig. 9.6a). Therrod outer segments (ROS) are aligned at the distal sclerad side of the ONL, and the cone outer segments (COS) are more proximal at the vitread side (Kreysing et al. 2012). The two plexiform layers are the main site for synaptic contacts between the retinal cells. Amacrine, bipolar, and horizontal cells in the

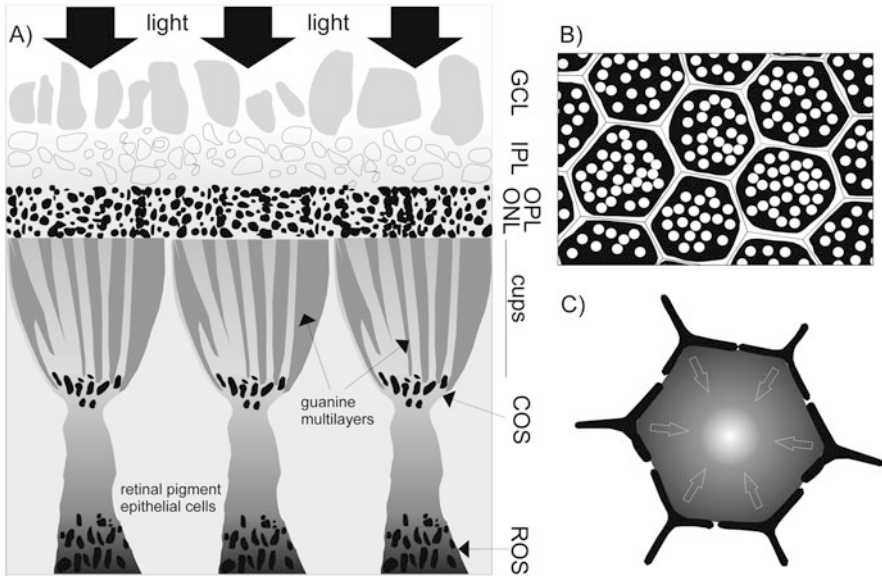


Fig. 9.6 (a) General morphology of the retina of *G. petersii* (light-adapted state). Light has to pass through the cellular layers of the retina, ganglion cell layer (GCL), inner plexiform layer (IPL), outer plexiform layer (OPL), and outer nuclear layer (ONL), before reaching the cups outlined by highly reflective guanine multilayers. (b) Top view onto the cups of the grouped retina slightly above the level of the COS (white circles). (c) Indication of light reflection by the walls of six retinal pigment epithelial cells forming the cuplike structure

INL mediate the intraretinal visual transfer properties (Wagner 2007; Dowling 2012).

The most striking difference to a “normal” fish retina is the observation that the photoreceptors in the *Gnathonemus* retina are grouped together in bundles consisting of about 330 rods located below about 25 cones. Each bundle of rods and cones lies in a hexagonal cuplike structure, which is formed by six large retinal pigment epithelial (RPE) cells (Landsberger et al. 2008; Kreysing et al. 2012) (Fig. 9.6b). A retina composed of such cups is called a grouped retina (Lockett 1977) and similar assemblies are found only in a few other teleostean fish groups, many of which are deep-sea fish (Francke et al. 2014). Each cup forms a macroreceptor unit and has a diameter of around 50 μm , giving rise to an angle of aperture of 2.5° (Francke et al. 2014). Thus, the spatial resolution of the *Gnathonemus* eye is very low compared to most other teleosts. *Gnathonemus* cannot separate objects less than about 3° apart (Kreysing et al. 2012). For comparison, the goldfish (which has no grouped retina) is known to visually resolve details at angles more than 15 times smaller, i.e., down to 0.14° (Land and Nilsson 2002).

The inner surface of the *Gnathonemus* retinal cups acts as a mirror, formed by the reflecting multilayers of guanine crystals, while a mirror surface below the cup is missing (Fig. 9.6). At the bottom of each cup, the cone outer segments (COS) are

located. They are thus exposed to the light, which is focused onto the cone outer segments with an increase of the incident light intensity by more than 500 %. In contrast, the rod outer segments (ROS) lie below the cup in a medium filled with light-scattering, submicron-sized guanine crystals and melanin granules, protecting them from the incoming light. Thus, the ROS receive a reduced level of illumination. While light levels for the cones at the bottom of the cup are amplified, the disordered phase of guanine crystallites underneath the cup attenuates the light leaking through the bottom of the cup and only a very small fraction of light reaches the ROS. The combined effect of this arrangement is that both the less sensitive cones and the very sensitive rods receive appropriate amounts of light to allow their simultaneous operation at mesopic light levels, which prevail in the dim habitat of the fish (Francke et al. 2014; Kreysing et al. 2012).

In *Gnathonemus*, the absorption maximum of the rod pigments is at 536 nm (green), while the single type of cone is most sensitive to 615 nm (red light) (Kreysing et al. 2012). In response to the daily changes of light and darkness, rods change their position to regulate light sensitivity or visual acuity via a process called retinomotor movement (Burnside and Nagle 1983). Under photopic daytime conditions, the bottoms of the cups are almost closed forming a small bottleneck through which the rods protrude into the light-protected area below. Thus, COS and ROS are separated from each other during daytime with the ROS being shielded from the light, while COS are fully light exposed. In contrast during dark adaptation, the bottleneck opens and the cups form a cylinder, in which the ROS are drawn inside the cup toward the inner retina. These movements are induced by rod myoid contractions.

The inner plexiform layer of the retina is rather thin, with about half the thickness as that of most other teleosts. Furthermore, the retina of *Gnathonemus* appears to lack local specializations such as a visual streak or a fovea centralis. All this suggests that information processing in the grouped retina is less complex than elsewhere. However, the presence of ten types of retinal ganglion cells suggests that like in other retinae, the visual stimuli are processed in several parallel pathways. In particular, fast and dynamic visual stimuli may be mediated by certain ganglion cells, while the amacrine cells may provide for direction and movement sensitivity (Francke et al. 2014). Interestingly, the information provided by rods and cones may be pooled already at the bipolar cell level such that color information is unlikely to be extracted by the brain.

In summary, the retina of *G. petersii* is a highly specialized and complex structure shaped by specialized epithelial cells. However, its spatial resolution is very low and there is only one type of cone, and also some retinal layers are rather thin and reduced. Information leaving the retina is colorblind but appears to be specialized for the processing of movement. The arrangement into reflecting cups by RPE cells reflects to a high degree the functional properties of the *Gnathonemus* retina. The apparent disadvantages this retinal arrangement imposes on the fish, however, might actually be advantageous when considering the habitat of the fish. In particular, we argue that the grouped retina forms a matched filter for certain

signal properties, namely, for the detection of large, fast-moving objects under dim and noisy light conditions.

9.5.2 Anatomy of Visual Brain Areas

The optic nerve (ON) consists of the bundled axons of retinal ganglion cells. In *G. petersii*, the ON is rather thin compared with the size of the eye or the brain, due to the relatively small numbers of retinal ganglion cells of each eye. Before entering the brain, the ON crosses the midline beneath the diencephalon at the optic chiasm and terminates as optic tract in the mesencephalic tectum and tegmentum and in the rostral diencephalon (thalamus, hypothalamus) (Lazar et al. 1984).

A detailed analysis of the retinal projections of *G. petersii* reveals that many well-established retinofugal connections into the teleost diencephalon are extremely reduced or even absent, while other primary visual regions receive only limited visual input but participate in active electrolocation, instead (Wullimann and Northcutt 1990; Northcutt and Wullimann 1988). In teleosts, retinal projections usually terminate in the suprachiasmatic nucleus (SCN) of the hypothalamus, driving the circadian rhythm. Large retinal terminal fields are also present in the thalamus and in the pretectal complex (central pretectal nucleus (CPN), periventricular pretectal nucleus (PPN), superficial pretectal nucleus (SPN)). The latter structure is further reciprocally connected to the optic tectum (OT) and by this probably involved in the detection of moving objects. In addition, the dorsal and ventral accessory optic nuclei located in the pretectal region receive direct retinal input and are involved in optokinetic oculomotor reflexes (Northcutt and Wullimann 1988; Rupp et al. 1996; Vanegas and Ito 1983).

In *G. petersii*, this general pattern is modified: retinal efferents terminate in the SCN, the thalamus, the PPN, as well as the OT. CPN receives reduced visual input, while an SPN and accessory visual nuclei are absent (Lazar et al. 1984; Wullimann and Northcutt 1990). The OT forms a relatively minor part of the whole brain, and it is differently located and shaped when compared to other teleosts (Fig. 9.7a). The very large, mostly electrosensory torus semicircularis pushes the two tecta rostrally and laterally, and the huge cerebellum covers the complete dorsal surface of the brain. The right and left tecta are interconnected by the intertectal commissure only at their rostralmost parts. The tectum is stratified as in other teleosts into seven laminae (Fig. 9.7b) (Pusch et al. 2013b; Meek 1983). The visual input to the OT is only poorly developed, as retinal fibers terminate exclusively in a narrow strip in the stratum fibrosum et griseum (Lazar et al. 1984), whereas in the majority of teleost species, retinal fibers terminate in three or four deeper layers of the tectum (Fig. 9.7b) (Wullimann 1998; Stürmer and Easter 1984).

The midbrain optic tectum integrates multisensory input and is the main visual center in teleosts. In *G. petersii*, tectal efferents project reciprocally into PPN, CPN, and the thalamus, while only restricted tectal terminations were detected in the preglomerular region (PG), which in most teleosts serves as a relay station for ascending visual information (Wullimann and Northcutt 1990). Because of limited

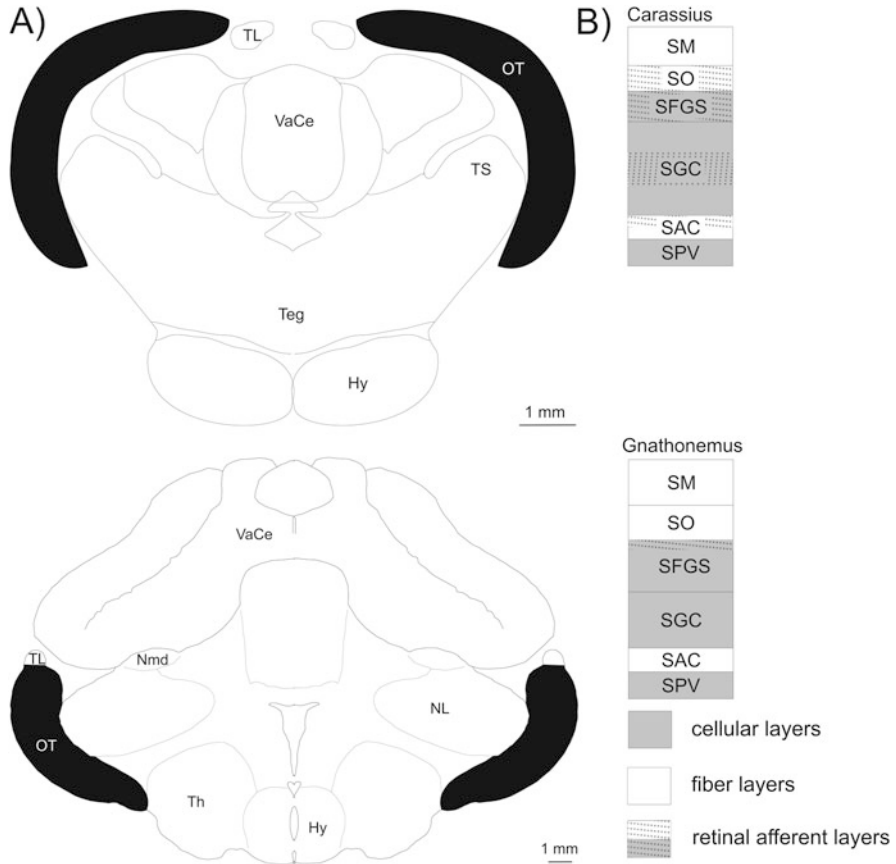


Fig. 9.7 (a) Brain sections on the level of the mesencephalon of *Carassius* and *Gnathonemus*. (b) General overview of layers of the OT in *Carassius* and *Gnathonemus*. For further explanation, see text. *Abbreviations:* Hy hypothalamus, Nmd mediodorsal mesencephalic nucleus, NL nucleus lateralis of the torus semicircularis, OT optic tectum, SAC stratum album centrale, SFGS stratum fibrosum et griseum, SGC stratum griseum centrale, SO stratum opticum, SPV stratum periventriculare, SM stratum marginale, Teg tegmentum, Th thalamus, TL torus longitudinalis, TS torus semicircularis, VaCe valvula cerebelli

tectofugal projections in the PG, it might be speculated that visual projections ascending to the dorsal telencephalon have to be provided by another route (Precht et al. 1998), maybe involving the torus semicircularis. Even though the tectum is thought to act as a multisensory neural processing area, which is essential for behavioral reactions, anatomical investigations in *Gnathonemus* showed only very weak electrosensory projections into the tectum (Ruhl et al. 2011; von der Emde unpublished data). However, there are tectal projections into the lateral nucleus of the torus semicircularis, representing the midbrain center for electrosensory processing (Wullmann and Northcutt 1990). Different parts of the

electrosensitive torus semicircularis project to the PG area in *Gnathonemus* (Bell 1981; Finger et al. 1981), suggesting that PG might be more involved in electroreception than in vision and thus might have different functions than those described for other teleosts (Braford et al. 1983).

In summary, even though the retina is highly specialized, the whole visual system in the *Gnathonemus* brain is clearly reduced. Anatomical findings suggest that during evolution, electroreception took over some visual regions, e.g., CPN, PG, SPN, and accessory visual nuclei. This suggests that in *Gnathonemus* vision might be subordinate to the active electric sense. However, it also could mean that the two senses are used for separate tasks. Here, we argue that there is a division of labor between vision and the active electric sense, which led to the development of separate and complementary matched filters in the visual and electric sensory systems. Anatomical and physiological findings indicate that the visual system evolved a matched filter for the detection of fast-moving, large objects and purposely filters out most other visual stimuli.

9.5.3 Functional Aspects of the Visual System

9.5.3.1 Detection of Visual Stimuli

In contrast to training *G. petersii* with electrosensory stimuli, pure visual training is quite difficult and time consuming. When the animals are trained for long enough, they can learn, however, to approach a black square projected onto a screen (Schuster and Amtsfeld 2002; Landsberger et al. 2008). These experiments confirmed that the spatial resolution is so poor that *Gnathonemus* cannot see objects smaller than about 3° of visual angle, no matter whether these objects are stationary or moving (Kreysing et al. 2012). *G. petersii* can also learn to discriminate between large, differently shaped visual patterns indicating that visual pattern recognition involves template matching (Schuster and Amtsfeld 2002).

Since the fish cannot see small particles, the involvement of the visual sense in finding their prey (small insect larvae) during foraging is negligible (von der Emde and Bleckmann 1998). In other behaviors, for example, during certain startle responses, it is much stronger. When presenting visual stimuli that rapidly expand in size mimicking the silhouette of an approaching predator, *G. petersii* consistently responds with a quick flight reaction away from the stimulus. Especially under dim light conditions, this response is much more reliable in *Gnathonemus* than in the goldfish (*Carassius auratus*), whereas under bright light, the two species show no differences (Kreysing et al. 2012). Startle experiments like this also showed the advantage of color blindness for *G. petersii*. The animals were significantly better than goldfish (which can see colors) at detecting an expanding virtual circle which was dynamically defined by the random exchange of equiluminant red and green floating particles. *Gnathonemus* detected such color-camouflaged stimuli significantly better than the goldfish, showing the advantage of missing color discrimination (i.e., “color pooling”) (Kreysing et al. 2012).

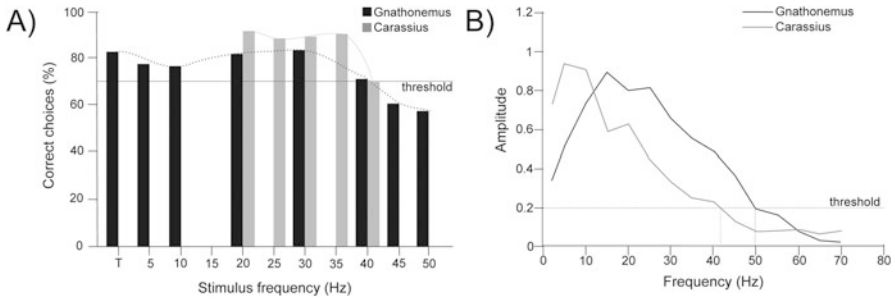


Fig. 9.8 (a) Behaviorally determined critical flicker fusion frequency in *G. petersii* (black) and *Carassius* (gray). The behavioral response to flickering light was tested in a two-alternative forced-choice procedure (Modified after Mora-Ferrer and Gangluff 2002; Pusch et al. 2013a). (b) Normalized amplitudes of visually evoked field potentials in the OT for the different flicker frequencies in *Gnathonemus* (dark gray) and *Carassius* (light gray) (Modified after Pusch et al. 2013a)

Another study described that *G. petersii* performs an optomotor response (OMR) when a moving stripe pattern was projected onto the bottom of the tank. Interestingly, the OMR of *G. petersii* is a very robust behavior, which does not adapt even after longer stimulus periods. The OMR is remarkably resistant to reduced light intensity with a constant gain over more than four orders of magnitude (Landsberger et al. 2008).

When trained in a two-alternative forced-choice paradigm to discriminate between a constant and a flickering light source, the flicker fusion frequency (FFF) of *G. petersii* was found to lie between 40 and 45 Hz (Fig. 9.8a) (Pusch et al. 2013a). In a similar experiment, the FFF of *Carassius* was measured at 35–40 Hz (Mora-Ferrer and Gangluff 2002). Behavioral measurements of the animals' FFF were substantiated by electrophysiological recordings (Fig. 9.8b), showing that in *G. petersii* the FFF thresholds of neurons in the tectum opticum were at about 50 Hz, while for *Carassius* it were at about 40 Hz (Pusch et al. 2013a). It follows that *G. petersii*'s visual system shows a higher temporal resolution than that of the goldfish (Fig. 9.8). In addition, *G. petersii*'s visual system is less sensitive to a reduction in contrast. In conclusion, both the retinal specializations and the brain circuits of the visual system of *G. petersii* enable the fish to be extremely effective in detecting fast-moving objects such as approaching predators under dim light conditions.

9.5.3.2 Noise Tolerance of the Visual System

Considering one macroreceptor of *G. petersii* with its wide spacing of 50 μm as being the smallest functional unit of the retina, visual spatial resolution is rather low. The bad spatial resolution of the *Gnathonemus* retina works like a low-pass filter and prevents the animals from seeing small objects and high spatial frequencies. When the fish were trained to respond to a sharp-edged square, *G. petersii* was easily outperformed by the sunfish (*Lepomis gibbosus*), a visual

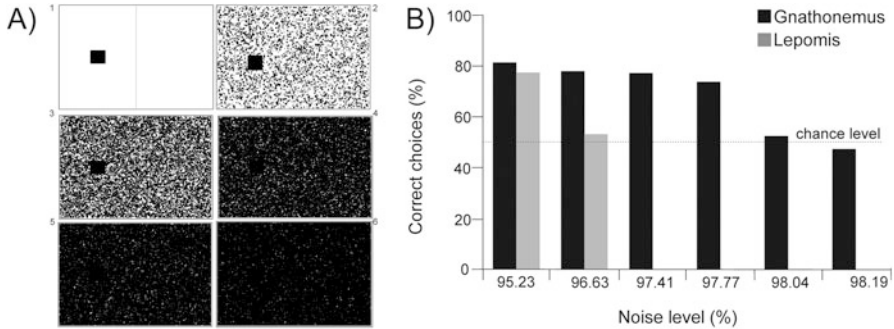


Fig. 9.9 (a) Different noise levels for disguising a square object during visual object detection: 1 – 0 %, 2 – 25.9 %, 3 – 62.4 %, 4 – 93.3 %, 5 – 96.6 %, 6 – 97.8 %. While *Gnathonemus* still could perceive the *large square* in 5 and 6, *Lepomis* was unable to do so. (b) In a noise suppression experiment with *Gnathonemus* (black) and *Lepomis* (gray) in a two-alternative forced-choice procedure, the fish had to swim toward that side of a screen which contained a *large black square*. The choice of the side with the *square* was rewarded. When different levels of visual noise were added, *Gnathonemus* could detect the *square* even with 97.8 % of noise, while *Lepomis* failed to do so at 96.6 %

specialist taken for comparison. However, if the stimuli were low-passed filtered, which removed all sharp edges, *G. petersii* could detect these objects better than *Lepomis* (Landsberger et al. 2008).

As mentioned above, *G. petersii* lives in blackwater streams carrying dissolved matter and many small particles making these waters very “noisy” (Moritz 2010). In a behavioral experiment, this effect was mimicked by adding small particles to a stripe pattern projected on the bottom of an aquarium, showing that the OMR of *G. petersii* is remarkably noise tolerant (Landsberger et al. 2008). Similar noise particles were also added to the stimuli in the abovementioned experiments with expanding circles eliciting a startle response in *G. petersii* and *Carassius*. The flight responses of both species declined when the threatening stimulus was disguised by dynamic gray noise particles. *Gnathonemus*, however, was less affected than *Carassius* (Kreysing et al. 2012). In a two-alternative forced-choice task, *Gnathonemus* and *Lepomis* were tested to recognize a black square moving over a screen. More and more dynamic noise particles were added, which concealed the object (Fig. 9.9a). It turned out that *Gnathonemus* was able to detect the object under higher noise levels than the sunfish, which does not have a grouped retina (Fig. 9.9b) (Petruschke and von der Emde unpublished data).

The abovementioned findings show that the fact that *G. petersii* cannot see high spatial frequencies and small objects can offer an advantage to these animals when the water is filled with small particles. Such visual noise is filtered out and the fish are able to see the larger objects behind the noise. This allows detection of approaching larger objects, e.g., a predator, which is additionally supported by the high temporal resolution of the visual system. In addition, when swept away by

the current, fish might be able to see the ground or approaching obstacles even under noisy conditions.

9.6 Partitioning of Environmental Sensing

In conclusion, weakly electric mormyrid fish possess an elaborated electrosensory system, which consists of peripheral matched filters and a large brain for processing of electrosensory information. The functions of the electric sense are clearly defined: it works very sensitively in a three-dimensional area around the fish up to a distance of about one fish length. It is very effective in detecting and recognizing small objects, mainly prey items, in a very complex environment containing many similar types of objects (“finding the needle in the haystack”). In addition, it can analyze the spatial and material properties of larger objects during close-up inspection very precisely. However, the electrosensory system does not work at larger distances: object detecting fails at distances larger than about 15 cm and object analysis ends even at a distance longer than 4–5 cm in a fish with a standard length of about 12 cm (von der Emde et al. 2010; Fechler and von der Emde 2013).

As shown above, these exceptional electric sensing abilities are made possible by the production of an optimal electric carrier signal, the EOD, and an elaborated processing of electrosensory information by the nervous system. Both EOD production and sensory processing depend to a high degree of peripheral structures, which take over certain aspects of processing and electromotor production and thus free the nervous system of processing duties. In the periphery, the fish have developed several matched filters, which tune the electric carrier by shaping the electric signals (tip effect, funneling effect, electric skin properties). On the sensory side, the fish have evolved two peripheral sensory foveae, one at the tip of the Schnauzenorgan (for prey detection and close-range object analysis) and one in the nasal region (for obstacle detection and short-range navigation). These areas contain specialized electroreceptor organs that due to their accessory structures form matched filters by responding primarily to certain types of electric stimuli. These electrosensory matched filters delegate several aspects of electrosensory processing to the periphery and thus make the system very fast and efficient. Nevertheless, the brain areas of *G. petersii* that are involved in signal production and perception of electrosensory stimuli are numerous and extremely large. *Gnathonemus* has a huge brain, which uses up to 60 % of the oxygen consumption of the fish (Nilsson 1996).

Like all mormyrids, *G. petersii* has highly evolved eyes of a very peculiar structure. Its grouped retina consists of retinal cups with a light-reflecting surface that focuses the light onto the outer segments of the cones and attenuates the light that reaches the rods. This leads to an alignment of the working ranges of rods and cones and enables simultaneous activity of both receptor types during daylight. As a consequence, *Gnathonemus* shows a superior response to visual stimuli in the mesopic range of illumination compared with fish without a grouped retina. In addition, the grouped retina of *G. petersii* filters out visual noise and responds extremely well to fast-moving stimuli.

The *Gnathonemus* retina thus forms a peripheral matched filter turning it into a highly specialized predator detector. Large objects moving at a distance from the fish are especially well detected. If a predator starts an attack against the fish by darting toward it, the grouped retina of *G. petersii* allows its detection even under unfavorable, “noisy” conditions. The peripheral matched filter frees the nervous system of processing tasks, which in other fishes are performed by the visual centers of the brain. In *G. petersii* visual brain structures are reduced and partly taken over by the electrosensory system. This “freeing up” of processing power in the brain leads to significant energy savings in the visual system and allows at least parts of the available computational capacity to be redirected to other tasks, e.g., to active electrolocation.

G. petersii has evolved a clear partitioning of sensing: in the near field, they employ active electrolocation and are thus able to find and identify their small prey items within a lot of background clutter in the absence of light during their nocturnal activity period. In addition, they can inspect nearby objects and detect their material and spatial properties. In the far field, the visual sense takes over, which, thanks to its matched filter in the retina, is well adapted to see fast-moving, large objects in dim light even under noisy conditions.

References

- Amey-Özel M, Hollmann M, von der Emde G (2012) From the Schnauzenorgan to the back: morphological comparison of mormyromast electroreceptor organs at different skin regions of *Gnathonemus petersii*. *J Morphol* 273(6):629–638. doi:[10.1002/jmor.20009](https://doi.org/10.1002/jmor.20009)
- Amey-Özel M, von der Emde G, Engelmann J, Grant K (2015) More a finger than a nose: the trigeminal motor and sensory innervation of the Schnauzenorgan in the elephant-nose fish *Gnathonemus petersii*. *J Comp Neurol* 523(5):769–789. doi:[10.1002/cne.23710](https://doi.org/10.1002/cne.23710)
- Bacelo J, Engelmann J, Hollmann M, von der Emde G, Grant K (2008) Functional foveae in an electrosensory system. *J Comp Neurol* 511(3):342–359. doi:[10.1002/cne.21843](https://doi.org/10.1002/cne.21843)
- Bell CC (1981) Some central connections of medullary octavolateral centers in a mormyrid fish. In: Fay RR, Popper AN, Tavolga WN (eds) *Hearing and sound communication in fishes*. Springer Verlag, Berlin, pp 383–392
- Bell CC (1990) Mormyromast electroreceptor organs and their afferent fibers in mormyrid fish. III. Physiological differences between two morphological types of fibers. *J Neurophysiol* 63(2):319–332
- Bodznick D, Montgomery JC (2005) The physiology of low-frequency electrosensory systems. In: Bullock TH, Hopkins CD, Popper AN, Fay RR (eds) *Electroreception*. Springer, New York, pp 132–153
- Braford MRJ, Northcutt RG, Davis RE, Demski LS, Kassel J, Overmier JB, Hollis KL (1983) *Fish neurobiology*, vol 2. The University of Michigan Press, Ann Arbor
- Bullock TH, Bodznick DA, Northcutt RG (1983) The phylogenetic distribution of electroreception: evidence for convergent evolution of a primitive vertebrate sense modality. *Brain Res Rev* 6:25–46
- Burnside B, Nagle B (1983) Retinomotor movements of photoreceptors and retinal pigment epithelium: mechanisms and regulation. In: Osborne NN, Chader GJ (eds) *Progress in retinal research*. Oxford Pergamon Press, Oxford, pp 67–109
- Carlson BA, Gallant J (2013) From sequence to spike to spark: evo-devo-neuroethology of electric communication in mormyrid fishes. *J Neurogenetics* 27(3):106–129. doi:[10.3109/01677063.2013.799670](https://doi.org/10.3109/01677063.2013.799670)

- Castello ME, Aguilera PA, Trujillo-Cenoz O, Caputi AA (2000) Electroreception in *Gymnotus carapo*: pre-receptor processing and the distribution of electroreceptor types. *J Exp Biol* 203 (Pt 21):3279–3287
- Cheng K (2012) Morphological correlates of signal variation in weakly electric mormyrid fish honors thesis. Cornell University, Ithaca
- Czech-Damal NU, Liebschner A, Miersch L, Klauer G, Hanke FD, Marshall C, Dehnhardt G, Hanke W (2012) Electroreception in the Guiana dolphin (*Sotalia guianensis*). *Proc Biol Sci R Soc* 279:663–668. doi:[10.1098/rspb.2011.1127](https://doi.org/10.1098/rspb.2011.1127)
- Dowling JE (2012) The retina. An approachable part of the brain. Belknap Press of Harvard University Press, Cambridge, MA
- Fechler K, von der Emde G (2013) Figure-ground separation during active electrolocation in the weakly electric fish, *Gnathonemus petersii*. *J Physiol Paris* 107:72–83, doi: <http://dx.doi.org/10.1016/j.jphysparis.2012.03.002>
- Finger TE, Bell CC, Russell CJ (1981) Electrosensory pathways to the valvula cerebelli in mormyrid fish. *Exp Brain Res* 42:22–33
- Francke M, Kreysing M, Mack A, Engelmann J, Karl A, Makarov F, Guck J, Kolle M, Wolburg H, Pusch R, von der Emde G, Schuster S, Wagner HJ, Reichenbach A (2014) Grouped retinæ and tapetal cups in some Teleostian fish: occurrence, structure, and function. *Prog Retin Eye Res* 38:43–69. doi:[10.1016/j.preteyeres.2013.10.001](https://doi.org/10.1016/j.preteyeres.2013.10.001)
- Franz V (1921) Zur mikroskopischen Anatomie der Mormyriden. *Zool Jahrb Abt Allg Zool Physiol Tiere* 42:91–146
- Harder W (1968) Die Beziehungen zwischen Elektrozepatoren, elektrischen Organen, Seitenlinienorganen und Nervensystem bei den Mormyridae (Teleostei, Pisces). *Z Vergl Physiol* 59:272–318
- Heiligenberg W (1973) Electrolocation of objects in the electric fish *Eigenmannia* (Rhamphichthyidae, Gymnotoidei). *J Comp Physiol* 87:137–164
- Hofmann M, Chagnaud B, Wilkens L (2005) Response properties of electrosensory afferent fibers and secondary brain stem neurons in the paddlefish. *J Exp Biol* 208:4213–4222
- Hollmann M, Engelmann J, von der Emde G (2008) Distribution, density and morphology of electroreceptor organs in mormyrid weakly electric fish: anatomical investigations of a receptor mosaic. *J Zool* 276:149–158
- Hopkins CD (2009) Electrical perception and communication. In: Squire L (ed) *Encyclopedia of neuroscience*, vol 3. Academic, Oxford, pp 813–831
- Kreysing M, Pusch R, Haverkate D, Landsberger M, Engelmann J, Ruiter J, Mora-Ferrer A, Ulbricht E, Grosche J, Franze K, Streif S, Schumacher S, Makarov F, Kacza J, Guck J, Wolburg H, Bowmaker JK, von der Emde G, Schuster S, Wagner HJ, Reichenbach A, Francke M (2012) Photonic crystal light collectors in fish retina improve vision in turbid water. *Science* 336:1700–1703. doi:[10.1126/science.1218072](https://doi.org/10.1126/science.1218072)
- Land MF, Nilsson D-E (2002) *Animal eyes*. Oxford University Press, Oxford
- Landsberger M, von der Emde G, Haverkate D, Schuster S, Gentsch J, Ulbricht E, Reichenbach A, Makarov F, Wagner HJ (2008) Dim light vision – morphological and functional adaptations of the eye of the mormyrid fish, *Gnathonemus petersii*. *J Physiol Paris* 102(4–6):291–303. doi:[10.1016/j.jphysparis.2008.10.015](https://doi.org/10.1016/j.jphysparis.2008.10.015)
- Lazar G, Libouban S, Szabo T (1984) The mormyrid mesencephalon. III. Retinal projections in a weakly electric fish, *Gnathonemus petersii*. *J Comp Neurol* 230(1):1–12. doi:[10.1002/cne.902300102](https://doi.org/10.1002/cne.902300102)
- Lissmann HW, Machin KE (1958) The mechanism of object location in *Gymnarchus niloticus* and similar fish. *J Exp Biol* 35(2):451–486
- Lockett NA (1977) Adaptations to the deep-sea environment. In: Crescitelli F (ed) *Handbook of sensory physiology*. VII the visual system in vertebrates. Springer Verlag, New York, pp 68–184
- McEwan MR (1938) A comparison of the retina of the mormyrids with that of various other teleosts. *Acta Zool* 19:427–465

- Meek J (1983) Functional anatomy of the tectum mesencephali of the goldfish. An explorative analysis of the functional implications of the laminar structural organization of the tectum. *Brain Res Rev* 6:247–297
- Moller P (1995) Electric fishes. History and behavior. Chapman & Hall, London
- Moller P, Serrier J, Belbenoit P, Push S (1979) Notes on ethology and ecology of the Swashi river mormyrids (Lake Kainji, Nigeria). *Behav Ecol Sociobiol* 4:357–368
- Mora-Ferrer C, Gangluff V (2002) D2-dopamine receptor blockade modulates temporal resolution in goldfish. *Vis Neurosci* 19:807–815
- Moritz T (2010) Fishes of Iguidi river – a small forest stream in south-east Benin. *Ichthyol Explor Freshw* 21(1):9–26
- Nilsson G (1996) Brain and body oxygen requirements of *Gnathonemus petersii*, a fish with an exceptionally large brain. *J Exp Biol* 199(Pt 3):603–607
- Northcutt RG, Wullimann MF (1988) The visual system in teleost fishes: morphological patterns and trends. In: Atema J, Fay RR, Popper AN, Tavolga WN (eds) *Sensory biology of aquatic animals*. Springer, New York, pp 515–552
- Nwani CD, Odoh GE, Ude EF, Okogwu OI (2011) Food and feeding habits of *Gnathonemus petersii* (Osteichthyes: Mormyridae) in Anambra River, Nigeria. *Int Aquat Res* 3:45–51
- Ogbeibu AE, Ezeunara P (2005) Studies on the food composition and feeding pattern of fish communities in the Ikpoba River, Southern Nigeria. *J Aquat Sci* 20(2):117–129
- Okedi J (1965) The biology and habits of the Mormyrid fishes: *Gnathonemus longibarbis*, *G. victoriana*, *Marcusenius grahamae*, *M. nigricans*, *Petrocephalus catostoma*. *J Appl Ecol* 2(2):408–409
- Pettigrew JD (1999) Electrosensory reception in monotremes. *J Exp Biol* 202(Pt 10):1447–1454
- Prechtl JC, von der Emde G, Wolfart J, Karamursel S, Akoev GN, Andrianov YN, Bullock TH (1998) Sensory processing in the pallium of a mormyrid fish. *J Neurosci Off J Soc Neurosci* 18(18):7381–7393
- Proske U, Gregory JE, Iggo A (1998) Sensory receptors in monotremes. *Philos Trans R Soc Lond* 353(1372):1187–1198
- Pusch R, von der Emde G, Hollmann M, Bacelo J, Nobel S, Grant K, Engelmann J (2008) Active sensing in a mormyrid fish: electric images and peripheral modifications of the signal carrier give evidence of dual foveation. *J Exp Biol* 211(Pt 6):921–934. doi:10.1242/jeb.014175
- Pusch R, Kassing V, Riemer U, Wagner HJ, von der Emde G, Engelmann J (2013a) A grouped retina provides high temporal resolution in the weakly electric fish *Gnathonemus petersii*. *J Physiol Paris* 107(1–2):84–94. doi:10.1016/j.jphysparis.2012.06.002
- Pusch R, Wagner HJ, von der Emde G, Engelmann J (2013b) Spatial resolution of an eye containing a grouped retina: ganglion cell morphology and tectal physiology in the weakly electric fish *Gnathonemus petersii*. *J Comp Neurol* 521(17):4075–4093. doi:10.1002/cne.23397
- Ruhl T, Mohr C, von der Emde G (2011) The mesencephalon of a mormyrid – sensory processing during active electrolocation in the weakly electric fish, *Gnathonemus petersii*. In: 33th Göttingen Neurobiology Conference, Göttingen. pp T17–14C
- Rupp B, Wullimann MF, Reichert H (1996) The zebrafish brain: a neuroanatomical comparison with the goldfish. *Anat Embryol* 194:187–203
- Salazar VL, Stoddard PK (2008) Sex differences in energetic costs explain sexual dimorphism in the circadian rhythm modulation of the electrocommunication signal of the gymnotiform fish *Brachyhyponomus pinnicaudatus*. *J Exp Biol* 211(Pt 6):1012–1020. doi:10.1242/jeb.014795
- Salazar VL, Krahe R, Lewis JE (2013) The energetics of electric organ discharge generation in gymnotiform weakly electric fish. *J Exp Biol* 216(Pt 13):2459–2468. doi:10.1242/jeb.082735
- Scheich H, Langner G, Tidemann C, Coles RB, Guppy A (1986) Electrosensory reception and electrolocation in platypus. *Nature* 319(6052):401–402. doi:10.1038/319401a0
- Schuster S, Amtsfeld S (2002) Template-matching describes visual pattern-recognition tasks in the weakly electric fish *Gnathonemus petersii*. *J Exp Biol* 205(Pt 4):549–557

- Schwan HP (1963) Determination of biological impedances. In: Nastuk WL (ed) *Physical techniques in biological research*, vol VI. Academic, New York, pp 323–407
- Speakman JR, Ravey PA (1991) No cost of echolocation for bats in flight. *Nature* 350:421–423
- Stoddard PK, Salazar VL (2011) Energetic cost of communication. *J Exp Biol* 214(Pt 2):200–205. doi:[10.1242/jeb.047910](https://doi.org/10.1242/jeb.047910)
- Stürmer CAO, Easter SSJ (1984) A comparison of the normal and regenerated retinotectal pathways of goldfish. *J Comp Neurol* 223:57–76
- Szabo T, Moller P (1984) Neuroethological basis for electrocommunication. In: Bolis C, Keynes RD, Maddrell SHP (eds) *Comparative physiology of sensory systems*. Cambridge University Press, Cambridge, pp 455–474
- Szabo T, Wersäll J (1970) Ultrastructure of an electroreceptor (Mormyromast) in a mormyrid fish, *Gnathonemus petersii*. II. *J Ultrastruct Res* 30:473–490
- Vanegas H, Ito H (1983) Morphological aspects of the teleostean visual system: a re-view. *Brain Res Rev* 6:117–137
- von der Emde G (1990) Discrimination of objects through electrolocation in the weakly electric fish, *Gnathonemus petersii*. *J Comp Physiol A* 167:413–421
- von der Emde G (1993) Capacitance discrimination in electrolocating, weakly electric pulse fish. *Naturwissenschaften* 80:231–233
- von der Emde G (2011) Remote electrical sensing: detection and analysis of objects by weakly electric fishes. In: Barth F, Humphrey J, Srinivasan M (eds) *Frontiers in sensing. From biology to engineering*. Springer, Wien, pp 313–326
- von der Emde G, Bleckmann H (1992a) Differential responses of two types of electroreceptive afferents to signal distortions may permit capacitance measurement in a weakly electric fish, *Gnathonemus petersii*. *J Comp Physiol A* 171:683–694
- von der Emde G, Bleckmann H (1992b) Extreme phase sensitivity of afferents which innervate mormyromast electroreceptors. *Naturwissenschaften* 79:131–133
- von der Emde G, Bleckmann H (1997) Waveform tuning of electroreceptor cells in the weakly electric fish, *Gnathonemus petersii*. *J Comp Physiol A* 181:511–524
- von der Emde G, Bleckmann H (1998) Finding food: senses involved in foraging for insect larvae in the electric fish, *Gnathonemus petersii*. *J Exp Biol* 201:969–980
- von der Emde G, Engelmann J (2011) Active electrolocation. In: Farrell A (ed) *Encyclopedia of fish physiology: from genome to environment*, vol 1. Academic, San Diego, pp 375–386
- von der Emde G, Fetz S (2007) Distance, shape and more: recognition of object features during active electrolocation in a weakly electric fish. *J Exp Biol* 210(Pt 17):3082–3095. doi:[10.1242/jeb.005694](https://doi.org/10.1242/jeb.005694)
- von der Emde G, Ringer T (1992) Electrolocation of capacitive objects in four species of pulse-type weakly electric fish. I. Discrimination performance. *Ethology* 91:326–338
- von der Emde G, Ronacher B (1994) Perception of electric properties of objects in electrolocating weakly electric fish: two-dimensional similarity scaling reveals a City-Block metric. *J Comp Physiol A* 175:801–812
- von der Emde G, Schwarz S (2001a) Detection of electric signals in jawed fishes. In: Kapoor BG (ed) *Sensory biology of jawed fishes – new insights*. Science Publishers, Enfield, pp 161–180
- von der Emde G, Schwarz S (2001b) How the electric fish brain controls the production and analysis of electric signals during active electrolocation. *Zoology* 103:112–124
- von der Emde G, Schwarz S (2002) Imaging of objects through active electrolocation in *Gnathonemus petersii*. *J Physiol Paris* 96(5–6):431–444. doi:[10.1016/S0928-4257\(03\)00021-4](https://doi.org/10.1016/S0928-4257(03)00021-4)
- von der Emde G, Amey M, Engelmann J, Fetz S, Folde C, Hollmann M, Metzen M, Pusch R (2008) Active electrolocation in *Gnathonemus petersii*: behaviour, sensory performance, and receptor systems. *J Physiol Paris* 102(4–6):279–290. doi:[10.1016/j.jphysparis.2008.10.017](https://doi.org/10.1016/j.jphysparis.2008.10.017)
- von der Emde G, Behr K, Bouton B, Engelmann J, Fetz S, Folde C (2010) 3-dimensional scene perception during active electrolocation in a weakly electric pulse fish. *Front Behav Neurosci* 4:26. doi:[10.3389/fnbeh.2010.00026](https://doi.org/10.3389/fnbeh.2010.00026)

- Wagner H-J (2007) Bipolar cells in the “grouped retina” of the elephantnose fish (*Gnathonemus petersii*). *Vis Neurosci* 24(3):355–362
- Wehner R (1987) “Matched filters” – neural models of the external world. *J Comp Physiol A* 161:511–531
- Wilkens L, Hofmann M (2005) Behavior of animals with passive, low-frequency electrosensory systems. In: Bullock T, Hopkins C, Popper A, Fay R (eds) *Electroreception*. Springer, New York, pp 229–263
- Wullimann MF (1998) The central nervous system. In: Evans DH (ed) *The physiology of fishes*, 2nd edn. CRC Press, Boca Raton, pp 245–282
- Wullimann MF, Northcutt RG (1990) Visual and electrosensory circuits of the diencephalon in mormyrids: an evolutionary perspective. *J Comp Neurol* 297:537–552

Index

A

- Acanthocnemus nigricans*
 - biology and behavior, 215
 - organ structure and function, 216–218
- African weakly electric fish. *See* Weakly electric fish
- AL. *See* Antennal lobe (AL)
- Ampullary receptor organs, 245
- Animal sensors, 28
- Antennal lobe (AL), 10, 12–13, 16, 17
- Aradus* bugs
 - biology and behavior, 225–226
 - organ structure and function, 226
 - species, 224–225
- Auditory system
 - anuran amphibians
 - Eupsophus roseus*, 136–137
 - Huia cavitimpanum*, 135
 - non-mammalian ear, 136
 - Odorrana tormota*, 134
 - Puerto Rican Coqui frog, 133
 - small-scale functional modifications, 136
 - decision criterion, 131
 - frequency response, 131
 - predators and prey, unmatched filter, 137–138
 - reduced CNS, 131
 - weakly electric fish
 - androgens effect, 132
 - electroreceptor tuning, 132
 - EOD, 132

C

- Central complex (CX), 162
- Central pattern generator (CPG), 68

Compound eyes

- acute zones, 149
- apposition eyes, 147
- eye radius, 149
- facet diameter, 149
- ommatidia, 147, 149
- photoreceptor, 149
- superposition eyes, 147
- Cone outer segments (COS), 251, 252
- “Co”-note, 133, 134
- Correlation detector, 119–126
 - Bayesian binary hypothesis test
 - confusion matrix, 120–122
 - correlation lag index, 120
 - decision rule, 120
 - desired signal, 119
 - multidimensional (vector) data, 122–123
 - ROC curve, 124
 - statistical confidence interval, 125–126
 - test statistics, 120
 - training and testing phases, 123–124
 - convolution and filtering, 117
 - correlation vs. convolution, 117
 - cross-correlation, 114
 - filter impulse response, 118
 - performance measurement, 118
- COS. *See* Cone outer segments (COS)
- CPG. *See* Central pattern generator (CPG)
- Cupiennius salei*. *See* Spider’s sense

D

- Distortion product otoacoustic emission (DPOAE), 134
- Drosophila melanogaster*, 5, 15, 94

E

- Electric organ discharge (EOD), 132, 238, 239, 243, 244, 247, 249
- Electroreception, 238
- EOD. *See* Electric organ discharge (EOD)
- Extralemniscal pathway, 67

F

- Flicker fusion frequency (FFF), 256

G

- Gnathonemus petersii*, 250–258
 - electric fovea, 245–246
 - electric signals, 246–250
 - environmental sense, 258–259
 - prey detection, 242–245
 - self-produced field, 246–250
 - in sensory ecology, 240–242
 - visual sense
 - fast-moving detection, 250
 - low-contrast objects detection, 250
 - noise tolerance, 256–258
 - retina, 250–253
 - visual brain areas, anatomy of, 253–255
 - visual stimuli detection, 255–256

I

- IID. *See* Interaural intensity difference (IID)
- Infrared radiation (IR), 208–211
- Infrared radiation (IR) receptors
 - in animal kingdom, 211–212
 - forest fires detection, 212–214
 - in pyrophilous insects, 215
 - Acanthocnemus nigricans*, 215–218
 - Aradus* bugs, 224–226
 - development of, 228–229
 - Filter 1, 230
 - Filter 2, 230
 - IR sensory organs, 214
 - Melanophila* beetles, 221–224
 - Merimna atrata*, 218–221

Insect olfactory system

- AL, 17
- aminergic and peptidergic plasticity, 16–17
- analytical chemical methods, 6
- antennal lobe, 12–13
- chemical detection system, 4
- filtering mechanisms, 5
- insect taxa, range of, 17
- LP, 13–15

MB, 15–16

- MB α -lobe output and LP neurons, 17
- olfactory receptor proteins, 5
- peripheral processing, 10–12
- stimulus sources, 4
- VOC, 4

- active movement, 9
- adaptation/sensitization, 9
- analytical and neurophysiological methods, 6
- chemical classes, 8
- definition, 7
- insect attraction, 8
- mixtures of, 8
- passive effects, 9
- plumes, 8–9
- stimulus-tracking ability, 9

Insects ears, mechanosensory organs, 92

Interaural intensity difference (IID), 87, 97

IR. *See* Infrared radiation (IR)**K**

Katydid

- distance estimation, 96
- intensity discrimination, 96–97
- noise filter, novelty detection, 97–98
- signal-to-noise ratio, 98

Kenyon cell (KC), 15, 16

L

- Lateral protocerebrum (LP), 13–15
- Lemniscal pathway, 67
- Local interneuron (LN), 12–13
- Locomotion, 42–45, 61, 156–160
- Long wavelength infrared (LWIR), 208, 210
- LP. *See* Lateral protocerebrum (LP)
- LWIR. *See* Long wavelength infrared (LWIR)

M

Matched filter

- auditory matched filter hypothesis (*see* Auditory system)
- classification, 113
- communication and radar systems, 112, 113
- confidence interval, 128–129
- correlation detector (*see* Correlation detector)
- desired signal, 112
- detection theory, 113
- experiment design, 126–127

- in insect audition, 96, 99–100
 - active mechanical processes, insect ear, 92
 - antennal and tympanal receivers, 92
 - chronological sequence ignore, 92
 - cricket case, 85–87
 - filiform hairs, 85
 - IIDs, 88
 - katydids (*see* Katydids)
 - low-intensity sound eliminate, 101–102
 - mismatched filters, 89–92
 - mosquitoes and flies, antennal ears of, 94–95
 - moth, simple ear of, 92–94
 - periphery, 95–96
 - reduced sensitivity, 102–103
 - species-specific temporal call pattern (*see* Temporal call pattern)
 - taxon and sensory modality, 85
 - time windows, 100–101
 - tympanal ears, 85
 - variable CFs, 87
 - noisy discrete-time temporal signal, 113
 - performance measurement, 145
 - ROC curve, 128–130
 - signal detection problem, 114
 - middle signal, 114
 - SNR, 115–116
 - top signal, 114
 - threshold detector, 113
 - Melanophila* beetles
 - biology and behavior, 221
 - detection range, 222–224
 - organ structure and function, 222–224
 - Merimna atrata*
 - biology and behavior, 218
 - organ structure and function, 218–221
 - Mid-wavelength infrared (MWIR), 208, 210, 230
 - Mormyrid fish, 250
 - Mormyromast, 243, 245
 - Mushroom body (MB), 15–16
 - MWIR. *See* Mid-wavelength infrared (MWIR)
- O**
- Oecanthus henry*, 87
 - Olfactory receptor cell (ORC), 10–12
 - Optomotor response (OMR), 256
 - ORC. *See* Olfactory receptor cell (ORC)
- P**
- Paralemniscal pathway, 67
 - Photoreceptors
 - shortwave radiation
 - deep-sea fish, lenses of, 178
 - distribution, 175
 - image quality improvement, 177–178
 - removing, function of, 176–178
 - retina protection, 177
 - spectral response of
 - inner segment filters, 183–186
 - retinal photosensitizer, 183
 - visual pigment, 171, 172, 181–183
 - PN. *See* Projection neuron (PN)
 - Polarisation filter
 - detection mechanism, 197
 - sense, 195–196
 - Post-retinal filters
 - melanin, 179
 - tapeta, 179–180
 - Projection neuron (PN), 12, 14, 15
- R**
- Rapid cessation of protraction (RCP), 70
 - Receiver Operating Characteristic (ROC) curve, 124–125, 131
 - Resonance condition, 210
 - ROC curve. *See* Receiver Operating Characteristic (ROC) curve
 - Rod outer segments (ROS), 250, 252
- S**
- Sensory ecology, 28, 54
 - Sensory images, 28
 - Sensory tuning, 89
 - Signal-to-noise ratio (SNR), 115–116
 - Spider's sense
 - forces, torques, and directionality, 38–40
 - information encode, 41
 - locomotion, adaptive control of, 42–45
 - mechanosensors, 29
 - physiological responses, 41
 - sensory dendrites, coupling of, 37–38
 - simple stereotyped behavior, 45–52
 - body raising, 47–48, 53
 - courtship and copulatory behavior, 50–52
 - mechanosensory neuronal circuit, 47–48

- Spider's sense (*cont.*)
 proprioception, leg joint, 48–50
 synergic withdrawal, 45–47
- tactile hair
 clever hair shaft, 34–37
 cuticular hairlike sensilla, 29
 density, 29
 distribution, 34
 hair socket, 32
 long smooth, 31
 micromechanical properties, 53
 morphological diversity of, 32
 primary afferents of, 53
 proprioceptive hairs, 54
 shaft length and shape, 32
 single sensory cell, 31
 socket diameter and hair shaft diameter,
 32–33
 stereotyped patterns, 53
 yellowish plume, 30
- tactile sense, 29
 vision, 29
- T**
- Temporal call pattern
 amplitude modulation, 99
 grasshoppers and crickets, 99
 neuronal network
 in crickets, 99–100
Drosophila, 100
- Terminal dendritic mass (TDM), 220
 Terminal nerve mass (TNM), 211
- V**
- Vibrissae. *See* Whisker
- Vision matched filter
 in insects, 150–151, 153–155
 animal's finite metabolic energy budget,
 144
 arthropods, 144
 compound eyes, 147–149
 energetic cost, 145, 146
 evolutionary process, 145
 locomotion, 156–160
 navigation, 160–164
 photoreceptor, 145
 physical terrain, 153–155
 prey detection and pursuit, 153
 resting potential, 145
 sex, 150–151
 in vertebrates, 171–186, 188, 195–197
- amphibious vision, problem of,
 188–189
 anterior eye, 171
 asymmetric eye, 188
 chameleon, 188
 in emmetropic eye, 187
 image focus, ramp retina, 188
 Lens, 190–191
 light-sensitive retina, 171
 lower-field myopia, 188
 magnetic compass calibration, 197
 myopic eyes, 187
 nutritive aqueous humour, 171
 optical imperfections, 186
 photoreceptors, spectral response of
 (*see* Photoreceptors)
- polarisation filter, 195–197
 post-retinal filters, 179–180
 pupil, 189–190
 retinal spatial filters, 191–194
 rods and cones functions, 173–174
 shortwave radiation, on photoreceptor,
 175–178
 tubular eyes, 194–195
 visual stimulus, 170
 wavelengths, 172–173
- W**
- Weakly electric fish
 acoustic signals, 239
 active electrolocation, 238
 electrocommunication, 239
 electroreception, 238
 electroreceptor organs, 240
 environmental sensing, 239
 EOD, 238, 239
Gnathonemus petersii (*see* *Gnathonemus petersii*)
 temporal and waveform cues, 239
- Whisker, 60, 62–66, 69–74, 77–78
 active sensory system, 61
 directly touch and sense, 61
 discrete arrangement, 68
 evolution, 76
 force and direction, 66
 function, 75
 in rat, 60
 balance, 74
 ipsilateral whisker, 72
 judge distance, 73
 macrovibrissae, 60, 69, 72
 microvibrissae, 60, 73

- mystacial musculature, 70–71
 - object exploration, 70
 - texture discrimination, 73
- locomotion, 72
- matched filters, 69
 - active touch sense, 77–78
- matched sensors
 - discrete sensors, 65
 - individual whiskers, 64–65
 - macrovibrissae, 66
 - microvibrissae, 65, 66
 - mystacial pad and design, 62–64
 - mystacial whiskers, 62
 - periphery, 62
 - shaft, 66
- mechanoreceptors, 61
- motor control, 68
- movement, 69, 72
- navigation, in mammals, 61
- neural maps, 66–67
- neuroscience, 61
- object discrimination, 61
- sensory pathways, 67–68
- shape of, 68
- social interactions, 74
- spatial arrangement and musculature of, 76
- specialists, 60
- tactile hairs, 61
- topographic maps, 66
- Whisking, 60, 69